Remediation of Cr(VI) and Ni(II) contaminated water by Metal Tolerant fungi isolated from Electroplating effluent

BABASAHEB BHIMRAO AMBEDKAR UNIVERSITY
LUCKNOW
प्रज्ञा शील करूणा
ESTABLISHED 1996

Thesis submitted for the award of the degree of

Doctor of Philosophy

in

ENVIRONMENTAL SCIENCE

Supervisor
Prof. S. K. Dwivedi

Submitted By
Vinay Kumar

Department of Environmental Science
School for Environmental Sciences
Babasaheb Bhimrao Ambedkar University
(A Central University, NAAC Accreditation 'A' Grade)
Vidya Vihar, Raebareli road, Lucknow-226025
Uttar Pradesh, India

Enrolment No. 1122/15

Year-2021

Declaration

I **Vinay Kumar**, declare that the material personified in the present Ph.D. work entitled **"Remediation of Cr(VI) and Ni(II) contaminated water by Metal Tolerant fungi isolated from Electroplating effluent"** which is being submitted to Department of Environmental Science, School for Environmental Sciences, Babasaheb Bhimrao Ambedkar University, Lucknow is an original piece of research work done by me. It has not been submitted in part or full form for any other diploma or degree in any university. I also declare that thesis is essentially free from all kinds of plagiarism.

Vinay Kumar

Dated: 01/03/2021

Department of Environmental Science

Certificate

This is to certify that the thesis entitled "**Remediation of Cr(VI) and Ni(II) contaminated water by Metal Tolerant fungi isolated from Electroplating effluent**" submitted by **Mr. Vinay Kumar** is an original research work and has not been previously submitted in part or full for the award of any other degree or diploma to this or any other university.

The thesis submitted to Babasaheb Bhimrao Ambedkar University, Lucknow satisfies all the requirements as stipulated in the Doctor of Philosophy (Ph.D.) regulations-1999 as an amended in 2008/2010/2013/2016 and it is fit for submission and evaluation for the award of the degree of Doctor of Philosophy of the University.

Date: 11.3.2021

Prof. S. K. Dwivedi 11.3.2021

Head of the Department 23/03/21

Acknowledgement

I hereby take the pride of presenting my thesis which is not solely the result of an individual's efforts. Many people have contributed to its development. At this moment, I am sincerely grateful to universe and all those who contributed in one way or another to complete this thesis. First of all, I thank almighty God for his protection and ability to do work.

I am awfully obliged to my supervisor ***Prof. S. K. Dwivedi, Ex-Head DES and Dean (presently) of School for Earth & Environmental Science, Babasaheb Bhimrao Ambedkar University, Lucknow*** *for his guidance and enlightened supervision during my research work. Prof. Dwivedi has always made oneself available to clarify all the doubts arose from my research work. His discipline, punctuality and fatherly behavior all the time astonished and encouraged me. He has given me much liberty to carry out this research work. I take it as salvo for me to consummate my PhD under his guidance & direction. I have learned a lot from him and his research expertise which I will promulgate to the world with his continuous benediction. Thank you sir, for your help and support.*

I would like to express my heartfelt gratitude to all the faculties of the Department of Environmental Science ***Prof. D. P. Singh, Prof. R. P. Singh****,* ***Prof. N. K. Arora****,* ***Prof. Shikha, Prof. V. Dutta****,* ***Asso. Professors Mr. N.K.S. More****, and* ***Dr. N. Kumar*** *and* ***Assistant Professors Dr. Jiwan Singh*** *for their support and encouragement which helped me to carry out this research work.*

I am also thankful to my seniors Dr. S. Shankar, Dr. N. Gupta, Dr. S. Ahmad, Dr. A. P. Rawat, Dr. G. Prasad, Mr. Indrajeet Chaudhary, Dr. G. Saxena, Ms. Roli Mishra, Ms. Deepti, Mr. Pawan Maddeshiya, Mr. Pawan Yadav, Mrs. Nisha Yadav, Ms. Divya Dibey, etc. for their co-operation.

I am highly indebted to my labmates Mr. R. S. Sharma, Mrs. Garima Singh, Mr. Ashvani K. Chaudhay, Mr. Suresh K. Chaudhary and Mr. Ajay R. Tripathi and to my friends and colleagues Ms. Saumya Tripathi, Mr. Deep N. Dixit, Mr. Shubham Sonkar, Ms. Shalu, Ms. Naincy Sahu, Ms. Lata Verma, Ms. Kashifa Iqbal and Mr. Chandrabhan and my juniors Saumya Singh, Deepa Kannaujiya,

Pragati Tripaathi, Kalpana Dubey and Sukhram for their availability as per my needs in the duration of my research work.

I would like to thanks to non-teaching staff of the Department of Environmental Science Mr. Anchal Jain, Mr. Aviral Dixit and Mr. Ranjeet Sharma for their co-operation.

I am also highly thankful to University Grants Commission (UGC), New Delhi, Government of India for providing fellowship (UGC Non-NET).

Above all, I cannot stop praising as well as expressing my unfailing gratitude and love to my father ***Mr. Vishnu Dayal****, my mother* ***Mrs. Prabha Vati****, my elder brother* ***Mr. Vijay Kumar****, my sister* ***Aradhana*** *and entire my family members for their kind support and help even under their hurdle situations they all were always stand just beside me. My parents are my source of inspiration. They have made teach me to take a rigid decision, do hard work and continuous efforts. They are the most important people in my world and I dedicate this thesis to them.*

Last but not least, I owe my thanks to all the persons and institutions that directly or indirectly played role to conquer the difficulties countered by me during research work.

Vinay Kumar

Preface

Environmental pollution is the burning issue of this era and has taken great attention of the society as well as governmental organizing bodies due to its detrimental impact on human health and the environment. Water pollution is one of it that causes serious health problem due to different types of hazardous substances such as heavy metal, pesticides, dyes, etc. Heavy metal polluted wastewater is generated from different types of industrial activities. Hexavalent chromium (Cr(VI)) and divalent nickel (Ni(II)) are two of most precious heavy metal widely used in different industrial process including electroplating, paint manufacturing, paper & pulp, leather tanning and mining of Cr and Ni. Huge amount of wastewater is generated from these processes containing Cr and Ni as contaminant and without proper treatment it is disposed off in natural water body or land that affect the flora and fauna of the environment. Contamination caused by these processes is directly or indirectly affect the human health too. Cr(VI) and Ni(II) are highly toxic, carcinogenic and mutagenic and number of human health dilemma such as eye and skin irritation, severe diarrhea, corrosion of skin and respiratory tract, kidney dysfunction and probably lung carcinoma has been reported that are caused by Cr(VI) and Ni(II) that's why World Health Organization (WHO) has set the permissible limit 0.05 mg/L for Cr and 0.07 mg/L for Ni for drinking water.

Many of the physicochemical techniques are utilizing for treatment of such type of wastewater but insufficient treatment efficacy, high associated cost, generation of huge amount of sludge, requirement of high energy and skilled man power are the major shortcoming of these techniques. Bioremediation implies microbes and plants that can destruct many of the physicochemical technique's drawbacks and can become a sustainable way for treatment of wastewater. Fungi exhibited high potency to survive in adverse environment and play crucial role in ecosystem functioning. Fungi that have high metal tolerance capability can be exploited for treatment of metal contaminated wastewater under *in situ* as well as engineered systems. The present study entitled "**Remediation of Cr(VI) and Ni(II) contaminated water by Metal Tolerant fungi isolated from Electroplating effluent**" is aimed to isolate the heavy

metal tolerant fungi from extremely heavy metal contaminated electroplating wastewater and give scientific knowledge about the Cr(VI) and Ni(II) tolerance and removal efficiency and mechanisms of isolated heavy metal tolerant fungal species for their potential application in the field of bioremediation of Cr(VI) and Ni(II) contaminated wastewater. In this investigation, the heavy metal tolerant fungal species were isolated from electroplating wastewater. Their heavy metal tolerance efficiency, Cr(VI) and Ni(II) reduction/removal potential was investigated and to establish the tolerance and reduction/removal mechanism of fungi for Cr(VI) and Ni(II), SEM-EDX, FTIR, XRD, XPS and many biochemical assays such as oxidative stress, enzymatic and non-enzymatic response that work as molecular signaling in the response of metal stress, were performed. The present thesis has been categorized into six chapters.

Chapter 1 is entitled **"Introduction"** that cover the background of the present work and describes the need for the treatment of Cr(VI) and Ni(II) contaminated wastewater.

Chapter 2 accomplished with seventh foremost objectives of the present work.

Chapter 3 is about **Review of Literature.** This chapter contains knowledge of the existing treatment techniques such physicochemical, filtration, adsorption, electrochemical, etc. Application of fungi and their mechanism that are involved in tolerance and removal of heavy metal including Cr(VI) and Ni(II) are also discussed.

Chapter 4 is on **"Materials and Methods"** that comprise the detail of methods and methodology followed during the journey of this study.

Chapter 5 is the **"Results and Discussion"**. This chapter is divided into 8 sections. **Section 5A** described the physicochemical characteristics of collected electroplating wastewater. **Section 5B** deals with isolated fungal species from electroplating wastewater. In **Section 5C** heavy metal tolerance efficacy of the fungi are discussed. **Section 5D** is explaining the molecular characterization of isolated fungal species. **Section 5E** is on Chromium reduction and Removal by *A. flavus* CR500: Biochemical and morphological response and phytotoxicity investigation. **Section 5F** comprises the detail investigation on *T. lixii* CR700

and its Cr(VI) remediation mechanism and entitled as "*T. lixii* CR700 and Cr(VI): Reduction, removal and Biochemical analysis". **Section 5G** and **5H** deals with Ni(II) removal and mechanism by *A. flavus* CR500 and *T. lixii* CR700 and entitled as "*A. flavus* CR500 and Ni(II): Removal, morphological and Biochemical analysis" and "*T. lixii* CR700 and Ni(II): Removal, morphological and Biochemical Study" respectively. The multiple-metal removal ability of *A. flavus* CR500 from wastewater is discussed in the **section 5I**.

Chapter 6 is emphasizing chief finding and conclusion of this investigation and entitled as **"Summary"**.

Chapter 7 is on **"conclusion"**. At the end of the thesis a list of publications (**Appendix I**) and conference and workshop attended (**Appendix II**) have been applauded.

Date **Vinay Kumar**

Abbreviation

Ar:	Argon
AAS:	Atomic absorption spectrophotometer
ANOVA:	Analysis of variance
ATP:	Adenosine tri phosphate
BOD:	Biological oxygen demand
CAT:	Catalase
CFE:	Cell free extract
ChrR:	Chromate reductase
COD:	Chemical oxygen demand
$Cr_{(III)/[III]}$:	Trivalent chromium
$Cr_{(VI)/[VI]}$:	Hexavalent chromium
DMRT:	Duncan multiple rage test
EDS/EDX:	Energy dispersive x-ray spectrophotometer
EDTA:	Ethylene diamine tetra acetate
Fig:	Figure
FTIR:	Fourier transform infrared spectrophotometer
FW:	Fresh weight
GSH:	Glutathione
GSSG:	Oxidized glutathione
HM:	Heavy metal
MDA:	Malondialdehyde

NBT:	Nitroblue tetrazolium
$Ni_{(II)}$:	Divalent nickel
PAL:	Phenyl ammonium lyase
PDA:	Potato dextrose agar
PDB:	Potato dextrose broth
POD:	Peroxidase
PPO:	Polyphenol oxidase
PVP:	Polyvinylpyrrolidone
ROS:	Reactive oxygen species
rpm:	Round per minutes
SEM:	Scanning electron microscope
SOD:	Superoxide dismutase
TDS:	Total dissolve solid
XPS:	X-ray Photoelectron Spectroscopy
XRD:	X-ray diffraction

General Symbol

°C:	degree centigrade
µ:	micro
µL:	micro litter
cm:	centimeter
g:	gram
h:	hour

kg:	kilo gram
L:	litter
m/mins:	minutes
M:	mole
mg:	Milligram
mL:	milliliter
mM:	mille mol
nm:	nano meter
U:	unit
v:	volume
w:	weight

Content

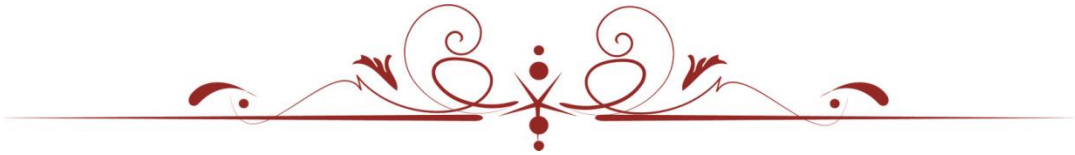

Chapter-1

Introduction

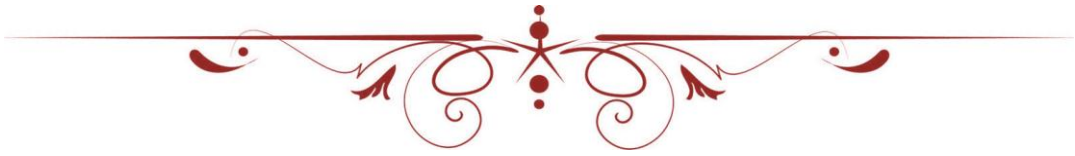

Chapter-1 Introduction

Present scenario of industrial and developmental activities are altering the natural flow of the materials and introducing foreign compounds into the environment (Faisal and Hasnain, 2004). Environmental pollutants including halogenated solvents, petroleum hydrocarbons, explosives, agro-chemicals, heavy metal/loids and radionuclide's are the serious problem to the environmental concern. Out of these pollutants, heavy metals (HMs) (cadmium, Cd; copper, Cu; mercury, Hg; lead, Pb; manganese, Mn; arsenic, As; nickel, Ni; zinc, Zn; iron, Fe etc.) are extensively used in different types of industries and released in high amount with their disposing effluents. These contaminants directly or indirectly come into the environment. A few number of metals including Fe, Mg, Cu, Mn, Co and Zn are the micronutrients for most of the organisms; while, not for all living organism and increasing concentration from their limit causes toxicity (Manorama et al., 2016; Singh et al., 2017). HMs as micronutrient may play essential role in metabolic activity e.g. metalloenzyme (Tahir et al., 2017). Because of high solubility of HMs in the aquatic medium, they can be easily absorbed or intake by the organisms. On another hand, being metal, they are non-biodegradable and have multiple threats to living organisms due to their persistence in nature, high toxicity characteristics and long half-lives after coming into the food chain (Ali et al., 2015; Jamali et al., 2007; Mondal et al., 2017). They have multiple ways to come into the food chain such as by seeping in ground water from wastewater, by drinking of water from polluted water body, crop irrigation by wastewater etc. (Jamali et al., 2007). After accumulation into the living organism they causes multiple threats to human (Table 1.1) as well as other organism. So, due to extensive use and toxic in nature heavy metal has rises number of environmental and human health issues and become a serious concern to resolve at present (Dhankar and Hooda, 2011; Mishra and Malik, 2012).

From the last four-five decades, it has been greatly focused to control hazardous chemical, especially toxic HMs. At present, there is a great requirement of economical and efficient techniques for treating HMs contaminated industrial wastewater (Dhankar and Hooda, 2011). There are some conventional technologies including chemical coagulation, adsorption, precipitation, membrane filtration, reduction and ion exchange that are being used to treat HMs polluted wastewater (Barakat, 2011; Fu and Wang, 2011). However, most of these methods are ineffective

to remove HMs below 100 mg/L (Dixit et al., 2015) and generate secondary pollution (Kumar et al. 2019). Their high cost and eco-unfriendly nature limits its application and required alternative cheap and ecofriendly technique to treat HMs contaminated wastewater. Bioremediation have been seen as cheaper and ecofriendly alternative which implies the application of bacteria, fungi and plant to treat wastewater, and have taken a great attention from the last 3-4 decades.

Table 1.1. Heavy metals permissible limit in drinking water (WHO Standard), their sources and Human health impact

Metal species	**Maximum permissible limit in drinking water* (mg L^{-1})**	****Major sources**	****Human health impact**
Hg	0.006	Pesticides, batteries and paper industries	Damage to nervous system, Protoplasm poisoning
Cd	0.003	Electroplating, welding, pesticide fertilizer, Cd and Ni battery industries	Kidney damage, bronchitis, gastrointestinal disorder, bone marrow, cancer
Pb	0.01	Paints, pesticides, smoking, automobile emission, mining, burning of coal	Liver, kidney & gastrointestinal damage, mental retardation in children
Cr	0.05	Chrome plating, ceramics, metallu-rgical processes, paints, dyes, magnetic tapes	Persisting diarrhoea, skin ulceration, "chrome holes", bronchial asthma
Cu	2.0	Agricultural fungicides, algicides, Fertilezers, plumbing corrosion, Electroplating, photography	Gastrointestinal disorder, liver and kidney malfunctioning, nausea, vomiting, diarrhoea, intestinal cramps, anaemia
As	0.01	Pesticides, fungicides, metal smelters, mining of coal and ores	Loss of appetite and nausea, vomiting, oesophageal and abdominal pain, and bloody "rice water" diarrhoea

			Bronchitis, dermatitis, skin thickening (hyperkeratosis) neurological disorders, muscular weakness
Mn	0.5	Welding, fuel addition, ferromanganese Production	Inhalation or contact causes damage to central nervous system
Ni	0.02	Nickel- or chromium-plated taps, bore-hole equipment	Skin sensitizer, dermatitis, prenatal mortality
Co	-	Aircraft engines, magnets, grinding and cutting tools, artificial hip and knee joints, glass, ceramics and paints	Congestive heart failure, dermatitis, liver and kidney effects, nausea, vomiting, diarrhoea, bleeding, coma
Zn	3.0	Refineries, brass manufacture, metal plating, plumbing	Zinc fumes have corrosive effect on skin, cause damage to nervous membrane
Fe	-	Blister packaging, iron pipes, and cookware	Liver, cardiovascular system, and kidney malfunctioning

***WHO's drinking water standards, 2017, **Sources of pollutants and their impact on human health is adopted from Ayangbenro and Babalola (2017) and Dhankar and Hooda (2011).**

Microorganisms have capacity to survive in almost every adverse environment because of their innate ability to take up the pollutants as nutrients like HMs due to accumulative and absorptive capability. Microorganism not only accumulates or adsorbs HMs but also having the ability to reduce HMs from toxic to non/less-toxic form (Chen et al., 2019; Sakthivel et al., 2016). Number of microorganisms has been explored for the mobilization and immobilization potential of metal ions, thereby varying their accessibility to plants (Birch, 1990; Bachofen, 1990; Deng et al., 2013; Rhee et al., 2014). Fungi have been reported to exhibit significant tolerance/resistance towards HMs and turn out to be dominant organisms in some contaminated aquatic

water bodies and other habitats (Gola et al., 2016; Mishra and Malik, 2012). The tolerance and accumulation characteristics of fungi are the major criteria for selection to introduce their application in the field of bioremediation. In case of growing fungi, their application in remediation is called as mycoremediation. *Aspergillus niger* (Fomina et al., 2017; Holda et al., 2016; Mondal et al., 2017; Sriharsha et al., 2017; Tahir et al., 2017), *Trichderma harzianum* (Adebiyi et al., 2017; Cecchi et al., 2017; Mohammadian et al., 2017) are reported as multi metal tolerant fungi. Numbers of species from diverse group of fungi (*Penicillium*, *Aspergillus*, *Trichoderma*, *Fusarium*, *Rhizopus*, etc.) have been reported which have different types of HMs removal capacity. A number of mechanistic strategies are involved in microorganisms (bacteria, fungi and algae) for resistance towards metals including enzymatic detoxification, accumulation inside the cell via active/passive uptake, adsorption on their outer cell structures, precipitation on cell surface, exclusion by permeability barrier, efflux pumps and alteration of the cellular objects (Bruins et al., 2000; Kumar et al., 2019; Merroun et al., 2001; Zhang et al., 2005; Cao et al., 2018; Yin et al., 2011; Dang et al., 2018). In the HMs removal, resistance/tolerance and homeostasis, fungi go through one or combination of more than one of the basic mechanisms.

The electroplating processes are widely used to deposit the preferred coating on metallic object via electrolysis to alter the characteristics of object surface in order to improve the physical appearance, protection from corrosion, surface properties or combination of them (US EPA, 2016; Martín-Laraet al., 2014; Ajmal et al., 2001). In the process, by passing the electricity through the electrolytic bath, the dissolved metal at the electrolytic bath are deposited on the cathode, whereas the platters dip the object into a series of the chemical bath to get desired result (US EPA, 2016; Martín-Laraet al., 2014). The metals including nickel (Ni), copper (Cu), zinc (Zn), chromium (Cr), cadmium (Cd), manganese (Mn), lead (Pb) or combination of them are commonly used in the electroplating process (US EPA, 2016; Martín-Laraet al., 2014; Machado et al., 2010a, b; Peng et al., 2005). Day by day, the growth of electroplating industries is increasing due to immense growth in developmental activities. Prominent factors that are playing a significant role in the growth of Electroplating Market are growing demand for automobiles, consumer goods and aircraft (MRR, 2017; Daylan et al., 2013). In India, as estimated by CPCB (Central Pollution Control Board) the growth of electroplating industries is going to increase by 100% in next ten years and also listed in the red category of industries (CPCB, 2007). There are above 15,000

electroplating plants or workshops in china producing about 4×10^9 m^3 electroplating wastewater per annum (Peng et al., 2005; Liu et al., 2011). However, in Europe, 1% of hazardous waste is generated by electroplating industries (Daylan et al., 2013). According to the Market Research Report (MRR) the global electroplating market has reached to 14,540.5 US$ in 2016 and expected to increase at a CAGR (Compound Annual Growth Rate) of 3.7 % during the periods of 2016-2026 (MRR, 2017).

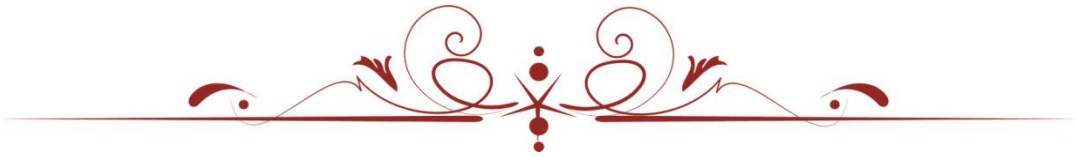

Chapter-2

Objectives

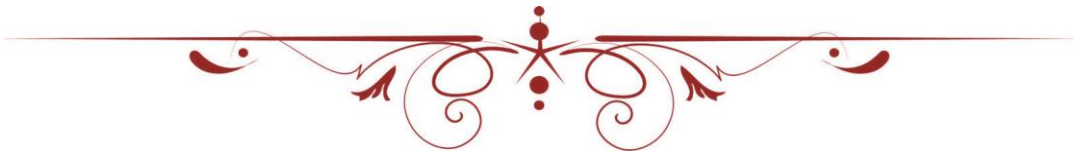

Chapter-2 Objectives

2.1. Isolation and identification (morphological and molecular) of fungi from electroplating waste water and sludge sample.

2.2. Screening of multi-metal tolerance capacity of isolated fungi against selected heavy metal.

2.3. Analysis of heavy metal removal capacity of HM tolerant fungi for specific metal and growth optimization at pH, temperature, time and metal concentration, a batch sorption study.

2.4. Analysis of heavy metal removal capacity of metal tolerant fungal isolates from multi-metal contaminated aqueous medium.

2.5. Determination of Catalase (CAT), Peroxidase (POD), Superoxide dismutase (SOD) Glutathione (GSH) and Protein, Proline and total phenolic content in tolerant fungi under the stress of $Cr_{(VI)}$ and $Ni_{(II)}$.

2.6. Absorption characterization of heavy metal in selected fungi by SEM, EDS, FTIR and XRD.

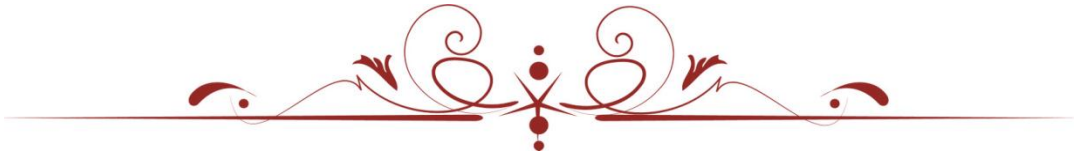

Chapter-3

Review of Literature

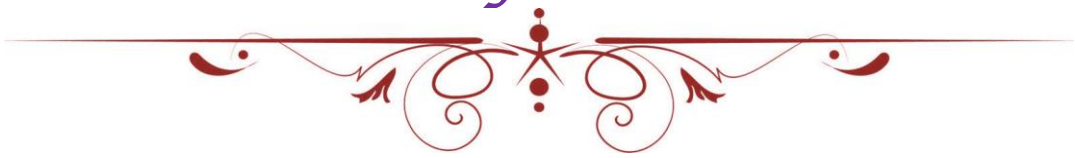

Chapter-3 Review of Literature

3.1 Sources and chemistry of Cr and Ni in wastewater

Chromium and Nickel are d-block transition element. Ni is the 24th most rich element of the earth crust with predictable concentration of 0.008%. The atomic number of Cr and Ni are 24 and 28 respectively. The electronic configuration of Cr is [Ar] $4s^1$, $3d^5$ and Ni is [Ar] $4s^2$, $3d^8$ with atomic mass of 51.9 and 58.71 amu respectively (Malaviya and Singh, 2016; Kerfoot, 2005). Cr shows -2, -1, 0, +1, +2, +3, +4, +5, and +6 and Ni shows -1, 0, +1, +2, +3 and +4 with an associated ample variety of chemical and physical characteristics (Coman et al., 2013; Pradhan et al. 2017). The most stable Ni is found when the oxidation state is +2 (divalent or $Ni_{(II)}$), while stable oxidation state for Cr are +6 ($Cr_{(VI)}$; hexavalent) and +3 ($Cr_{(III)}$; trivalent). The common species of $Cr_{(VI)}$ in water are CrO_4^{2-}, $Cr_2O_7^{2-}$, H_2CrO_4 and $HCrO_4$ and the species of $Cr_{(III)}$ are Cr^{3+}, $Cr(OH)_2^-$, CrO_2^-, CrO^+, $HCrO_2$ (Barrera-Díaz et al., 2012). $Ni_{(II)}$ occur in water in the form of Ni^{2+} and with persulfate or halides generate the insoluble Ni(III) oxide (β-NiO(OH)) whereas $Ni_{(II)}$ hydroxide oxidation by persulfate results in Ni(IV) oxide (NiO_2) (Coman et al., 2013).

Nickel a silver white, hard and squashy metal, usually found as face-centered cubic crystal lattice with ferromagnetic characteristics at room temperature. With non-ferromagnetic characteristics, a hexagonal form of Ni is also known. There are numbers of uses are associated with Ni, Ni-compound and Ni alloys for industrial and commercial purposes. It is mostly used in the production of temperature and corrosion resistance stainless steel, non-ferrous alloys and Ni-based super alloys. Its alloys are used in range of areas from industrial machineries to precision electronic (Coman et al., 2013). Its compound and complex are also used as potential catalyst in a variety of syntheses. $NiSO_4$ and $NiCl_2$ is the common $Ni_{(II)}$ compound very excessively used for electroplating purpose in electroplating plants (Kiptoo et al., 2004). However, phosphorus, organic chelating agents and high amount of $Ni_{(II)}$ are used for without electric current plating where chelating agents prevent the $Ni_{(II)}$ precipitation and phosphorus work as reductant in the deposition of Ni on the object (Ying et al., 1988; Shih et al., 2013). This mechanism complete in following reaction:

$$2C_6H_8O_{7(aq)} + 3Ni^{2+}{}_{(aq)} \rightarrow C_{12}H_{10}Ni_3O_{14(aq)} + 6H^+ \quad (1)$$

$C_{12}H_{10}Ni_3O_{14(aq)} + 2H_2PO_4^-{}_{(aq)} + 2H_2O \rightarrow 3Ni_{(s)} + 2HPO_3^-{}_{(aq)} + 2C_6H_8O_{7(aq)} + 2H^+ + H_2$ (2)

These sources collectively generate huge amount of Ni contaminated wastewater via seepage and discharge of Ni-containing effluents. Ni laterite ores usually produces by open cut mining and produces huge amount of potentially acidic waste rock. There downstream flow to the environment via surface water flow also causes Ni contamination. In water, Ni typically occurs in soluble of Ni^{2+}, but its other form may also occur predominantly combined with sulfate and chloride. However, Ni speciation is dependent upon different types of factors including pH, temperature, ionic strength, ligand type and concentration, dissolved organic carbon (DOC), hardness (e.g., Ca and Mg concentration) and other cations etc. (Binet et al., 2018).

Chromium metal has a metallic shine, steely-grey in color, hard and breakable, resists tarnishing, and has high melting (1907 °C) and boiling point (2671 °C). It is passivated by oxidation reaction which form protective thin layer and prevent the oxygen diffusion onto the core metal. It shows a BCC crystal system analogous to α-iron crafting, proficient in stainless steel alloy (Malaviya and Singh, 2016; Haynes, 2014). These characteristics make it appropriate element to improve alloy and change the hardness, metallic lusture and colour and boost corrosion resistance property (Wallwork, 1976). The fraction of stainless steel and oxidation of used Cr in refractory bricks contaminate the soil and water as a result of leaching. Na_2CrO_4, a $Cr_{(VI)}$ compound is generated in huge amount throughout the lime treatment of ferrous-chromite and chromite ores which result into the formation of different highly water soluble $Cr_{(VI)}$ compound such as CrO_4^{2-}, $CrOCl_4$, $H_2Cr_2O_7$, CrF_6, CrO_3, $Cr_2O_7^{2-}$, H_2CrO_4 and $HCrO_4^-$ (Langard, 1990). Potassium dichromate ($K_2Cr_2O_{7)}$ and $Na_2Cr_2O_7$ (sodium dichromate) are used as titration standard. However, $Na_2Cr_2O_7$ is less preferable due its hygroscopic property for the redox titration. $H_2Cr_2O_2$ is extensively used in various manufacturing industries including dyes and paint pigments, electroplating, analytical grade chemicals, leather tanning and others. Huge amount of effluent is produced from these industries, major cause of $Cr_{(VI)}$ contamination of water and soil (Fig. 3.1).

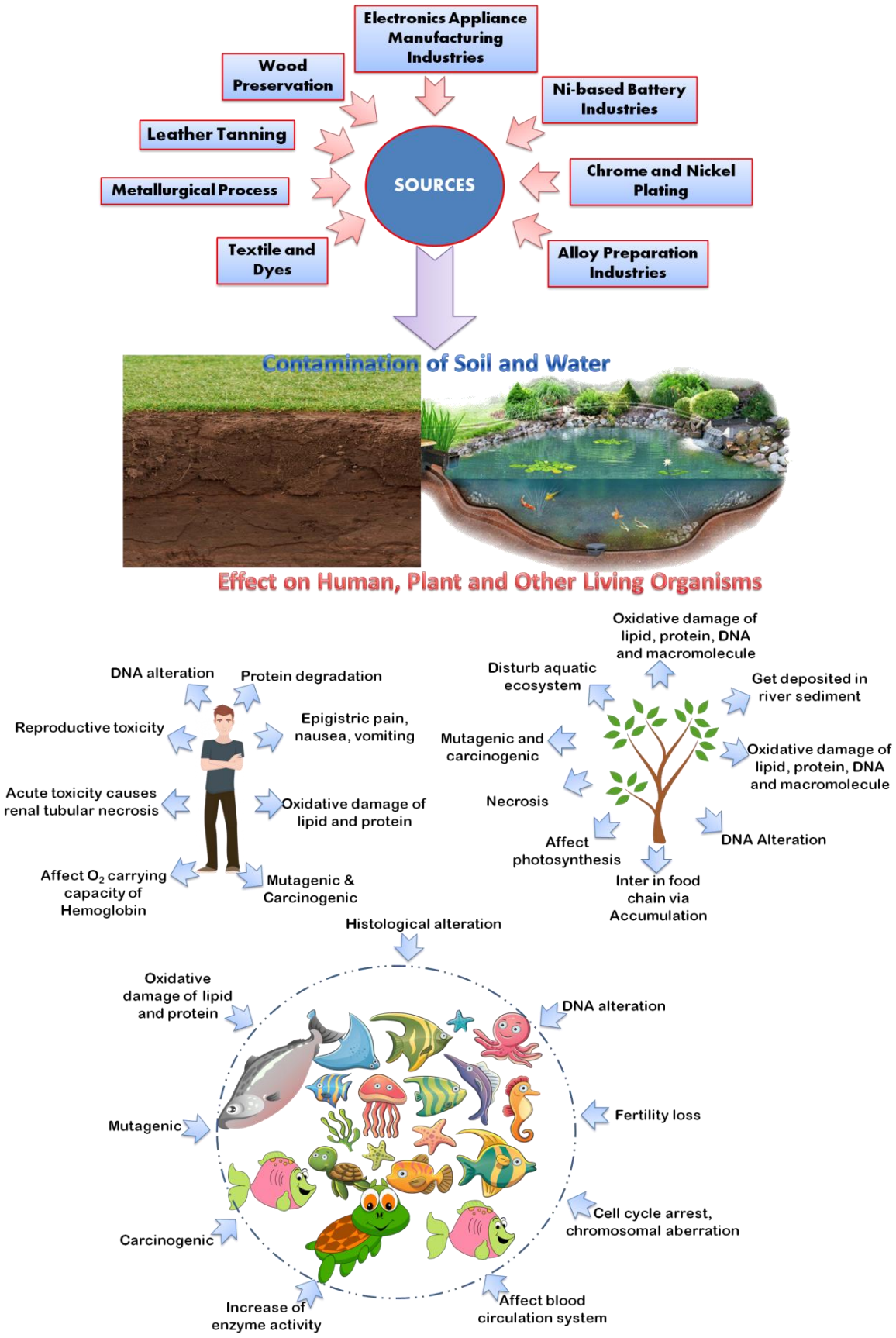

Fig. 3.1. Sources and Effect of $Ni_{(II)}$ and $Cr_{(VI)}$ on Human health and other organisms.

The compound of $Cr_{(III)}$ form several octahedral co-ordination complexes, show various colour as a result of diverse crystal field transition in the association of coordinating ligands and the stability of the complexes confirmed by crystal field stabilization energy as of configuration of d^3. $Cr_{(III)}$ easily oxidized into $Cr_{(VI)}$ in alkaline condition but stable in acidic condition, while $Cr_{(III)}$ compounds are less soluble than $Cr_{(VI)}$ in water. The oxides of $Cr_{(III)}$ to some extent is water soluble below pH 5.0 and pH 5.0 forms hydrated $Cr_{(III)}$ compounds, very less soluble in water. In water, $Cr_{(VI)}$ forms anionic species increases solubility up to 60 g/L in a broad range of temperature (Kimbrough et al., 1999).

3.2 Toxicity of $Cr_{(VI)}$ and $Ni_{(II)}$

Chromium is basically found in its trivalent and hexavalent state in which $Cr_{(III)}$ is a vital trace element necessary for metabolism of lipid, glucose and amino acid (Pradhan et al., 2017). However, $Cr_{(VI)}$ and $Ni_{(II)}$ are highly toxic species even at low concentration. $Cr_{(VI)}$ is basically found in the form of CrO_4^{2-}, structurally similar to SO_4^{2-} (sulphate ion), by replacing the SO_4^{2-} species, CrO_4^{2-} easily transported inside the cell via sulphate transport system (Zhitkovich et al., 2011). After uptake inside the cell, both of the species ($Cr_{(VI)}$ and $Ni_{(II)}$) are redox active and induces the reactive oxygen species (ROS) production such as O (nascent oxygen), O_2^- (superoxide anion), OH^- (hydroxide ion), HO_2^- (peroxo ions) and $OH^\bullet$ (hydroxyl radicals) (Das et al., 2013; Barrera-Díaz et al., 2012). ROS inside the cell depends on the concentration of $Cr_{(VI)}$ and $Ni_{(II)}$ as high concentration exposure increases free radical generation inside the cell. High content of ROS causes oxidative stress inside the cell and oxidative damages to cellular micro and macro constituent. $Cr_{(VI)}$ also known to cause non-oxidative damage of DNA. The most unambiguous form of damage caused by Cr is its binding with DNA (Cr-DNA), detected in various cultural cell, the major cause of Cr induced mutations and chromosomal breaks (Zhitkovich et al., 2011). $Cr_{(III)}$, end products of $Cr_{(VI)}$ metabolism inside the cell can make Cr(III)-DNA complex via electrostatic interaction with negatively charged phosphate group of DNA. Cr(III)-DNA complex is mutagenic and toxic which affect DNA replication and translation and can lead mutagenesis. While, produced ROS during $Ni_{(II)}$ and $Cr_{(VI)}$ metabolism react with DNA-proteins to form variety of intermediary products and byproducts, described as oxidative DNA damage. $Cr_{(VI)}$ metabolism also linked with the fabrication of single strand breaks, can affect the cell functions and cause

cancer in kidney, liver and lungs (Singh and Chowdhuri, 2017). It has been also reported that $Ni_{(II)}$ can replace Fe(II) from hemoglobin and produces hybrid non-functional hemoglobin that affect the O_2 carrying capacity of blood and causes permanent intracellular hypoxia (Lynn et al., 1998).

Direct contact of $Ni_{(II)}$ and $Cr_{(VI)}$ causes dermatitis, dermal corrosion and dermal necrosis (Kadota and Kurita, 1955; Kimbrough et al., 1999). Occupational contact via inhalation of $Ni_{(II)}$ and $Cr_{(VI)}$ increases the chance of respiratory cancer (USEPA, 1998). Nickel carbonyl is highly hazardous species of Ni causes lungs disorder (Sunderman et al., 1975). Long term occupational $Ni_{(II)}$ and $Cr_{(VI)}$ exposure from mining and industrial areas can cause carcinomas in bronchial system (Gibb et al., 2000). $Ni_{(II)}$ is also marked as immune sensitive and allergen and reduces the antibody circulation response (Fig. 3.1) (Das et al., 2020). $Cr_{(VI)}$ causes neurotoxicity by reducing the neuronal cells (Pradhan et al. 2017), while significant neurological disorder is also reported due to Ni(II) toxicity in mice (ABC, 1988).

3.3 Treatment methods for $Ni_{(II)}$ and $Cr_{(VI)}$ contaminated wastewater

3.3.1 Physicochemical methods

3.3.1.1 Chemical Precipitation

The most frequent way of $Cr_{(VI)}$ removal is its reduction in trivalent chromium $Cr_{(III)}$ subsequently $Cr_{(III)}$ precipitation as $Cr_{(III)}$ hydroxide. Typically sulfur compound such as sulfur dioxide (SO_2) and sodiumbisulfite ($NaHSO_3$) are abundantly used for reduction of $Cr_{(VI)}$ (Barrera-Díaz et al., 2012; Canning, 1982). After dissolution in water SO_2 and $NaHSO_3$ converted into reducing agent H_2SO_3 as shown in equation.

$$SO_2 + H_2O \rightarrow H_2SO_{3(aq)} \quad (1)$$

$$NaHSO_{3(aq)} + H^+_{(aq)} \rightarrow H_2SO_{3(aq)} \quad (2)$$

After the production of reducing agent, the equation (3) takes place in the system almost instantaneously at pH of 2.5 and reduces the $Cr_{(VI)}$ to $Cr_{(III)}$. However, theoretically 3 kg of $NaHSO_3$ (sodium bisulfite) and 2–3 kg of H_2SO_4 (sulfuric acid) are needed to reduce the 1 kg of $Cr_{(VI)}$.

$$4CrO_4^{2-}{}_{(aq)} + 6NaHSO_{3(aq)} + 3H_2SO_4 + 8H^+{}_{(aq)} \rightarrow 2Cr_2(SO4)_{3(aq)} + 3Na_2SO_{4(aq)} + 10H_2O \quad (3)$$

The SO_2 can react as follows (equation 4).

$$2CrO_4^{2-}{}_{(aq)} + 3SO_{2(g)} + 4H^+{}_{(aq)} \rightarrow Cr_2(SO4)_{3(aq)} + 2H_2O \quad (4)$$

After getting reduced of $Cr_{(VI)}$ into $Cr_{(III)}$, it is precipitated as $Cr(OH)_3$ by adding NaOH or $Ca(OH)_2$ slurry into the system to neutralize the pH.

$$Cr_2(SO_4)_3 + 6NaOH_{(aq)} \rightarrow Cr(OH)_{3(s)} + 3Na_2SO_{4(aq)} \quad (5)$$

The nickel is chemically removed from the system by elevating the solution pH up to 9.0-10.0 (Kurniawan et al., 2006; Coman et al., 2013). With rise in the pH of the $Ni_{(II)}$ containing solution, $Ni_{(II)}$ get precipitated as $Ni(OH)_2$.

$$Ni^{2+}{}_{(aq)} + 2OH^-{}_{(aq)} \rightarrow Ni(OH)_{2(s)} \quad (6)$$

The most basic problem of this technique is the generation of large amount of sludge. The generated sludge make difficulties in managing, transporting as well as in its final disposal and also the associated cost of this technique is adding another disadvantage with this technique. Thus, it is required to develop new technology to address these issues.

Iron is another probable agent for the reduction of $Cr_{(VI)}$ that is used for treatment of $Cr_{(VI)}$ containing wastewater (Jacobs et al., 2001; Jobby et al., 2018). Iron mediated $Cr_{(VI)}$ reduction mainly occur at lower pH value due to presence of iron in its divalent and trivalent forms and easily participate in $Cr_{(VI)}$ reduction. The most common iron salts, iron chloride ($FeCl_2$) and iron sulfate ($FeSO_4$) are basically utilized in this process subsequently precipitated by raising the pH of the solution as mentioned above (Barrera-Díaz et al., 2012). Iron induced $Cr_{(VI)}$ reduction occur as follows:

$$6Fe^{2+}{}_{(aq)} + Cr_2O_7^{2-}{}_{(aq)} + 14H^+{}_{(aq)} \rightarrow 6Fe^{3+}{}_{(aq)} + 2Cr^{3+}{}_{(aq)} + 7H_2O \quad (7)$$

$$Cr^{3+}{}_{(aq)} + 3OH^-{}_{(aq)} \rightarrow Cr(OH)_{3(S)}\downarrow \quad (8)$$

3.3.1.2 Ion flotation

Some time pollutants are also present in non-surface active form that can be removed by adding surfactant. Surfactants basically react with pollutants via either electrostatic attraction or chelation mechanism and are removed by creating foam phase via sparging of air into the solution. Sodium dodecyl sulfate was used for Ni^{2+} removal and was successfully removed from the solution (Doyle and Liu, 2003). In another study, dodecyldiethylenetriamine was used which revealed its selective ion flotation behavior of Ni^{2+} and other pollutant. At pH 9.0, the removal effectiveness for Ni^{2+} was almost 93%. Lu et al. (2020) utilized the binary solution of sapindus saponin and cetyl trimethyl ammonium bromide surfactant for removal of $Cr_{(VI)}$ and recorded 94% removal. Some studies also reported high removal potential of $Cr_{(VI)}$ by cationic surfactant modified adsorbent (Jin et al., 2014).

3.3.1.3 Ion exchange

Basically in ion exchange, undesired ions are replaced by non-toxic ions. Ion exchange is widely used for treating heavy metal containing wastewater. Various types of resins and zeolite have been applied for efficient elimination of $Ni_{(II)}$ and $Cr_{(VI)}$. In many of the work, ion exchange was applied with other treatment technique to enhance the removal potential of the system. A water-stable cationic metal-organic framework $\{[Cu(L)_{0.5}(bpe)(H_2O)](NO_3)\bullet(H_2O)_{0.5}\}_{\boldsymbol{n}}$ (**1**) (H_4L = bis(3,5-dicarboxypyridinium)-p-xylylene) fabricated by Shao et al. (2019) was used for exclusion of chromate ion from aqueous medium. Synthesized material showed high uptake efficiency (190 mg/g) for $Cr_{(VI)}$ via substituting the Cu(II) cation from the central metal ion positions. In another work, silica-based pyridine resin (SiPyR-N4) was able to remove 99.3% of $Cr_{(VI)}$ via ion exchange and reduction mechanism (Ye et al., 2019). Abbasi et al. (2018) investigated the $Ni_{(II)}$ loading onto an iminodiacetic acid ion exchange resin (TP207XL), $Ni_{(II)}$ loading happened via the combination of intraparticle diffusion/ion exchange reaction mechanisms.

3.3.2 Membrane filtration

Membrane filtration is advanced and broadly used technology for management of heavy metal contaminated wastewater. It is mainly used due to its several compensation such as semi-permeability, require less chemical and space and has

high adoptability. In respect of $Ni_{(II)}$ and $Cr_{(VI)}$ treatment, the membrane filtration can be categorized into ultrafiltration, nanofiltration and reverse osmosis. The fundamental design of membrane technique is illustrated in Fig. 3.2b that is commonly used in treatment of water.

The pore size of the ultrafiltration membrane is higher (2-100 nm) than dissolved, hydrated and low molecular weight metal complexes. The heavy metal ions can easily pass through the membrane as it is not applied in treatment of dissolved metal containing wastewater. But, by modifying the surface of the membrane as adsorptive membrane, can be used with dual-function by adsorptive-filtration membrane. The adsorbing material may be natural material, silica, synthetic polymer and industrial by-product. In a study, Bisheh et al. (2020) used porous organic polymer modified adsorptive ultrafiltration membrane and also functionalized with amino monomer for $Ni_{(II)}$ and Pb(II) removal. They found 86 and 92 % elimination of $Ni_{(II)}$ and Pb(II) respectively from the solution. In another research, ultrafiltration membrane synthesized from cellulose acetate polymer mixed with polyethylene glycol additive and amine modified TiO_2 was used for exclusion of $Cr_{(VI)}$. The membrane illustrated high removal potential of $Cr_{(VI)}$ which was 99.8% (Gebru and Das, 2018). Li et al. (2018a) prepared a hybrid ultrafiltration membrane (PAA/ZIF-8/PVDF-membrane). They used the prepared membrane for exclusion of $Ni_{(II)}$ from highly saline conditions and hybrid ultrafiltration membrane, could effectively remove $Ni_{(II)}$ (219.09 mg/g).

Nanofiltration (NF) is an advance membrane filtration technique, as low pressure driven membrane with molecular weight cut-off in the range 200 –1000 Da have been widely used in the studies for the separation of different types of salts and heavy metal. It can be operated at the pressure ~0.5–2 MPa. NF membrane possesses electrostatic charge on surface for better selectivity of ion together than size selectivity. Thus, the main separation mechanism of NF membrane filtration in removal of pollutants is charge effect and size exclusion (Hosseini et al., 2017; Otero-Fernandez et al., 2017; Coman et al., 2013). In a study, polyether-imide-thin film nanocomposite nanofiltration membrane was fabricated for the separation of $CrSO_4$ and some other pollutant and reported 81% removal of $CrSO_4$ from water (Bandehali et al., 2020). In another research, NF membrane AFC80 reduced the $Cr_{(VI)}$ concentration below WHO standard permissible limit of drinking water (Otero-

Fernandez et al., 2017). Basaran et al. (2016) investigated the Ni^{2+} and Cr^{6+} rejection efficiency of commercial NF90 and NF270 membrane. They reported 99.2 and 96.5% rejection of Ni^{2+} and Cr^{6+} by NF90 membrane and 98.7 and 95.7% by NF270 membrane respectively. NF300 and PN40 membrane also has high rejection competence for $Cr_{(VI)}$ which are able to remove 97 % and 88% respectively (Gaikwad et al., 2017).

Reverse osmosis is the trendiest technique. This technique is being applied presently for treatment of drinking water and can be also used for treatment of wastewater. RO is the pressure driven technique. Through RO membrane, water molecule easily passed while ionic compounds are retained (Fig. 3.2a). The pore size of RO membrane can be 0.1nm or less. RO can be applied to treat contaminated water containing metal concentration in the range of micromole to mille mole (Coman et al., 2013). Gaikwad and Balomajumder (2017) studied $Cr_{(VI)}$ rejection efficiency of sheet polyamide RO membrane and reported 99.97% rejection of $Cr_{(VI)}$ from binary solution of $Cr_{(VI)}$-fluoride. In a research, two types of membrane namely sea water high rejection membrane (SWHR-membrane) and high rejection brackish water membrane (AG-membrane) was employed for removal of $Cr_{(VI)}$ and 91% rejection was recorded with AG membrane (Çimen et al., 2014). In low pressure reverse osmosis process associated with EDTA complexation using commercial flat membrane of polyamide, 99% $Ni_{(II)}$ removal was recorded (da Silva et al., 2015). Ipek (2005) also found high rejection efficiency of $Ni_{(II)}$ and other pollutant using RO membrane.

Many others types of filtration membrane including forward membrane, direct membrane, adsorptive membrane, nano-fibrous membrane, ceramic membrane, chemically modified microporus membrane, ion exchange membrane etc. have been investigated by many researcher and also showed high rejection/removal efficiency for different types of pollutant including $Ni_{(II)}$ and $Cr_{(VI)}$ (Taha et al., 2012; Daraei et al., 2013; Pagana et al., 2008; Coman et al., 2013; Hosseini et al., 2017). These membrane become an option to chemical and environmental engineers for $Ni_{(II)}$ and $Cr_{(VI)}$ contaminated water treatment.

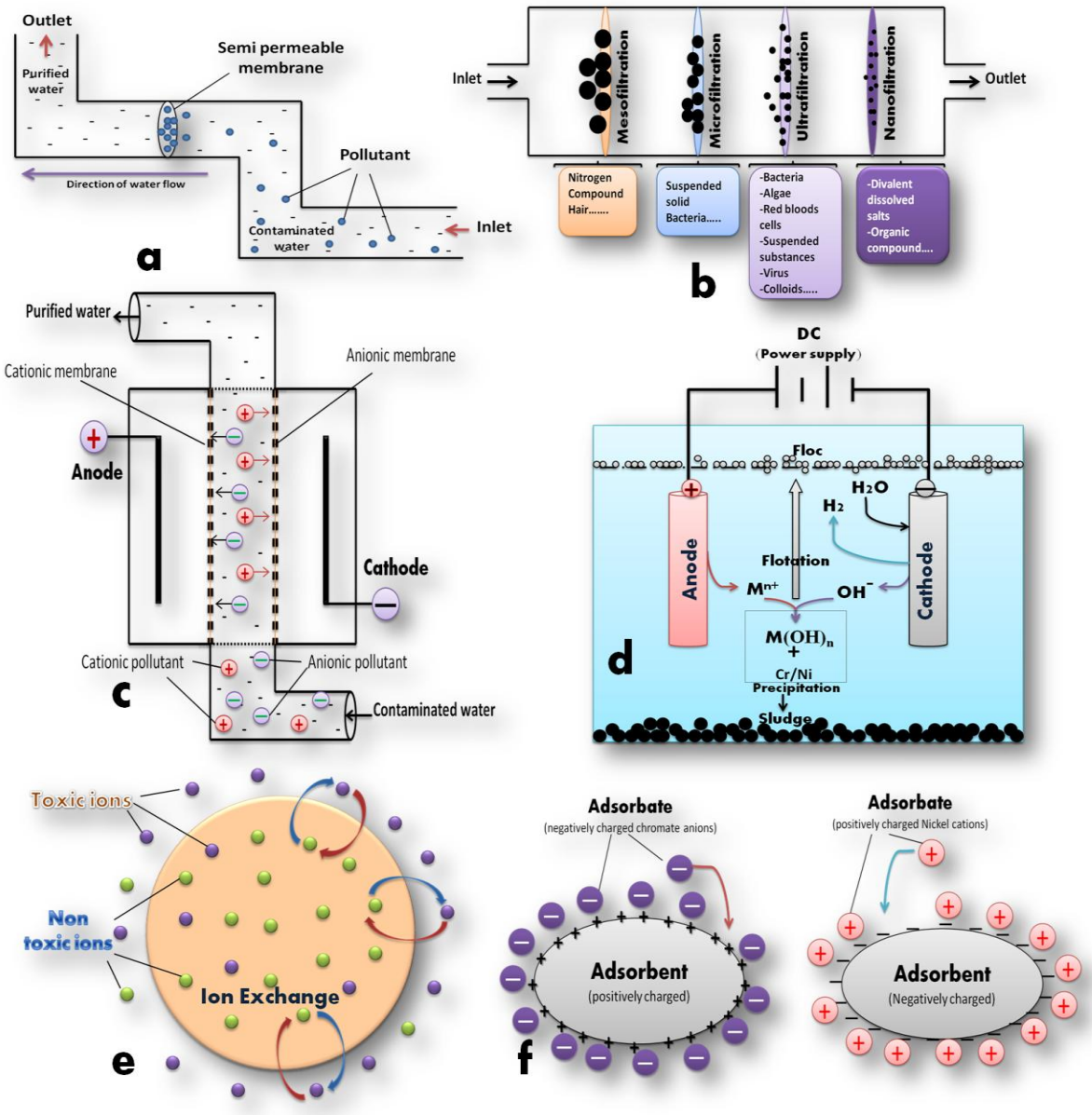

Fig. 3.2. Different types of treatment strategies for $Cr_{(VI)}$ and $Ni_{(II)}$ contaminated industrial wastewater. (a) reverse osmosis, (b) different filtration methods, (c) electrodialysis, (d) electrocoagulation/electroflotation, (e) Ion exchange and (f) Adsorption.

3.3.3 Adsorption

Presently many types of material have been investigated for removal of contaminants from industrial wastewater. Adsorption is mainly preferred due low cost, easy operation and simple design. Adsorption is basically physical phenomenon where molecules adhere on the surface of solid material via physical forces or

chemical bond. The substance that adsorb on the solid surface is known as adsorbate and the solid surface where phenomenon occur is called adsorbent. There are many types of material including activated carbon, nano, micro and meso particle, agro waste biochar, agro-waste ash, low cost agriculture originated material, zeolite, nanofibers, nanotubes, nanocomposites, nanoparticle assisted membrane etc. have been reported for their high potential to remove diverse range of organic and inorganic contaminants including $Cr_{(VI)}$ and $Ni_{(II)}$ (Table 3.1; Fig. 3.2f).

3.3.3.1 Biochar

Biochar is by-product of pyrolysis of woody organic matter. Mostly it contains high lignin content when prepared at low temperature (200-400 °C) and with increase in the pyrolytic temperature, the content of ash also increases while the amount of biochar decreases (Georgieva et al., 2020; Wang et al., 2019). Biochar has high adsorption efficiency for pollutants due to presence of adsorptive active surface functional group, high surface area and present surface charge on the biochar (Table 3.1) (Bogusz et al., 2017; Fan et al., 2019). However, the adsorption properties of biochar vary with feed stock material, pyrolysis temperature, particle size, nature of pollutant, pH of the medium, interaction rate etc. (Fan et al., 2019; Wang et al., 2019; An et al., 2019). Most of the studies has focuses on production with minimal cost for successful removal of contaminants hence, the researcher have utilizes many types of agricultural residue, municipal waste, industrial waste etc. for the preparation of cost effective biochar for the removal of various types of contaminant as well as $Cr_{(VI)}$ and $Ni_{(II)}$. In some studies mineral rich ash prepared at high pyrolysis temperature (above 700 °C) have been utilized for removal of $Cr_{(VI)}$ and $Ni_{(II)}$ from aqueous conditions and effective removal of $Ni_{(II)}$ and $Cr_{(VI)}$ was reported. Qu et al. (2020) used KOH to amplify the surface area of biochar prepared from corn straw by two steps pyrolysis and employed for removal of $Cr_{(VI)}$. They reported that after activation of biochar, the adsorption ability of biochar was raised and was 116.97 mg/g. An et al. (2019) studied the $Ni_{(II)}$ removal capacity of peanut shell derived biochar activated with $KMnO_4$ and KOH. They reported 87.15 mg/g of Ni(II) removal and removal was driven by co-precipitation and complexation (chemi-sorption). Number of studies have also explored several types of activated and without activated biochar for efficient removal of Cr(VI) and Ni(II) from contaminated industrial wastewater (Bogusz et al., 2017; Fan et al., 2019; Georgieva et al., 2020; Gazi et al., 2018). However, activation of

biochar is another way of the biochar utilization with high removal efficiency for pollutants that has taken the attention of the research community.

3.3.3.2 Activated carbon

Activated carbon is carbon rich material prepared by physicochemical pre-treatment of feed stock and post-treatment of biochar. In addition of pyrolysis of feed stocks, hydrothermal carbonization is also claimed as effective method for preparation of carbon rich material and obtained product from hydrothermal process is known as hydrochar (Wong et al., 2018). In recent days, microwave assisted preparation of activated carbon is also reported in many studies (Ao et al., 2018). Frequently exploited feed stocks for the preparation of activated carbon for wastewater treatment are coal, coconut shell, lignite and woods (Demirbas, 2009; Wong et al., 2018). Most of the time, different types of chemical such as KOH, zerovalent, iron oxide etc. are used for activation of carbon rich material hence, it is termed as activated carbon (Basta et al., 2009). Acid-base treatment has been reported by several researchers that enhance the adsorption characteristic of activated carbon (Wong et al., 2018; Kan et al., 2017). Adsorption property of activated carbon is basically owing to its high porosity and large surface area together with surface chemistry of adsorptive functional group. The activated carbon has been reported in many studies for effective removal of $Ni_{(II)}$ and $Cr_{(VI)}$ from contaminated aqueous medium (Table 3.1). Tu et al. (2020) conducted an study using Bermuda grass derived activated carbon in the removal of $Cr_{(VI)}$ and they reported 403.23 mg/g of adsorption capacity for $Cr_{(VI)}$. However, the removal was happened via reduction and precipitation in addition of adsorption. In a study, carbon rich material was extracted from waste lignocellulosic material of *Ziziphus jujuba* cores and activated with rubidium carbonate to enhance the surface area. The activated carbon showed high removal efficiency for $Cr_{(VI)}$ which was 62% (Benturki et al., 2018). Effective removal of $Ni_{(II)}$ was also found with graphite derived activated carbon functionalized by Tetraethylenepentamine (El-Magied et al., 2018). In a research, Onundi et al. (2010) studied the $Ni_{(II)}$ removal ability of granular activated carbon prepared from shell of palm kernel and reported 55% $Ni_{(II)}$ removal. $Cr_{(VI)}$ and $Ni_{(II)}$ removal efficiency of activated carbon have been reported in many studies with successful removal (Chen et al., 2018; Krishnan et al., 2011; Niazi et al., 2018; Maneechakr and Karnjanakom, 2017).

Table 3.1. $Cr_{(VI)}$ and $Ni_{(II)}$ experimental conditions, removal efficiency and mechanism by different types of adsorbent

Adsorbent	$Cr_{(VI)}/Ni_{(II)}$	Concentration (mg/L), dose (g/L), pH, temperature (° C), time (min) and shaking rate (rpm)	Adsorption capacity	Mechanism	Fitted Kinetic model	Isotherm model	References
Biochar							
Rice straw biochar prepared at 400 °C	$Ni_{(II)}$	20, 1.0, 5.5, 25, 1440 and 200	27.3 mg/g	Cation exchange, precipitation, adsorption and surface complexation	Pseudo-second order	Langmuir model	Deng et al. (2019)
Rice straw biochar prepared at 700 °C	$Ni_{(II)}$	20, 1.0, 5.5, 25, 1440 and 200	54.6 mg/g	Cation exchange, precipitation, adsorption and surface complexation	Pseudo-second order	Langmuir model	Deng et al. (2019)
pine cone biochar –Na-alginate hybrid adsorbent	$Ni_{(II)}$	25, 1.0, 5.5, 25, 120, and 130	15.82 mg/g	Adsorption	Pseudo-first, Pseudo second order and Weber – Morris model	Langmuir model	Biswas et al. (2019)
Date fruit biochar pretreated with HCl	$Ni_{(II)}$	4.0 (mmol/L), 10, 6.0, 23, 1440 and 30	0.34 mmol/g	C=C, C=O, C-O, and phenolic groups mediated adsorption	Pseudo-second order	Sips model	Mahdi et al. (2019)
distillers grains (DG)-biochar	$Cr_{(VI)}$	50, 1.25, 2.0, 25, 1440 and 300	8.1 mg/L	Adsorption	Pseudo-second order	Langmuir	Lian et al. (2019)
Phosphogypsum modified (PM)-biochar	$Cr_{(VI)}$	50, 1.25, 2.0, 25, 1440 and 300	38.2 mg/L	Adsorption	Pseudo-second order	Freundlich model	Lian et al. (2019)
Wheat straw biochar	$Cr_{(VI)}$	100, 1.25, 5.6,	2.4 mg/L	Adsorption	-	-	Zhang et al.

		room temperature, 1440 and 160					(2019)
Wheat straw biochar-nZVI	$Cr_{(VI)}$	100, 1.25, 5.6, room temperature, 1440 and 160	8.06 mg/L	Adsorption	-	-	Zhang et al. (2019)
Sweet lime peels biochar	$Cr_{(VI)}$	20, 0.50, 2.0, 30, 720 and 120	9.92 mg/L	O-H, C=O, COOH participated in $Cr_{(VI)}$ adsorption	pseudo second order	Langmuir	Shakya et al. (2019)
Activated carbon							
Banana peels hydrothermally prepared activated BAC600-H	$Ni_{(II)}$	100, 1.0, 6.0, 20, 1440 and 150	78%	Electrostatic attraction b/w COO^{-} and Ni^{2+}	-	Langmuir – Freundlich model	Bibaj et al. (2019)
Banana peels pyrolysed activated carbon BAC600-P	$Ni_{(II)}$	100, 1.0, 6.0, 20, 1440 and 150	84%	Electrostatic attraction b/w COO^{-} and Ni^{2+}	-	Langmuir – Freundlich model	Bibaj et al. (2019)
Activated carbon prepard from *Phragmites Australis*	$Ni_{(II)}$	30, 0.6, 6.0, 25, 160 and 125	12.3 mg/g	Complexation by Oxygen containing functional group, electrostatic attraction ion exchange by deprotonated Phenolic and Carboxyl group	pseudo second order	Langmuir	Yu et al. (2019)
Activated carbon prepared from *Phragmites Australis* activated by manganese formate hydrate	$Ni_{(II)}$	30, 0.6, 6.0, 25, 160 and 125	20.9 mg/g	Complexation by Oxygen containing functional group, electrostatic attraction ion exchange by deprotonated Phenolic and Carboxyl group	pseudo second order	Langmuir	Yu et al. (2019)
Modified Powdered activated carbon with 15% nitric acid	$Ni_{(II)}$	2, 1.0, 7.0, room temperature, 120, and 120	98%	Deprotonated COOH and PhOH cause electrostatic attraction with Ni2+	Pseudo-second order	Langmuir model	Su et al. (2019)
ZnO-tetrapods/activated	$Cr_{(VI)}$	10, 2, 2, room	96%	Electrostatic attraction	Pseudo-	-	Sharma et al.

carbon (ZAC) nanocomposite		temperature, 420, 240			second-order and Elovich model		(2019)
ZnO-nanoparticles loaded parthenium weed activated carbon (ZnONPs-PWAC)	$Cr_{(VI)}$	50, 1.0, 3, -, 90, -	99%	Electrostatic interaction and chemical reaction	-	-	Kamaraj et al. (2020)
Polysulfide rubber (PSR) coated granular activated carbon	$Cr_{(VI)}$	10, 11.0, 4.0, 22, 2880, 40	100%	diffusion, electrostatic attraction by protonated polysulfide	Pseudo-second order	Langmuir model	Mortazavian et al. (2019)
Nano-adsorbent							
Fe_3O_4 nanoparticles incorporated with hydroxyapatite nanorods	$Ni_{(II)}$	10, 2.0, 7.0, room temperature, 1440, -	94%	Surface complexation, calcium exchange, electrostatic attraction and precipitation	Pseudo-second order	Freundlich model	Thanh et al. (2018)
Polyacrylonitrile (PAN)–titanium oxide (TiO_2) nanofiber functionalized with aminopropyltriethoxysilane (APTES)	$Ni_{(II)}$	100, 1.0, 5.0, 25, 300, -	30 mg/g	Complexation and Electrostatic attraction	Double-exponential model	Langmuir isotherm	Mokhtari and Keshtkar (2016)
sodium dodecyl sulphate coated magnetite nanoparticles	$Ni_{(II)}$	10, 1.0, 6.0, 25, 5,	69.80%	Adsorption	-	-	Adeli et al. (2017)
Magnetic magnetite (Fe_3O_4) nanoparticles	$Cr_{(VI)}$	25, 1.0, 2.0, 25 and 1440, -	9.69 mg/L	electrostatic attraction	pseudo-second-order	Sips and Langmuir	Rajput et al. (2016)
Magnetic nanoparticle-multiwalled carbon nanotubes composites	$Cr_{(VI)}$	5, 1.0, 2.0, 25, 240 and 150	95%	Adsorption, intraparticle diffusion	Pseudo-second-order	Langmuir	Lu et al. (2017)
carbonaceous nanofi bers	$Cr_{(VI)}$	0.3 mmol, 0.2, 30, -, -	90%	Reduction, adsorption		Langmuir	Cheng et al. (2016)
Zeolite							

Zeolite P hydrothermally synthesized from C Fly ash	$Ni_{(II)}$	100, 2, -, 480 and 150	32 mg/g	Adsorption	first-order empirical kinetic model	Langmuir	Liu et al. (2019a)
Zeolite 3A modified with $Mg(OH)_2$	$Ni_{(II)}$	200, 12, 7.0, 300, -	95%	Adsorption	pseudo-second-order kinetic model and intraparticle diffusion model	Freundlich	Pahlavanzadeh and Motamedi (2020)
Core-Double-Shell Structured Magnetic Polydopamine@Zeolitic Idazolate Frameworks- 8 Microspheres	$Cr_{(VI)}$	30, 0.2, 5.0, 20, 960, -	82%	Reduction, chelation, electrostatic attraction	pseudo-second-order kinetic model	-	Zhu et al. (2017)
Zeolitic imidazolate framework-8	$Cr_{(VI)}$	5, 20, 7.0, -, 60, -	57%	electrostatic attraction	-	Langmuir, Sips and Toth	Shahrak et al. (2017)

3.3.3.3 Nanomaterial

The pollutant removal performance of different types of nano-scaled material is reported in many studies. The materials, which size is less than 100 nm are considered as nanomaterial which includes nano-particle, nanofiber, nanosheet, nanotubes, nano-composite, etc. (Table 3.1) (Cai et al., 2019; Agarwal et al., 2018; Adeli et al., 2017; Mokhtari and Keshtkar, 2016; Cheng et al., 2016; Lu et al., 2017; Samuel et al., 2019). Nanomaterial have been extensively explored for removal of $Cr_{(VI)}$, $Ni_{(II)}$ and other inorganic and organic pollutants. Agarwal et al. (2018) synthesized γ-alumina nanoparticles and multiwalled carbon nanotubes for $Ni_{(II)}$ removal and reported 99.41 and 87.65 % removal respectively from aqueous medium. The sodium dodecyl sulphate-coated Fe_3O_4 nanoparticles (SDS–Fe_3O_4NPs) can remove 41.2 mg/g of $Ni_{(II)}$ via adsorption (Adeli et al., 2017). Liu et al. (2017) synthesized birnessite/carbon nanotubes (HB/CNTs) nanocomposites for removal of Ni^{2+} and Zn^{2+} from wastewater and found highest removal ability of 89.5 and 96.6 mg/g. While, polyacrylonitrile (PAN)–titanium oxide (TiO_2) nanofiber activated with aminopropyltriethoxysilane (APTES) removed 147 mg/g of $Ni_{(II)}$ (Mokhtari and Keshtkar, 2016) and green extract capped superparamagnetic iron oxide nanoparticles showed 227.20 mg/g of $Ni_{(II)}$ removal. Successful removal of $Cr_{(VI)}$ have been also explored in different study using various types of nanomaterial. Some of the utilized nanomaterials are bifunctional MOF/Titanate nanotube composites (Wang et al., 2019), chitosan grafted graphene oxide (CS-GO) nanocomposite (Samuel et al., 2018), magnetic iron oxide nanoparticle-multiwalled carbon nanotube composites (Lu et al., 2017), chitosan-modified multi-walled carbon nanotube composite (Huang et al., 2018a), graphene/SiO_2@polypyrrole nanocomposites (Fang et al., 2018), carbonaceous nanofibers (Cheng et al., 2016), chitosan/MWCNT/Fe_3O_4 composite nanofibers (Beheshti et al., 2015) that showed high efficiency for evacuation of $Ni_{(II)}$ and $Cr_{(VI)}$.

3.3.3.4 Zeolite

Zeolite is the crystalline, porous structure composed of silicon, allumium and oxygen as aluminosilicate ($[AlO_4]^{4-}$ and $[SiO_4]^{4-}$) on three dimensional networks which form open frame work with cations positioned cavities and channels (Abdullahi et al., 2017; Zhu et al., 2017). The cations neutralize the negative charge on the lattice

and add unique features like catalytic and ion-exchange property on zeolites or similar materials (Table 3.1) (Xu et al., 2008; Abdullahi et al., 2017). An important characteristic of zeolite is that their frame works basically build up of four co-ordinated atoms forming tetrahedral (Baerlocher et al., 2007). Zeolite is also some time referred as molecular sieve. Numbers of zeolite are known presently but most of them are synthesized from different types of materials including agro-waste ash, fly ash, Kiolinite, Bauxite residue, glass and alum sludge (Abdullahi et al., 2017; Collins et al., 2020; Liu et al., 2018; Shahrak et al., 2017). Shahrak et al. (2017) synthesized zinc-based zeolitic imidazolate framework materials (ZIF-8) for its application in $Cr_{(VI)}$ removal. They recorded 70% removal efficiency of ZIF-8 for $Cr_{(VI)}$. Zeolite P synthesized by hydrothermal process from fly ash for removal of $Ni_{(II)}$ and achieved 77.0 mg/g of $Ni_{(II)}$ removal (Liu et al., 2019a). In another work, Liu et al. (2018) synthesized zeolite Y using the same stock material by fusion-hydrothermal method and successful removal of $Ni_{(II)}$ and $Cu_{(II)}$ was recorded. Effective removal of $Cr_{(VI)}$ and $Ni_{(II)}$ is also reported in many other studies using synthesized zeolite (Zhu et al., 2017).

3.3.4 Photocatalysis

Photocatalysis is one of the advance treatment technique where semiconductors such as TiO_2 is used for photocatalytic degradation (oxidative reduction) of pollutants from wastewater. In the photocatlytic reaction, when UV-A (315-400 nm) or visible light fall on the semiconductors surface, the electron of the valence bond gain energy from absorbed photon and become excited, as a result budge to conduction band (Gopinath et al., 2020). This incident creates positive (Hole; h^+) as well as negative charge (electron; e^-) on the surface of semiconductors (Eq. 9). In case of $Cr_{(VI)}$, it reduces in its trivalent form $Cr_{(III)}$ by one electron transfer from conduction band via making charge transfer complex (semiconductor-$Cr_{(VI)}$ complex for Ex. $Cr_{(VI)}$-TiO_2 complex) for fast photocatalytic reduction (Eq. 10-12) (Kretschmer et al., 2019). While, attack of holes to absorb water produces hydroxyl group produces $OH^{\bullet}$, H_2O_2, superoxide radical ($O_2^{\bullet-}$) as proposed in several studies (Eq. 13-16) (Kretschmer et al., 2019; Chen et al., 2017a).

$$TiO_2 + h\upsilon \text{ (photon)} \rightarrow e^- \text{ (electron)} + h^+ \text{ (hole)} \quad (9)$$

$$Cr_{(VI)} + e^- \rightarrow Cr(V) \quad (10)$$

$$Cr(V) + e^{-} \rightarrow Cr_{(VI)} \quad (11)$$

$$Cr_{(VI)} + \rightarrow Cr_{(III)} \quad (12)$$

$$H_2O + h^{+} \rightarrow OH^{\bullet} \quad (13)$$

$$OH^{-} + h^{+} \rightarrow OH^{\bullet} \quad (14)$$

$$2OH^{\bullet} \rightarrow H_2O_2 \quad (15)$$

$$H_2O_2 + h+ \rightarrow HO_2^{\bullet} + H^{+} \quad (16)$$

Presently, this technique is trending and taken lot of attention of the researcher to develop effective photocatalyst. Number of effort have been made for synthesizing photocatalyst for reduction of $Cr_{(VI)}$. For example, Chen et al. (2017a) designed and synthesized TiO_2 by thermal hydrolysis of titanium tetra chloride ($TiCl_4$) under the presence of diethylene glycol (DEG). Further they found that DEG was chemically bonded on TiO_2 and increased the internal hole-scavenging consequences and electron releasing ability of the material. In $Cr_{(VI)}$ reduction assessment, the synthesized TiO_2 nanocrystal showed 95% $Cr_{(VI)}$ reduction potential up to three cycle. In a research, nontoxic Nitrogen−sulfur codoped carbon dots (NSCD) was fabricated by single-step microwave-assisted method. The synthesized NSCD successfully used for photocatalytic reduction of $Cr_{(VI)}$ and showed high $Cr_{(VI)}$ reduction efficiency (Saini et al., 2020). However, the synthesis of photocatalyst by physicochemical method has some disadvantages. Thus, to get greener way for synthesis of photocatalyst many researches have been conducted. In most studies plant extract were used for the green synthesis of photocatalyst (Goutam et al., 2018; Padhi et al., 2017; Khosravi et al., 2019; Esfahani et al., 2020) whereas in some of the studies microorganism were applied (Chatterjee et al., 2020). The green synthesize photocatalyst also showed high efficiency in the reduction of $Cr_{(VI)}$ from aqueous medium. Padhi et al. (2017) hydrothermally synthesized photocatalytically stable and magnetically separable g-Fe_3O_4/RGO nanocomposite with *Averrhoa carambola* leaf extract. *Averrhoa carambola* leaf extract changed the structural, electronic and optical features of the Fe_3O_4 nanoparticle and at room temperature g-Fe_3O_4/RGO nanocomposite showed high photocatalytic $Cr_{(VI)}$ (97%) reduction performance. Similarly, in another work, *Jatropha curcas* L. was used for the synthesis of TiO_2 nanoparticle which showed

efficient photocatalytic $Cr_{(VI)}$ reduction and COD removal capability (Goutam et al., 2018).

3.3.5 Electrochemical method

3.3.5.1 Electrocoagulation

Electrocoagulation (EC) is different from conventional coagulation, has wide application for the treatment of wastewater. EC unit consist of electrolytic cell that contain anode and cathode metal electrodes and tenuously connected with direct current (DC) control source (Fig. 3.2d) (Ye et al., 2016). EC is a complex successive process that comprises the release of cations from "Sacrificial electrode", hydrogen generation at the cathode and coagulant development by aggregation of released cations in the system solution. The important stage in EC is the encroachment of coagulant. It is advancement in the area of wastewater treatment that colonizes the workplace of floatation/coagulation and electrochemistry. EC can remove many of the pollutants such as suspended solid, dissolve organic matter, heavy metal, microorganism etc. from wastewater. In the process, the adsorption effect of flocs escorted by many mechanism such as adsorption, coagulation, electrophoresis, electrostatic attraction, electro-oxidation, electro-deposition, electrical neutrilization and co-precipitation of the pollutants (Un et al., 2017; Ye et al., 2016; Lu et al., 2016; GracePavithra et al., 2019). The pollutants removal effectiveness of EC depends upon turbidity, conductivity and suspended solid of the wastewater, and high electricity and skilled man-power requirement become major disadvantage of electrocoagulation. Electrocoagulation process deals with Faraday Law. According to Faraday Law the number of moles transmitted in an electrochemical process is specifically equivalent to quantify of charge delivered between the elctrodes (GracePavithra et al., 2019). In an investigation, Un et al. (2017) studied the competence of iron (Fe) electrode for evacuation of $Cr_{(VI)}$ from electroplating wastewater which contains 1000 mg/L of $Cr_{(VI)}$. Under the optimum operational parameters current density 20 mA /cm2, 0.05 M NaCl electrolyte and pH 2.4, the removal efficiency of iron electrode was 100%. The resulting sludge from EC process was also utilized for ceramic pigment synthesis which was black and reddish brown color in transparent glaze. Further they stated that this process can be applied for $Cr_{(VI)}$ removal from wastewater with zero waste production. Lu et al. (2016) also studied iron electrode for removal of $Cr_{(VI)}$. They

reported that the maximum removal competence of $Cr_{(VI)}$ from water was highest at lower pH (2.0) and with rise in the pH of the system solution, the residual amount of $Cr_{(VI)}$ in the medium was increased. They suggested that removal of $Cr_{(VI)}$ was done via reduction in its trivalent $Cr_{(III)}$ form by release of Fe^{2+} ion subsequently precipitation, co-precipitation and also specific adsorption on iron hydroxide. However, the current density, electrolytic time and type of used electrode also affected the removal of $Cr_{(VI)}$. In a research, Liu et al. (2017a) utilizes the aluminium/iron/carbon (Al/Fe/C) hybrid electrodes for $Ni_{(II)}$ and fluoride (F) removal from wastewater generated by real flue gas desulfurization in coal-fired power plant. The affecting parameters such as pH of the solution, applied current density and time were considered. It was found that with increase in time and current density removal of $Ni_{(II)}$ and F positively affected and maximum removal with a current density of 5.00 mA/cm2 in 25 min at pH 4 and was 98% and 86% respectively.

Presently, In the EC process many types of electrode are applied for treatment of wastewater. Aluminium and iron electrode are the two most trending electrode and are frequently studied. In the acidic and basic medium the iron electrode differently act with two types of mechanism. When iron electrode used in acidic medium, the following mechanism happened on cathode and anode (Ye et al., 2016; Lu et al., 2016):

Anode

$$4Fe_{(S)} \rightarrow 4\ Fe^{2+}_{(aq)} + 8e^{-} \quad (17)$$

$$4Fe^{2+} + 10H_2O + O_2 \rightarrow 4Fe(OH)_{3(S)}\downarrow + 8H^{+}_{(aq)} \quad (18)$$

Cathode

$$8H^{+}_{(aq)} + 8e^{-} \rightarrow 4H_{2(g)}\uparrow \quad (19)$$

Overall

$$4Fe_{(S)} + 10H_2O_{(l)} + O_{2(g)} \rightarrow 4Fe(OH)_{3(S)} + 4H_{2(g)}\uparrow \quad (20)$$

While, in basic condition the following mechanisms occur in the electrolytic cell:

Anode

$$Fe_{(S)} \rightarrow 4Fe^{2+}_{(aq)} + 2e^{-} \quad (21)$$

$$Fe^{2+}_{(aq)} + 2OH^{-}_{(aq)} \rightarrow Fe(OH)_{2(S)}\downarrow \quad (22)$$

Cathode

$$2H_2O + 2e^{-} \rightarrow H_{2(g)}\uparrow + 2OH^{-}_{(aq)} \quad (23)$$

Overall

$$Fe_{(S)} + 2H_2O_{(l)} \rightarrow Fe(OH)_{2(s)}\downarrow + H_{2(g)}\uparrow \quad (24)$$

The $Fe(OH)_{n(S)}$ precipitate in wastewater as gelatinous suspension can drive out the $Cr_{(VI)}$ and $Ni_{(II)}$ from solution by electrostatic attraction or complexation, subsequently coagulation. The released ferrous ion from the electrode reduces the $Cr_{(VI)}$ into $Cr_{(III)}$ at basic and acidic condition both but precipitation of $Cr_{(III)}$ and $Ni_{(II)}$ occur in basic condition as shown in following reactions (Liu et al., 2017; Un et al., 2017):

$$CrO_4^{2-}{}_{(aq)} + 3Fe^{2+}_{(aq)} + 4H_2O_{(l)} + 4OH^{-}_{(aq)} \rightarrow 3Fe(OH)_{3(S)}\downarrow + Cr(OH)_{3(S)}\downarrow \quad (25)$$

$$xNi^{2+}_{(aq)} + Fe_n(OH)_{3n(S)} \leftrightarrow Fe_n(OH)_{3n-x}Ni_{x(S)}\downarrow + xOH^{-} \quad (26)$$

$$Ni^{2+}_{(aq)} + 2OH^{-}_{(aq)} \rightarrow Ni(OH)_{2(S)}\downarrow \quad (27)$$

Couple of reaction also occurs with using aluminium (Al) electrode and it also differently work in the basic and acidic medium. Aluminium ion generated from Al-electrode (anode) and form hydroxylated species of Al. In basic condition, following mechanism happen in electrolytic cell (Al-Qodah and Al-Shannag 2017):

Anode

$$Al_{(S)} \rightarrow Al^{3+}_{(aq)} + 3e^{-} \quad (28)$$

Cathode

$$3H_2O_{(l)} + 3e^{-} \rightarrow 1.5H_{2(g)} + 3OH^{-}_{(aq)} \quad (29)$$

Overall

$$Al_{(S)} + 3H_2O_{(l)} \rightarrow Al(OH)_{3(S)}\downarrow + 1.5H_{2(g)}\uparrow \quad (30)$$

In acidic medium the reactant and product were the same but reaction happen differently as follows:

Anode

$$Al_{(S)} \rightarrow Al^{3+}_{(aq)} + 3e^{-} \quad (31)$$

$$Al^{3+}_{(aq)} + 3H_2O_{(l)} \rightarrow Al(OH)_{3(S)}\downarrow + 3H^{+}_{(aq)} \quad (32)$$

Cathode

$$3H^{+}_{(aq)} + 3e^{-} \rightarrow 1.5H_{2(g)}\uparrow \quad (33)$$

Overall

$$Al_{(S)} + 3H_2O_{(l)} \rightarrow Al(OH)_{3(S)}\downarrow + 1.5H_{2(g)}\uparrow \quad (34)$$

In above reaction produced Al^{3+} react with OH^{-} and generate $Al(OH)_{3(s)}$, the present $Ni_{(II)}$ and $Cr_{(VI)}$ and other pollutant in the wastewater adsorbed on $Al(OH)_{3(s)}$. In an investigation, Heidmann and Calmano (2008) studied the effect of removal efficiency of Al-electrode in removal of different heavy metal. They also considered the parameters like initial metal ion concentration and applied current density in the study. It was found in the study that rise in the initial concentration of $Ni_{(II)}$ and other metal did not affect their removal rate, but increase in $Cr_{(VI)}$ concentration increases its removal rate. They stated that, all the tested metal other than $Cr_{(VI)}$ have same electrochemical behavior, get hydrolyzed and co-precipitated as hydroxide while, $Cr_{(VI)}$ first reduced to $Cr_{(III)}$ subsequently co-precipitated as $Cr_{(III)}$ hydroxide. They also found that increased current density enhances the $Cr_{(VI)}$ removal rate but reduces the efficiency of Al-electrode but highly efficient for $Ni_{(II)}$ removal. In another investigation, Zongo et al. (2009) also found the same problem in $Cr_{(VI)}$ removal by Al-electrode. While, successful and efficient removal of $Cr_{(III)}$ and COD (chemical oxygen demand) was reported by Elabbas et al. (2016) using Al-electrode. To increase the $Cr_{(VI)}$ removal efficiency of Al-electrode in electrocoagulation process, hybrid technologies and pairship with other electrode has been reported in some studies (Liu et al., 2017; Akbal and Camci, 2011). Akbal and Camci (2011) applied pair of aluminium-iron electrode for removal of Ni, Cr and other metal and at pH 3.0 and a current density of 10 mA/cm^2 in electrocoagulation time of 20 min, the removal rate of Ni and Cr was 100%. In another investigation, high removal efficiency was

recorded with Al-Titanium composite electrode and authors stated that Al-Ti composite electrode can be applied in $Cr_{(VI)}$ removal that will not change in color index of the solution (Li et al., 2019b).

The development and study on some other types of electrode were also carried out by many researchers. In an experiment, Rana-Madaria et al. (2005) tested the carbon aerogels as an electrode for the $Cr_{(VI)}$ decontamination from water. In this study, $Cr_{(VI)}$ concentration was reduced from 2 to 0.008 mg/L with a removal efficiency of 99.6%. Velasco et al. (2016) studied titanium and graphite electrodes for the reduction of $Cr_{(VI)}$ at steady state potential employing electrochemical reactor. With change in the hydrogen and oxygen and reducing the current efficiency, the $Cr_{(VI)}$ reduction was reported. A research was conducted using cylindrical graphite as cathode and packed-bed made up of iron scrap used as anode. This arrangement was applied for $Ni_{(II)}$-EDTA removal. Optimum condition for maximum removal of $Ni_{(II)}$-EDTA was 0.5 A (applied current), air-purged rate 0.2 L min-1, initial pH 3.0, temperature of 313 K, anode packed density of 400 kg m^3 and time of 30 min. Gaikwad and Bolamajumdar (2017) derived activated carbon from *Limonia acidissima* shells and prepared carbon electrode. By utilizing the prepared carbon electrode successful reduction of $Cr_{(VI)}$ and removal of F was reported simultaneously. However, this study is different from EC process, but providing an insight to move greener way to synthesize new bio-based-electrode for such type of treatment processes. The authors concluded that it will be useful for $Cr_{(VI)}$ and F removal from less contaminated water (Gaikwad and Bolamajumdar, 2017).

3.3.5.2 Electrodialysis

Electrodialysis (ED) method is broadly used for removal and recovery of ionic species from contaminated water (Fig. 3.2c). It is a separation process where ions transport through the ionic-membrane from the solution by electrostatic force generated by the electric potential between anode and cathode (dos Santos et al., 2019). Solid membrane application have been extensively studied for heavy metal removal including $Cr_{(VI)}$ and $Ni_{(II)}$. Using Dowex HCR-S ion exchange resin in ED process, $Ni_{(II)}$ efficient recovery was observed from the 1 M $NiSO_4$ solution but other ion exchange membrane such Dowex MSC- 1, Purolite C 100E and KU 2-8 was less effective (Dzyazko et al., 2004). In the recent years, liquid membrane integration with

ED process is trending. In a study, a liquid membranes having tri-n-octylamine or trialkylbenzylammonium chloride in 1,2-dichloroethane was used for separation of $Ni_{(II)}$ by galvanostatic electrodialysis process. The effect of electrodialysis parameters were studied and at optimum conditions, with rise in the concentration of $Ni_{(II)}$ the separation was increased (Sadyrbaeva, 2015). In another study, ionic liquid-based polymer inclusion membrane (PIM) and integrated ED was successfully applied for $Cr_{(VI)}$ separation (Li et al., 2020). Similarly, Wang et al. (2020) also studied poly vinylidene fluoride-co-hexafluoropropylene) (PVDF-HFP) in PIM and found higher $Cr_{(VI)}$ transport with PVDF-HFP in comparison to cellulose triacetate (CTA) and poly (vinyl chloride) (PVC) based membrane.

3.3.5.3 Electrodeioization

Electrodeionization (EDI) process combines the resin and ion-exchange membrane and removes ions from the solution by applying the electricity between cathode and anode (Coman et al., 2013; GracePavithra et al., 2019). EDI is basically a hybrid process of ion exchange and the electrodialysis. Combination of ED and ion exchange membrane resin hybrid process employed for recovery of $Ni_{(II)}$ from contaminated solution and successfully demonstrated the $Ni_{(II)}$ recovery using Amberjet 1200 H cation-exchange resin (Gabli et al., 2020). Zhang et al. (2014) applied ion exchange resin in the EDI process for continuous recovery and removal of $Cr_{(VI)}$ and $Cr_{(III)}$ and reported high removal efficiency with very low electricity consumption. In a study, using an integrated two-stage electrodeionization (EDI) process, $Ni_{(II)}$ removal and pure water production was done from simulated Ni-electroplating rinse water. In the process, 94% removal was found in first stage of EDI with 99.8% (as compare to initial Ni concentration) removal from final stage of EDI (Lu et al., 2015). In continuous EDI process, $Cr_{(VI)}$ removal was investigated by Xing et al. (2009) and they suggested that voltage required in $Cr_{(VI)}$ removal was not only dependent on applied current density but also vary with flow rate of effluent.

3.3.5.4 Electroflotation

Electroflotation (EF) is efficient for removal of different types of organic and inorganic pollutant removal. In the EF process, hydrogen (H_2) and oxygen (O_2) are produced by electrolysis of water via electrochemical reaction on cathode and anode

(applied electrode) respectively (Fig. 3.2d). Due to bubbling of water, the present contaminants came out from the wastewater and float on the surface. While, bubble generation by electrolysis is completed in three steps: nucleation, growth and detachment (Santos et al. 2018). In an investigation, EF process was investigated for removal of less soluble $Cr_{(III)}$ from wastewater. EF affecting parameters such as solution pH, presence of flocculants, surfactants particle size, ionic composition, electrokinetic potential, current density and solution temperature were optimized. It was found in the study that removal potential depend upon solution composition, size of the particle and minimum surface charge (Perfil'eva et al., 2016). They also found that using anionic M-10 and LT-30 flocculants and rising in solution temperature enhance the particle size that increases the removal efficiency from 81-99%. Kolesnikov et al. (2018) studied the EF process in removal of $Ni_{(II)}$, $Cr_{(III)}$ and other metal hydroxide from solution by using sodium sulfate as supporting electrolyte. They reported that non-ionogenic flocculant N-300 rise the EF efficiency in removal of metal. Increase in the efficiency for removal of $Ni_{(II)}$ and other metal was also reported by applying different types of surfactant in EF process (Kolesnikov et al., 2015). In a study, Ti and RuO2/TiO2-Ti were utilized as cathode and anode respectively in two compartments of EF membrane reactor. Nafion 117 membrane was used to separate the catholyte (spent liquor effluent) and anolyte (0.01 N $H2SO_4$). Highest removal was reported for $Cr_{(III)}$ with successful application of recovered $Cr(OH)_3$ in tanning of cowhide (Selvaraj et al., 2018). To advance the removal competence, EF process was also studied with combination of electrocoagulation process. Khelifa et al. (2013) reported that EF process effectively remove the $Ni_{(II)}$ and $Cu_{(II)}$ by utilizing Ti/RuO2 (anode) and stainless steel (cathode) but the presence of EDTA, drastically inhibited the removal capacity of EF. To overcome this problem, the combination of EC-EF was applied and removal efficiency of $Ni_{(II)}$ was increased up to 77% and 78% for copper under the same condition. Similar technique was investigated for $Cr_{(VI)}$ removal where, $Cr_{(VI)}$ first reduced into $Cr_{(III)}$ by EC-process and further removed from the solution by combination of EF-EC process (Gao et al., 2005).

3.3.5.5 Electrochemical reduction

Electrochemical reduction (ECR) of $Cr_{(VI)}$ to $Cr_{(III)}$ is extensively reported in $Cr_{(VI)}$ removal from contaminated water. In an investigation, single chambered cell

with titanium anode was utilized for indirect reduction of $Cr_{(VI)}$ and precipitation of $Cr_{(III)}$. Decreased in the pH of the solution increases the $Cr_{(VI)}$ reduction, but reduces the $Cr_{(III)}$ precipitation. It was also found that during the reaction mechanism, Ti anode could corrode and produces the Ti^{2+} and Ti^{3+} make available the free electron for $Cr_{(VI)}$ reduction. Simultaneously, the continuous generation of OH anion on cathode caused formation of solid product ($TiO2_{(6x-y-z+5/2)}Cl_{2y}$ $Cr_{2x}(OH)_{2z}(s)$) as precipitate (Yao et al., 2020). Hu et al. (2017) investigated the $Cr_{(VI)}$ reduction followed by precipitation in an stirred batch reactor using a low-carbon steel electrode. They reported high removal effectiveness of $Cr_{(VI)}$ from seawater, synthetic wastewater and concentration of $Cr_{(VI)}$ was dropdown below the permissible limit (0.5 mg/L) from all the types of water. In a recent study, discarded cigarette filters (DCFs) were utilized as a bed for immobilization of palladium nanoparticle placed between porous anode and as cathode, graphite felt was used in the study. The system was intended for the $Cr_{(VI)}$ removal and disinfection of water via producing chlorine gas (Cl_2) from ground water. On cathode, produced hydrogen gas converted into hydrogen radical, act as an effective reducing agent for $Cr_{(VI)}$ reduction and produced hydroxyl anions on the surface of cathode increases the medium pH, resulted into $Cr_{(III)}$ precipitation with 96% efficiency. While, Cl_2 produced on the surface of anode was effective for water disinfection (Dorosti et al., 2020). Effective electrochemical $Cr_{(VI)}$ reduction followed by $Cr_{(III)}$ precipitation using steel rods connected in unipolar mode and NaCl as electrolyte was reported by Lakshmipathiraj et al. (2008). The modification of cathode and anode with nanoparticle and other substances also proven for enhanced $Cr_{(VI)}$ reduction in ECR process. For example: Pd-coated copper rod enhanced the $Cr_{(VI)}$ reduction in ECR process (Tabatabaei et al., 2020). Use of organic material as electrolyte such as urea and oxalic acid in ECR process also influences the reduction efficiency of ECR process (Sriram et al., 2018; Liu et al., 2018).

3.3.6 Biological remediation

$Cr_{(VI)}$ and $Ni_{(II)}$ are toxic for living organism, affect the growth and developmental activity of plant, animal and microbes. Their toxicity have been reported at cell organelles, cellular, tissue and whole organism level. In most of the studies it has been reported that $Cr_{(VI)}$ and $Ni_{(II)}$ causes oxidative stress can affect the cell membrane, protein, lipid and DNA via oxidative and non-oxidative damages (Das

et al., 2018; Barrera-Díaz et al., 2012; Zhitkovich et al., 2011). Cellular level toxicity is also detected using scanning and transmission electron microscopy. In addition, some of the metal tolerant species of microbes and plants have hyper accumulation ability of Cr and Ni inside the cytoplasm and cell organelles. Some species also have the potential to reduce $Cr_{(VI)}$ to $Cr_{(III)}$ via enzyme catalyzed or electron mediated mechanism. Cell wall of plant and microbes is also made up of carbohydrate, protein and lipid which carry number of functional group on their surface and provide better opportunity for adsorption of pollutants including $Cr_{(VI)}$ and $Ni_{(II)}$ on their surface. Thus, combinely the surface functional group and accumulation mechanism offering best applicability of metal tolerant plant and microbes for removal of $Ni_{(II)}$ and $Cr_{(VI)}$.

Bioremediation of heavy metal as well as organic pollutant have been reported extensively in the literature. The living organism such as bacteria, yeast, fungi, algae and plant has been found as efficient bioremediation agents (Table 3.2). Biosorption is another phenomenon where bio-originated product and byproduct are used as adsorbent. In the biosorption process, pollutant removal is basically driven by the functional group present on the surface of applied bio-adsorbent. Many types of bioadsorbent such biochar, saw dust, straw, dried fungal, bacterial, algal and plant biomass have been utilized by researchers for successful removal of $Ni_{(II)}$, $Cr_{(VI)}$ and other various types of pollutants (Georgieva et al., 2020; Wong et al., 2018; Liu et al., 2018; Fan et al., 2019). In the biosorption of pollutant, the most affecting parameters are pH of the medium, initial pollutants concentration, temperature and surface properties of bio-adsorbent including functional group. But, the bioremediation is different from biosorption, performed by living organism via accumulation, degradation, mineralization, transformation and also sorption by the functional group present on the organism cell surface. The degradation, mineralization and transformation are basically performed by different types of enzyme-catalyzed mechanism which convert the pollutant into carbon dioxide, methane, water and biomass. The accumulation is reported for heavy metal and some recalcitrant organic compound such as DDT accumulation in plant, involved whole cell system, makes a chain of different types of bio-process such as interaction with organism, surface sorption, transportation outside to inside the cell, intracellular precipitation or translocation inside vacuoles. Living organism, most preferably utilized the pollutant as nutrient and energy sources to catalyze them in less toxic forms. Some time,

pollutant also exported to outside of the cell by microbes through efflux pump to lessen the toxicity of pollutant and maintaining cellular homeostasis. Temperature, pH, moisture, initial metal concentration, chemical nature of pollutant, availability of nutrients and microbial community of the contaminated sites are the most considerable parameters that can affect the bioremediation process. Microbial interaction with $Ni_{(II)}$ and $Cr_{(VI)}$ causes surface sorption of $Ni_{(II)}$ and $Cr_{(VI)}$ with chemical binding between available functional group surface. Surface absorbed $Cr_{(VI)}$ and $Ni_{(II)}$ accelerate their transportation in microbial cell. Transported $Ni_{(II)}$ may accumulate or transported to outside of the cell while, $Cr_{(VI)}$ either accumulated or transformed into less toxic $Cr_{(III)}$ by chromate reductase or $Cr_{(VI)}$ to $Cr_{(III)}$ happen spontaneously inside the cell.

Table 3.2. Experimental condition, removal efficiency and mechanism of microbes and plant for $Cr_{(VI)}$ and $Ni_{(II)}$.

Name of the species	$Cr_{(VI)}/Ni_{(II)}$	Initial metal concentration (mg/L), pH, temperature (°C), time (h or d) and agitation rate (rpm)	Removal rate (%)	Associated mechanisms in removal of $Cr_{(VI)}/Ni_{(II)}$	References
BACTERIA					
Rhodococcus erythropolis	$Cr_{(VI)}$	50, 5.0, 28, 120h, -	89.5	Accumulation, biosorption and bioreduction	Banerjee et al. (2017)
Serratta marcescens	$Cr_{(VI)}$	25, 8.0, 30, 36h, -	100	Accumulation, biosorption and bioreduction	Kafi lzadeh and Saberifard (2016)
Pediococcus acidilactici applied in anaerobic two-phase bioreactor	$Cr_{(VI)}$	900, -, -, -, -	100	Reduction happen by extracellular secreted lactate produced in glycolysis path way	Lytras et al. (2017)
Geobacter or *Desulfovibrio* with combination of *Ferrovibrio* in presence of Fe(0)	$Cr_{(VI)}$	5, -, -, 60d, -	98.1 ± 1.2	Reduction happened by providing electron from Fe (solid state electron transfer) to $Cr_{(VI)}$ anaerobic bacteria (Geobacter or Desulfovibrio)	Shi et al. (2019)
Bacillus megaterium 1295S	$Ni_{(II)}$	0.5, -, -, -, -	80.46	accumulation and surface sorption	Gheethi et al. (2017)
Bacillus aryabhattai HU-39	$Ni_{(II)}$	25, -, 30, 72h, -	89	Accumulation and surface sorption	Khadim et al. (2019)
YEAST					
Saccharomyces cerevisiae BY4741	$Cr_{(VI)}$	300 µM, -, 30, 24h, 180	48.43 µM/g FW	Accumulation	Huang et al. (2013)
Wickerhamomyces anomalus M10	$Cr_{(VI)}$	1 (mM), -, 25, 72, 250	95	Accumulation	Fernández et al. (2017)
Saccharomyces cerevisiae	Cr(VI)	90, 5.0, 25, 3h, 120	99.6	Biosorption	Rossi et al. (2018)

Yarrowia lipolytica	$Ni_{(II)}$	100, 6.0, 30, 60h, 120	68.99	Biosorption	Wierzba et al. (2017)
Candida sp.	$Ni_{(II)}$	321.5, 4.0, 25, 8d, 150	46.8 mg/g	Bioaccumulation	Donmez and Aksu (2001)
FUNGI					
Penicillium oxalicumSL2 used in stired tank bioreactor	$Cr_{(VI)}$	164.6, -, 30, +	89.1	Reduction of $Cr_{(VI)}$ driven by acidic metabolite such as oxalic acid, gluconic acid, malic acid, citric acid subsequently absorb or precipitated on cell surface as chromium oxalate	Long et al. (2020)
Phanerochaete chrysosporium	$Ni_{(II)}$	16, 6.0, 36, 9h, well mixing condition	89.4	adsorption by surface functional group	Noormohamadi et al. (2019)
Trichoderma harzianum	$Ni_{(II)}$	400, -, 24, 14d, -	11,000 mg/Kg	Accumulation inside of the mycelia	Cecchi et al. (2017)
Aspergillus flavus CR500	$Ni_{(II)}$	10, 7.0, 28, 144h, 80	73.1	Accumulation inside of the mycelia as well as biosorption on mycelia	Kumar and Dwivedi (2020)
Trichoderma asperellum TS141	$Ni_{(II)}$	200, 8.0, 29, 8d, 200	78	Accumulation inside of the mycelia	Hoseinzadeh et al. (2017)
ALGAE					
Oscillatoria subbrevis and *Gloeocapsa atrata*	$Cr_{(VI)}$	17.5, 7.0, -, 6.5, -	71.65		Kushwaha et al. (2014)
Chlorella sp.	$Cr_{(VI)}$	12.7, 5.6, 27.5, 12d, -	73.1	Binding on cell surface and accumulation inside the cell	Ajayan et al. (2018)
Limnococcus limneticus and *Leptolyngbya subtilis*	$Cr_{(VI)}$	10, 9.0, 25±2, 9d, -	52	Bioaccumulation and binding on cell surface	Sen et al. (2017)
Chlorella vulgaris	$Cr_{(VI)}$	1, -, 25, 3d	88.1	Reduction of $Cr_{(VI)}$ to $Cr_{(III)}$ by oxidation-reduction reactions between $Cr_{(VI)}$ and the acetate-type ligand in addition of Chromate reductase, binding on surface and intracellular accumulation	Zou et al.(2020)
Dunaliella sp.	$Ni_{(II)}$	300, -, 29 ±1, 7d, -	80.8	Bioaccumulation and binding on cell surface	Moussa et al. (2018)

Durvillaea antarctica	$Ni_{(II)}$	50, 5.0, 20±1, 4h, 150	32.8 mg/g	Biosorption	Guarí n-Romero et al. (2019)
Cystoseria indica	$Ni_{(II)}$	100, 6.0, 25, 1.5, 175	18.17mg/g	Biosorption	Khajavian et al. (2019)

3.3.6.1 Bacteria

Microorganisms have potential application in removal of $Ni_{(II)}$ and $Cr_{(VI)}$ (Table 2.2). Both types of bacteria (gram negative and gram positive) have shown high efficiency in removal of $Ni_{(II)}$ and $Cr_{(VI)}$ and also enzyme-catalyzed $Cr_{(VI)}$ reduction into $Cr_{(III)}$. A study demonstrated the $Ni_{(II)}$ removal efficiency of *Bacillus aryabhattai* HU-39. At 250 mg/L of initial $Ni_{(II)}$ concentration and at 30°C, the removal of $Ni_{(II)}$ by strain HU-39 was 89%, $Ni_{(II)}$ removal happen via bio-precipitation of $Ni_{(II)}$ as $NiCO_3$ (Khadim et al., 2019). Gheethi et al. (2017) investigated the potential of *Bacillus megaterium* 1295S and *Sporosarcina pasteurii* 586S for removal of $Ni_{(II)}$. They reported that with rise in the concentration of $Ni_{(II)}$ the removal effectiveness of *B. megaterium* 1295S and *S. pasteurii* 586S was decreased and highest at lower concentration. The major mechanism involved in removal of $Ni_{(II)}$ are intracellular accumulation and surface sorption, driven by cell surface functional group (Ozturk, 2007; Khadim et al., 2019). In the case of $Cr_{(VI)}$, in addition of accumulation and surface sorption, its reduction to $Cr_{(III)}$ is reported extensively. A research showed that *Rhodococcus erythropolis* has high $Cr_{(VI)}$ reduction efficiency, it accumulated inside the cell and adsorbed outside of the cell $Cr_{(VI)}$ in the form of $Cr_{(III)}$ with great removal efficiency (Banerjee et al., 2017). In another investigation, a bacterium that have 99% similarity with *Pediococcus acidilactici*, was utilized for removing $Cr_{(VI)}$ in Sequencing Batch Reactor (SBR) in anaerobic and mesophilic conditions. The authors achieved 100 % $Cr_{(VI)}$ removal using sequencing batch reactor process. The authors reported extracellular $Cr_{(VI)}$ reduction, mediated by lactate, extracellularly generated by *Pediococcus acidilactici* from the glycolysis process (Lytras et al., 2017). A research conducted by Karthik et al. (2017) isolated a new aloalkaliphilic bacterial strain, *Cellulosimicrobium funkei* AR8. The complete $Cr_{(VI)}$ reduction was reported at optimum pH 7.0 within 120 h and the reduced $Cr_{(III)}$ either extracellularly absorbed on its cell surface or accumulated inside the cell as detected by TEM, fourier transform infrared (FTIR) and x-ray diffraction analysis. A quinone-reducing bacteria, *Shewanella* strain Y2 investigated for $Cr_{(VI)}$ reduction with the function of electron shuttling compounds (DOM), sodium formate (NaFc) and $Fe_{(III)}$. Results illustrated that Fe(III)/DOM appreciably endorsed the reduction of $Cr_{(VI)}$ at 0.8 mM of anthraquinone-2-sodium sulfonate and 5 mM of sodium formate concentration (Huang et al., 2016). In an investigation conducted by Zinicovscaia et

al. (2020), the biofilm of *Shewanella xiamenensis* supported on zeolite was utilized in selective exclusion of $Ni_{(II)}$, $Cr_{(VI)}$ and other metal from metal complex system with different combination. The greatest removal of $Ni_{(II)}$ was attained within one hour at pH 5.0 and 6.0 by bio-sorption and bioaccumulation. $Cr_{(VI)}$ removal was occurred via bio-sorption, bioaccumulation and long time reduction process but the removal rate for $Cr_{(VI)}$ was less as compare to $Ni_{(II)}$ and inclusive reduction of $Cr_{(VI)}$ was recorded in 35 days. The mechanism that deals with $Cr_{(VI)}$ reduction is differently performed by aerobic and anaerobic bacteria.

3.3.6.2 Yeast

Yeast broadly utilized in fermentation and also has promising capability in removal of different types of pollutant (Table 3.2). In an investigation, Baker's yeast (*Saccharomyces cerevisiae*) immobilized on mango leaves was employed in the removal of $Ni_{(II)}$. The highest $Ni_{(II)}$ removal was recorded at neutral pH (7.0) and the biosorption of $Ni_{(II)}$ was 250 mg/g, even it was highly efficient in removal of $Ni_{(II)}$ after 5^{th} cycle of regeneration using 0.2 M HCl (Yakout et al., 2016). In a study, Luo et al. (2016) examined intracellular content of $Ni_{(II)}$ in different sensitive and $Ni_{(II)}$-tolerant mutant budding yeast *Saccharomyces cerevisiae*. They found that intracellular $Ni_{(II)}$ content was increased in the response of $Ni_{(II)}$ concentration in Ni-tolerant mutant as compare to wild type but decreased in sensitive strains. Further, in functional genomics study they identified 22 nickel-tolerant diploid deletion mutants of budding yeast genes that were involved in transportation, vacuolar translocation, protein synthesis, Ni-sensitivity etc., collectively in Ni-homeostasis. Fernández et al. (2017) examined the evacuation of $Cr_{(VI)}$ by *Wickerhamomyces anomalus* M10 in an alternative culture and using the Plackett-Burman design. They found that K_2HPO_4, inoculum size and sucrose had noteworthy effect on $Cr_{(VI)}$ removal. For complete reduction of $Cr_{(VI)}$, the optimum culture condition was 1mM $Cr_{(VI)}$ concentration, 400 rpm agitation and air flow (1 vvm). Rossi et al. (2018) treated the *Saccharomyces cerevisiae* biomass with KOH and also thermally treated to enhance its biosorption potential of $Cr_{(VI)}$. They studied the affecting factor such as initial $Cr_{(VI)}$ concentration, pH and contact time, under optimum conditions the removal of $Cr_{(VI)}$ was 99.66%. Chromate reductase (ChrR), responsible for $Cr_{(VI)}$ have been reported in bacteria, fungi and also in yeast. To confirm the yeast ChrR activity and its potential

to reduce the $Cr_{(VI)}$, Martorell et al. (2012) isolated *Pichia anomala* M10 and *Pichia jadinii* M9 from textile effluent and analyzes the ChrR activity in the both strains. They found that ChrR activity was increased in both strain after addition of NAD(P)H as an electron donor but the presence of Hg^{2+} and Mn^{2+} inhibited the activity of ChrR. In a study, demonstrated by Guillén-Jiménez et al. (2008) reported that the sulfate ion can improve the growth and tolerance ability of *Candida* sp. FGSFEP towards $Cr_{(VI)}$. The yeast strain was capable in complete reduction of $Cr_{(VI)}$ at 1.7 mM concentration in the presence 23.92 mM sulfate concentration. These studies suggested the potential of yeast exploitation in $Cr_{(VI)}$ and $Ni_{(II)}$ removal.

3.3.6.3 Fungi

Fungi are the key player of ecosystem; naturally cleaning the environment by their saprophytic characteristics, have wide application in industrial, food and beverage processing. In addition, fungi are the consortium of enzymes and have potential application in degradation of organic pollutant for environmental cleanup. Heavy metal including $Cr_{(VI)}$ and $Ni_{(II)}$ accumulation, detoxification, mineralization, transformation etc. are greatly reported in fungi (Table 3.2). A study examined the biosorption potential of *Phanerochaete chrysosporium* for removal of $Ni_{(II)}$. *P. chrysosporium* can accumulate 16 mg/L with high removal efficiency at pH 6.0 and 30 °C within under well mixing conditions (Noormohamadi et al., 2019). In our study, the multiple metal removal potential of *A. flavus* CR500 was investigated from multi-metal contaminated tannery wastewater. Under the optimized condition (pH 7.0, 28 ± 1 °C), the removal of $Ni_{(II)}$ and $Cr_{(VI)}$ was 38.6 and 58.2 % from Pb(II), $Cr_{(VI)}$, $Ni_{(II)}$ and As(III) amended (5 mg/L of all metal/loid) and diluted (1:2) tannery wastewater (Kumar and Dwivedi, 2020). In an investigation, Cecchi et al. (2017) reported high Ni accumulation efficiency (11,000 mg Ni/kg of fungal biomass) of *Trichoderma harzianum* at 24 °C in 14d. *T. asperellum* TS141 and *T. harzianum* TS103 also has excellent $Ni_{(II)}$ removal ability from aqueous medium (Hoseinzadeh et al. 2017). In addition, fungi also exhibited outstanding $Cr_{(VI)}$ reduction performance in aqueous medium. Some amount of $Cr_{(VI)}$ was accumulated inside the cell and also absorb on the surface of fungus cell via surface functional group or as precipitate of $Cr_{(III)}$ species. ChrR enzyme played role in reduction of $Cr_{(VI)}$ with the help of electron donor such as NADH or NADPH (Irazusta et al. 2018). Long et al. (2020) reported

that *Penicillium oxalicum* SL2 can reduce $Cr_{(VI)}$ extracellularely by secreting acid metabolite such as gluconic acid, oxalic acid, citric acid, malic acid, and tartaric acid. The $Cr_{(VI)}$ removal performance of SL2 was 89.1% in a stirred tank bioreactor, cylindrical 10×40 (diameter and height) oxygen supplied from the bottom of the reactor and operated at 30 °C using potato dextrose liquid (PDL) medium amended with $Cr_{(VI)}$. Consortium development with metal resistant species of fungi or bacteria is also studied by several researchers for the treatment of wastewater. In a study, *Penicillium commune*, *Cladosporeum perangustum*, *Paecilomyces lilacinus* and *Fusarium equiseti* were used to develop fungal consortium in tannery wastewater treatment. Fungal consortium was immobilized on Nylon mesh. Wastewater treatment efficiency of fungal consortium immobilized with nylon mesh was investigated in stirred tank bio-reactor (12 cm diameter and 20 cm height). With 1L of working tannery wastewater (amended with glucose (1%) and ammonium nitrate (0.01%)) at pH 4.0 and 28 °C, the treatment performance of immobilized fungal consortium was very high with removal efficiency of 82.52% for COD (chemical oxygen demand), 86.19% for color, 100% for $Cr_{(VI)}$ and 99.92% for total Cr (Sharma and Malaviya, 2016). Talukdar et al. (2020) tested the metal $Cr_{(VI)}$ removal efficiency of *A. flavus* (FS4) and *A. fumigatus* (FS6) for consortium development. Both fungal spore suspension was used as fungal consortium for removal of $Cr_{(VI)}$ from liquid medium and industrial wastewater too. Developed fungal consortium can remove 81.25 ± 0.25% of $Cr_{(VI)}$ from PDB medium while 68 % removal was recorded from battery effluent.

3.3.6.4 Algae

Algae have excellent biological characteristic such as high photosynthetic competence and simple in structure, can grow in extreme ecological situation such as high salinity, presence of heavy metal, polluted water streams, nutrient stress conditions, high temperature (Leong and Chang, 2020; Moussa et al., 2018). Algae have been reported for production of lipid, so algae have dual approach as their utilization in wastewater treatment and use of produced biomass in energy production (Ramadoss and Subramaniam, 2018; Sen et al., 2017). In case of $Cr_{(VI)}$ and $Ni_{(II)}$ removal, algae have been utilized in live as well as in dead form. For example, dry and dead biomas of *Cladophora glomerata* was employed for adsorptive evacuation

of $Cr_{(VI)}$ from polluted aqueous medium. At the operational condition 20 mg/L $Cr_{(VI)}$, 45 ºC and pH 2.0, *C. glomerata* removed 66.6% in 60 minutes of contact time (Al-Homaidan et al., 2018). In another work, blue-green marine algae were utilized for $Ni_{(II)}$ removal and at the experimental conditions of pH 6.0, biomass dose 2 g, and shaking rate 120 rpm, the removal of $Ni_{(II)}$ was 42.05 mg/g (Ramadoss and Subramaniam, 2018). But, in case dried biomass application another energy production strategy can't be implemented. While, live application of algae in removal of $Cr_{(VI)}$ have been studied with efficient removal and high amount of biomass production was reported in many studies that can be used for production of bio-fuel. Sen et al. (2017) studied $Cr_{(VI)}$ removal efficiency of cynobacterial consortium. The consortium was consisted of *Leptolyngbya subtil* and *Limnococcus limneticus*. They found efficient removal rate at an initial concentration 15 mg/L of $Cr_{(VI)}$, pH 9.0 and with an inoculum size of 10% in 12 days. When both alga were applied in consortium, raise in dry biomass, the lipid content was reported with high $Cr_{(VI)}$ removal performance as compared to individual use. Similarly, Moussa et al. (2017) studied the $Ni_{(II)}$ removal capability of live alga *Dunaliella* sp. which reduces the $Ni_{(II)}$ concentration solution with removal efficiency of 93.63%. Excess of $Ni_{(II)}$ concentration reduced the growth of the alga, level of protein and carbohydrate content while, significantly accelerated the total lipid, carotenoid content and phenolic content. The algal species such as *Oscillatoria subbrevis*, *Gloeocapsa atrata* and *Chlorella* sp. can also remove the pollutants including $Cr_{(VI)}$ and $Ni_{(II)}$ with enhanced lipid content in obtained biomass (Ajayan et al., 2018; Kushwaha et al., 2014). An experiment was conducted for the assessment of tannery wastewater treatment efficiency of *Scenedesmus* sp. The alga had removed 96% of Cr and other pollutants (Cu, Pb, Zn) and nutrients (phosphate and nitrate) within 12 days from diluted tannery wastewater amended with BG11 culture medium (Ajayan et al., 2015).

3.3.6.5 Plants

Plants have enormous potential in remediation of heavy metal contaminated sites and can be applied *in situ* for effective remediation in sustainable way. Phytoremediation is a cheapest, ecofriendly and economical technique for remediation purposes, uses their growth for removal, extraction, reduction, degradation and stabilization of pollutants that are driven by plant and sun light (as energy source) (Bello et al., 2018). Plants use various mechanisms in removing heavy metal from soil

and water such as accumulation, trans-evaporization, transformation, stabilization etc. (Table 3.2) (Saha et al., 2017). Several studies have reported the successful utilization of plants in treatment of $Cr_{(VI)}$ and $Ni_{(II)}$ contaminated wastewater especially aquatic plant has more advantage in wastewater remediation. In a study, the $Ni_{(II)}$ and other heavy metal removal potential of *Phragmites australis* was performed. The study was conducted in deep-water hydroponic system and $Ni_{(II)}$ concentration was 5 mg/L. Over 6^{th} week periods, the removal of $Ni_{(II)}$ was very high with removal rate of 93% via phytostabilation (Bello et al., 2018). Bingöl et al. (2017) utilized *Lythrum salicaria* L. in removal of $Ni_{(II)}$ from contaminated water. The maximum accumulation of $Ni_{(II)}$ was at pH 7.0, 10 mg/L of $Ni_{(II)}$ concentration and $Ni_{(II)}$ distribution was higher in root followed by shoot and leaves. In another work, Chaudhary and Sharma (2019) evaluated the Cr removal potential of *Lemna gibba* from liquid nutrient medium. At 5 mg/L of Cr concentration, removal of Cr was highly increased up to 98.6%. In a study *Limnobium laevigatum* efficacy for removal of Cr, Ni, Pb and Zn from multi-metal contaminated aqueous system was performed. Accumulation of these heavy metals was reported much higher in root as compare to shoot and with rise in the concentration of metal; the concentration of metal in root was extremely higher than metal concentration in the solution (Arán et al., 2017). Saha et al. (2017) utilized water hyacinth (*Eichhornia crassipes*) on large scale (100 L) for chromite mine wastewater treatment. Hundred liter of chromite mine wastewater was taken in rectangular container and experiment was performed in ambient condition (25-30 °C). At 15^{th} day of experiment, the water hyacinth achieved 99.5 % removal of $Cr_{(VI)}$ with efficient reduction in BOD (biological oxygen demand), COD and TDS (total dissolve solid). Phytoremediation is a time taking process, the main disadvantage of this technique. However, researchers have also investigated the effect of plant on removal of $Cr_{(VI)}$, $Ni_{(II)}$ and other pollutants in constructed wetland. Studies have successfully demonstrated the plant utilization in constructed wetland and effective removal of $Cr_{(VI)}$ and $Ni_{(II)}$ was recorded (Li et al., 2017; Madera-Parra et al., 2015). In an investigation, *Typha domingensis* was utilized for treatment of metallurgical effluent containing Cr, Ni and other pollutants in free-water surface constructed wetland for 5 years. Higher Cr and Ni concentration was reported in root and rhizome than aerial and submerged part of leaves (Hadad et al., 2018).

3.4. Heavy metal tolerance and removal by fungi including $Cr_{(VI)}$ and $Ni_{(II)}$

3.4.1 Metal tolerance in fungi

Tolerance is the ability of organism to survive in an adverse environment. HMs are toxic in nature for most of the organisms. Ability of fungi to grow in HMs polluted environment is the metal tolerance of the fungi (Mondal et al, 2017, Mohammadian et al, 2017). There are some mechanisms in fungi to tolerate and detoxify the HMs such as enzymatic detoxification, accumulation inside the cell via active (transport systems) and/or passive (diffusion) uptake mechanism, exclusion by permeability barrier, adsorption on extracellular structures (cell wall, capsule, slime), extra and intracellular precipitation, efflux pumps, adjustment in the cellular targets, methylation, volatilization and chelation of metal/loids etc. (Baldrian, 2003; Gadd, 2017; Merroun et al., 2001; Zhang et al., 2005) in which some mechanisms are based on the production of extracellular and intracellular chelating agent (for molecular mechanism of HMs tolerance and removal see **Section 3.4.3**) (Gadd, 2007; Cao et al., 2018; Yin et al., 2011; Dang et al., 2018). Many morphological responses also have been observed in fungi under the presence of HMs. Growth inhibition, change in colour morphology, cell elongation, constriction, protrusion less, ruptured, snubbed/flatted, outward growth of mycelia are reported in presence of HMs in several studies (Chen et al., 2017). Contaminated sites (soil and water) are the major source to isolate the metal tolerant fungi (Mohammadian et al., 2017). Fungal response to metal and their resistance depends on the concentration, toxicity and bioavailability of HMs and characteristics of the fungi (Baldrian, 2003). The resistance nature of the fungi varies with genetic background of the fungi, HMs concentration, existing environmental condition, nutrient availability and types of HMs. *Aspergillus niger* (Cu , Pb , Cr, Zn, Cr, Ni and V) (Coreño-Alonso et al., 2014; Sepehr et al., 2014; Iram et al., 2015; Saravanan et al., 2015; Holda et al., 2016; Sakthivel et al., 2016; Fomina et al., 2017) and *Trichoderma harzianum* (Cd, Pb, Cu, Zn Ni, Fe) (Adebiyi et al., 2017; Cecchi et al., 2017; Mohsenzadeh et al., 2014) are multimetal resistant fungal species. Table 3.3 is listed for many fungal species which have the potential to tolerate HMs.

Table 3.3 depicted that most of the fungal species that are reported for tolerance towards HMs belongs to the class ascomycetes. This class of fungi is also very widely distributed in different type of habitats and play important role in ecosystem like nutrient cycling and soil stabilization (Challacombe et al., 2019). However, there is no any clear evidence that relates them with each-other that why they are highly metal tolerant and belongs from the same class of fungi. To get insight on the ascomycetes, here it is to be mentioned that Challacombe et al. (2019) investigated the genomic and secrotomic similarities to assess their role in biomass decomposition and pathogenesis in arid environment by five different fungal species (*Aspergillus* CK392, *Coniochaeta* CK134, *Embellisia* CK46, *Chaetomium* CK152 and *Phoma* CK108) of ascomycetes class. In genomes and secretomes analysis, they found that all the tested fungi have melanized structure and genetically capable to synthesize melanin which make survivable to these tested ascomycetous fungus in arid environment. There is also some category of proteins that expressed in all tested condition and common for some of the fungi which provids common nature of ascomycete fungus.

Table 3.3. The Heavy metal tolerant fungi applied in removal HMs in growing form.

Class of Fungi	Name of the Fungi	Name of the Pollutants	References
Ascomycetes	*Aspergillus aculeatus*	Cd	Xie et al. (2014)
	Aspergillus flavus	Cu, Pb, & Cr	Iram et al. (2015), Qayyum et al. (2016)
	Aspergillus flavus strain KRP1	Hg	Kurniati et al. (2014)
	Aspergillus foetidus	Cd	(Chakraborty et al., 2014)
	Aspergillus fumigates	Cr	Panda et al. (2014), Sakthivel et al. (2016)
	Aspergillus fumigatus PD-18	Cd, Cr,Ni, Pb and Zn	Dey et al. (2016)
	Aspergillus niger	Cu , Pb , Cr, Zn, Cr, Ni & V	Coreño-Alonso et al. (2014), Sepehr et al. (2014), Mirazimi et al. (2015), Iram et al. (2015), Saravanan et al. (2015), Holda et al. (2016), Olubunmi et al. (2016), Sakthivel et al. (2016),

		Fomina et al. (2017), Mondal et al. (2017), Sriharsha et al. (2017), Tahir et al. (2017)
Aspergillus niger (CMCC98003)	Pb, Hg, & Cd	Cui et al. (2018)
Aspergillus niger A40	Pb	Sharma et al. (2017)
Aspergillus niger MSR4	Cr	Melvin et al. (2015)
Aspergillus niger strain SF-6095	Cr	Manorama et al. (2016)
Aspergillus oryzae	Cr	Sepehr et al. (2014)
Aspergillus sp.	Cu, Zn & Cr	Pundir et al. (2015), Sathvika et al. (2015), Pundir et al. (2018)
Aspergillus sp. UF3	Lead and Strontium	Dhami et al. (2017)
Aspergillus terreus	Pb, Cr and Cu	Khadiga et al. (2017), Sriharsha et al. (2017)
Aspergillus terreus AML02	Cd, Pb & Zn	Dey et al. (2016)
Aspergillus terreus PD-17	Cd, Cr, Ni, Pb & Zn	Dey et al. (2016)
Acremonium persicinum	Cd, Pb, Cu & Zn	Mohammadian et al. (2017)
Acremonium sp.	Cr	Herath et al. (2014)
Beauveria bassiana	Zn, Cu, Cd, Cr & Ni	Gola et al. (2016)
Beauveria bassiana 4580	Cd, Cr, Ni, Pb & Zn	Dey et al., (2016)
Botrytis cinerea	CuO	Kovacec et al. (2017)
Candida albicans	Cd	Nadeem et al. (2015)
Chaetomium globosum	Cu	Karunasekera et al. (2017)
Cheatomium .sp	Co, Zn, Cd	Sani et al. (2017)
Cyberlindnera jadinii M9	Cr	Irazusta et al. (2018)
Exophiala sideris	As	Seyedmousavi et al. (2011)
Flammulina velutipes	Cu, Zn & Hg	Li et al. (2018)
Fusarium oxysporium	Cr and Pb	Migahed et al. (2017)
Fusarium oxysporum UF8	Pb & Sr	Dhami et al. (2017)
Fusarimum solani	Cd	Kumar et al. (2019)
Humicola sp.	Cd	Netpae et al. (2015)
Neurospora sp.	Pb, Ni, Co, Cr, Cu, & Zn	Joshi et al. (2014), Desai et al. (2016)

Paecilomyces chysogenum	Cr	Olubunmi et al. (2016)
Paecilomyces fumosoroseus 4099	Cd, Cr, Pb & Zn	Dey et al. (2016)
Paecilomyces javanicus	Pb	Rhee et al. (2016)
Penicillium chrysogenum	Zn & Cu	Tahir et al. (2017)
Penicillium chrysogenum CS1	Cr & Pb	Qian et al. (2017)
Penicillium griseofulvum MSR1	Cr	Abigail et al. (2014)
Penicillium janthinillum (GXCR)	Cu, Pb, & Cd	Cai et al. (2016)
Penicillium simplicissimum	Cd, Pb, Cu, Zn & Cr	Xu et al. (2015), Mohammadian et al. (2017)
Penicillium simplicissimum (iso 10, KP713758)	Al, Cr, Pb	Chen et al. (2017)
Penicillium sp.	Ni, Cd & Cr	Netpae et al. (2015), Butt et al. (2017), Costa et al. (2017)
Phialophora malorum	Cu	Karunasekera et al. (2016)
Phialophora mutabilis	Cu	Karunasekera et al. (2016)
Saccharomyces cerevisiae	Cu	Sivakumar et al. (2017)
*Saccharomyces cerevisiae (*transgenic strains*)*	Co, Mn & Ni	Ruta et al., (2017)
Simplicillium chinense	Al, Cr & Pb	Chen et al. (2017)
Trichoderma asperellum	Cd	Mohsenzadeh et al. (2014)
Trichoderma asperellum (iso 11, KP792512)	Al, Cr & Pb	Chen et al. (2017)
Trichoderma asperellum PTN7	Cr	Chang et al. (2016)
Trichoderma ghanense	Cd, Cu, Pb, As & Fe	Oladipo et al. (2018)
Trichoderma harzianum	Cd, Pb, Cu, Zn Ni, Fe	Mohsenzadeh et al. (2014), Adebiyi et al. (2017), Cecchi et al. (2017), Mohammadian et al. (2017)
Trichoderma koningiopsis	Cu	Salvadori et al. (2014)
Trichoderma logibrachiatum	Pb	Devi et al. (2017)
Trichoderma sp.	Cd	Bazrafshan et al. (2015)
Trichoderma tomentosum	Cd	Mohsenzadeh et al. (2014)
Trichoderma viride	Cr & Pb	Sugasini et al. (2015), Migahed et al. (2017)
Wickerhamomyces anomalus M10	Cr	Irazusta et al. (2018)

Basidimycetes	*Antrodia xantha Shiga-1F*	Cu	Hattori et al. (2015)
	Auricularia polytricha	Cu, Zn & Hg	Yang et al. (2014), Li et al. (2018)
	Cantharellus cibarius Fr.	Cd	Drewnowska et al. (2017)
	Coriolopsis sp. (1c3 KM403574)	Al, Cr, Pb	Chen et al. (2017)
	Fomitopsis cf. meliae	Zn, Cu, & Pb	Kaewdoung et al. (2016)
	Fomitopsis meliae	Cd, Cu, Pb, & Fe	Oladipo et al. (2017)
	Fomitopsis palustris TYP-0507	Cu	Hattori et al. (2015)
	Ganoderma aff. Steyaertanum	Zn, Cu, Cd and Pb	Kaewdoung et al. (2016)
	Phanerochaete chrysosporium	Cd, Cr, Zn, Pb, Cu, & Ni	Sepehr et al. (2014), Chen et al. (2015), Zuo et al. (2015), Huang et al. (2017)
	Pleurotus eryngii	Cu, Zn & Hg	Li et al., (2018)
	Pleurotus florida	Cu	Packiyam et al. (2014)
	Pleurotus ostreatus	Cu, Zn, Hg & CdS	Borovaya et al. (2015), Li et al. (2018)
	Pleurotus ostreatus HAU-2	Cd & Cr	Li et al. (2017)
Deuteromycetes	*Alternaria sp.*	Ni & Cd	Netpae et al. (2015), Costa et al. (2017)
Zygomycetes	*Mucor*	Cr	Sakthivel et al. (2016)
	Mucor indicus	Pb	Samadi et al. (2017)
	Rhizomucor pusillus	Pb, Cr & Cd	Qayyum et al. (2016)
	Rhizophagus irregularis	Cd	Yao et al. (2013), Huang et al. (2018)
	Rhizopus arrhizus UCP 402	Cd	Freitas et al. (2015)
	Rhizopus microspores	Cd, Cu, As and Fe	Oladipo et al. (2017)
	Rhizopus oryzae	Zn and Cu	Tahir et al. (2017)

In case of metal tolerance in fungi, the listed studies in Table 3.3 are not much focused on HMs tolerance mechanism, so a clear insight on fungal (from ascomycete class) tolerance towards HMs is not clear. But, metal tolerance and removal mechanism that have been discussed in **section 3.4.3** are common for all the types of fungi, not specific to ascomyctes. Besides, it is a question remains to resolve that why

majority of HMs tolerant fungus belong to ascomycete class and need detailed experimentation as investigated by Challacombe et al. (2019) to resolve this question.

3.4.2 Heavy metal removal by fungi

The interaction between fungi and HMs may be positive (no or less affected with presence of HMs) or negative (inhibition of growth and metabolic rate or death of the fungus in presence of HMs). The positive interaction of fungi with HMs (higher fungal resistance towards HMs) are seems to a new approach of fungi in HMs removal from wastewater. The researchers have reported number of fungi having multi-metal removal capacity in growing/viable form and in dead biomass form of the fungi (Chakraborty et al., 2014; Kan et al., 2015; Kariuki et al., 2017; Li et al., 2018; Xu et al., 2015; Zang et al., 2016). In the field of bioremediation, fungi have great potential for their application in HMs remediation. In the ecosystem, fungi are already working as decomposer with number of enzymatic activity which specifying them for remediation of HMs and other pollutants.

3.4.2.1 Fungi and their process of Application

The HMs pollution is the serious problem of the environment to be concern. The issues of HMs pollution in water are important to concern due to their harmful impact on human health as well as the environment. The researcher reported diverse group of fungi for the reduction of HMs from wastewater in which *Aspergillus, Trichoderma, Fusarium, Penicllium* species have potential to remediate many HMs contaminated wastewater (Chen et al., 2017; Dey et al., 2016; Dhami et al., 2017; Mohsenzadeh et al., 2014; Pundir et al., 2018; Sharma et al., 2016; Xie et al., 2014). In remediation of HMs, fungi have been used in two ways; (a) in growing form (b) in dead biomass form. In growing/viable form, fungus should have tolerance ability towards pollutant (HMs) because HMs may toxic in nature and can inhibit the growth of the fungi. While, in case of dead or dried biomass form, the heavy metal removal is basically driven by surface functional groups of biomass, so there is no need of tolerance characteristics of fungus. Infact there is importance of adsorption characteristics of fungus biomass for a particular pollutant that has been selected to be removed from contaminated water. An overview on remediation of HMs by fungi from wastewater is shown in Fig. 3.3.

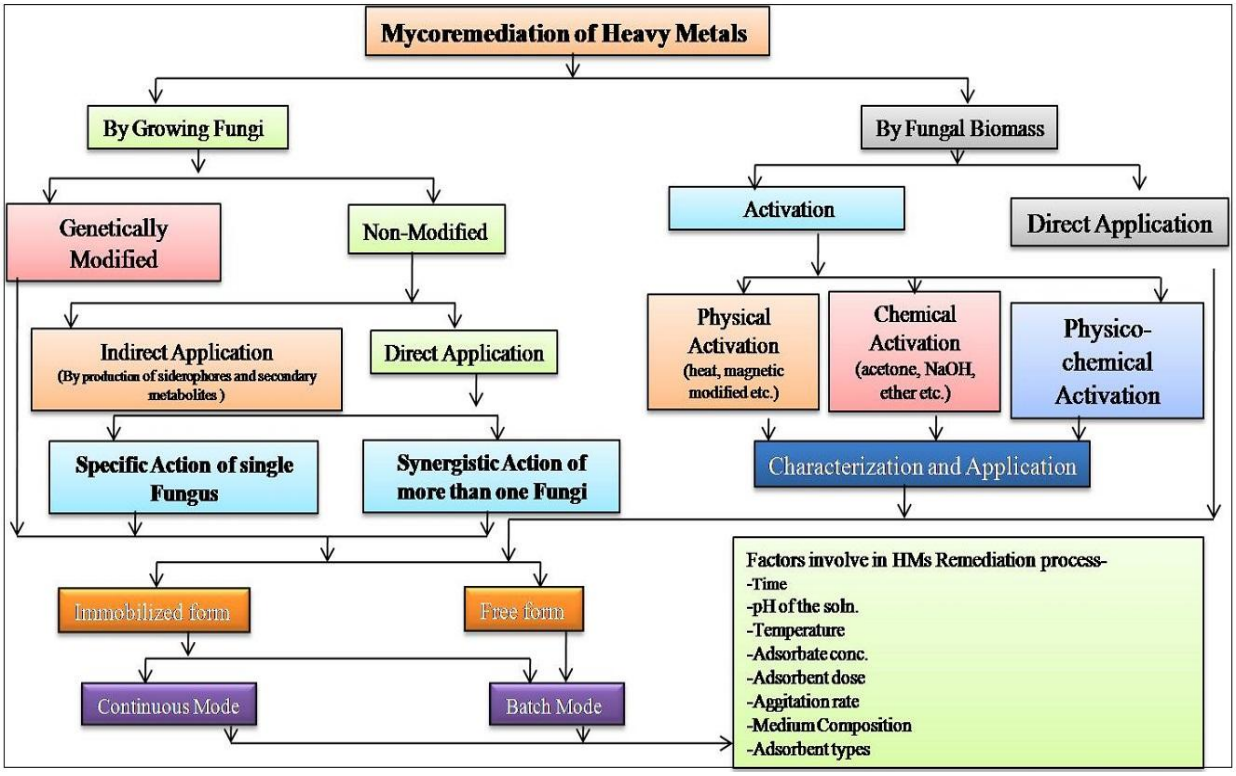

Fig. 3.3. Techniques in removal of heavy metal by growing fungi and fungal biomass from waste water.

3.4.2.1.1 Growing form of fungi

Fungi application in growing form is an important method which is based on the tolerance and metabolic rate of selected fungi against particular pollutant. The benefit of growing fungi utilization in wastewater is that it has self-replenishment ability which specified its use in continuous condition. Fungal tolerance towards HMs may be because of bio-accumulation or biotransformation (bio-synthesis or bio-reduction) or surface adsorption etc. In the growing form, fungi are applied by their immobilization on any supporting medium for application in continuous mode (Sathvika et al., 2015; Sriharsha et al., 2017) or their direct implementation with contaminant solution in batch mode (Chang et al., 2016; Li et al., 2018; Oladipo et al., 2017). Some fungal species such as *Aspergillus niger* has capacity to remove different types of HMs such as lead; Pb, cadmium; Cd, nickel; Ni, chromium; Cr, copper; Cu, cobalt; Co, zinc; Zn and manganese; Mn (Fomina et al., 2017; Iram et al., 2015; Holda et al., 2016; Mirazimi et al., 2015; Mondal et al., 2017; Olubunmi et al., 2016; Sakthivel et al., 2016; Sriharsha et al., 2017; Tahir et al., 2017). *Trichoderma harzianum* and *Trichoderma viride* showed the tolerance against Cd, Pb, Cu, Zn Ni, Fe and reported as multi-metal adsorptive fungi (Joshi et al., 2011; Mohsenzadeh et

al., 2014; Migahed et al., 2017; Sugasini et al., 2015; Wang et al., 2013). A number of fungal species have been reported to remove HMs from aqueous system and some of them are listed in Table 3.4 which has been used in growing form in batch mode and some of them in continuous mode too.

3.4.2.1.2 Fungal biomass form

Fungal biomass basically represents the dead and dried biomass of the fungi. In this case, HMs removal is mainly driven by adsorption mechanism which depends on functional group available on the cell-surface of the applied fungal biomass. Surface functional groups availability varies with molecular composition of adsorbent (fungal biomass) and its surface area. However, physicochemical modification of biomass enhanced the adsorption potential of pollutant. There are two types of techniques used to enhance the adsorption properties of biomass; physical and chemical treatment.

Physical treatment: Physical modification is basically done to create uniqueness (such as increase the surface area) in fungal biomass such as heat treatment which generally applies to remove the moisture from adsorbent. But some time it is helpful in reduction of anti-adsorptive functional group and also helpful to expose some adsorptive functional group (active sites). Heat or thermal activation of biomass are using from the ancient time such as biochar preparation. Conversion of fungal biomass into micro/nano scale adsorbent is the emerging research field which attributed with fast growing fungi. Because the fast growing fungi can be easily cultivated for the large scale biomass production. The micro/nano conversion of fungal biomass increases the surface area which is directly associated with increase in availability of active sites. Inthorn et al. (2014) reported magnetically modified biogenic manganese oxides (MMBMOs) by *Acremonium strictum* strain KR21-2 as adsorbent in removal of Cd^{2+}, Cu^{2+}, Ni^{2+} and Co^{2+} which revealed a new field in biomass treatment.

Table 3.4. Fungal species and their heavy metal removal capacity from different type of medium and their affecting factors

S.N.	Name of the Fungi	Name of the Pollutant	Removed amount	Applied Medium	Initial Concentration of pollutant	pH of the Medium	Incubation Temperature	Duration of Experiment	Agitation rate	Reference
1	*Aspergillus flavus*	$Cu_{(II)}$	97%	Aqueous solutions	-	9	-	20 hours	150rpm	Iram et al. (2015)
		$Pb_{(II)}$	99%	Yeast peptone glucose medium	-	-	25°C	7 days	two step process, 150 rpm	Qayyum et al. (2016)
		Fe	94%	Fe treated PDB medium	1000mg/L	-	room temperature	14 days	-	Bano et al. (2018)
		Mn	91%	Mn treated PDB medium	1000mg/L	-	room temperature	14 days	-	Bano et al. (2018)
2	*Aspergillus flavus strain KRP1*	Hg	97.50%	-	10 mg/L	5.7	30°C	7 days	130 rpm	Kurniati et al. (2014)
3	*Aspergillus foetidus*	Cd	79%	Liquid medium	100 mM	5	32 ±1°C	24 hours	175rpm	Chakraborty et al. (2014)
4	*Aspergillus niger*	Pb(II)	23%	Liquid medium	250 Mm	-	28 °C	24 hours	120 rpm	(Chakraborty et al., 2014)
5	*Beauveria bassiana*	$Cr_{(VI)}$	61.10%	Cr treated composite media	30 mg/L	6.5–7.0	30°C	5 days	150 rpm	Gola et al. (2016)
		Cd(II)	63.40%	Cd treated composite media	30 mg/L	6.5–7.0	30°C	5 days	150 rpm	Gola et al. (2016)
		Zn(II)	67.80%	Zn treated composite media	30 mg/L	6.5–7.0	30°C	5 days	150 rpm	Gola et al. (2016)
6	Indigenous	Pb(II)	92.73%	Pb treated	-	6	28–30 °C	96 hours	150 rpm	Gururajan et

	fungal isolates (Mangalore, India)			Dextrose Peptone medium						al. (2018)
7	*Mucor indicus*	Pb(II)	97–99%	Lead treated sugar soln.	300 mg/L	-	-	24 hours	-	Samadi et al. (2017)
8	*Penicillium simplicissimum*	Cu	230 mmol/kg	Cu treated PDB medium	-	-	28±1°C	4 days	-	Mohammadian et al. (2017)
9	*Penicillium sp.*	Cd	140mg/g	Aqueous solutions	100mg/L	-	37°C	-	150 rpm	Costa et al. (2017)
10	*Phanerochaete chrysosporium*	Pb(II)	91.30%	aqueous medium	50 mg/L	-		168 hours	-	Huang et al. (2017)
11	*Rhizomucur pusillus*	Cd	77%	Yeast peptone glucose medium	-	-	25°C	7 days	two step process, 150 rpm	Qayyum et al. (2016)
12	*Simplicillium chinense (KX425621)*	Pb(II)	80.60%	Aqueous solutions	100mg/L	5 ± 0.2	25 ± 2°C	7 days	150 rpm	Chen et al. (2017)
13	*Sterigmatomyces halophilus*	Cd	91%	Cd treated PDB medium	1000mg/L	-	room temperature	14 days	-	Bano et al. (2018)
14	*Trichoderma asperellum*	Cd	91.06%	Aqueous solutions	100mg/L	9	room temperature	2 months	-	Mohsenzadeh et al. (2014)
15	*Trichoderma asperellum (KP792512)*	Pb(II)	57.10%	Aqueous solutions	100mg/L	5 ± 0.2	25 ± 2°C	7 days	150 rpm	Chen et al. (2017)

Chemical treatment: Chemical treatments are generally used to enhance the active sites and its uniform distribution on surface of adsorbent which are responsible for adsorption of HMs. In case of plant biomass, the researchers have used many types of chemical (such as zero valent iron) to enhance the adsorptive properties. While, for fungal biomass activation workers have reported the use of some chemical such as NaOH, HCl, acetone, ether etc. to enhance the adsorptive properties of fungal biomass (Zang et al., 2017).

Generally fast growing fungi are used for adsorption of HMs because the biomass cultivation is easy in case of fast growing fungi. *Pleurotus ostreatus* (Vaseem et al., 2017), *Pleurotus eryngii* (Kan et al., 2015; Amin et al., 2016), *Aspergillus niger* (Hajahmadi et al., 2015; Holda et al., 2016) and *Agaricus* sp. (Ertugay et al., 2010) are well known as fast growing fungal species which have been applied in dead form as an efficient adsorbent. Many fungal species have been used in dead forms which are listed in Table 3.5. Some time fungal biomass is also applied after treatment with some chemicals to increase active sites on its surface. Zang et al. (2017) boiled *Auricularia auricular* biomass in 0.5N NaOH solution, then applied in adsorption of $Cr_{(VI)}$ and reported incremental change in adsorption of $Cr_{(VI)}$.

Fungal biomass have high potential to remove HMs from wastewater, however their adsorption vary with types of pollutants, medium pH, pollutant's concentration and agitation rate. Another most important thing is the characteristics of biomass, basically surface functional groups which primarily affect the adsorption of HMs, has been discussed in **section 3.4.3.1**. In the HMs adsorption investigation many types of kinetic and isotherm model have been used to describe the effect of time on adsorption and HMs interaction with applied adsorbent. Most fitted kinetic model in adsorption of HMs by fungal biomass is pseudo-second-order kinetic model (Hassan et al., 2018; Rashid et al., 2016), however some studies also found that pseudo-first-order kinetic model is best fitted in HMs adsorption to explain adsorption rate (Shokoohi et al., 2019) (Table 3.5).

To examine the relationship between the adsorption and equilibrium concentration, various sorption isotherm models are widely employed for fitting the data. These models basically determine the adsorption behavior of adsorbate (pollutant) on adsorbent (fungal biomass). Most fitted isotherm model in adsorption

are Langmuir and Freundlich isotherm model that describes the adsorption of HMs on fungal biomass (Amin et al., 2016; Hassan et al., 2018; Manorama et al., 2016). The Langmuir isotherm theory assumes monolayer adsoprtion of HMs over a homogeneous biosorbent surface. It support single-layer biosorption theory based on the assumption that all the biosorption sites have equal affinity for adsorbate molecules and there is no transmigration of adsorbate on the surface. While, the Freundlich isotherm is an empirical isotherm employed to describe heterogeneity of system and support the multilayer adsorption of adsorbate on the surface of the adsorbent. Hassan et al. (2018) used *Neopestalotiopsis* sp ASU1 biomass for the biosorption of Cd(II) and Zn(II) and they found that Langmuir isotherm model is best fitted in the Cd(II) and Zn(II) biosorption. While, Freundlich isotherm model is well fitted in the biosoprtion of Hg(II) on the surface of *Pleurotus eryngii* (Amin et al., 2016). Some studies are listed in Table 3.5 which showed that Langmuir and Freundlich isotherm model are the most fitted and can be used to describe the HMs biosorption onto the fungal biomass.

In recent days, plant biomass originated biochar has also attracted the researcher and has been broadly investigated its application in HMs biosorption. Studies showed it as an efficient biosorbent for HMs removal. Biosorption basically varied with characteristic of biosorbent and nature of the pollutants, but the preparation cost of biochar may affect its use in the treatment of contaminated water. Because, studies have suggested that biochar prepared at high temperature (above 400 °C) are efficient in biosorption of HMs (Shi et al., 2019). However, fungi can be cultivated on low graded waste materials (agro-waste) that enhance their applicability in treatment of wastewater and thus, water treatment cost can be reduced.

Table 3.5. HMs adsorption efficiency of some fungal bio-adsorbent and plant originated biochar

Name of the adsorbent	Name of the pollutant	metal concentration	pH	Temperature	dose of adsorbent	contact time	Removal	fitted kinetic model	Isotherm model	Reference
Fungi used as bio-adsorbent										
Pleurotus eryngii	Hg(II)	1 mg/L	7	30 °C	0.35 g	30 min	77.40%	pseudo- second order	Freundlich model	Amin et al. (2016)
Neopestalotiopsis sp ASU1	Cd(II)	200 mg/L	7	30 °C	50 mg	30 min	185.3 mg/g	pseudo-second-order	Langmuir model	Hassan et al. (2018)
Neopestalotiopsis sp ASU1	Zn (II)	200 mg/L	6	30 °C	50 mg	30 min	153.8 mg/g	pseudo-second-order	Langmuir model	Hassan et al. (2018)
Pencillium fellutinum biomass immobilzed with Na-bentonite	Ni(II)	100 mg/L	6	30 °C	0.05 g	60 min	76 mg/g	pseudo-second-order	Langmuir model	Rashid et al. (2016)
Pencillium fellutinum biomass immobilzed with Na-bentonite	Zn (II)	100 mg/L	5	30 °C	0.05 g	60 min	56 mg/g	pseudo-second-order	Langmuir model	Rashid et al. (2016)
Aspergillus niger strain SF-6095	$Cr_{(VI)}$	200 mg/L	2	room temperature	1 g/L	300 min	98.25%	-	Langmuir Model	Manorama et al. (2016)
Aspergillus awamori	Ni (II)	55 mg/L	6	25 °C	0.25 g/ 100 mL	3 h	7.5 mg/L	-	Redlich–Peterson	Shahverdi et al. (2015)
Aspergillus terreus	Cd(II)	20 mg/L	7	25 °C	1g	90 min	94%	pseudo-first-order	Freundlich isotherm	Shokoohi et al. (2019)

Aspergillus terreus	$Cr_{(VI)}$	20 mg/L	7	25 °C	1 g	90 min	89%	pseudo-first-order	Freundlich isotherm	Shokoohi et al. (2019)
Penicillium sp . M RF1	Ni(II)	639 mg/L	5.5	30 °C	7.5 g/L	140 min	74.60%	-	Freundlich isotherm model	Sundararaju et al. (2020)
Plant biomass originated Biochar										
Artemisia argyi (AS600)	Cu(II)	50 mg/L	-	-	0.1 g/50 mL	45	18 mg/g	pseudo-second-order	Langmuir model	Song et al. (2019)
Artemisia argyi (AS600)	$Cr_{(VI)}$	50 mg/L	-	-	0.1 g/50 mL	45	15 mg/g	pseudo-second-order	Freundlich isotherm	Song et al. (2019)
Tobacco petiole pyrolytic biochar (TPBC300)	$Cr_{(VI)}$	250 mg/L	1	ambient temperature	2.5g/L	540 min	99.02%	pseudo-second-order	Temkin model	Zhang et al. (2019)
Rice husk biochar (RH700)	Pb	1 mM	6	-	0.1g/20 mL	48 h	26.7 mg/g	pseudo-second-order	Freundlich isotherm	Shi et al. (2019)
Date seed-derived biochar	Pb	0.50 mM	6	23 ± 2 °C	0.10 g/10mL	24 h	0.045 mM/g	pseudo-second-order	Langmuir and Freundlich	Mahdi et al. (2018)

Another basic problem which is associated with the use of biochar as well as fungal biomass is its treatment and disposal after its final application in wastewater treatment which needs high cost. To remove this disadvantage, researcher applied reuse approach for these adsorbent where it can be washed with low (pH<4) or high (pH>8) pH washing solution to desorbs the adsorbed HMs from the surface of the adsorbent and can be reused (Rashid et al., 2016). But, after few cycles, the adsorption efficiency of adsorbent gets reduced. On another hand used washing solution is corrosive and its direct disposal can cause harmful impact on the environment. As an alternative to these disadvantages, different techniques are developed and can be applied including production of composite material and production of construction bricks etc. (Isaza-Pérez et al., 2020).

3.4.2.2 Application of growing form of fungi

3.4.2.2.1 HMs removal by single fungal species

Most of the studies in the field of bioremediation have applied as single bioremediation agent for the study. Here this approach is more basic and easy to optimize the other influencing parameter. Similarly, in mycoremediation one fungus has been utilized for removal of one HM (Table 3.4) or more than one HMs in most of the studies (Xu et al., 2015; Desai et al., 2016; Chen et al., 2017; Qian et al., 2017). It is found in the literature that most studies are focussed on only single heavy metal for removal because all the fungal species are unable to tolerate all the types of HMs and due to metal toxicity the growth of the fungus is severely inhibited at very less concentration of some HMs. Several studies targeted the binary metal solution for removal by tolerant fungus and some recent studies also targeted multiple metal contaminated aqueous solution or wastewater for removal of multiple HMs with single fungal isolate (Bano et al., 2018; Gola et al., 2016). But, it is to be remembered that very few isolate has been reported that have the potential to remove more than two HMs. So, this field is remains to explore and has great importance for industrial effluent treatment due to the fact that industrial effluent contains multiple HMs. *Aspergillus flavus*, *A. gracilis* (Bano et al., 2018), *Beauveria bassiana* (Gola et al., 2016), *Aspergillus lentulus* (Mishra and Malik, 2012) are the species that have the potential to remove multiple HMs from wastewater.

It is right that all the types of fungal species are unable to tolerate more than one metal but posses many types of metabolic activities and are the major sources of enzyme that are able to degrade many types of organic pollutants. The industrial, developmental and agricultural activities produce not only heavy metal but they also produces number of organic pollutant that have serious environmental concern. These pollutants may be dyes, phenolic products, pesticides, polyaeromatic hydrocarbon etc. In the recent year it attracted the researcher for simultaneous removal/bio-transformation of HM and degradation of organic contaminant. This field of the study is very emerging that offering a big gap for the study. Gola et al. (2018) investigated the applicability of *Beauveria bassiana* for the removal of dyes (Reactive remazol red, Yellow 3RS, Indanthrene blue and Vatnovatic grey) and HMs [$Cr_{(VI)}$., Zn(II), Cu(II), Cd(II), Pb(II) and Ni(II)] from mix solution and significant amount of removal was reported. *Acremonium* sp. P0997 showed efficient removal potential for polyaeromatic hydrocarbon (naphthalene, fluorene, phenanthrene, anthracene, and fluoranthene present alone) and also has high resistance to HMs (Mn^{2+}, Fe^{2+}, Zn^{2+}, Cu^{2+}, Al^{3+}, and Pb^{2+}) (Ma et al., 2014).

3.4.2.2.2 Synergistic application of two or more microbes

Synergistic microbial utilization is a novel approach in HMs remediation where two microbes are used with their synergistic action in HMs removal. But here compatibility test is needed for both microbes with each-other because microbe generally produces many types of metabolites in normal as well as in stressed conditions. So, these metabolites may have negative consequences on the synergist microbes, can inhibit the growth of synergist and affect the HMs removal potential of the implemented system. Therefore, compatibility test is an important step in this method and by this test we can verify the survivability of both microbes with each-other in normal or stress conditions. There can be made a pair-ship of fungus-fungus or fungus-bacteria. The synergistic mechanism also played by large plant with their rhizospheric fungi and other microbes which increases the HMs tolerance capacity of plants (Xie et al., 2014; Yao et al., 2013). Some researchers worked on synergistic action of fungus with another fungi and bacterial species in HMs remediation (Herath et al., 2014; Huang et al., 2018; Migahed et al., 2017; Olubunmi et al., 2016). Fungal consortium is the best example of synergistic action in fungi that have more efficiency to remove HM from wastewater.

3.4.3 Heavy metal tolerance and Removal mechanism in fungi

3.4.3.1 Fungal cell wall and its role in metal sorption

Heavy metal frequently found in the polluted environment. HMs present in polluted environment first interacts with cell surface of the organism. The fungal cell surface is different from the other organism. So, to understand the interaction of cell surface of the fungi with HMs and its possible role in adsorption and accumulation of metal, the structure of the cell wall of the fungi and its composition should be known. It is found with the electron microscopic investigation of the negative stained cell wall of the fungi that the thickness of electron-transparent internal layer is of about 70-100 nm. However, thickness of the cell wall may vary with fungal growth conditions and their genetic status, and an electron-dense outer layer (Osumi et al., 1998). The brewing yeast may be composed of 200 nm of the electron-transparent inner layer. The inner layer maintained the mechanical strength of the wall which is made up of chitin and β1, 3-glucan. It carries about 50-60% weight of the total dry weight of cell wall (Moukadiri et al., 1999; Kang et al., 2018). The carbohydrate of the cell surface contains multiple phosphodiester bridges by their side chains resulting in abundant negative charges on surface of the cell at physiological pH values (Jigami et al., 1999). The negative charged cell wall surface play crucial role in adsorption of positively charged metal ion via electrostatic attraction. The heavily glycosylated mannoproteins of outer layer of the cell wall (Cappellaro et al., 1994; Kang et al., 2018) is implicated among in others cell-cell recognition mechanism (Reynolds et al., 2001) and also restricts the accessibility of plasma membrane and internal part of the cell to foreign compounds (enzymes, protein and pollutants) (Cappellaro et al., 1994). Polysaccharides and β 1, 3-glucon generate alkaline sensitive linkage in cell wall which supports fungal growth in acidic medium (Moukadiri et al., 1999). These side chains also provide hydrophilic properties to the cell wall which may be useful to retain water on fungal cell surface and provide resistance to drought conditions. About one third part of the wall (dry weight) is accounted by the outer protein layer. The carbohydrate fraction of well glycosylated mannoproteins of the outer cell wall layer is frequently accounts over 90% (w/w). The proteins of the cell wall covalently linked to β 1, 3-glucan-chitin network either directly or indirectly via a β 1, 6-glucan moiety (Fig. 3.4). Furthermore, some of proteins are also disulfide-bonded to other proteins of the cell wall that may also provide active sites for metal sorption via

metal-thiol group complexation (Moukadiri et al., 1999; Kang et al., 2018). The numerous negative charges are on the cell surface of yeast due to phosphodiester bridges in both N- and O-linked mannosyl side chains (Jigami et al., 1999) which is also helpful in metal binding via electrostatic attraction. It can be concluded that fungal cell wall mostly made up of protein, polysaccharides, polyphosphates, polypeptide, lipid, chitin, inorganic ions etc. (Ayangbenro et al., 2017; Kang et al., 2018) which contain number of functional groups such as –COOH, -OH, $-NH_2$, =NH, -SH, $–O-CH_3$ etc. These functional groups are also detected at different spectra with FTIR analysis and with some other techniques on dead fungal biomass (Sathvika et al., 2015; Kumar et al. 2019) which is mainly responsible for the adsorption of HMs on the surface of fungal cell.

Bioadsorption is basically a surface phenomenon that occurred on the surface of biomass. In case of fungi, it can also be pronounced as mycoadsorption. Mondal et al. (2017) reported that IR (infra red) bands 3265 cm^{-1} (alcoholic –OH stretching), 1618 cm^{-1} (carboxylic acid (–COOH), and 1417 cm^{-1} (–C–H and –N–H stretching) of unloaded *Aspergillus niger* are shifted to 3280 cm^{-1} (─OH and –NH stretching), 1614 cm^{-1} and 1361 cm^{-1} after adsorption of $Cr_{(VI)}$. They concluded that –OH and –N–H group are mostly accountable for the decontamination of $Cr_{(VI)}$. Lopez-Fernandez et al. (2018) reported a new band of 938 cm^{-1} in adsorption of $U_{(VI)}$ which was shifted from 917 cm^{-1} (Romero-Gonzalez et al., 2016) represent the stretching of U=O associated to the accumulation of UO_2^{2+} on the surface of fungal cell wall. Role of oxalic acid as signified by the IR spectrum at 2495 ± 5, 1700 ± 5, 1201 ± 5, 1261 ± 5 and 1126 ± 5 cm^{-1} and thiol groups (-SH) at 2561 ± 5 cm^{-1} respectively in the biosynthesis of PbS by *Aspergillus terreus* have been studied (Jacob et al., 2016) (Table 3.6). Decrease in the intensities of IR spectrum ranges from 1650 to 1450 cm-1 and 1230 to 1030 cm^{-1} are recognized after adsorption of Cd(II) in *Thamnidium elegans* cells embedded in acrylic network of p(3-Methoxyprophyl) acrylamide p(MPA) enriched with 2-Akrylamido-2-methyl-1-propane sulfonic acid (AMPS). Copper ions adsorption with the amine, carboxyl and phosphate groups was reported by Majumdar et al. (2008) (Table 3.6). Majumder et al. (2017) reported that C–O groups oxidized into C=O under $Cr_{(VI)}$ and also found the involvement of phosphate and sulfonyl groups in coordination of chromate ions. They also found the shift in the peak from 1029 cm^{-1} to 1033 cm^{-1} and 531 cm^{-1} to 576 cm^{-1} which represents the formation of $Cr_{(III)}$-phosphate compound and formation of $Cr(OH)_3$. Mohanty et al.

(2016) reported that IR band of 476.33 cm^{-1} and 417.51 cm^{-1} attributed to MnOx stretching, bending and wagging vibrations for Mn_2O_3 and MnO_2 respectively in Mn treated *Aspergillus oryzae* biomass.

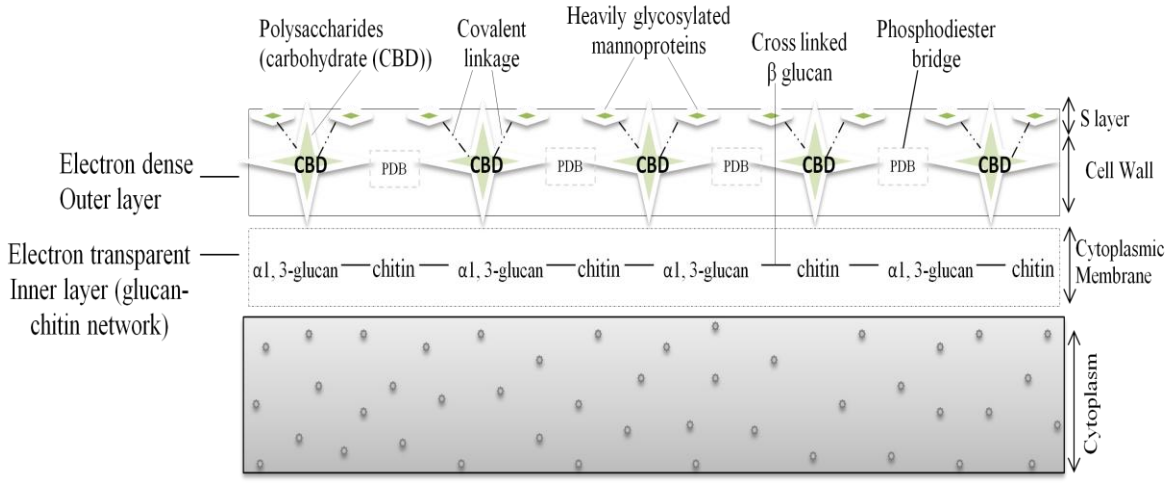

Fig. 3.4. Schematic diagram shows the structure of fungal cell wall.

Table 3.6. IR bands and observed Functional group in HMs treated fungal biomass

Fungal Biomass	IR Band	Functional Group Stretching	Reference
Aspergillus niger	3265 cm^{-1} 1618 cm^{-1} 1417 cm^{-1} 1031 cm^{-1}	alcoholic –OH stretching carboxylic acid –COOH, –C–H, –N–H stretching amine –C–N stretching	Mondal et al. (2017)
Rhodotorula mucilaginosa	1543 cm^{-1} 1050 and 1150 and 1070-1150 cm^{-1} 1390 cm^{-1}	double bond of the carbonyl, C=O, group from amides C-O stretching stretching of carboxylate anions (COO^-)	Lopez-Fernandez et al. (2018)
Mucorales fungi	3447 cm^{-1} 2888 cm^{-1} 1657 cm^{-1} 1555 cm^{-1} 1381 cm^{-1} 1086 cm^{-1}	O-H stretching vibrations stretching vibrations of aliphatic C-H; carbonyl groups stretching of C=O N-H deformation in CONH plane, including amide CN bond stretching plus CH_3 wagging C-O-C bonds	Berger et al. (2018)
Aspergillus	2561±5 cm^{-1}	thiol groups	Jacob et al.

terreus	2495±5, 1700±5, 1261±5, 1201±5 and 1126±5 cm^{-1}	involvement of biosynthesis of PbSe	(2016)
Aspergillus fumagatus	3383 cm^{-1}	Amide C=O	Kalyani et al. (2018)
	2361 cm^{-1}	O-H stretching acid	
	1723 cm^{-1}	C=O stretching of Aldehyde, Ketone, Ester	
	1581 cm^{-1}	C=C stretching Aromats	
	1389 cm^{-1}	C-O stretching	
	1112 cm^{-1}	C-C stretching of Ketones	
	616 cm^{-1}	C-Cl stretching Chloroalkanes	
Polyethylenimine-Modified *Penicillium chrysogenum* biomass	3200 to 3600 cm-1	overlapping of OH and NH stretching	Deng et al. (2005)
	1115 cm^{-1}	alcoholic C-O stretching	
	1161 cm^{-1}	C-N stretching vibration	
	1663 cm^{-1}	CdO stretching in carboxyl or amide groups	
	1551 cm^{-1}	N-H bending	
	1740 cm^{-1}	$-COO^{-}$ stretching of ester	
Thamnidium elegans cells in acrylic network of p(3-Methoxyprophyl)acrylamide p(MPA) enriched with 2-Akrylamido-2-methyl 1-propane sulfonic acid (AMPS)	3442 and 3078 cm^{-1}	O-H and N-H stretching	Çelik et al. (2017)
	2932 cm^{-1}	C-H stretching vibrations of CH_2 and CH_3	
	1404 cm^{-1}	CH_2 bending vibrations	
	1363 cm^{-1}	CH_3 bending vibrations	
	1663 cm^{-1}	C=O stretching of acids and amides (amide I)	
	1555 cm 1 and 1458 cm^{-1}	N-H and C-N stretching of the amide II and III	
	1223 cm^{-1}	asymmetric stretching of C-O-C vibrations	
	1192 cm^{-1}	symmetric stretching of C-O-C vibrations	
	1042 cm^{-1}	S=O stretching vibration	
	627 and 528 cm^{-1}	C-N-C scissoring vibrations	
Hexadecyl-trimethylammonium bromide and dodecylamine treated *Penicillium chrysogenum*	3423.8 cm^{-1}	NH_2 asymmetric stretch mode of amines	Loukidou et al. (2003)
	2925.1 cm^{-1}	C–H groups stretching	
	1636.1 cm^{-1}	CO stretching mode, conjugated to a NH deformation mode (amide 1)	
	1559.7 cm^{-1}	NH deformation mode conjugated to C=N (amide 2)	
	1384.2 cm^{-1}	amide 3 or sulfamide band	

biomass	1071 cm^{-1}	C–O stretching in carbonyl	
	1673 cm^{-1}	C=O stretching in carboxyl groups	
	1150 cm^{-1}	P=O stretching	
	1040–910 cm^{-1}	P–OH stretching	
	1050–970 cm^{-1}	P–O–C stretching	
Mucor rouxii	3398.3 cm^{-1}	N–H or O–H stretching vibrations	Majumdar et al. (2008)
	2920–2850 cm^{-1}	alkyl chains	
	1654.8 cm^{-1}	C=O stretching mode (amide 1)	
	1654.8 cm^{-1}	N–H bending (amide II)	
	1544.9 cm^{-1}	C–N stretching	
	1407.9 cm^{-1}	COO^- of the carboxylate group	
	1078.1–995.2 cm^{-1}	phosphate group	
Arthrinium malaysianum	3422 cm^{-1}	–NH stretching in amides and O–H stretching vibration in alcohol and/or phenol	Majumder et al. (2017)
	2958 cm^{-1}	C–H stretching vibrations of $–CH_3$	
	2927 cm^{-1}	C–H stretching vibrations of CH_2	
	1404 cm^{-1}	C–N stretching	
	1239 cm^{-1}	C–H stretching in amide III and C–O stretching	
	1077 cm^{-1}	P–O–C and P–OH stretching	
Aspergillus oryzae	1089.58 cm^{-1}	C-N stretching of Aliphatic amines	Mohanty et al. (2016)
	775.24 cm^{-1}	N-H wag of Primary and Secondary amines	
	688.46 cm^{-1}	C=C stretch of alkynes	
	540.94, 464.76 cm^{-1}	CH_2 vibrations of Polysaccharides	
	1377.89 cm^{-1}	C-O stretching of Alcohols, Carboxylic acid, esters, ethers	
	1249.65 cm^{-1}	C-N stretching of Aliphatic amines	
Termitomyces clypeatus	1299.79 cm^{-1}	P=O bands of polysaccharides	Ramrakhiani et al. (2011)
	1078.01 cm^{-1}	C–O bands of polysaccharides	
	1500 to 1650 cm^{-1}	primary, secondary and tertiary amines and ammonium salts of carboxylic acid	
	1403.92 cm^{-1}	sulfonyl, sulfonamide	

3.4.3.2 Reactive oxygen species (ROS) production and Heavy metal

All living organisms showed many types of responses (morphological, physiological and molecular) in stress conditions and also under HMs stress condition due to its toxic characteristic. ROS production under HMs stress is more frequently reported phenomenon in plant and other living organisms (Singh et al., 2016). This

phenomenon is also reported in fungi such as *Fusarium solani*, *Penicillium janthinellum* and *Pleurotus ostreatus* HAU-2 in the presence of $Cr_{(VI)}$, Cd and Pb (Li et al., 2018b; Kumar et al., 2019; Teng et al. 2017). In higher plant, many pathways have been reported for ROS production such as chloroplast, mitochondria, peroxisome etc. (Singh et al 2016). However, in fungi, over reduction of electron transport chain in mitochondria is might be possible site for ROS production (Keunen et al., 2011). The well known mechanism Haber–Weiss and Fenton reactions may also involve in production of ROS via reacting with redox active heavy metals (Halliwell, 2006; Keunen et al., 2011). Although the ROS production is common phenomenon and its alleviation depends upon its production and consumption. Toxic HMs possibly accelerates the production of ROS in comparison to its consumption in fungi and also in other organism such as $Cr_{(VI)}$ increases the production of ROS. The hydroxyl ($OH^{\bullet}$), superoxide radical ($O_2^{\bullet-}$), singlet oxygen (O) and hydrogen peroxide (H_2O_2) are collectively called as reactive oxygen species due their high reactivity. Out of them hydroxyl radical is most reactive and highly damaging one (Singh et al., 2016). The ROS have positive and negative consequences for all types of organism. ROS are unstable and very reactive and can react with protein, membrane lipid, peptides and macromolecules and oxidizes them, causes many types of negative consequences or oxidative injuries and some time causes cell death (Sharma and Dietz, 2009; Hossain et al., 2012). Collectively negative consequences are called as oxidative stress (Singh et al. 2016). Conversely, ROS has been also seen as signaling molecule and reported as regulator of the several biomolecules. In HMs stress condition, ROS may work as signaling molecules for the production of glutathione, metallothionine, phytochelatines and other thiolic compound that work as metal chelating agents and transport them into vacuoles or outside of the cell through efflux pump (Kumar et al. 2019; Chen et al. 2019; Singh et al. 2016; Banerjee et al., 2019). A complex mechanism of metal tolerance, response, transportation and accumulation in fungi are shown in Fig. 3.5.

3.4.3.3 Fungal response to oxidative stress and Heavy metal

3.4.3.3.1 Enzymatic response to oxidative stress

The redox active HMs highly induces the production of ROS in fungi, one of the major factors for damaging the cell constituents due to oxidative injuries. Fungi

generally counter the oxidative stress by multiple antioxidants mechanism. The antioxidant mechanisms are driven by many types of antioxidants (enzymatic and non-enzymatic) as the cellular immune system. The catalase (CAT), peroxidase (POD) and superoxide dismutase (SOD) are the major enzymatic antioxidants produced under HMs stress. *Pleurotus ostreatus* HAU-2 produces CAT, POD and SOD under the presence of Pb stress (Li et al. 2017a). They reduces/neutralizes the ROS. SOD act with super oxide radical, while CAT react with H_2O_2 and catalyses it into H_2O (Xu et al., 2012; Li et al., 2017a; Karigar et al., 2011; Irazusta et at., 2012, 2018). Bannister et al. (1987) classified the SOD into two families on the basis of their evolutionary homology and metal binding cofactor at the active sites; copper or zinc-containing SOD (Cu/ZnSOD) and manganese or iron-containing SOD (Mn/FeSOD). Cu/ZnSOD and MnSOD induced in the response of ROS toxicity. Jacob et al. (2004) reported that SOD activity increases with increase in incubation period in cadmium-treated ectomycorrhizal fungus *Paxillus involutus* which is essential in detoxification mechanisms of ROS. Teng et al. (2017) found a significant increase in activity of SOD, CAT, POD, Glutathione reductase (GR), glutathione-S–transferase (GST), and level of GSH, GSSG in *Penicillium janthinellum* BC109-2 under Zn stress. The increase in the activity of CAT also reported in *Fusarium solani* (Kumar et al., 2019). The extracellular activity of glucose oxidase (GOD) reported in bioleaching of Cd, Cu, Pb, Zn, Mn, and Cr (Deng et al., 2013). Extracellular GOD activity influences the excretion of metabolites by HMs (Ren et al., 2009). Bbakr1, a member of aldo-keto reductase (AKRs) family, homologous to 2,5-diketo-D-gluconic acid reductase, involved in the development of *Beauveria bassiana* against Cr stress (Wang et al., 2018).

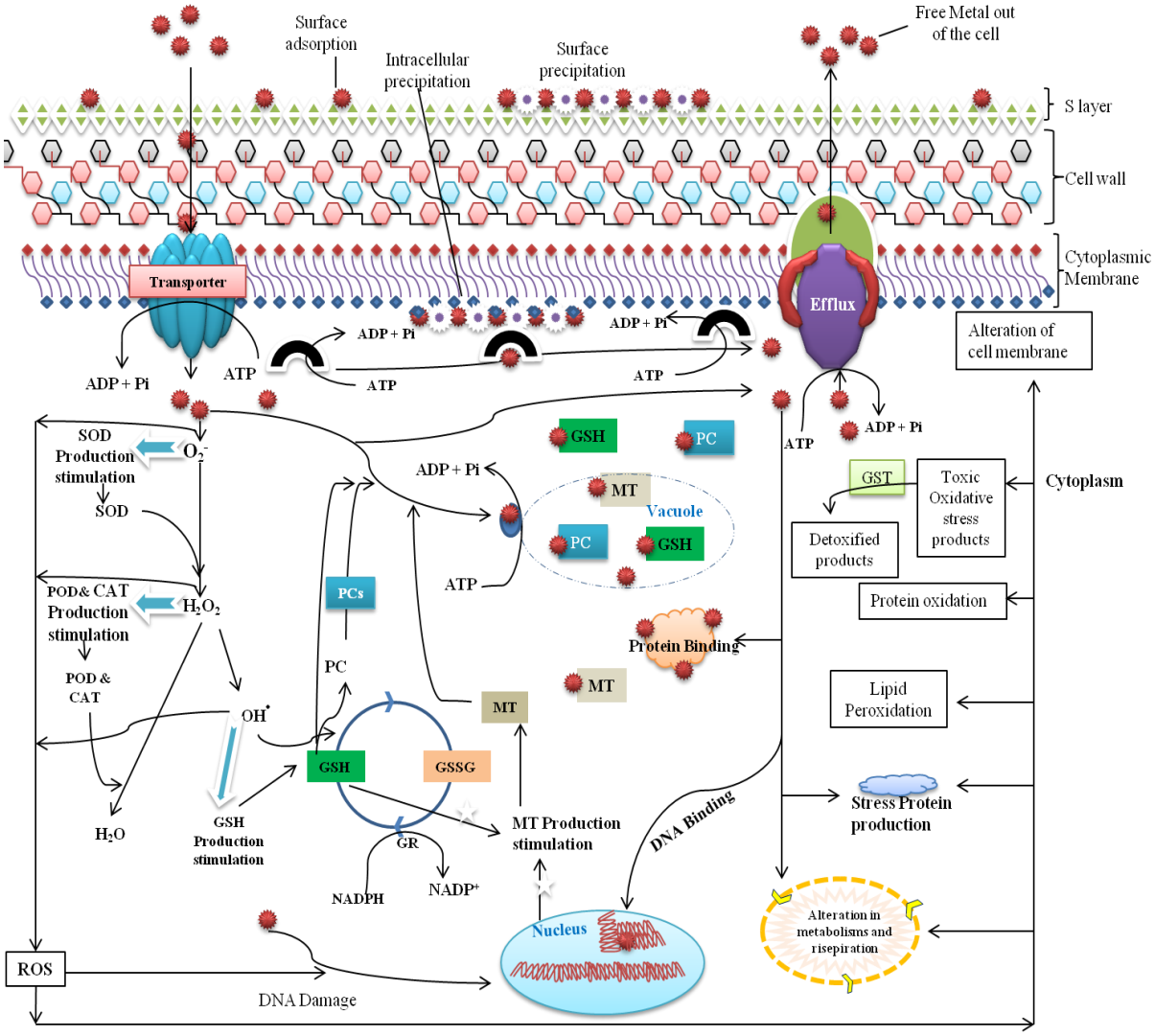

Fig. 3.5. Heavy metal sorption mechanism in fungi, figure (schematic representation) shows the hypothesized metal ion (red sphere) stress response or tolerance mechanisms in fungi. Metal interact with surface cell wall and may adsorb on the surface or uptake by cell inside with the help of transporter. After coming inside of the cell, metal stress produces superoxide anion (O_2^-) which stimulate the production of superoxide peroxidase (SOD) and SOD react with O_2^- and coverted it into H_2O_2. Hydrogen peroxide stimulates the production of peroxidase (POD) and catalase (CAT). POD and CAT catalyzes H_2O_2 into H_2O. The remaining H_2O_2 convert into OH (hydroxyl radical) which is most active agent of reactive oxygen species (ROS) and stimulate the production of glutathione (GSH). GSH and/or metal stimulate the metallaothioneine (MT) and phytochelatein (PC) production, bind metal ion, and also react with OH and form oxidized glutathione (GSSG). Glutathione reductase (GR) reduces GSSG into GSH. MT, PC and GSH involved in metal chelation may transport inside vacuole with the help of transporter. ROS causes alteration in

metabolisms and respiration, DNA damage, protein oxidation, lipid peroxidation, alteration of cell membrane and some time cell death. Diffused metal ion in cytoplasm causes binding of protein, DNA and –SH and -COOH containing molecule and alteration of cell metabolisms and respiration.

3.4.3.3.2 Non-enzymatic response to oxidative stress

Uptake of essential and non-essential metal is a well-known mechanism in the removal of HMs. The essential characteristic of live fungi in the removal of HMs is its tolerance and accumulation of a particular metal (Rehman et al., 2010). The tolerance of the fungi is maintained by many mechanisms. Other than enzymatic antioxidants, non-enzymatic antioxidants also are the major factor that provides tolerance ability to specific fungus for specific metal. However, it is often seen that in single organism, more than one antioxidant are involved in antioxidation mechanism which can be pronounced as multiple antioxidants system. It has been also found that antioxidants vary with the types of pollutant (HMs) within the same organism. Glutathione (GSH) reduces Cd^{2+} toxicity and induces the production of metallothionein to increase the tolerance of the fungi (Singhal et al., 1987). While, in the yeast, glutathione (GSH)-metal complex formation and its exporting into the vacuoles of the cell is one of the major mechanisms of Cd(II) tolerance and detoxification (Li et al., 1997). Rehman et al. (2010) incubated *Candida tropicalis* in Cd(II) and glutathione amended medium and found that intracellular oxidized glutathione level raised from control level, an increase in glutathione and non-protein thiole content was also observed. Thiole is an essential agent in cellular redox signaling and it control/management in fungi and other living organism (algae and plant) (Moran et al., 2001; Pócsi et al., 2004). The presence of Mn(II) induces manganese peroxide (MnP) in detoxification of metal (Karigar et al., 2011). GSH could also react with H_2O_2 in the presence of peroxidase (POD) enzyme and produces oxidized glutathione (GSSG) (Huang et al., 2017; Zhang et al., 2016). In another report, it was found that GSH accumulated inside the cell and could involve in the synthesis of metal sulphide (de Almeida et al., 2004). Li et al. (2017c) reported that Cd improve the level of GSH content while, $Cr_{(VI)}$ did not affected the level of GSH in *Pleurotus ostreatus* HAU-2 . Delalande et al. (2010) suggested that GSH contain two-tailed structure: one tail has thiole groups which can react with Cd and form cadmium-bis-glutathionate (Cd-GS_2) and another tail have γ-Glu residue which is not associated with Cd chelation. Total phenolic component and

proline has also been reported in plant as non-enzymatic antioxidants to relive the oxidative stress by donating the H^+ in neutralization of ROS. The non-protein thiol content was found as $Cr_{(VI)}$ and arsenate complexing agent in fungus (Chen et al. 2019; Wu et al., 2015).

3.4.3.3.3 Role of Protein under HMs stress

Several specific proteins such as heat shocked protein over synthesis are also reported in fungi (Irazusta et al. 2018). They have important role in detoxification and accumulation of HMs. Chaperones protein helped to protect *Candida fukuya-maensis* RCL-3 and *Rhodotorula mucilaginosa* RCL-11 against copper-induced oxidative stress (Irazusta et al., 2016, 2018). A detailed proteomic-based investigation of Cu tolerant *Penicillium janthinellum* strain GXCR and EC-6 have been done by Feng et al. (2017). They found that many proteins are in abundance such as heat shock proteins (Hsps), 60S ribosomal proteins (RPs)/ATP-dependent RNA helicases (ADRHs), 40S RPs/eukaryotic translation initiation actors, elongation factor 1, histone/26S protease regulatory subunit, actin, and proteasome/protein transport proteins. Palmieri et al. (2000) reported over expression of 14-3-3 proteins in *Pleurotus ostreatus* under the exposure of Cu.

3.4.3.3.4 Role organic organic acid under HMs stress

Organic acid secretion has been also reported to relive the HMs stress via binding/chelating of heavy metal in plants. Similarly, the synthesis of organic acid such as malic acid, oxalic acid, pyruvic acid, citric acid, gluconic acid, and succinic acid were detected in *Penicillium chrysogenum* in bioleaching of Cd, Cu, Pb, Zn, Mn and Cr (Deng et al., 2013; Rhee et al., 2016). These organic acid productions have been reported as extracellular and intracellular metabolites. Extracellular secretion mostly causes solubilization of metal and minerals from their surroundings. Extracellular organic acid production by fungi emphasizes its use in biomining purpose to extract metal from low graded ores. However, intracellular organic acid production causes intracellular precipitation of metal and also their translocation for compartmentation in vacuoles (Borovaya et al., 2015; Rhee et al., 2015). The intracellular production of these organic acids may also belong to their intracellular HMs precipitation (Rhee et al., 2015).

3.4.3.3.5 Energy metabolism under HMs stress

Several researchers have reported that metal stress increases the energy demand in fungi (Feng et al., 2017; Irazusta et at., 2016). Some metal transporter or hyper-accumulation processes are closely associated with energy metabolisms or ATP-driven mechanism (Visioli and Marmiroli, 2013; Feng et al., 2017; Irazusta et al., 2018). Decreased in the level of glucose and D-fructose indicates that the demand of energy increase under Cu stress (Feng et al., 2017). Glycolysis, gluconeogenesis and the citrate cycle (TCA) greatly affected by Cu treatment in *P. janthinellum* strain GXCR. Decreased in acetyl-CoA, carboxylase and fatty acid synthetase are found in *P. janthinellum* strain GXCR and EC-6 under the stress of Cu (Feng et al., 2017). Over synthesis of alcohol dehydrogenase, enolase 1, phosphoglycerate kinase, and glyceraldehyde-3-phosphate dehydrogenase increases the demand of energy because these enzymes are related to the glycolytic pathway (Irazusta et al., 2018). The first responder of imbalanced homeostasis is the mitochondria which act as an important place for the Cu dependent ATP production (Zischka and Lichtmannegger, 2014). Mitochondrial cristae was greatly affected by Cu stress toxicity and causes deformity via peroxidation and inhibited the ATP transport to outside of mitochondria (intercellular ATP deficit) (Zischka and Lichtmannegger, 2014; Visioli and Marmiroli, 2013).

3.4.3.4 Metal transportation

Metal is generally occur in the environment, come into the contact of organisms and adhere on their surface. But after adherence on the surface, organisms accumulate the metal from outside to inside the cell via active (metabolic dependent) or passive mechanisms. In passive mechanism the metal may come inside the cell via ion exchange, osmotic mechanism etc. while in case of active transport it is driven by many type of transporting agents which are called as transporter. The transporter also involved in transport of the metal from cytoplasm to periplasm or vacuoles of the cell. Similarly, in fungi many types of transporters have been reported for the transport of the HMs from outside to inside of the cell or from periplasm to cytoplasm or from cytoplasm to vacuoles or from inside to outside of the cell (in case efflux pump). Cd-conjugate ATP- binding cassette (ABC) transporter, manganese transporter, iron transporter, copper transporter, metal transporting ATPase and some other metal

transporter are involved in metal transport from outside to cytoplasm and from cytoplasm to cell organelles (Bellion et al., 2006). Functionally ABC transporters are diverse and mediate ATP dependent import and/or export of solute. Structurally it revealed a transmembrane domain that contains substrate or nucleotide binding domain that bind and hydrolyzes ATP to drive the transport cycle (Verhalen et al., 2017). The copper transporters (CTR) are the small integral membrane proteins. It contains three transmembrane domains with the C-terminus and N-terminus located at cytosol and extracellular respectively (Tamayo et al., 2014). CTR1 and CTR3 are the efficient transporters found in the plasma membrane of *Saccharomyces cerevisiae* that obtain Cu from the environment, while CTR2 found in tonoplast which transport Cu into the cytosol (Puig and Thiele, 2002). Copper-transporting ATPases belongs to HMs P-type ATPase family (HMA), posses eight transmembrane domain. These proteins coupled with ATP hydrolysis for the efflux of metal cation from the cytoplasm (Tamayo et al., 2014). Siderophore production and special group protein are involved in uptake of Fe (Haas et al., 2008). Fungal siderophore is basically hydroxamates. A set of hydroxamates siderophore production was reported in *Laccaria bicolor* (Haselwandter et al., 2013). Putative ferrireductase, a protein present in *Rhizophagus irregularis* can reduce Cu^{2+} and Fe^{3+}, which is taken up by Fe-oxidase and permease complex consisted high-affinity transporter, oxidase-dependent Fe^{2+} transporter (Tamayo et al., 2014). Vacuolar iron transporters are implicated in the transfer of metal from the cytoplasm to the vacuoles (Li et al., 2001). Zinc-iron-permease and cation diffusion facilitators are a family of protein for the transportation of Zn (Eide, 2006).

Transmembrane containing histone-rich region is necessary for the selectivity of Zn for the fungi (Nishida et al., 2008). Cation diffusion facilitators transport the metal from the outside to the cytoplasm and from cytoplasm to lumen of cell organelles and classified into three groups (Tamayo et al., 2014). The proton gradient of transmembrane is usually used by divalent metal transporters to facilitate the transport of many types of divalent metal cations (Tamayo et al., 2014). In *Saccharomyces cerevisiae* four types of transporter are involved in uptake of Zn, Zrt1p (transport Zn from low concentrated environment), Zrt2p (transport Zn from high concentrated environment), Fet4p (involve in uptake of Cu, Fe and Zn) and Pho84p (involve in transportation of phosphate and Zn) (Tangsombatvichit et al.,

2015; Khouja et al., 2013). The Zhf1 and HcZnT1 from *Schizosaccharomyces pombe* and *Hebeloma cylindrosporum* respectively are localized on endoplasmic reticulum membrane and involve in Zn tolerance (Blaudez and Chalot, 2011). Cu enhanced the many Cu-responding signaling pathway such as calcium signaling pathway (CSP), insulin signaling pathway (ISP), NOD-like receptor signaling pathway (NOD), Hedgehog signaling pathway (HD), GnRH signaling pathway (GnRH), MAPK signaling pathway (MAPK), neurotrophin signaling pathway (NSP) in *Penicillium janthinellum* strain GXCR and EC-6 (Feng et al. 2017). Vaccaro et al. (2016) reported that proton motive forces drive the CDF protein or P-type ATPase to transport the HMs inside to outside of the cell via multiple transportation steps such as from cytoplasm to periplasm and from periplasm to outside of the cell that is also called as active efflux mechanism.

3.4.3.5 Metal compartmentation

Metal localization in fungi has great importance in metal accumulation inside the cell of fungus. Cd proportion has been quantified in the cytosol and vacuoles of *Paxillus involutus* which are 20% and 30% respectively (Blaudez et al., 2000). Cd-conjugated glutathione (Cd-GSH) or Cd-conjugated PCs and/or Cd-conjugated MTs may involve in detoxification of Cd via ATP-binding and transport it into vacuoles which is a crucial step in Cd detoxification (Bellion et al., 2005). X-ray microanalysis revealed the Cd accumulation correlated with electron dense accumulated sulfur in the vacuolar compartment which also indicated the involvement of thiolic compound in metal complexation (Ott et al., 2002). Compartmentalization or sequestration of metal depends on ionic radius of metal and electronegativity (Teng et al., 2017). Soluble fraction contains organo-ligands such as sulfur-rich organic alkali, peptides and organic acids which detoxify the metal by complexation are stored in vacuoles (Bhatia et al., 2005). Metal compartmentation in vacuoles is well known intracellular detoxification mechanisms which driven by metal transporter (Li et al., 2001; Blaudez et al., 2000). Vacuolar proton-pyrophosphatase (V-Ppase) pump and vacuolar proton ATPase (V-ATPase) pump energizes vacuolar uptake of metal in plants (Singh et al., 2016). Schematic presentation of metal compartmentation is shown in Fig. 3.6.

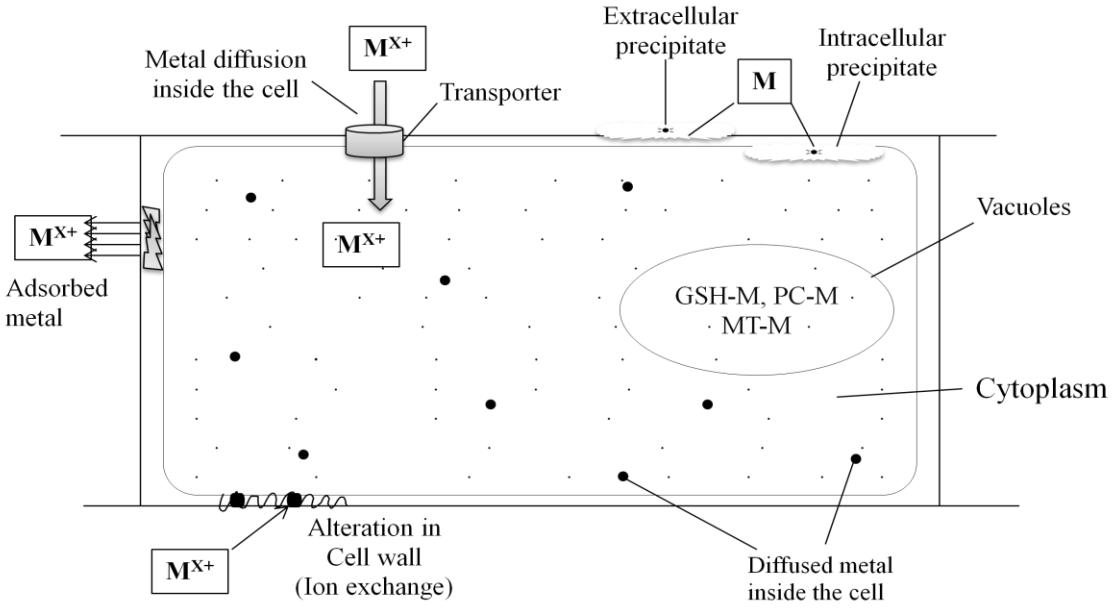

Fig. 3.6. Schematic diagram shows the possible metal accumulation site in a cell of the fungi. Dark black sphere (metal ion) diffused in cytoplasm and conjugated metal with glutathione (GSH-M), phytochelateine (PC-M) and metallothioneine (MT-M) are transported in vacuole. M=metal ion.

3.4.3.6 Metal chelating agents

3.4.3.6.1 Phytochelatins

Out of above mentioned mechanisms biochelation and biocomplexation, bio-oxidation etc. are also involved to remove HMs by fungi. Some chelating agents such as Metallothionein (MT) (Vaseem et al., 2017) and phytochelatins (PC) (Jacob et al., 2016) are present inside the fungal cells and play an important role in detoxification of HMs. These chelating agents form complex compounds by binding with the metal ion which are usually secreted by fungi as secondary metabolites or can be accumulated inside the vacuoles of the cell (Vaseem et al., 2017). The PCs are the family of small cysteine-rich peptides which carry –SH group having the capacity to bind metal ion. The PC synthesis catalyzes by phytochelatins synthetase (e.g. dipeptidyltranspeptidase, γ-glutamylcysteine dipeptidyl transpeptidase; EC 2.3.2.15), enzymes required HMs as an activating factor (Grill et al., 1989). GSH works as an activator for phytochelatin synthetase production which reduces the ROS into GSSG. Induction of ROS by the toxicity of HMs has been reported in many fungi (Xiang et al., 1998; Hirata et al., 2005). *Candida glabrata* produces PC in the response of Cd

(Mehra and Winge, 1991). Courbot et al. (2004) isolated thiol compound Cys and their derivates, γ-GluCys and glutathione to PC (up to polymerization degree n=8) from *Paxillus involutus* mycelium treated with Cd. Increase in glutathione and γ-GluCys in Cd-stressed in *P. involutus* formed a stable complex compound of Cd and other thiophilic metal (e.g. Hg, Cu, and Zn). Specific permease such as the Ycf1 membrane transporter is involved in Cd-γ-GluCys2 transportation to vacuoles in fungi (Li et al., 1997; Courbot et al., 2004). In *Penicillium janthinellum* EC-6 (a mutant strain), the synthesis of PC significantly increased under the stress of Cu that form a complex PC-Cu (Feng et al., 2017).

3.4.3.6.2 Metallothionein

High cysteine containing the low molecular mass of polypeptide is metallothionein, first reported in the equine kidney (Ruta et al., 2017). Three metallothionein protein classes are recognized as: class I resemble with equine kidney protein; class II has different extensive sequence homology from class I protein (Howe et al., 1997). Poly(γ-glutamylcysteinyl)-glycin is the general structure of metallothioneine (MT). These MTs are known to be widespread in fungi (Kneer et al., 1992). Howe et al. (1997) reported Cu binding metallothioneine in *Paxillus involutus* GPaxRSp2, *Paxillus involutus* Pax4 and *Laccaria laccata* (GLac4 and ELacl). In Brewer's yeast and *Candida glabrata*, MTs are reported for Cu tolerance (Jensen et al., 1996; Sutherland and Stillman, 2014). Transpeptidase works as an intracellular metal sensor in control of (y-EC)nG peptide formation by the metalloactivation mechanism. It was found in yeast that transpeptidase is involved in structural metal discrimination of Zn and Cu (Mehra and Winge, 1991; Sutherland and Stillman, 2014). In *Schizosaccharomyces pombe*, copper binding component (y-EC)nG peptides of (y-EC)2G through (y-EC)4G devoid of sulfide have been reported (Reese et al. 1980). The absorption spectroscopy and luminescence measurement suggested the Cu(I)-thiolate cluster in peptides (Mehra and Winge, 1991). The low-molecular-weight cysteine-rich protein found in *Neurospora crassa* in the presence of Cu, classified as MTs because of the presence of N-terminal sequences of animal MT and Cys-X-Cys motif (Lerch, 1980). Two domains exist in metallothiooneine: α-domain containing 11 cysteine residues have potential to react with four Cd^{2+} and Zn^{2+} or six Cu^{+2} ions while β-domains including 9 cysteines have potential to chelate three Cd^{2+}, three Zn^{2+} or six Cu^{+} ions (Sutherland and Stillman, 2014).

3.4.3.6.3 Melanin

Negatively charged hydrophobic dark-brown pigment containing high molecular weight produced by some fungal species is known as melanin (Sandra et al., 2017; Eisenman et al., 2012). Generally, it is found in outermost layer of the cell wall linked with chitin; and in some fungi, it is also located at outside of the fungal cell in granulous form. Oxidative polymerization of compounds (indolic and/or phenolic compounds) such as glutaminyl-3,4-dihydroxybenzene (GDHB) or 3,4-dihydroxyphenylalanine (DOPA) or catechol or 1,8-dihydroxynaphthalene (DHN) is the major mechanism involved in the formation of melanin (Eisenman et al., 2012). High antioxidant potential of melanin reported in *Fonsecaea pedrosoi* which showed via reducing Fe(III) to Fe(II) (Cunha et al., 2010). Various functional (phenolic, carboxyl, alcoholic hydroxyl, carbonyl and methoxy groups etc.) present in the melanin are mainly responsible for the chelating potential of fungi (Butler et al., 1998; Sandra et al., 2017). Siegel (1987) reported that melanin-rich fungal strain *Cladosporium cladosporioides* has more potential to biosorbed Cd, Ni, Cu, Zn, and Pb compared to non-melanized *Penicillium digitatum* (Gonçalves et al., 2012). Melanin over producing *A. nidulans* mutant strain (MEL1) has more potential to biosorption of neodymium and lanthanum. Significant uptake of radio cesium (^{137}Cs) and radio cobalt (^{60}Co) is reported in *A. alternate* and *Aspergillus pulverulents* (Mahmoud, 2004). Antioxidant characteristic of melanin is reported by Hoogduijn et al. (2003). They found that melanin defends keratinocytes and melanocytes from the induction of DNA strand broken down by ROS (H_2O_2).

3.4.3.6.4 Siderophore

Chemically siderophore is made up of alcoholates, hydroxamates and α-hydroxycarboxylates which contain negatively charged oxygen atoms and have the capacity to make tight interaction with metal ions such as Fe^{3+} ion (Kurth et al., 2017). Nitrogen and sulfur are also present as bidentate ligands but they exhibited lower selectivity. These moieties are featured by siderophore which is capable to make a complex with metal ion other than ferric ion (Hider and Kong, 2010). Siderophore mostly involves in the uptake of ferric ion. In the presence of water, ferric ion react with water molecules and produces octahedral $Fe(H_2O)_6^{3+}$ complexes (Kurth et al., 2017). Hexadentate ligands (siderophore) can make a stable complex

with Fe^{3+} ion. *Cupriavidus metallidurans* applied in metal contaminated soil treatment in bioreactor produces citrate siderophore staphyloferrin B with a 16-fold reduction in HMs (Diels et al., 2009). Arsenic contaminated soil washing with siderophore removed 92.8% arsenic from the soil as compared to washing with medium (Kurth et al., 2017). However, bacteria are mostly reported for production of siderophore which is important in metal bioremediation. Some plants are dependent on bacterial siderophore for uptake of ferric ion and they uptake ferric ion by direct uptake of bacterial metal chelates or chelate degradation, or ligand exchange reactions. Bioaugmented Cr polluted soil with *Ralstonia metallidurans* and *Pseudomonas aeruginosa* increased Cr accumulation up to 5.4 times in maize plant (Braud et al., 2009). Dimkpa et al. (2009) found that culture filtrate of *Streptomyces tendae* F4 containing siderophores improved the Fe and Cd uptake capacity in sunflower and increases its growth. It is investigated by Yun et al. (2001) that ferrireductase (Fre) protein might involve in the uptake of Fe by siderophore.

3.4.3.7 Bioreduction

In the bioreduction mechanism toxicity of metal is reduced due to the reduction in their oxidation state which is driven by living organisms (Li et al., 2017a). Chromium is commonly exist in the environment in its stable form $Cr_{(III)}$ and $Cr_{(VI)}$ however, $Cr_{(VI)}$ almost 100 times more toxic than its $Cr_{(III)}$ form (Ramırez-Ramırez et al. 2004; Romo-Rodríguez et al. 2015; Long et al. 2018). Its reduction in $Cr_{(III)}$ form mitigate its toxicity potential. *Aspergillus tubingensis* Ed8 produces glucose oxidase (GOX) in $Cr_{(VI)}$ reduction into $Cr_{(III)}$ which indicate that GOX enzyme is important for the transformation of $Cr_{(VI)}$ to $Cr_{(III)}$ and this transformation reaction is dependent on glucose, indicated that $Cr_{(VI)}$ reduction require more energy (Romo-Rodríguez et al., 2015), it was also confirmed by over synthesis of phosphoglycerate kinase, enolase 1, glyceraldehyde-3-phosphate dehydrogenase and alcohol dehydrogenase under the presence of $Cr_{(VI)}$ that is commonly involved in glycolytic pathway (Irazusta et al., 2018). Organic acids including citrate and salicylate enhanced the rate of $Cr_{(VI)}$ bioreduction which indicate that decrease of medium pH is more favorable for $Cr_{(VI)}$ reduction (Coreño-Alonso et al., 2009; Romo-Rodríguez et al., 2015). Shi et al. (2018) reported the production of citric acid, oxalic acid and maleic acid to decrease the pH of the solution that lead higher reduction of $Cr_{(VI)}$ to $Cr_{(III)}$ by *Pisolithus* sp1. Increase in the ROS (H_2O_2) production is also

associated with $Cr_{(VI)}$ reduction via multiple steps mechanism by forming Cr(V) and Cr(IV) (as intermediate mediate product) and final product of $Cr_{(III)}$ (Wani et al., 2018). This mechanism is called a multistep electron transfer reaction which may enzyme dependent or substrate dependent (Qamar et al., 2011). Sometimes these mechanisms are extracellularly completed and do not dependent on the enzyme and driven by the functional group or negative charges present on the cell surface of the fungi (Cao et al., 2018; Yin et al., 2011; Dang et al., 2018).

Mitochondrial Ferredoxin-NADP reductase Yah1 was over synthesized under the stress of $Cr_{(VI)}$ may involve in the reduction of $Cr_{(VI)}$ (Irazusta et at., 2018). Chromate reductase enzyme reported in several fungal and bacterial species that is responsible for the reduction of $Cr_{(VI)}$ to $Cr_{(III)}$ via electron transfer mechanism donated from NADH or electron donating agents (Irazusta et al., 2018). Wani et al. (2018) hypothesized two types of mechanisms for reduction of $Cr_{(VI)}$: Direct mechanism and indirect mechanism. Direct mechanism includes $Cr_{(VI)}$ reduction under aerobic and anaerobic condition while indirect mechanisms include extracellular $Cr_{(VI)}$ reduction, membrane-bound $Cr_{(VI)}$ reduction, cytochrome c (Cyt-c) dependent reduction and intracellular $Cr_{(VI)}$ reduction etc. In case of growing fungi, bioreduction is mostly metabolic dependent but in the case of dead fungal biomass, it happened mostly extracellular or through surface attached reaction. Electrostatic attraction and one electron transfer reaction mechanisms are reported by many researchers for the reduction of $Cr_{(VI)}$ by dead fungal biomass (Pradhan et al., 2017). It is investigated by Yun et al. (2001) that Ferrireductase (Fre) protein might involve in the uptake of Fe by siderophore. Fre1p, a plasma membrane is necessary for the uptake of Fe inside the cell of the fungi and plants from their growth medium or environment (Radisky and Kaplan, 1999). The reductase abundant plasma membrane of *S. cerevisiae* contained Fre1 protein exhibited a comparable activity towards Fe^{3+} and Cu^{2+} and one electron acceptor activity was found by paraquat (methyl viologen), INT (iodophenyl nitrophenyl tetrazolium chloride) and TTC (triphenyltetrazolium chloride) (Hassett and Kosman, 1995).

3.4.3.8 Mycoprecipitaion

Bioprecipitation is one of the main mechanisms which involve in the removal of HMs by microbes from wastewater (Maisa et al., 2018). In case of fungi, it can be pronounced as mycoprecipitation which is the part of bio-precipitation. The main

anionic species involved in bio-precipitation are PO_4^{2-}, CO_3^{2-}, S^{2-}, OH^-, $C_2O_4^{2-}$, O^{2-}, Cl^- etc. Bioprecipitation can be categorized into two types: 1) extracellular bio-precipitation and 2) intracellular bio-precipitation. In intracellular precipitation, metal ion come inside the cell through the fungal cell wall and precipitate (sable/insoluble compound) as their minerals by reacting with respective anionic species while, in extracellular precipitation, metal ion extracellularly synthesized into their precipitate where anionic species is donated by the fungus or may provided from their surrounding medium. While fungal cell surface provide base to take place the reaction. In intracellular precipitation, precipitate products are mostly adhere to intracellular surface of the cell, while in extracellular precipitation the precipitate product may occur on the fungal cell surface or diffused in the surrounding medium after precipitation. Liang et al. (2015) reported phosphate, sulfate, oxide anion involvement for removal of lead and found lead phosphate ($Pb_3(PO_4)_2$), anglesite ($PbSO_4$) and pyromorphite ($Pb_5(PO_4)_3Cl$) the lead oxides massicot and litharge (PbO) as lead precipitate. Phosphate ion is also reported for the precipitation of uranium (U) that form uranium complex compound such as meta-ankoleite, chernikovite, bassetite and uramphite (Liang et al., 2016). *Aspergillus niger* produces uranyl acetate hydrate (organo-uranyl complex) mineral from low grades ore of uranium (Maisa et al., 2018). Sutjaritvorakul et al. (2015) reported zinc oxide (ZnO) formation fungus isolated from the zinc mining site. Li et al. (2015) studied Ca and Sr precipitation by fungus and found $CaCl_2$ and/or $SrCl_2$, calcite($CaCO_3$), strontianite ($SrCO_3$), vaterite in different forms [$CaCO_3$, ($CaxSr_1-x)CO_3$] and olekminskite [$Sr(Sr,Ca)(CO_3)_2$] as bio-precipitate. Sulfide and Phosphate of Cd was found by Borovaya et al. (2015) and Kumar et al. (2019) in fungal mediated Cd precipitation. *Paecilomyces javanicus* precipitated the lead as plumbonacrite ($Pb_{10}(CO_3)_6O(OH)_6$), cerussite ($PbCO_3$) and lead oxalate (PbC_2O_4) (Rhee et al., 2014). Dhami et al. (2017) also reported Pb co-precipitation into lead carbonate, Plumbonacrite, Shannonite ($Pb_2O(CO_3)$), vaterite and aragonite and Sr into Strontianite, Strontium calcium carbonate ($SrO_5CaO_5(CO_3)$), carbocernaite along with calcite by two calcifying fungal isolates *Aspergillus* sp. UF3 and *Fusarium oxysporum* UF8.

3.4.3.9 Biovolatilization

Biovolatilization is basically deal with the biological volatilization of metal/loid from the water and soil into the environment. Biovolatilization is broadly

reported for volatilization of As and Hg by microorganism (bacteria, fungi and algae) and plants. In case of As, the methylation is the basic mechanism that convert the non-volatile As-species to volatile As-species. The methylation of As was firstly observed in fungus *Scopulariopsis brevicaulis* involving As(V) reduction into As(III) followed by the oxidative addition of a methyl group (-CH_3) (Challenger, 1945). Challenger (1945) proposed the pathway of As methylation where, As(V) ($AsO(OH)_3$; arsenic acid) is first reduced to As(III) ($As(OH)_3$; arsenious acid) and then bio-methylated to monomethylarsonic acid ($AsO(OH)_2(CH_3)$) → dimethylarsinic acid ($AsO(OH)(CH_3)_2$) → trimethylarsineoxide ($AsO(CH_3)_3$) → arsenobetaine ($(CH_3)_3As^+(CH_2)COO^-$), and other multifarious As-compounds such as arsenoribosides (AsRib). Recently, these compounds also have been reported in many other fungi such as *Penicillium* sp., *Aspergillus* sp. (Guimarães et al., 2019) and *Rhizophagus irregularis* (Li et al., 2018d) that interlinked with the methylation pathway as proposed by Challenger (1945). In addition, some microorganism also degrade or/and synthesize As-compound into volatile As (such as arsine (AsH_3), monomethylarsine ($AsH_2(CH_3)$), dimethylarsine ($AsH(CH_3)_2$) and trimethylarsine ($As(CH_3)_3$). This mechanism has been also reported by Guimarães et al. (2019) in *Penicillium* sp., *Aspergillus* sp. at the time As-volatilization using potato dextrose broth medium. However, the methylation and bio-volatilization is commonly occured in ecosystem (contaminated with As) and majorly contributed in As global flux (Wang et al., 2014; Mestrot et al., 2013).

Hg is one of toxic metal and volatile in nature, can also bio-volatilize by microorganism. Bacterial as well as fungal-volatilization of Hg is frequently reported in many studies that play important role in decontamination of Hg-polluted site (Urík et al., 2014; Chen et al., 2018; Chang et al., 2020). Generally, bacteria and archaea utilize the *mer* operon which is capable in enzymatic reduction of Hg(II) or methyl mercury (MeHg) to less toxic Hg(0), volatile species of Hg (Boyd and Barkay, 2012; Giovanella et al., 2016). In fungi, the mechanism of bio-volatilization of Hg is not well characterized. However, in a recent report, it is found that *mer* genes (*merA*) up-regulated in the exposure of Hg(II) in *Penicillium* spp. DC-F11, a potential isolate for volatilization of Hg (Chang et al., 2020). They have also analyzed the activity of mercuric reductase that is responsible for reduction of Hg(II) to Hg(0). Thus, *mer* operon is basically involved in enzymatic reduction of Hg(II) to Hg(0) as well as its

volatilization. Some other fungal species such as *Candida albicans*, *Saccharomyces cerevisiae* (Yannai et al., 1991), *Scopulariopsis brevicaulis* (Boriova et al., 2014), *Aspergillus niger* and *Cladosporium* sp. (Urík et al., 2014) also have been reported for volatilization of Hg, but no any other clear Hg volatilization pathway has yet been observed in fungi. Some other metal/loid such as Se (Selenium), Sb (Antimony), Tl (Thallium) and Bi (Bismuth) are also reported for volatilization by fungi (Boriova et al., 2014). Despite it, some time fungi change the less toxic form of metal/loid into its high toxic form. Yannai et al. (1991) tested the tolerance ability of *Candida albicans* and *Saccharomyces cerevisiae* towards Hg ($HgCl_2$) and reported that *Candida albicans* and *Saccharomyces cerevisiae* are unable to grow above 0.75 µg/mL. Further they investigated the end product of Hg at the tested concentration (below 0.75 µg/mL) and found that an amount of Hg (proportional to Hg tested concentration) is transformed in organo-mercury (methyl mercury) compound. Methyl mercury, highly toxic species of Hg, can inhibit the growth of fungi as well as other organism.

3.4.3.10 Methylation

The synthesis and transfer of methyl group is a vital metabolic process (Bentley et al., 2002). Basically the C, O, N and S atom of organic compounds serve as methyl group acceptor in metabolic process. Metal and metalloids also reported in many studies as methyl group acceptor and resultant into methylated end products. However, the term "biomethylation" consider the formation of both either volatile or non-volatile methylated compound of metals and metalloids. The methylation of As is widespread, occurring in bacteria, fungi, algae and plants. As methylation was first proposed in fungus *S. brevicaulis* by Challenger (1945). In As methylation, As(V) first reduced in As(III) followed by oxidative addition of methyl ($-CH_3$) (earlier discussed in **section 3.4.3.9**). Similar pathway has been proposed for antimony (Sb) methylation, it was first proposed for Sb methylation in fungus *S. brevicaulis* and *P. notatum* as methylation of phenylstibonic acid ($C_6H_5SbO(OH)_2$) to phenyldimethylstibine ($C_6H_5SbO(CH_3)_2$) via reduction of Sb(V) to Sb(III) followed by methylation (Challenger, 1945). Later some other fungal species are reported for methylation of Sb such as *Cryptococcus humicolus* (Hartmann et al., 2003) and *Phaeolus schweinitzii* (Andrew et al., 2001). Andrew et al. (2001) reported that *P.*

schweinitzii efficiently transforms the antimony (III) compounds potassium antimony tartrate and antimony trioxide (Sb_2O_3) to nonvolatile dimethylantimony and trimethylantimony species. Mercury is another metal reported for its methylation by bacteria and fungi. In bacteria, clear Hg-methylation pathway, genes responsible for Hg-methylation and Hg transporting agents have been reported (Regnell and Watras, 2018). Fungi such as *Coprinus comatus*, *C. radians*, *Candida albicans* and *Saccharomyces cerevisiae* have been reported for Hg-methylation potential (Fischer et al., 1995; Yannai et al., 1991). But in fungi, mechanism of Hg-methylation is least known.

3.4.3.11 Biooxidation

Manganese peroxidase is a heme enzyme extracellularly produced by lignin-degrading fungus (basidiomycetes) that can oxidize Mn^{2+} to oxidant Mn^{3+} in a multiple step electron transfer reaction (Have et al., 2001). Extracellular protein involvement in Mn oxidation in anamorphic ascomycete strain KR21–2 and *L. discophora* SS-1 has been reported by Miyata et al. (2004). The proteins such as p-phenylenediamine and 2,2'-azinobis (3-ethylbenzothiazoline-6-sulfonic acid) are the extracellular Mn oxidizer. The peroxide-oxidized enzyme catalyzes Mn(II) into Mn(III) in the presence of suitable Mn(III) chelator. Purified laccase enzyme isolated from *Stropharia rugosoannulata* can catalyze the Mn(II) into Mn(III) (Schlosser et al., 2002).

3.4.3.12 Other mechanisms

Many of known and unknown other mechanism may also involved in the tolerance and accumulation of HMs in fungi. Such as the ion exchange is the major interactive manner among some divalent metal ions and the extracellular polymeric substances (EPS) (Sheng et al., 2010). It was found that the binding between the metal ions (divalent; Ca^{2+}, Ni^{2+} and Mg^{2+}) and EPS is one of the most important intermolecular interactions behind microbial aggregate structures. Simultaneous release of Ca^{2+} and Mg^{2+} into solution during metal removal mechanism by microbial aggregate indicating the ion exchange involvement (Yuncu et al., 2006). However, strong binding capacity are also seen in neutral and extreme acidic eukaryotic biofilms for heavy metals (Co, Ni, Zn, Cu, As, Cd, Cr, Hg and Pb) which might be by producing colloidal materials such as protein, or affecting the ionic values of metal

(e.g., the transformation of Hg^{2+} to Hg0 or transformation of $Cr_{(VI)}$ into Cr(III)) (Choi et al., 2009; Neu and Lawrence, 2010). There are some specific transport systems involved through the membrane and carriers may consist of all the metabolically-coupled and H+ gradient drove transport system. They play important role in metal efflux pump system. Metal efflux pump maintains the salinity inside of the cell and their surroundings. Adriaensen (2005) found enhanced in Zn efflux which may act as a tolerance mechanism in *Suillus bovines*. The GSH as above discussed is reported for the binding of HMs.

3.4.3.13 Genes involved in HMs tolerance and detoxification

Exploration of basic molecular mechanism of tolerance and adaptation of fungi in HMs stress environment is an important field of scientific interest. Gene expression have imperative role on biological process which establish the growth and development of fungi as well as HMs tolerance in HMs stress condition. In plants, many types of set of gene expression have been triggered under HMs stress. Different types of stressor induces the expression of a set of gene in microbes and plants in order to link the signaling pathway with HMs and other stress tolerance (Viti et al., 2013; Singh et al., 2016). The regulatory genes and functional genes are the two group of genes expressed under stress condition. Various transcription factors (TFs) encoded by group of genes are called as the regulatory genes group. It can regulate many stress responsive genes separately or cooperatively and make up a gene system. However, metabolic compound such as amines, alcohol, sugar, enzymes etc. play important role in tolerance of HMs are encoded by group genes, known as the functional genes group (Singh et al., 2016).

Flores-Alvarez et al. (2012) reported *CHR-1* gene expression under $Cr_{(VI)}$ exposure in *Neurospora crassa* that encoded CHR-1 protein (homologous to ChrA protein), sensitive upon $Cr_{(VI)}$ exposure and promote its accumulation inside the cell. The expression of Glutathione-S-Transferase (GST) encoding six *GintGst* genes found in an arbuscular mycorrhizal fungus *Glomus intraradices* in exposure of Cd, Zn, and Cu (Waschke et al., 2006) which confirm its role in adaptation of *G. intraradices* in Cu, Cd and Zn contaminated environment. However, Shen et al. (2015) identified 24 GST genes in *Exophiala pisciphila*. These all *EpGSTs* up-regulated by Pb stress but differentially expressed some of them under stress of Cd, Cu and Zn. Metallothionein (MT) is cystolic peptides reported for binding of HMs via

cysteinyl-thiolate bonds and participate in metal homeostasis. MT family genes expression belongs to functional genes group are reported in many fungal species in exposure of heavy metal: *Neclu_MT1* gene induced by Cd in *Heliscus lugdunensis* (Loebus et al., 2013), Cu-specific MT genes (*CMT1* and *CMT2*) expressed under exposure of Cu in *Cryptococcus neoformans* (Palacios et al., 2014), *LbMT1* gene up-regulated by Cu and Cd in *Laccaria bicolor* (Reddy et al., 2014), Cu-dependent expression of *HcMT1*and *HcMT2* genes in *Hebeloma cylindrosporum* (Ramesh et al., 2009), Transcription of AsMT1s and AsMT3 in *Amanita strobiliformis* inducible with treatment of Ag and Cu and Zn and Cd respectively (Hlozkova et al., 2015).

Recently, Bakti et al. (2018) reported *PcaA* gene expression in *A. fumigatus* induced under exposure of Cd which was associated with induction of GFP-PcaA fusion protein. This protein is specifically produced under exposure of Cd neither Cu nor Zn or Fe and localized in membrane as found in confocal microscopic observation and strongly correlated with detoxification of Cd. However, Bakti et al. (2018) also studied the role of AfYap1 (ortholog of the yeast Yap1 transcription factor) in metal sensing by *A. fumagatus* Af293 (Wild Type) and they found that AfYap1 is involved in sensing of Cd and Cu both. The Cd and Cu are also up-regulated the *GintABC1* gene in *Glomus intraradices* that encoded the GintABC1 protein which belong to the sub-family of ABC transporter and possibly involved in Cu and Cd detoxification (González-Guerrero et al., 2010). In recent study, Li et al. (2018) investigated Cd tolerance in *Pleurotus eryngii* which differentially expressed 15 unigenes. These differentially expressed genes (DEGs) are specifically up-regulated upon Cd exposure which is mainly related with heat shocked protein (HSP) genes including three HSP 70 genes, one HSP 9 gene, one HSP 20, one HSP 60, and one HSP 78. Some other unigenes such as "carbohydrate-binding module family 13 protein", "3-beta-hydroxy-delta 5-steroid dehydrogenase activity", "uncharacterized aromatic compound mono-oxygenase", and "mannose-6-phosphate isomerase" are of them that up-regulated in Cd stress. Further, they were added NO with Cd stress and found an increase in the biomass of *P. eryngii*. They found in transcriptomic analysis that putative oxidoreductase, transferase, reductase, dehydrogenase genes and TFs such as "GTPase activator activity", "GTP binding", "transcription factor complex", "enzyme activator activity" and "ATP binding" are up-regulated significantly and enhance the Cd tolerance capacity in *P. eryngii*. These studies confirmed that there are sets of gene

expression in fungi that up-regulated under HMs stress and interlinked with metabolic activity and development of fungi. However, single HM induced gene expression may vary from species to species and also in a same fungal species different HMs may induce various set of genes expression which might be specific for each HM. These expressed set of genes are strongly associated with tolerance and detoxification mechanisms of HMs in fungi and very essential for fungi to survive in HMs stressed environmental condition.

Chapter-4

Materials and Methods

Chapter -4 Materials and Methods

4.1 Collection of Electroplating wastewater sample

The pre-sterilized glass bottle was used to collect the electroplating wastewater from electroplating industrial area, Ballabhgarh, Faridabad (28°19'19"N, 77°17'59" E), India in the month of April 2018,brought to the Laboratory of Department of Environmental Science, BBAU, Lucknow, India (26°49'03" N, 80°55'37" E), stored at 4 ℃ and further experiments were conducted.

4.2 Physicochemical analysis of Electroplating wastewater

The physicochemical parameters of electroplating wastewater; pH and Electrical Conductivity (ELICO, PE 138, Water Quality Analyzer), biochemical oxygen demand (BOD) (5-day dilution methods), chemical oxygen demand (COD), Total solid and selected heavy metal (nitric-perchloric acid digestion method) was analyzed as per the standard protocol outlined in "Standard Methods for the Examination of Water and Wastewater" (APHA, 2012). Heavy metals (Cr, Cd, Cu, Ni and Pb) were analyzed in acid digested electroplating wastewater using atomic absorption spectrophotometer (AAS) (Varian, AA240FS) and As was analyzed using a publish standard method (Dhar et al., 2004) and absorbance was read at 880 nm using double beam spectrophotometer (Systronics, Model: 2203).

4.3. Microorganism Isolation

The chromium tolerant fungal species were isolated by serial dilution method (Sharma et al., 2016). To isolate the chromium tolerant fungal species, the serial dilution was made up to 10^{-3} and vertex for a minute. The wastewater suspension (0.5 mL) was spread on $Cr_{(VI)}$ (100 mg/L; $K_2Cr_2O_7$, Purity; 99.5%, Molychem, Mumbai, India) amended potato dextrose agar (PDA) (HiMedia, Mumbai, India) plate and was incubated at 28 ± 1°C for six days. Four morphologically distinct fungi grew on 100 mg/L of $Cr_{(VI)}$ amended potato dextrose agar (PDA) plate.

4.4 Heavy metal Tolerance assay

First, the tolerance assay of isolates was conducted towards Cr(VI) for screening purpose to select the isolate for detail investigation and minimize the

number of isolates. Two fungal isolate showed high tolerance towards Cr(VI) and on the basis of their tolerance towards $Cr_{(VI)}$ they were renamed as isolate CR500 and isolate CR700. After selecting the best Cr-tolerant fungal isolates, their tolerance towards other heavy metal was also conducted including Ni(II). The tolerance of fungal isolates towards different heavy metal/oid was evaluated using the plate assay method. The stock solution of Cr, Mn, Cu, Ni, Cd, Pb and As was prepared using their respective salts ($K_2Cr_2O_7$ and $MnSO_4$ were obtained from Molychem, Mumbai, India; $CuSO_4.5H_2O$, $NiSO_4.6H_2O$, $CdCl_2$, $PbSO_4$ and As_2O_3 were procured from Loba Chemie, Mumbai, India). The metal concentrations: 0, 100, 200, 400, 600, 800, 1000, 1200, 1400, 1600 and 2000 mg/L was used for the study of tolerance of selected isolates using plate assay method (Kumar et al., 2019). A disc of 0.5 cm diameter of seventh day grown mycelia of fungal isolate was inoculated on different concentration of heavy metal amended PDA plates separately. The inoculated plates were incubated for ten days in the incubator at 28 ± 1°C. The growth of isolates was estimated by measuring the colony diameter on tenth day after incubation. The formula [Ti = T/C] was used to calculate the tolerance index (Ti) where T; growth of fungus on metal contaminated PDA plate and C; growth of fungus on without heavy metal contaminated PDA plate (Chen et al., 2017).

4.5 Molecular Identification

The molecular identification of isolate was carried out at the sequencing facility of the National Centre for Microbial Resource (NCMR), National Centre for Cell Science, Pune, India. For DNA isolation, the mycelia (50 mg) of isolates were collected from 7^{th} day grown on PDA plate. The genomic DNA was isolated by the standard phenol/chloroform extraction method (Sambrook et al., 1989), followed by PCR amplification of the ITS regions using universal primers ITS1 [5'-TCCGTAGGTGAACCTGCGG -3'] and ITS4 [5'-TCCTCCGCTTATTGATATGC -3'] (White et al. 1998). The amplified ITS PCR product was purified by PEG-NaCl precipitation and directly sequenced on ABI® 3730XL automated DNA Sequencer (Applied Biosystems, Inc., Foster City, CA) as per manufacturer's instructions. Essentially, sequencing was carried out from both ends so that each position was read at least twice. For identification, the sequenced data were analyzed and assembled using BLAST (Basic Local Alignment Search Tool; https://blast.ncbi.nlm.nih.gov/Blast.cgi) NCBI (National Center for Biotechnology

Information) (Boratyn et al. 2013). The ITS region sequence of fungal isolates was deposited in GenBank, NCBI. To assess the confidence limits of the branching, the Bootstrap analysis was performed. The neighbor-joining tree was reconstructed using a standard parameter of CLUSTAL W alignment with a gap opening penalty 15 and a gap extension penalty of 6.66 for both pairwise alignment and multiple alignments. The evolutionary analysis was inferred using the Neighbor-Joining method (Saitou and Nei 1987). The tree is drawn to scale, with branch lengths in the same units as those of the evolutionary distances used to infer the phylogenetic tree. The evolutionary distances were computed using the Maximum Composite Likelihood method (Tamura et al. 2004) and are in the units of the number of base substitutions per site. Evolutionary analysis was conducted in MEGA X (Kumar et al. 2018).

4.6 Experimental design

The batch study was conducted in 250 mL Erlenmeyer flask containing 100 mL $Cr_{(VI)}$ ($K_2Cr_2O_7$) or Ni(II) ($NiSO_4$) amended potato dextrose broth (PDB) at pH 6.5 separately. The concentration of metal ranged from 0 to 200 mg/L (0, 5, 20, 50, 70, 100, 200 and 500 mg/L) and inoculated with 1 mL of 3×10^4 mL fungal spore suspension (in case of isolate CR500) or 0.5 cm block mycelia grown on PDA plate (in case of isolate CR700) (Kumar et al., 2019). Inoculated flasks were incubated at 28 ± 1 °C for 6 d in an incubator shaker at 80 rpm. Five mL of culture was taken out from the incubated flask after incubation period of 24, 48, 72, 96, 120 and 144 h and centrifuged at 10000 rpm for 10 min. All the treatments were made in triplicates. The supernatant was used for the determination of the concentration of $Ni_{(II)}$, $Cr_{(VI)}$ and total Cr. The same process with different $Cr_{(VI)}$ and $Ni_{(II)}$ concentration (0, 5, 20, 50 and 100 mg/L) was followed to obtain the biomass for enzymatic and biochemical analysis and the biomass was harvested by centrifuging at 5000 rpm and 4°C for 10 min.

The $Cr_{(VI)}$ reduction and Ni(II) removal experiment was also conducted under the presence of 10 mg/L of heavy metal/loid (As, Cd, Cu, Mn, Ni and Pb individually), 5 mM of phenol, EDTA, glutathione (GSH) and acetate and 2% glucose amended PDB medium separately (Arévalo-Rangel et al., 2013). For the assessment of Cr(VI) reduction and removal potential of isolates in real wastewater, the PDB medium was diluted with sterilized tannery effluent (TEF) and amended with 50 mg/L

of $Cr_{(VI)}$. To study the effect of pH and temperature, the $Cr_{(VI)}$ reduction and $Ni_{(II)}$ removal ability of isolates was determined at different temperature (20, 28, 35 and 40 °C) and pH (5.0, 6.5 and 8.0 and 9.0; 0.1M HCl and NaOH was used to adjust the pH) at 50 mg/L of $Cr_{(VI)}$ concentration (Liu et al., 2007). Inoculation and incubation were done as above mentioned condition and 5 mL of culture medium was taken out on 6th day after incubation for determination of $Cr_{(VI)}$ and $Ni_{(II)}$ concentration.

To get the obtained biomass, the culture was filtered through pre-dried and weighed Whatman filter paper No. 1 and dried (60 °C for 4 h) and weighed using the weighing balance (Sartorius BT224S). For the estimation of accumulated Cr and Ni concentration, the dried biomass was washed with 0.1M HNO_3 (Shen et al., 2019) to remove adsorbed chromium from the fungal cell surface and digested using acid oxidative solution of HNO_3:H_2SO_4 (3:1 ratio) (Li et al., 2017a). Without acid washed biomass was also subjected to acid digestion for the determination of total immobilized Cr and Ni, by subtracting the accumulated Cr and Ni from total immobilized Cr and Ni, the surface adsorbed Cr and Ni concentration was calculated.

Total Cr and Ni concentration in the supernatant and acid digested samples was determined using a fast sequential atomic absorption spectrophotometer (Varian, AA240FS). The hexavalent chromium concentration in the supernatant was determined by 1, 5-diphenylcarbazide method as described by American Public Health Association (APHA, 1992; Bai et al., 2018). The percentage of removal and reduction was calculated using the equation (Eq. 1) and (Eq. 2) respectively.

$$A = \frac{Ci - Cf}{Ci} \times 100 \qquad \text{(Eq. 1)}$$

$$y = \frac{Ci - Cb}{Ci} \times 100 \qquad \text{(Eq. 2)}$$

[Where, A; Removal percentage, y; Reduction percentage, C_i; Initial $Cr_{(VI)}$ or $Ni_{(II)}$ concentration, C_f; final Cr or $Ni_{(II)}$ concentration, C_b; final $Cr_{(VI)}$ concentration]

4.7 Multipl metal Removal from simulated Wastewater by isolate CR500

For determination of multimetal removal ability of the *A. flavus* CR500, three types of SWW were prepared: i) 5 mg/L, ii) 10 mg/L and iii) 20 mg/L of each metal (Pb, As, Ni, and Cr using the respected salts) in PDB medium. To study the effect of

pH on the removal of metal from SWW, the pH of the SWW (containing 10 mg/L of each metal in PDB medium) was adjusted to 5.0, 6.0, 7.0, 8.0 and 9.0 using 0.1M HCl and 0.1M NaOH. Fifty mL of prepared SWW was taken in different 250 mL Erlenmeyer flask separately and further autoclaved, inoculated and incubated as per above mentioned condition.

4.8 Growth and multimetal removal from TWW by isolate CR500

The growth and multimetal removal ability of *A. flavus* CR500 was also investigated in TWW collected from the Common Effluent Treatment Plant (CETP), Jajmau Unit, Kanpur (26°24'51"N and 80°25'09"E), Uttar Pradesh, India (physicochemical parameters of TWW are shown in supplementary section). The TWW was diluted with distilled water (in the ratio of 1:2 and 1:4 (TWW: distilled water) in separate flask) to optimize the growth and metal removal ability of *A. flavus* CR500. Fifty mL of undiluted and diluted TWW was taken in 250 mL flask and supplemented with 1.2 g PDB and 0.25 mL of 1000 mg/L of metal (Cr, Ni, Pb and As) solution to get 5 mg/L of multimetal contaminated TWW and the pH of the obtained solution was adjusted to 7.0. Further, the solution was inoculated and incubated as per the condition mentioned in **section 4.6**. After ten days of incubation, the culture medium was centrifuged at 5000 rpm and metal concentration and obtained biomass was determined as explained in **section 4.6**.

4.9 SEM-EDS analysis

Fresh fungal biomass was fixed in 2.5 % of glutaraldehyde at 4 °C for 6 hours, washed with phosphate buffer (pH 7.0) and subsequently dehydrated with different concentration of ethanol (20, 30, 40, 50, 60, 70, 80, 90 and 100%) for 10 min at each concentration. The final dehydration was carried out with absolute acetone for 20 minutes and samples were mounted on aluminium studs with help of carbon tape (Coreño-Alonso et al., 2014). The surface analysis was done using a scanning electron microscope (JEOL, Japan; model JSM-6490LV) coupled with an energy dispersive x-ray spectrophotometer (EDS).

4.10 FTIR and XRD analysis

For FTIR analysis, dried fungal biomass (60 °C for 6 h) was ground with potassium bromide (KBr) in the ratio of 1:100 (w/w). The hydraulic press (130 lbs)

was used to form pellets and IR absorbance of the sample was read using Fourier transform infrared spectroscopy (Thermo-Scientific Nicole 6700, USA) in the range from 400-4000 cm^{-1}. After $Cr_{(VI)}$ biosorption, the crystalline structure in the biomass of Isolate CR500 was determined using the x-ray diffraction (XRD) technique (Mini Flex 600).

4.11 XPS analysis

The x-ray photoelectron spectroscopic (XPS) analysis was performed to determine the valence state of chromium adsorbed on the mycelia surface of Isolate CR700. The fungal biomass was harvested from reduction experiment at 100 mg/L of $Cr_{(VI)}$ by centrifugation at 10000 rpm for 10 minutes. The pellet was dried at 70°C for 6 h and subjected to XPS analysis using X-ray photoelectron spectroscopy (PHI Versa Probe II with AES).

4.12 Lipid peroxidation assay

The malondialdehyde (MDA) is the final decomposition product of lipid peroxidation used for the indexing of lipid peroxidation. Five mL of the solution containing 20 % trichloroacetic acid and 0.5 % 2-thiobarbituric acid was used to homogenize the 200 mg of fungal pellets. The homogenized mixture was heated at 95 °C for 30 minutes and the reaction was arrested by quickly transferring into an ice bath. The reaction mixture was centrifuged at 5000 × g for 10 min and the absorbance of the supernatant was recorded at 532 nm and 600 nm. After subtracting the turbidity at 600 nm, MDA concentration was calculated by its molar extinction coefficients 155 mmol L^{-1} cm (Zhang et al. 2007).

4.13 Determination of H_2O_2

The total phenolic compound was estimated following the method described by Qiu et al. (2010). The reaction mixture was prepared to contain 100 µL of sample (culture broth), 0.5 mL of Folin-Ciocalteau reagent, 1.5 mL distilled water and 1 mL of 20 % sodium carbonate (w/v) and incubated for two hours at room temperature in the dark condition. The absorbance was taken at 760 nm using the UV-visible double beam spectrophotometer (Systronics 2203 Smart UV-VIS. Spectrophotometer). Different concentration of gallic acid was prepared in 95 % ethanol to obtain the

calibration curve and absorbance was taken at 273 nm. The results were expressed in milligram of gallic acid equivalent per milliliter of culture broths.

4.14 Determination of Total phenolic content

Fungal biomass (0.5 g) was homogenized in 5.0 mL of 0.1 % trichloroacetic acid in the ice bath followed by centrifugation at 12000 × g for 15 min. The reaction mixture was prepared by adding 0.5 mL of the supernatant, 0.5 mL of 10 mmol potassium phosphate buffer (pH 7.0) and 1 mL of 1 mol Potassium Iodide (KI). After shaking the absorbance of the mixture was recorded at 390 nm. The concentration of H_2O_2 was calculated using the standard curve of H_2O_2 (Velikova et al. 2000).

4.15 Proline, GSH and Non-protein thiol content

Proline content was estimated as described by Gratao et al. (2012). Fresh washed fungal pellets (0.5 g) was homogenized with 5 mL of 3 % sulphosalicylic acid and the homogenate was centrifuged at 10000 rpm for 10 min at 4 °C. The reaction mixture was prepared by adding 2 mL of supernatant, 2 mL of glacial acetic acid, 2 mL of ninhydrin and kept in boiling water for 45 minutes. Cold toluene (4 mL) was added and separated. Absorbance was taken at 520 nm against toluene reference.

To estimate the GSH content, 1 mL of supernatant and 100 µL of 3 mmol 5′dithio-bis-(2-nitrobenzoic acid) was added in 1 mL of reaction buffer [0.1 M phosphate buffer (pH 7.0), 0.5 mM EDTA] and kept at room temperature for 5 minutes; absorbance was read at 412 nm. Reduced GSH was used to prepare a standard curve to calculate GSH content (Rehman and Anjum 2010).

To estimate the non-protein thiol content, 200 µL of supernatant and 1 mL of 1 mM 5′ dithio-bis-(2-nitrobenzoic acid) was added to 1 mL of reaction buffer containing 0.1 M phosphate buffer (pH 7.0) and 0.5 mM EDTA. The mixture solution was incubated at room temperature for 10 minutes and absorbance was taken at 412 nm. Non-protein thiol content was calculated by comparing with the cysteine standard curve (Rehman and Anjum 2010).

4.16 Estimation of intracellular protein content, activity of Chromate reductase, Polyphenol oxidase (PPO) and Phenyl ammonia lyase (PAL)

Fresh fungal pellet (0.5 g) was grinded with mortar pestle in 2 mL of phosphate buffer (pH 7.0) and centrifuged at 1000 rpm for 10 minutes. Filtered supernatant was employed as cell-free extract (CFE) for the estimation of protein and activity of chromate reductase. Intracellular protein content was estimated by following the method described by Lowery et al. (1951).

To determine the activity of **PPO**, 100 µL of CFE was added in the reaction mixture (1.5 mL of 0.1 mol L^{-1} sodium phosphate buffer (pH 7.0) and 200 µL 0.01 mol L^{-1} catechol). The changes in absorbance was recorded every 30 s for 3 minutes at 495 nm. PPO activity was expressed as unit per minute per milligram of protein (Mayer et al. 1965).

Phenyl ammonia lyase (**PAL**) activity was assayed by determining the production of trans-cinnamic acid. 0.4 ml of CFE was added with the reaction mixture containing 1.5 mL of 0.1 mol L^{-1} sodium borate buffer (pH 8.8) and 0.5 mL of 12 mmol L^{-1} of phenylalanine and incubated at 25 °C under light for 1hour. The reaction was stopped by incubating at 47 °C for 10 min and the absorbance was taken at 290 nm, and the amount of trans-cinnamic acid was calculated (Dickerson et al. 1984).

4.17 Estimation of activity of SOD, POD and CAT

Total protein was extracted by grinding 0.5 g of fresh mycelia in chilled mortar pestle and suspended in 3 mL of extraction buffer which contained 1 % (w/v) polyvinylpyrrolidone (PVP), 50 mM sodium phosphate buffer (pH 7.5) and 0.1 mM ethylenediaminetetraacetic acid (EDTA).

SOD activity was determined by the method as described by Xu et al. (2010). Three mL of the reaction mixture was prepared, which contained 25 mM nitroblue tetrazolium (NBT), 50 mM phosphate buffer (pH 7.8), 10 mmol methionine, 0.1 mmol EDTA, 2 µmol riboflavin, 50 mM sodium carbonate and 100 µL extract. The reaction mixture was incubated at 30 °C for 15 minutes under a light intensity of 150 µ mol m^{-2} s^{-1}. The absorbance of the obtained mixture was read at 560 nm.

To determine the **CAT activity**, 3 mL of reaction mixture was prepared containing 25 mM sodium phosphate buffer (pH 7.0), 0.05% guaiacol, 0.1 mM EDTA, 1 mM H_2O_2, and 50 µL extract. The activity CAT was determined via a decrease in H_2O_2 and absorbance was taken at 470 nm. CAT activity was calculated with an extinction coefficient of 39.4 mM^{-1} cm^{-1} and expressed as µ mol H_2O_2 min^{-1} mg^{-1} protein (Xu et al. 2010).

To determine the **POD activity**, Three mL reaction mixture was prepared which contained, 25 mM sodium phosphate buffer (pH 7.0), 0.05% guaiacol, 0.1 mM EDTA, 1 mM H_2O_2, and 50 µL of extract. The activity of POD was determined via measuring the change in absorbance at 470 nm and values were calculated with molar extinction coefficient of 26.6 $mM^{-1}cm^{-1}$ (Zhu et al. 2004).

4.18 Chromate reductase

The activity of **chromate reductase (ChrR)** was determined by following the method explained by McLean and Beveridge (2001) and modified by Ontañon et al. (2018). Fresh fungal pellet (0.5 g) was ground with chilled mortar pestle in 2 mL of phosphate buffer (pH 7.0) and centrifuged at 3000 rpm for 10 min. Three mL of reaction mixture was prepared which contained 100 µL CFE, 10 mg/L $Cr_{(VI)}$, 50 mmol phosphate buffer (pH 7), with and without 6.5 mg/L NADH. The obtained reaction mixture was incubated at 30 ℃ for 60 min, the sample was taken every 15 minutes to analyze the remaining $Cr_{(VI)}$ concentration using 1,5-diphenylcarbazide reagent. The specific activity of ChrR was defined as units of activity of chromate reductase per milligram of protein.

4.19 Phytotoxicity test

The $Cr_{(VI)}$ detoxification ability of *A. flavus* CR500 and *T. lixii* CR700 was studied using Mung bean (*Vigna radiata*) and chickpea (*Cicer arietinum*) seeds. Fungal treated (supernatant of 100 mg/L of $Cr_{(VI)}/Ni_{(II)}$ from **Section 4.6**) and without treated 100 mg/L of $Cr_{(VI)}/Ni_{(II)}$ and sterilized distilled water was taken for comparative study. *Vigna radiata* and *Cicer arietinum* seeds were surface sterilized using 10% H_2O_2 (Ahmad et al., 2008) and washed thrice with sterilized distilled water, distributed at equidistance in Petri plate (90 mm diameter) containing sterilized double layered Whatman filter paper No. 1 (Chen et al. 2019). The plates were

watered at alternate day with above-taken solution separately for comparative study and incubated at room temperature. The shoot and root length of seedling was measured at the sixth day and the seed germination rate was calculated using the following equation (Kannan and Upreti, 2008):

$$Germination\ Rate = \frac{Number\ of\ seeds\ germinated}{Total\ number\ of\ seeds} \times 100 \qquad \text{(Eq. 3)}$$

4.20 Statistical analysis

To improve the analytical precisions of the variables, all the experiments were conducted in three replicate. The obtained data were statistically analyzed using SPSS software (version 20.0) with one Way Analysis of Variance (ANOVA) and the mean of the data were compared using post-hoc DMRT ($p \leq 0.05$). Paired t-test ($p \leq 0.05$) was performed to compare the chromate reductase activity.

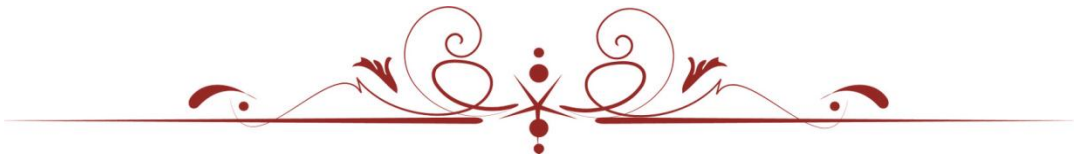

Chapter-5

Results and Discussion

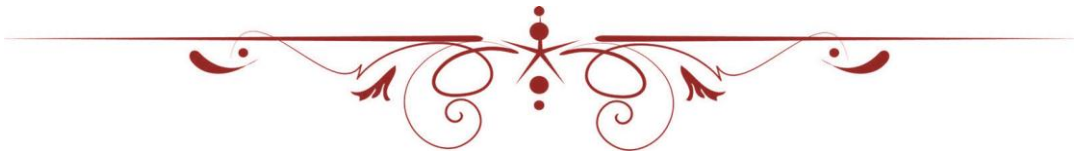

5A. Physicochemical characteristic of collected Electroplating wastewater

Plating industries use a large amount of water as raw material to prepare electrolytic bath using respective chemical as per their requirement for the plating and finishing purposes. Another use of water in plating industries is rinsing and cleaning of objects as the pretreatment process (US EPA, 2016; Martín-Lara et al., 2014). The electroplating industries uses number of metals and chemicals; therefore, the generated waste contain high amount of toxic metals and chemicals via rinsing of products, due to spillage and dumping of baths (CPCB, 2007; US EPA, 2016). The wastewater stream generated from plating industries is usually extremely variable (1 liter to 500 liters per square meter of surface plated) but frequently high in heavy metals (including Cd, Cr, Pb, Cu, Zn, and Ni), cyanide (CN), fluoride (F), and oil and grease, all of which are process dependent (Table 5.1) (WBG, 1999; Cui et al., 2014; Sochacki et al., 2014; Bhateria and Dhaka, 2017). Some studies reported the high content of TS, TDS, COD, total hardness, sulfates, phosphate, nitrate and metals such as sodium, potassium, calcium, magnesium and manganese in electroplating wastewater (Bhateria and Dhaka, 2017; Borgia et al., 2015; Angelin et al., 2015; Machado et al., 2016). Moreover, air emissions from the electroplating industries may contain toxic organics such as trichloroethylene and trichloroethane (WBG, 1999; CPCB, 2007).

EWW is very toxic and hazardous due to the presence of high amount of toxic heavy metals and chemicals. In most of the cases, the EWW is dominated with heavy metal as contaminant that is a major cause of its hazardous in nature (Borgia et al., 2018; Bhateria and Dhaka, 2017; Borgia et al., 2015; Angelin et al., 2015). All the organic and inorganic pollutants present in EWW have a serious impact on human health and the environment. Out of the heavy metal contaminants, Cr, Cd, Sn and Pb are the most concernable pollutants due to their toxic, carcinogenic, mutagenic in nature even they can cause serious impact to living being at very least concentration (Vutukuru, 2005; Golovanova, 2008; Cima, 2011; Balabaskaran et al., 1987; Eisler, 1989). EWW is of serious environmental concern to all the national and international pollution control organizations.

Fig. 5.1. Image showing the electroplating wastewater sample collection site.

In the present study it was found that the collected electroplating wastewater was basic in nature and highly dominated with Ni, Cr and Cu. Total solid of the wastewater was 3830.6 ± 13.13 and the BOD and COD was 670.00 ± 6.6 and 1130.0 ± 11.12 mg/L respectively. The concentration of Ni, Cr, Cu and Cd was 140.21 ± 1.2, 54.84 ± 2.09, 23.76 ± 0.02 and 2.43 ± 1.20 mg/L respectively (Table 5.1). Trace amount of As and Pb was also detected in collected electroplating wastewater. These parameters also investigated in some previous studies and their results are shown in Table 5.1 to compare with present study. The concentration of Ni, Cr, and Cu varied from 0.8-27562, 0.2-36756 and 2.2-335.0 mg/L respectively in different types of electroplating wastewater as reported in different studies (Bhateria and Dhaka, 2017; Borgia et al., 2015; Machado et al., 2016). The results of the previous studies (Table 5.1) and present study suggested that pollutant types and their concentration vary with the use of their respective chemical and type electroplating industries (Angelin et al., 2015; Choi and Meier, 2001; Bhateria and Dhaka, 2017; Borgia et al., 2015; Zare et al., 2015).

Table 5.1. The physicochemical characteristic of Electroplating wastewater.

Collected place	pH	EC (µS)	Pollutants in Electroplating Wastewater (mg/L)																		Reference
			TS	TDS	BOD	DO	COD	Total hardness	Oil & Grease	CN	Ca	Cr	Cu	Ni	sulphate	Zn	Cd	Mn	Co	Pb	Fe	
Chrome plating industry*	1.75	78	39860	2100	-	6.49	2228	2000	59	-	500	15147.5	287.6	798.6	-	84.5	-	-	-	-	-	Angelin et al. (2015)
-	6.8	-	-	-	-	-	620	340	-	-	-	14.7	12.8	1.86	-	81.6	-	-	-	-	17	Choi & Meier (2001)
**	2.2	24750	2597	2228	205	18	1359	2997	20	-	-	2.7	-	0.8	-	4.6	4.7	1.6		13.8	3.31	Bhateria & Dhaka (2017)
-	-	-	-	-	-	-	-	-	-	-	-	75	-	-	-	16.8	-	-	-	-	11.5	Godet et al. (1996)
Isfahan, Iran	3	15.3	93.1	-	-	1.5	806	-	-	-	-	-	-	-	-	-	-	-	-	-	-	Zare et al. (2015)
	<1	-	-	105320	-	-	-	-	-	-	265	36756	335	27562	-	-	-	0.94	-	11.64	16.4	Borgia et al. (2015)
Waste water ***	7.44	29.7	-	27.0	-	-	-	-	-	-	-	0.22	2.2	1.4	-	0.44	-	-	-	-	-	Machado et al. (2016)

****	-	-	-	-	-	-	-	-	-	-	-	36756	335	27562	-	206.7	-	-	-	11.64	16.48	Borgia et al. (2018)
*****	9.49	39.60	3830.6	-	670.0	-	1130.0	-	-	-	-	54.8	23.7	140.2	-	-	2.43	-	-	0.83	-	Present Study[#]

"-" represent parameter did not evaluated in the respective study, EC (Electrical Conductivity), TS (Total Solid), TDS (Total Dissolve solid), BOD (Biological Oxygen Demand), DO (Dissolve Oxygen), COD (Chemical Oxygen Demand), CN (Cynide), Ca (Calcium), Cr(chromium), Cu (Copper), Ni (Nickel), Zn(Zink), Cd(Cadmium), Mn(Manganese), Co(Cobalt), Pb (Lead), Fe(Iron) , *Ozhuhinasery Tamilnadu, India, **Electroplating, effluent treatment plant, Rohtak, Haryana, India, ***collected at neutralization step from Vale dos Sinos, Rio Grande do Sul, Brazil, ****Electroplating unit near Choolaimedu at Chennai, Tamil Nadu, India, ***** Ballabhgarh, Faridabad, India, [#]In the present study, values are mean of two replicates.

5B. Fungal species isolated from Electroplating wastewater

The isolated fungal species from electroplating wastewater are shown in Fig. 5.2. Four morphologically different fungal isolates were grown on the 100 mg/L amended PDA plate. These isolates were purified on without metal amended PDA plate and denoted as Isolate A, B, C and D. The colony of Isolate A was greenish in color and isolate B was brownish black, whereas cottony mycelia with white colony was appeared by isolate C which later transformed into green in color at the periphery of the colony after 3-4 d of incubation period while at the centre of PDA plate no mycelia was appeared but after 6-7 d of incubation the plate was fully occupied by the isolate C with vertical mycelia. The pinkish brown color colony was observed in isolate D.

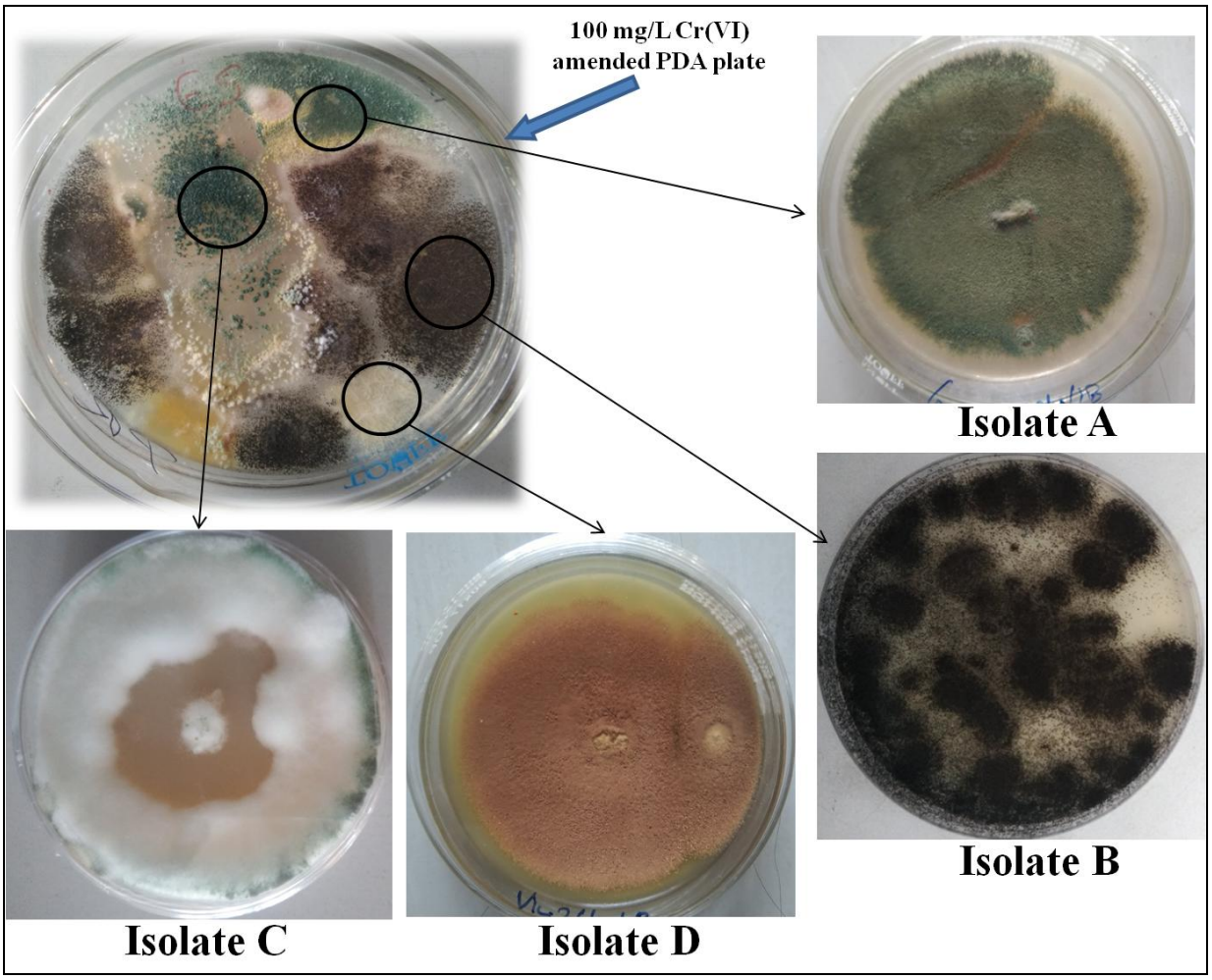

Fig. 5.2. Isolated fungal species on 100 mg/l of $Cr_{(VI)}$ amended PDA plate.

5C. Heavy metal Tolerance and coding of Fungal isolates

The tolerance of isolated fungal isolates was first tested at different concentration of $Cr_{(VI)}$. However, before conducting the tolerance assay it was hypothesized that the fungal isolate which will not be able to tolerate above 300 mg/l of $Cr_{(VI)}$ concentration, will not be selected to proceed for further study and 300 mg/L of $Cr_{(VI)}$ concentration will be considered as CR0 (critical minimum $Cr_{(VI)}$ concentration for selection of fungal isolate for further study) for nomenclature purposes of the isolates. In the tolerance test, Isolate B and D was unable to grow above 300 mg/L of $Cr_{(VI)}$ concentration. Isolate A and C showed their growth up to the concentration of 800 and 1000 mg/L of $Cr_{(VI)}$ respectively, subsequently renamed as Isolate CR500 and Isolate CR700 by following the equation.

$$CR? = Tm - CR0$$

Where, CR? represent the unknown $Cr_{(VI)}$ tolerant fungal isolate, Tm represent the maximum $Cr_{(VI)}$ tolerance concentration of isolate and CR0 represent critical minimum concentration (300 mg/L) for the selection of isolate.

5C.1 Tolerance of Isolate CR500 at different concentration of selected heavy metals

The tolerance of Isolate CR500 at different heavy metals is presented in Fig. 5.3. Cd and Cu were extremely toxic to Isolate CR500 and the growth was severely inhibited above 100 and 200 mg/L respectively. However, Cu is micronutrients, but the extreme concentration of Cu (200 mg/L) and Cd (100 mg/L) inhibited the growth of Isolate CR500. It was previously reported that oxidative damages caused by Cd inhibited the growth of *Phanerochaete chrysosporium* and *Fusarium solani* (Chen et al., 2019; Kumar et al., 2019). Severe inhibition in the growth of CR500 above 800 mg/L of $Cr_{(VI)}$ might be due to ROS production (**see section 5E.4**) and 1200 mg/L of Pb was found and the Ti (Tolerance index) was 0.15 ± 0.01 and 0.09 ± 0.01 respectively, which suggested that the above these concentrations toxic effects of both the metals were more prominent. Ni and Mn showed the toxic effect above 1600 mg/L in Isolate CR500 (Fig. 5.3). *Trichoderma harzianum* exhibited tolerance above the concentration of 500 mg/L of Ni (Cecchi et al., 2017). *Aspergillus humicola* strain SKP102 produces oxalic acid in the response of Ni stress to minimize its toxic impact and exhibited the tolerance above 9.0 mmol (Ghosh and Paul, 2016). In the present

work, Isolate CR500 showed most significant tolerance towards As (2000 mg/L; Ti: 0.22) among the tested metal/loid (Fig. 5.3). Oladipo et al. (2018) investigated the tolerance potential of *Aspergillus* spp. towards As and recorded the growth at 500 mg/L concentration of As. The higher concentration of As, Pb and Ni might produces H_2O_2 in CR500 (Table 5.2), causes oxidative stress thereby the growth of Isolate CR500 might be inhibited at elevated concentration of As, Pb and Ni. However, at the lower concentration, multiple antioxidants (SOD, POD, CAT, proline and phenolic content; Table 5.2) involve in scavenging of ROS and minimize the oxidative stress impact. These antioxidants may enable the fungus to tolerate 1200, 1600 and 2000 mg/L of Pb, Ni and As respectively. Metal tolerance index revealed that Isolate CR500 is a multimetal tolerant fungus while above a specific concentration of the metal the growth of the fungus was inhibited. Tolerance of Isolate CR500 was most significant towards As, Pb and Ni and were selected for further study.

5C.2 Tolerance of Isolate CR700 at different concentration of selected heavy metals

The Isolate CR700 showed strong tolerance towards As, Ni, Cr, Zn, and Cu and poor tolerance towards Pb and Cd (Fig. 5.4). With the increase in the concentration of heavy metal (in case of As and Ni above 200 mg/L) significant ($p \leq 0.05$) decrease in value of Ti (Tolerance index) of isolate CR700 was found. No growth of isolate CR700 was recorded above 100 mg/L of Pb and Cd (Ti: 0.00) while towards Cu and Zn the growth of isolate CR700 was recorded up to 1200 mg/L and the values of Ti were 0.15 ± 0.02 and 0.11 ± 0.02 respectively. In this work, it was found that beyond a certain concentration, Cu and Zn toxicity were prominent, although both metals are the essential micronutrient (Chen et al., 2019). Due to oxidative stress caused by cadmium, it was toxic to *Phanerochaete chrysosporium* and *Penicillium simplicissimum* at the concentration of 0.5 mmol and 100 mg/L respectively (Bhainsa et al., 2014; Chen et al., 2019). In the present study, at the concentration of 1000 mg/L of $Cr_{(VI)}$, the Ti was 0.20 ± 0.02 and no growth of Isolate CR700 was found over 1000 mg/L of $Cr_{(VI)}$. It was evaluated in this study that $Cr_{(VI)}$ causes oxidative stress via generating ROS (Fig. 5.17), however; it minimizes the oxidative stress impact by scavenging the ROS by enzymatic (CAT, POD and PPO) and non enzymatic (proline and Phenolic content) (Fig. 5. 18) antioxidants but the

excess of $Cr_{(VI)}$ might caused severe cellular damages and inhibited the growth of isolate CR700 after 1000 mg/L concentration of $Cr_{(VI)}$.

Moreover, Isolate CR700 showed growth up to 1500 mg/L of Ni (Ti: 0.07 ± 0.02) and 2000 mg/L of As (Ti: 0.20 ± 0.02) (Fig.S1), while *Trichoderma harzianum* was able to tolerate 500 mg/L of Ni (Cecchi et al., 2017). *Aspergillus humicola* strain SKP102 exhibited tolerance up to the concentration of 9.0 mmol of Ni and produces oxalic acid to minimize its toxic impact (Ghosh et al., 2016). Oladipo et al. (2018) investigated the As tolerance ability of *A. tubingensis*, *A. fumigatus*, *A. terreus*, *A. nidulans* and *A. nomius* and reported the tolerance up to the concentration of 500 mg/L. In this work, based on the tolerance potential of isolate CR700 the tested metal can be categorized into three groups for isolate CR700; strongly tolerable: As and Ni, medially tolerable: Cr, Zn and Cu and poorly tolerable: Pb and Cd.

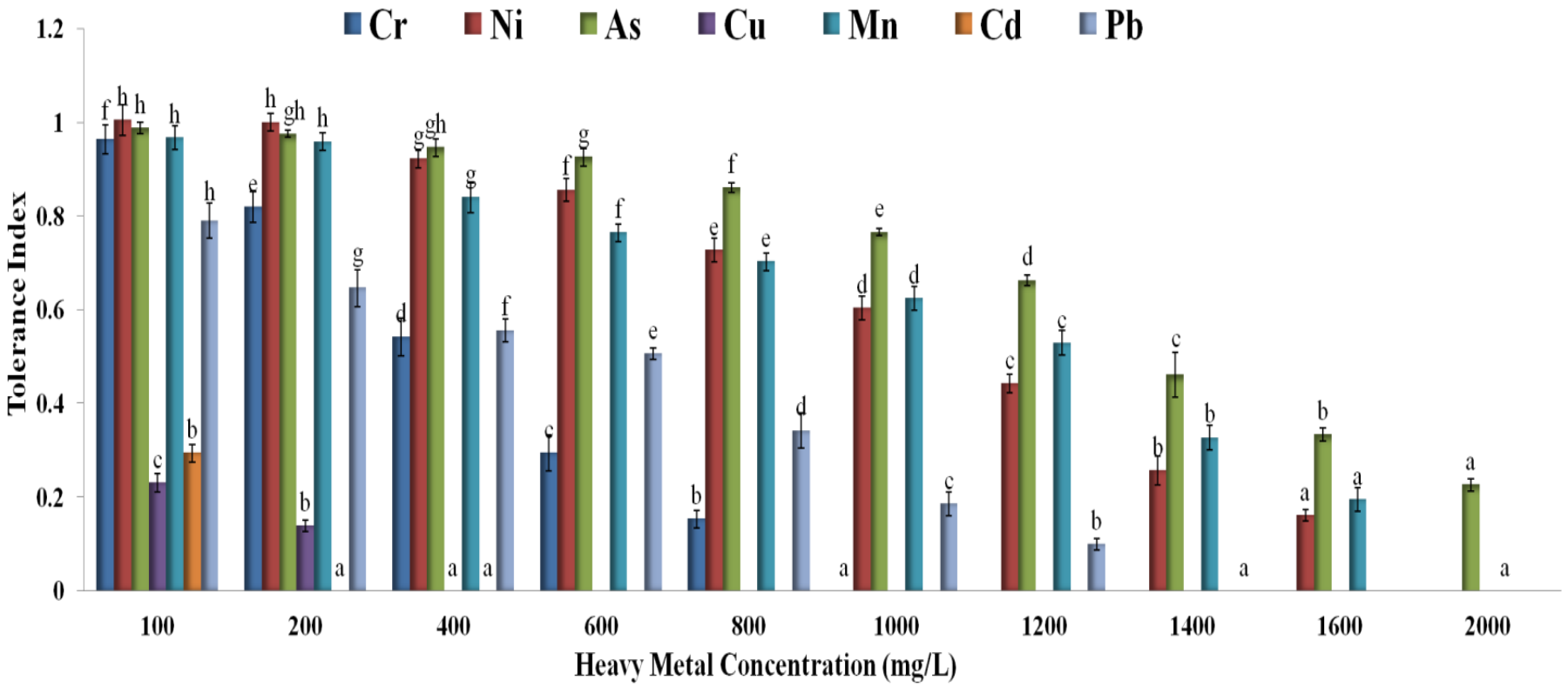

Fig. 5.3. Tolerance index of Isolate CR500 against different concentration of Cr, Ni, As, Cu, Mn, Cd and Pb (Mean ± standard deviation of three replicates, Value within each column followed by the same letter are not significantly different using DMRT$_{[p < 0.05]}$).

5D. Molecular Identification fungal isolates

The ITS region sequence of *A. flavus* isolate CR500 was determined for phylogenetic analysis. As can be seen in Fig. 5.5, Isolate CR500 showed the closest relation with *A. flavus*, *A. flavus* strain APBSMLF54, *A. flavus* strain M68, and *A. flavus* isolate DTO 213 I2. The neighbor-joining tree (Fig. 5.5) based on ITS region sequences showed that Isolate CR500 formed a distinct branch with the most closely related species, *A. flavus*, *A. flavus* strain APBSMLF54, *A. flavus* strain M68 and *A. minisclerotigenes* isolate DTO 045-I9 separated from the other member of genus *Aspergillus*. Similar to this study, some previous studies was also performed the ITS region sequencing of fungal DNA for their identification using BLAST, NCBI and identified the fungi at their species level (Dey et al., 2016; Lotlikar et al., 2018; Sharma et al., 2016; Shi et al., 2018).

The ITS region sequence of *Trichoderma lixii* isolate CR700 was determined for phylogenetic analysis. Isolate CR700 showed highest sequence similarities with *Trichoderma lixii* isolate A705, *Trichoderma* sp. isolate yi0852_1, *Trichoderma* sp. isolate yi0413_1 and *Trichoderma* sp. isolate yi0091_1. A neighbor-joining tree based on ITS region sequences showed that isolate CR700 formed a distinct branch with most closely related species, *Trichoderma lixii* isolate A705, *Trichoderma* sp. isolate yi0852_1, *Trichoderma* sp. isolate yi0413_1 and *Trichoderma* sp. isolate yi0091_1, separated from the other members of the genus *Trichoderma* (Fig.5.6)

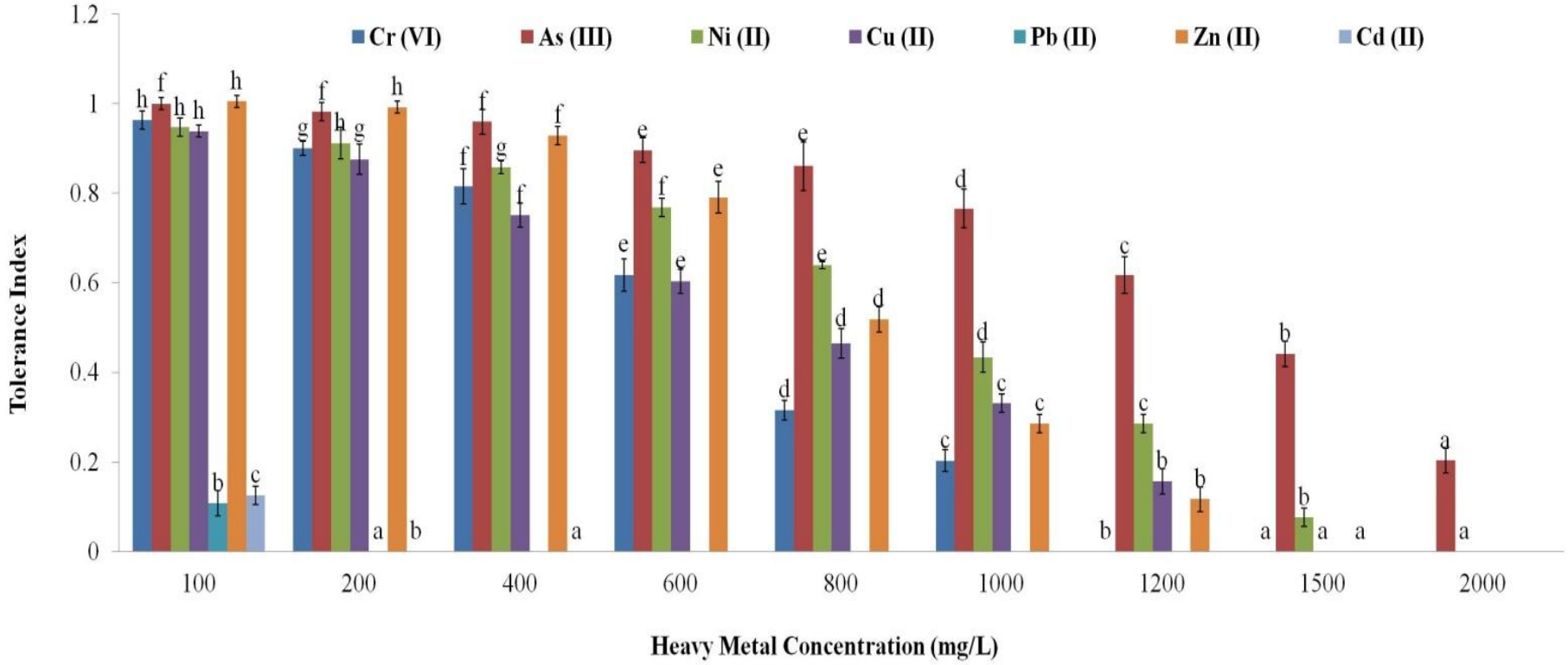

Fig. 5.4. Tolerance index of *T. lixii* CR700 towards heavy metals (Mean ± standard deviation of three replicates, Value within each column followed by the same letter are not significantly different ($p < 0.05$) using Duncan's Multiple Range Test).

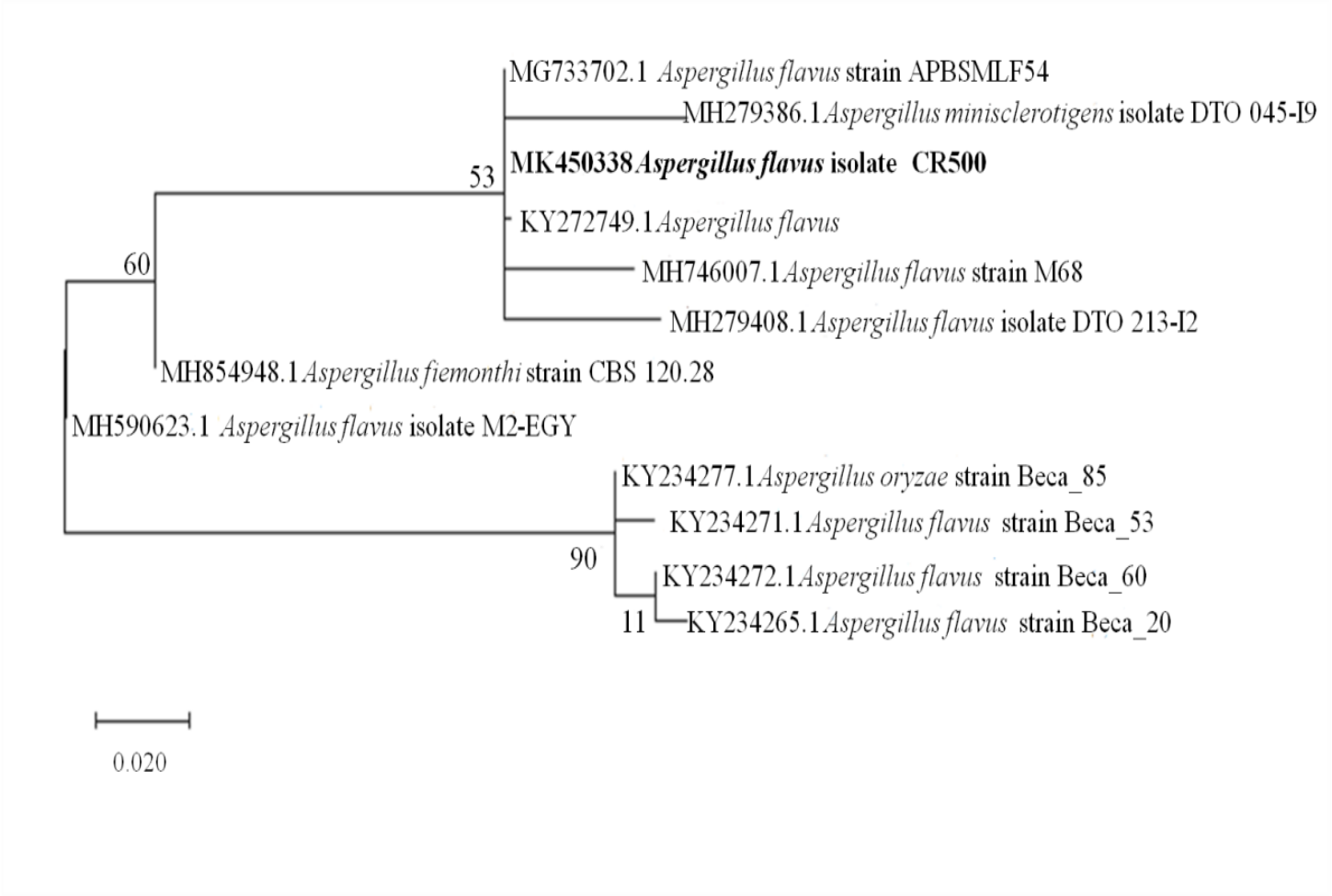

Fig. 5.5. Phylogenetic position of *A. flavus* isolate CR500 along with other closely related species of the genus *Aspergillus*. The percentage of replicate trees in which the associated taxa clustered together in the bootstrap test (1000 replicates) is shown next to the branches. The tree was reconstructed using neighbor-joining analysis based on 578 bases of aligned ITS region sequences

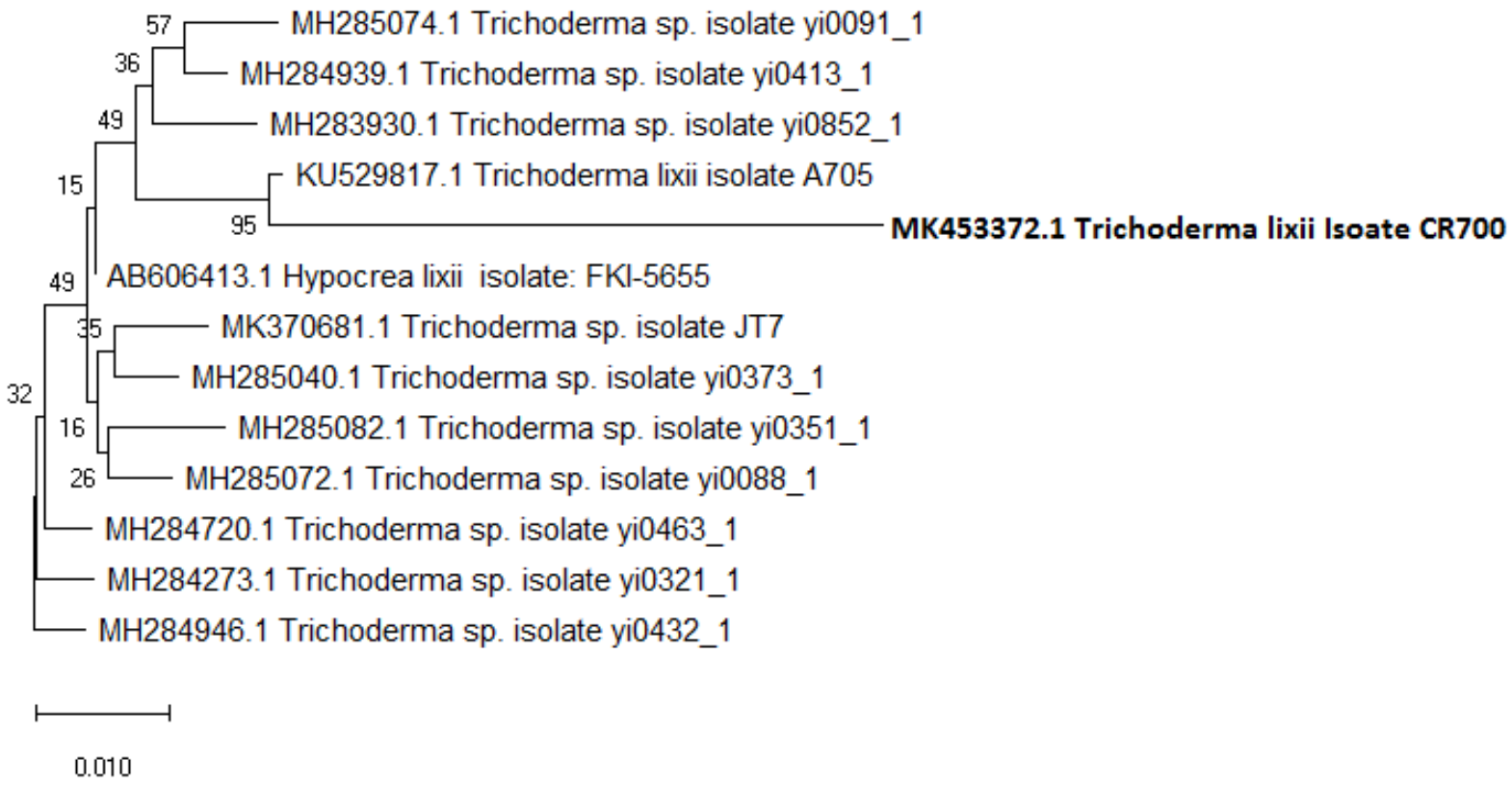

Fig. 5.6. Phylogenetic position of *T. lixii* isolate CR700 along with other closely related species of the genus *Trichoderma*. The percentage of replicate tree in which the associated taxa clustered together in the bootstrap test (1000 replicates) are shown next to the branches. The tree was constructed using neighbor-joining analysis (on MEGA X) based on 641 bases of aligned ITS region sequences and the optimal tree with the sum of branch length 0.18467182 is shown.

5E. Chromium reduction and Removal by *A. flavus* CR500: Biochemical and morphological response and phytotoxicity study

5E.1 Reduction of $Cr_{(VI)}$ by *A. flavus* CR500

A. flavus CR500 showed efficient reduction potential in the concentration range from 5 to 100 mg/L and reduces almost 99% of $Cr_{(VI)}$ to $Cr_{(III)}$ at all the concentration (Fig. 5.7a) which was higher than *Paecilomyces lilacinus* XLA (96.6%) at 100 mg/L (Xu et al., 2017a). Further increase in the $Cr_{(VI)}$ concentration up to 200 mg/L, the reduction potential of isolate CR500 was decrease to 77.5%. However, *Trichoderma asperellum* strain PTN7 and *T. asperellum* strain PTN10 reduces 2.70 and 8.35 mg/L of $Cr_{(VI)}$ at concentration of 10 mg/L (Chang et al., 2016). In this study, with increase in the $Cr_{(VI)}$ concentration the removal of $Cr_{(VI)}$ decreased significantly ($p < 0.05$) up to 50 mg/L and an instant increase of 73.4% in the removal was recorded at 70 mg/L of $Cr_{(VI)}$ (Fig. 5.7a). Chen et al. (2019) reported 88% $Cr_{(VI)}$removal by *Penicillium simplicissimum* at 100 mg/L concentration of $Cr_{(VI)}$ in seven days and *S. rolfsii* showed 60% removal of $Cr_{(VI)}$ at the concentration of 10 mg/L (Rafi et al., 2017) via accumulation and surface adsorption mechanisms. In this study, decrease in the removal percentage with increase in the $Cr_{(VI)}$ concentration might be due to decrease in obtained biomass that reduces the availability of functional group and also affect the accumulation potential of isolate CR500 (Kumar et al., 2019; Chen et al., 2019). Increase in the $Cr_{(VI)}$ concentration also saturate active sites that is responsible for $Cr_{(VI)}$ surface adsorption as found in FTIR analysis (**section 5E.8**) that's why removal percentage was decreased with increase in $Cr_{(VI)}$ concentration. Interestingly, with increase in the $Cr_{(VI)}$ concentration from 50 to 100 mg/L, the level of non-protein thiol and proline content instantly increased (Table 5.3) in which non protein-thiol is the metal complex forming agents (Chakraborty et al., 2014; Mukharjee et al., 2010) and proline is the oxidative stress reducing components (Gratao et al., 2008; Islam et al., 2016) that might be led the maximum accumulation of Cr at 70 mg/L. However, in the present study, removal of Cr by isolate CR500 happened via accumulation, adsorption and precipitation mechanism.

The $Cr_{(VI)}$ reduction experiment was also conducted at different incubation periods and results revealed that *A. flavus* CR500 could reduce 90% $Cr_{(VI)}$ to $Cr_{(III)}$ within 24 h at 50 mg/L which was increased up to 99.3% at 72 h of incubation (Fig.

5.7b). *A. niger* reduces 99% of $Cr_{(VI)}$ within 84 h at the same concentration (Gu et al., 2015). A previous study also reported complete $Cr_{(VI)}$ reduction by *Shewanella oneidensis* MR-1 below 16 mg/L of $Cr_{(VI)}$ concentration (Xafenias et al., 2013). Moreover, in this study 4.9 ± 0.12 and 0.53 ± 0.02 mg Cr per gram of dried biomass accumulation and adsorption respectively was recorded at 50 mg/L of $Cr_{(VI)}$ concentration after six days of incubation which revealed that *A. flavus* CR500 not only reduces the $Cr_{(VI)}$ into $Cr_{(III)}$ but is able to remove the Cr via accumulation inside the cell and adsorption/precipitation on mycelia surface.

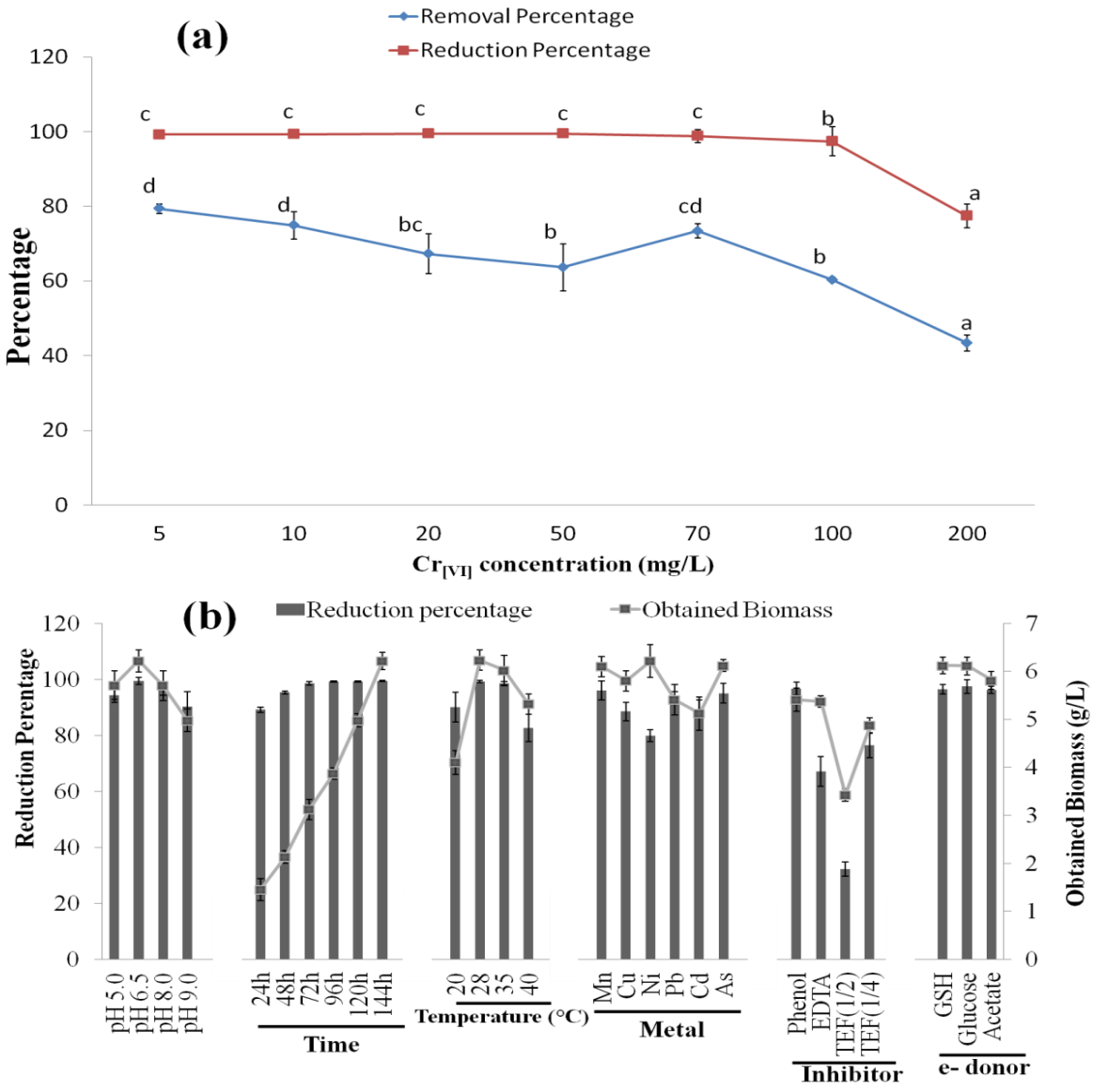

Fig. 5.7. Effect of (a) different initial concentration on reduction and removal of $Cr_{(VI)}$ *A. flavus* CR500 (Mean ± standard deviation of three replicates, Value within each column followed by the same letter are not significantly different using $DMRT_{(p < 0.05)}$). (b) Effect of various pH, time, temperature, metals (Mn; $MnSO_4$, Cu; $CuSO_4$, Ni; $NiCl_2$,

Pb; $PbSO_4$, Cd; $CdCl_2$, As; As_2O_3), metabolic inhibitor, electron donor and sterilized tannery effluent on reduction of $Cr_{(VI)}$to $Cr_{(III)}$by *A. flavus* CR500 and biomass production (values within each are representing mean of two replicates and bar representing standard deviation).

Schematic diagram of $Cr_{(VI)}$ reduction and removal mechanism by isolate CR500 is shown in Fig. 5.9. Reduction of $Cr_{(VI)}$ to $Cr_{(III)}$ in isolate CR500 was mainly driven by the enzyme ChrR (Martorell et al., 2012; Irazusta et al., 2018). $Cr_{(VI)}$ induced ChrR activity was recorded in *A. flavus* CR500 which was a major factor that driven the $Cr_{(VI)}$ reduction into $Cr_{(III)}$ where NADH, GSH, acetate and glucose (Fig. 5.7b) played a role of electron donor (Arévalo-Rangel et al., 2013; Banarjee et al., 2019). Some studies also suggested that one electron transfer mechanism might involve in $Cr_{(VI)}$ reduction (Pradhan et al., 2017; Cui et al., 2011). Reduced $Cr_{(III)}$ might be either efflux to outside of the cell through efflux pump such as proton motive force, CDF protein (able to transport the heavy metal from cytoplasm to periplasm and outside of the cell) (Vaccaro et al., 2016; Banerjee et al., 2019) or went to vacuolar compartmentation via Cr-thiol complex formation (Bhatia et al., 2005; Cánovas et al., 2003). Chromium removal by *A. flavus* CR500 was occurred due to accumulation and adsorption/precipitation. Increased in GSH and non-protein thiol content (Table 5.3) might lead to Cr-thiol complexation which went to vacuolar compartmentation also inferred by SEM analysis (Fig. 5.10) (Cánovas et al., 2003; Long et al., 2018). Cr bioadsorption and precipitation was inferred by EDS, FTIR and XRD analysis (Fig. 5.10, 5.11, 5.12). Cr precipitation happened on the surface of fungi mainly in the form of Cr_2O_3 as reported in some previous studies (Karthik et al., 2017; Raza et al., 2016; Dhal et al., 2018).

5E.2 Bioreduction potential under different stress conditions

In the bioremediation process, natural sites have multiple factors (conditions) that can reduce the growth and bioremediation efficiency of bio-remediators. In this context, the growth and reduction ability of *A. flavus* CR500 was also determined under the different stress conditions (Fig. 5.7b). The *A. flavus* CR500 could able to reduce 50 mg/L of $Cr_{(VI)}$ efficiently in a range of temperature 20 to 40°C. The reduction percentage was 90, 99.3, 98.5 and 82.5 % at the temperature of 20, 28, 35 and 40 °C respectively (Fig. 5.7b). Murugavelh et al. (2013) investigated the

reduction efficiency of immobilized *Phanerochaete chrysosporium* in the temperature ranges from 10-40 °C and maximum was 98.3 at 25 °C which is lower than the present study at 28 °C (99.3%). In this work, reduced in the reduction percentage at 20 and 40 °C might be due to decrease in the activity of ChrR and obtained biomass at these temperature played a role in reduction of $Cr_{(VI)}$in isolate CR500 (Kathiravan et al., 2010). However, the most favorable temperature was 28 to 35 °C for $Cr_{(VI)}$ reduction by isolate CR500.

The pH of the solution is an important factor that can influence the metal solubility, microbial growth, surface functional group of the cell and ultimately reduction efficiency of the microbes (Das et al., 2014; Kathiravan et al., 2010). In the present work, isolate CR500 exhibited efficient $Cr_{(VI)}$ reduction ability in the pH ranges from 5.0 to 9.0. However, a maximum of 99.4% reduction of $Cr_{(VI)}$ was recorded at pH 6.5 followed by 96.4, 94.3 and 90.0% at the pH 8.0, 5.0 and 9.0 respectively (Fig. 5.7b). Murugavelh et al. (2013) reported an increase removal (98.3%) at pH 5.0 using immobilized spore of *Phenerocheate chrysosporium* on Ca alginate due to physicochemical interaction between metal ion and matrix. *Bacillus amyloliquefaciens* showed maximum reduction (92.4%) at pH 7.0 (Das et al., 2014) and Xu et al. (2017) reported maximum $Cr_{(VI)}$reduction in the pH ranges from 5.5 to 6.5 by fungus *Paecilomyces lilacinus* XLA. In the present study, decrease in the biomass productivity (Fig. 5.7b) and the activity of ChrR enzyme with change in the pH (optimum pH 6.5) of the solution might be possible explanation for decrease in reduction percentage with change in the solution pH (Das et al., 2014; Xu et al., 2017). However, at higher pH the negatively charged mycelia may cause the repulsion between the mycelia surface and chromate ions that also could negatively influence the reduction ability of isolate CR500.

Most of the studies investigated the reduction potential of fungi at different pH, temperature and initial concentration of $Cr_{(VI)}$ (Murugavelh et al., 2013; Xu et al., 2017; Chang et al., 2016; Gu et al., 2015). The presence of heavy metals and different types of metabolic inhibitor in wastewater is common which can affect the growth and reduction capability of fungi due to their toxicity. However, in the present study, isolate CR500 showed efficient reduction potential and high biomass productivity with different heavy metal and metabolic inhibitors that's really harsh to grow for all fungi. Isolate CR500 exhibited 96, 95, 91.4, 89.5, 88.5 and 79.8% reduction of $Cr_{(VI)}$

with 10 mg/L of Mn, As, Pb, Cd, Cu, Ni respectively (Fig. 5.7b). The presence of EDTA (a metabolic inhibitor) decreased the reduction percentage to 67% (Arévalo-Rangel et al., 2013), while 96% reduction was recorded in presence of phenol by isolate CR500. The GSH, glucose and acetate are the electron donor provide the electron in the $Cr_{(VI)}$ reduction via enzyme chromate reductase (Banerjee et al., 2019) and positively affect the reduction ability of isolate CR500 (Fig. 5.7b).

Moreover, isolate CR500 showed slow growth in 50% diluted PDB medium with sterilized TEF and reduce 32.2% of the externally added 50 mg/L of $Cr_{(VI)}$, however, showed fast growth in one fourth diluted PDB medium with sterilized TEF and reduce 74.4% of the externally added 50 mg/L of $Cr_{(VI)}$ (Fig. 5.7b) and also showed 39% removal of total Cr at the same concentration. The ability of *A. flavus* CR500 to grow and reduce the $Cr_{(VI)}$ under such conditions especially TEF and heavy metals which are the key challenges in the bioremediation process, that make it promising bio-agent for bioremediation of $Cr_{(VI)}$. None of the studies is available over the reduction potential of fungi under such stress conditions (metals and metabolic inhibitors); however, some studies have been reported the multimetal tolerance potential of fungi (Li et al., 2017; Chen et al., 2019; Gola et al., 2016).

5E.3 Chromate reductase (ChrR) activity

The ChrR activity was determined as $Cr_{(VI)}$ reduction potential of $Cr_{(VI)}$induced CFE (ChrR at 50 mg/L of $Cr_{(VI)}$) and without $Cr_{(VI)}$ induced CFE (ChrR at 0 mg/L of $Cr_{(VI)}$) of Isolate CR500. The activity of ChrR increased from 6.3 ± 0.16 to 10.4 ± 0.31 U/mg proteins in without $Cr_{(VI)}$ induced CFE and $Cr_{(VI)}$ induced CFE (Fig. 5.8f). The $Cr_{(VI)}$reduction by without $Cr_{(VI)}$ treated CFE indicate that either ChrR is involved in the mechanism other than $Cr_{(VI)}$ reduction or some other enzymes are also accountable in $Cr_{(VI)}$ reduction. However, the activity of ChrR was increased up to 63.7% by the exposure of $Cr_{(VI)}$ in isolate CR500 compared to control. A similar result was reported in *Cyberlindnera jadinii* M9 and *Wickerhamomyces anomalus* M10 (Irazusta et al., 2018). The ChrR is a soluble intracellular type of enzyme (Martorell et al., 2012) and its activity is also reported on the plasma membrane of *C. jadinii* M9 and *W. anomalus* M10 (Irazusta et al., 2018; Martorell et al., 2012) which is responsible for the extracellular reduction of hexavalent chromium. Other than ChrR, flavoprotein wrbA (Ycp4), Type II nitroreductase (Frm2) and putative nitroreductase-

like proteins Hbn1 might be responsible for $Cr_{(VI)}$ reduction; were over-synthesized under chromium exposure in *Saccharomyces cerevisiae*, *W. anomalus* M10 and *C. jadinii* M9 (de Oliveira et al., 2007; Irazusta et al., 2018; Kwak et al., 2003).

5E.4 Oxidative stress under $Cr_{(VI)}$ exposure

Hexavalent chromium is redox active transition metal, catalyzes the production of ROS such as $O_2^{\bullet-}$, H_2O_2 and $OH^{\bullet}$ by Haiveber–Weiss and Fenton reactions and thus causes oxidative damage inside the cells (Halliwell and Gutteridge, 1984; Wu et al., 2010). The strong oxidative property of ROS oxidizes unsaturated fatty acid, protein and DNA and giving rise into multiple oxidative damages (Scandalios, 2005). In this study, the levels of H_2O_2 and lipid peroxidation were significantly increased in isolate CR500 under the stress of $Cr_{(VI)}$ (Table 5.2). This study directly correlates to increase in lipid peroxidation with hydrogen peroxide production under $Cr_{(VI)}$ stress and indicated that the $Cr_{(VI)}$ toxicity was due to ROS production. However, a maximum of 9.18 n mol/g FW H_2O_2 and 35.2 mU/mg protein of MDA was recorded at 100 mg/L of $Cr_{(VI)}$. Li et al. (2017a) reported that higher concentration of Cr and Cd exhibited the production of H_2O_2 and increase the lipid peroxidation in *Pleurotus ostreatus* HAU-2.

5E.5 Enzymatic antioxidants response

The ROS scavenging properties of the antioxidants make them an important component of cellular immune system (Scandalios, 2005; Zhang et al., 2016). SOD, POD, CAT, and PAL belongs to the group of induced enzymatic antioxidants and reduce the impact caused by oxidative stress (Xu et al., 2012). In this study, the activity of polyphenol oxidase (PPO) significantly increased with increase in the $Cr_{(VI)}$ concentration ($p < 0.05$) (Fig. 5.8b). The similar result for PPO and PAL was reported in *S. rolfsii* under Cr stress (Rafi et al., 2017). In present study, the activity of SOD and CAT increased significantly ($p \leq 0.05$) with the increase in the concentration of $Cr_{(VI)}$ (Fig. 5.8a,d). Similarly, with increase in the $Cr_{(VI)}$concentration the activity of POD and PAL was also increased in *A. flavus* CR500 (Fig. 5.8c,e). Increase in the activity of SOD, POD and CAT were also reported in *Pleurotus ostreatus* HAU-2 and *Fusarium solani* under stress of Cr and Cd (Li et al., 2017; Kumar et al., 2019). The significant increase in activities of PPO, SOD, POD, CAT and PAL is directly associated with an increase in the production of H_2O_2 and lipid peroxidation (Table

5.2). The results revealed that CAT, SOD, POD, and PPO are associated with scavenging of ROS as reported in plants (Wu et al., 2010; Yang and Li, 2011; Xu et al., 2012).

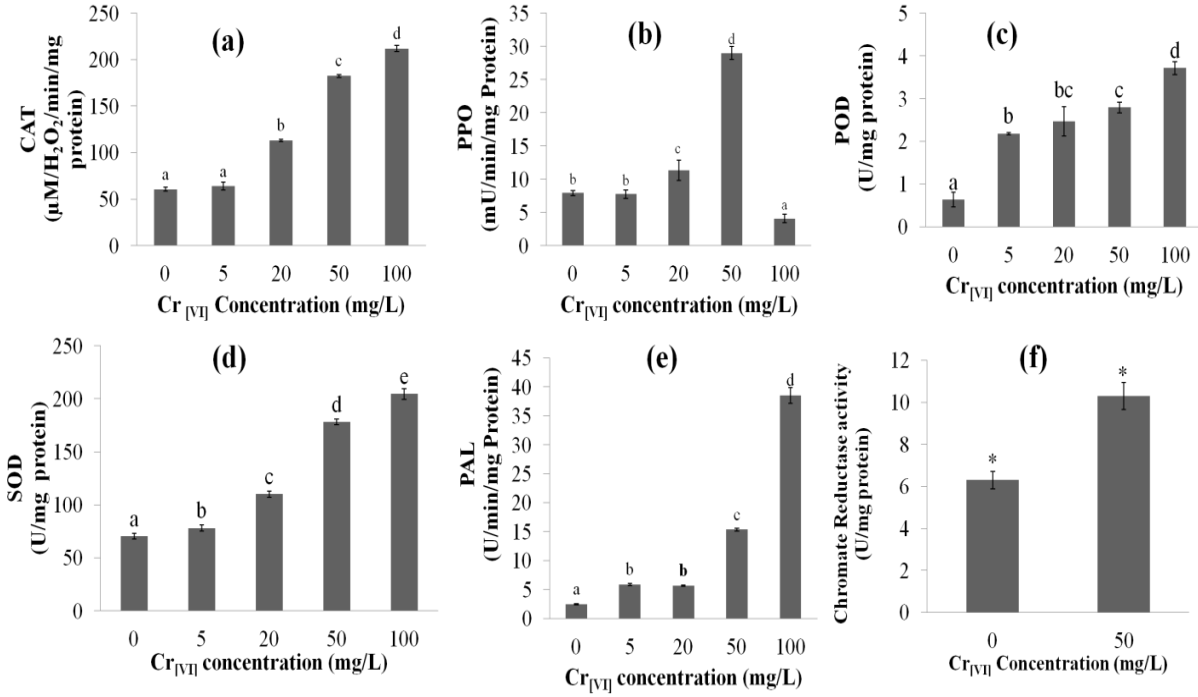

Fig. 5.8. Effect of $Cr_{(VI)}$ on activity of (a) CAT, (b) Polyphenol oxidase (PPO), (c) POD, (d) SOD, (e) Phenyl ammonia lysae (PAL), and (f) Chromate reductase in *A. flavus* CR500 (Mean ± standard deviation of three replicates, Value within each column followed by the same letter are not significantly different using $DMRT_{(p < 0.05)}$) (*data are significantly different using Paired $t\text{-}Test_{(p < 0.05)}$).

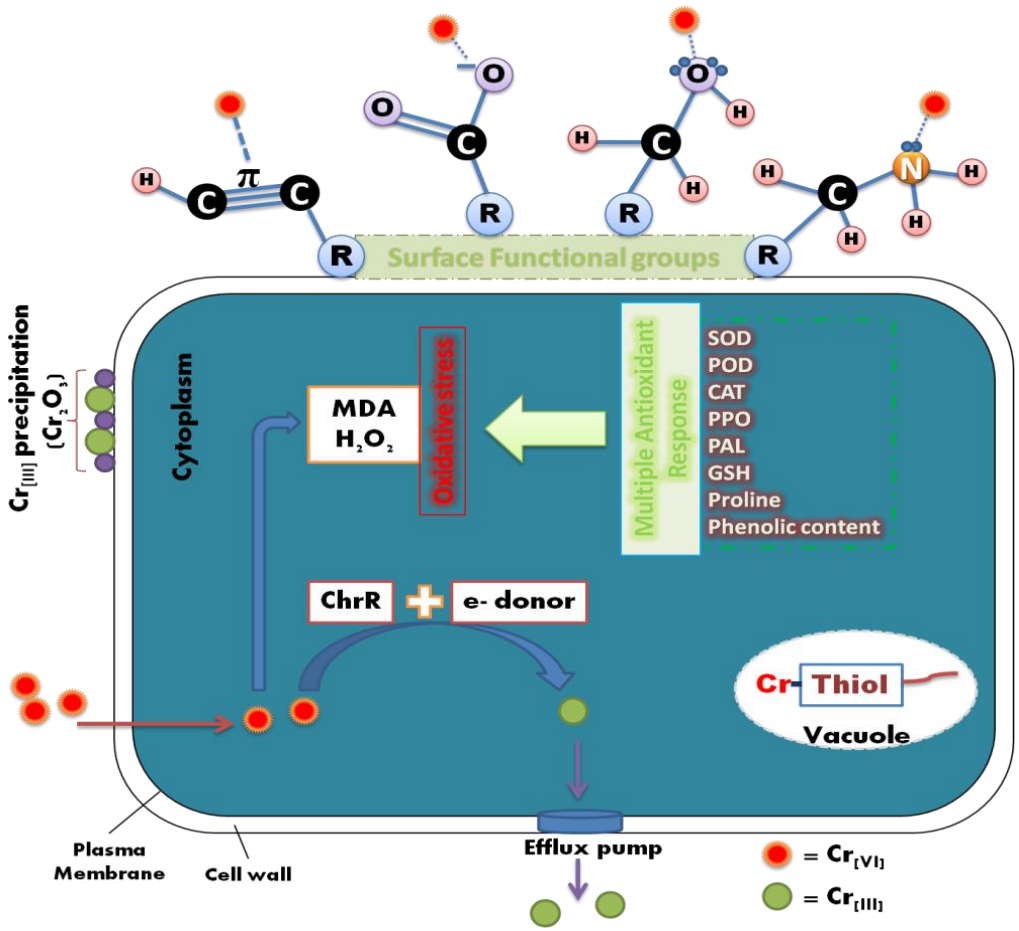

Fig. 5.9. Schematic diagram showing that $Cr_{(VI)}$ (red ball) after coming in the contact of isolate CR500, inter inside the cell of the fungus and causes oxidative stress via producing the ROS. In response of the oxidative stress, the level of multiple antioxidants increase inside the cell to minimize the oxidative impact by scavenging the ROS and on another hand $Cr_{(VI)}$ induces the activity of ChrR that detoxified $Cr_{(VI)}$via transferring into its less toxic $Cr_{(III)}$ form (green ball). $Cr_{(III)}$ might be effluxes from inside to outside of the cell of the isolate CR500 or accumulated inside the cell via thiol-Cr complex formation and vacuolar compartmentation. Effluxes $Cr_{(III)}$ might goes to extracellular precipitation in the form of Cr_2O_3 on the surface of the fungus. Some cell surface functional groups (─C≡C─, NH_2, COO^-, C=O and O─H) also contributed to total Cr removal from the aqueous medium via adsorption by electrostatic attraction and π-bond─Cr interaction.

5E.6 Biochemical and Non-enzymatic antioxidants

The intracellular protein content was first increased with increase in $Cr_{(VI)}$concentration up to 20 mg/L and then significantly ($p \leq 0.05$) decreased (Table 5.2). The level of GSH and non-protein-thiol-content in *A. flavus* CR500 was

significantly ($p \leq 0.05$) increased with increase in $Cr_{(VI)}$ concentration (Table 5.2) and maximum of 40.4 mmol/g FW and 473.4 µmol/g FW was recorded at 100 mg/L of $Cr_{(VI)}$. The GSH is less abundant than Non-protein thiol content. It might minimize the $Cr_{(VI)}$ stress via chelation and antioxidation mechanisms (Qin et al., 2007). Increase in the level of GSH was also recorded in *Pleurotus ostreatus* HAU-2 under Cd and Cr (Li et al., 2017). In plants, GSH not only involved as an antioxidant in redox homeostasis of the cell but it is also a defender of heavy metal detoxification by inducing the phytochelatins production (Rausch and Wachter, 2005; Anjum et al., 2012). In this study, a significant increase in non-protein-thiol content indicates its involvement in Cr-thiol complexation. Similar results were reported for the complexation of cadmium-thiol and arsenic-thiol in *A. foetidus* and *A. niger* respectively (Chakraborty e al., 2014; Mukharjee et al., 2010). Total phenolic content, GSH and proline are the non-enzymatic antioxidant and play a significant role in the scavenging of ROS (Islam et al., 2016). In this study, with the increase in the $Cr_{(VI)}$ concentration the proline and total phenolic content production was also significantly ($p \leq 0.05$) increased in *A. flavus* CR500 and maximum production of proline (0.89 µ mol/g FW) and phenolic content (53.84 µg/mL) was recorded at 100 mg/L of $Cr_{(VI)}$ (Table 5.2). The phenolic content protects the cell from the adverse effect of heavy metal stress through scavenging the reactive oxygen species via donating the hydrogen atoms from its hydroxyl group (Hernandez et al., 2009). However, in plants, proline and phenolic content production were found in the response of heavy metal stress, drought, osmotic stress, and high levels of salinity (Ashraf and Foolad, 2007; Gratao et al., 2008; Islam et al., 2016).

Table 5.2. Effect of different concentration of $Cr_{(VI)}$ on biomass production, intracellular protein content, proline, total phenolic content, Lipid peroxidation (MDA), H_2O_2 content, GSH and non-protein thiol content in *A. flavus* CR500. All the values are mean of three replicates ± SD. ANOVA post hoc DMRT was done to check the variation within the variable. Identical letter denote no significance differences at the level of $p \leq 0.05$.

$Cr_{(VI)}$concentration (mg/L)	Obtained Biomass (g/L)	Protein (µg/g FW)	Proline (µ mol/g FW)	Total Phenolic Content (µg/mL)	MDA (mU/mg protein)	H2O2 (n mol/g FW)	GSH (mmol/g FW)	Non-protein thiol content (µmol/g FW)
0	6.18 ± 0.41^{d}	469.6 ± 6.3^{c}	0.69 ± 0.018^{d}	0.65 ± 0.10^{a}	16.7 ± 0.7^{a}	0.92 ± 0.14^{a}	15.5 ± 0.77^{a}	87.1 ± 4.3^{a}
5	6.10 ± 0.33^{d}	454.3 ± 2.5^{b}	0.40 ± 0.007^{c}	2.94 ± 1.51^{a}	24.2 ± 0.5^{b}	1.45 ± 0.14^{a}	19.3 ± 0.61^{ab}	143.5 ± 6.2^{b}
20	5.84 ± 0.10^{c}	518.3 ± 4.5^{d}	0.13 ± 0.004^{a}	23.26 ± 1.30^{b}	27.1 ± 0.4^{c}	2.36 ± 0.57^{b}	22.4 ± 4.78^{b}	233.7 ± 7.3^{c}
50	5.53 ± 0.17^{b}	479 ± 7.4^{c}	0.31 ± 0.023^{b}	42.70 ± 2.14^{c}	29.7 ± 0.5^{d}	5.44 ± 0.11^{c}	32.2 ± 0.84^{c}	308.2 ± 7.8^{d}
100	4.85 ± 0.15^{a}	303 ± 13.0^{a}	0.89 ± 0.011^{e}	53.84 ± 2.23^{d}	35.2 ± 1.5^{e}	9.18 ± 0.55^{d}	40.4 ± 1.39^{d}	473.4 ± 11.3^{e}

5E.7 SEM analysis

$Cr_{(VI)}$ accumulation and biosorption were inferred from the lack of globular protrusions mycelia (smooth hyphae) after exposure of $Cr_{(VI)}$ (Fig. 5.10a, f; red and black arrow). While rough with dense globular protrusions mycelia of Isolate CR500 was found in the absence of $Cr_{(VI)}$ (Fig. 5.10a, e; red arrow). A similar result was also reported in *Penicillium simplicissimum* for the adsorption and accumulation of Zn, Cu, and Cd (Chen et al., 2019). The constriction in hyphae also occurred under the exposure of 100 mg/L of $Cr_{(VI)}$ (Fig. 5.10c; yellow circle) which might be associated with the tolerance mechanism of Isolate CR500. Liu et al. (2011) reported the aggregation of *P. simplicissimum* mycelia under the stress of Cd which leads to detoxification by reducing the surface area. However, under the exposure of 500 mg/L of $Cr_{(VI)}$, swelled or outward growth (Fig. 5.10f; yellow arrow) and ruptured hyphae of isolate CR500 (Fig. 5.10f; black circle) was found which might be associated with an increase in number/size of vacuoles due to compartmentation of chromium thiolic/organic compound (Cánovas et al., 2003; Wu et al., 2015; Chen et al., 2019). In this study, the increase in level of non-protein thiol content (Table 5.2) might associated with Cr-thiol production and due to its vacuolar compartmentation, intracellular outward pressure was increased and causes swelling/outward growth and rupture of mycelia. Similar result was reported in *Aspergillus sp.* and *P. oxalicum* SL2 under arsenate stress and Cr stress respectively (Cánovas et al., 2003: Long et al., 2018). Moreover, the presence of Cr (1.82 weight%) was also detected by EDS (Fig. 5.10b, d) analysis at 100 mg/L treatment of $Cr_{(VI)}$ which is a shred of evidence to the biosorption of $Cr_{(VI)}$on the mycelia surface of *A. flavus* Isolate CR500. Zn, Cu, and Cd biosorption was also detected on the surface of *P. simplicissimum* by EDS analysis (Chen et al., 2019).

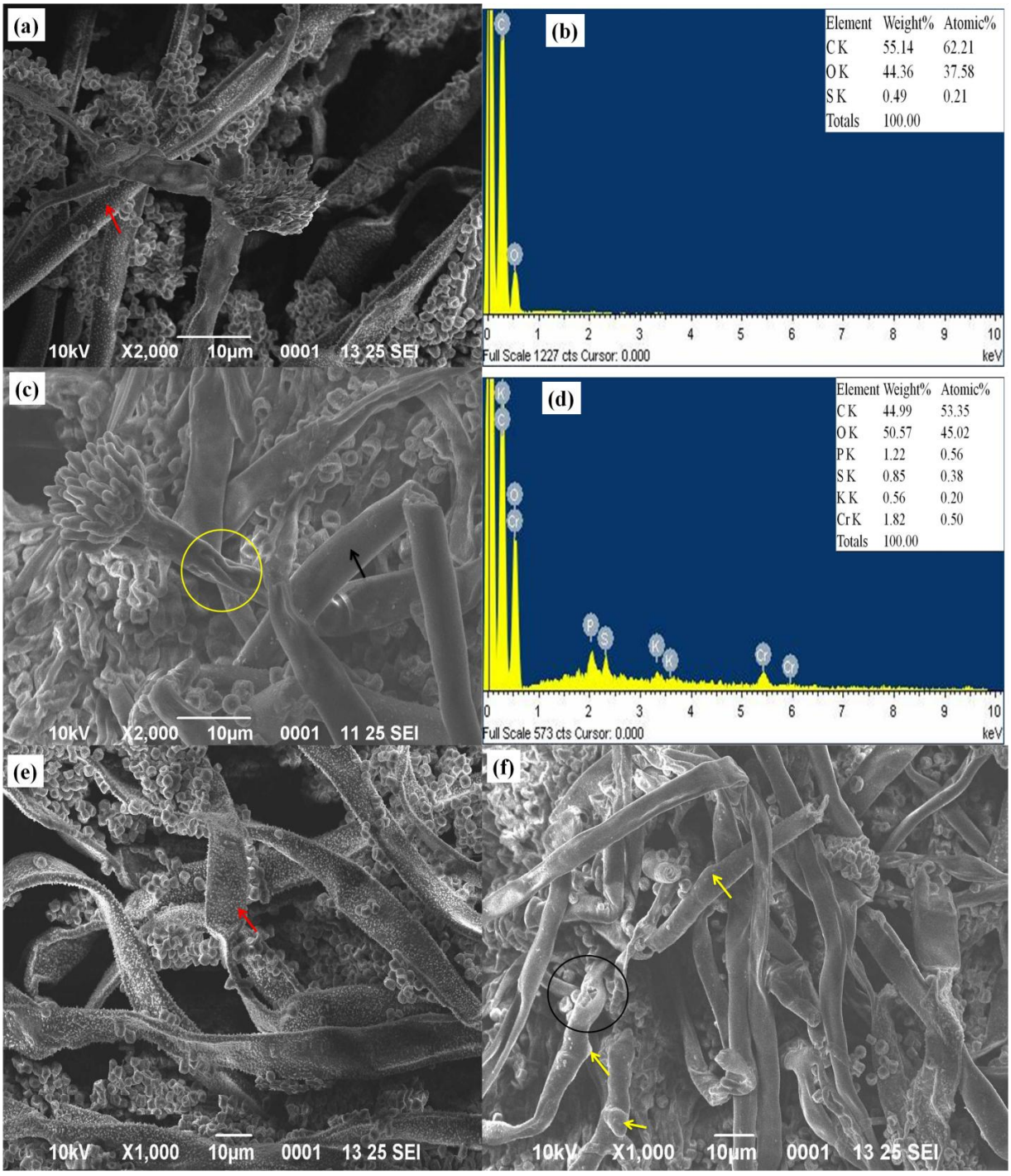

Fig. 5.10. Effect of $Cr_{(VI)}$ on the morphology of *A. flavus* Isolate CR500 (a) and (e) SEM image at different magnitude (red aero sowing the rough mycelia of isolate CR500) (c) at 100 mg/L (yellow circle showing mycelial constriction under $Cr_{(VI)}$ and black aero showing protrusionless mycelia) (F) 500 mg/L (black circle representing to ruptured hyphae and yellow aero showing swelling/outward growth) (b) EDS micrograph of control and (d) treated with 100 mg/L of $Cr_{[VI]}$.

5E.8 FTIR and XRD analysis

The change in the vibrational frequencies was detected using FTIR analysis (Fig. 5.11a, b; Table 5.3) which is associated with $Cr_{(VI)}$ biosorption (Liu et al., 2011). The disappeared peak from $Cr_{(VI)}$ treated biomass at 2134.8 cm^{-1} (C≡C Stretching) indicated to metal-π bond ($Cr_{[VI]}$─π) interaction involvement in $Cr_{(VI)}$ biosorption . The disappeared peak at 1374.3 and 1744.6 cm^{-1} assigned to amide III band represents to COO^- anions and stretching of C═O group respectively which indicate the electrostatic attraction involved in biosorption of $Cr_{(VI)}$. The shift in the peak 3407.5 to 3375.6 cm^{-1} assigned to ─OH stretching vibration and ─NH stretching of the protein, indicated to lone pair (lp)-metal interaction in the binding of $Cr_{(VI)}$ where, OH have two lp and NH have one lp (Fig. 5.11a, b; Table 5.3). The shift in the peak 1648.9 cm^{-1} to 1650.5 cm^{-1} and 1554.9 cm^{-1} to 1549.0 cm^{-1} was clearly indicated the involvement of the protein associated functional group in the complexation of $Cr_{(VI)}$ (Fig. 5.11a, b; Table 5.3) (Damodaran et al., 2013). Heavy metal biosorption using fungi is known to engage different functional groups (Chen et al., 2019; Xu et al., 2017a). The involvement of amine and hydroxyl group of *Rhizopus arrhizus* was found in $Cr_{(III)}$ biosorption (Shoaib et al., 2013) whereas, OH, NH, C=O and phosphate groups of *P. simplicissimum* were involved in the removal of Cd, Cr, Cu and Pb (Chen et al., 2019).

To identify the presence of Cr minerals, $Cr_{(VI)}$ treated fungal biomass of isolate CR500 was scanned by the XRD. The diffract gram of $Cr_{(VI)}$ treated fungal biomass is shown in Fig. 12, carried multiple peaks of Cr_2O_3. The peaks at $2\theta = 23°$, 35.8° and 41° corresponding to (220), (221) and (221) planes respectively, assigned the presence of Cr_2O_3 (Nayak et al., 2018, Raza et al., 2016). Some similar results of $Cr_{(VI)}$ reduction were reported in *A. fumigatus*, *Cellulosimicrobium funkei* strain AR8 and *Bacillus cereus* strain and concluded the same (Karthik et al., 2017; Dhal et al., 2018; Nayak et al., 2018).

5E.9 Phytotoxicity test

In sight of ecotoxicological assessment, the phytotoxicity test of fungal treated and without treated 100 mg/L of $Cr_{(VI)}$ and sterilized distilled water was subjected to phytotoxicity test using Mung bean (*Vigna radiata*) seeds. The *Vigna radiata* was also used in some previous studies to assess the toxicity of treated and without treated

heavy metal solution (Chen et al., 2019; Sharma and Malaviya, 2016). In the present study, Longer shoot (13.2 ± 1.6 and 14.1 ± 1.4 cm) and root (4.5 ± 2.1 and 4.0 ± 0.9 cm) of *Vigna radiata* was recorded for sterilized distilled water and fungal treated 100 mg/L of $Cr_{(VI)}$ respectively (Fig. 5.13a). However, the root and shoot growth of *Vigna radiata* was 0.0 and 0.14 ± .05 cm respectively in without fungal treated 100 mg/L of $Cr_{(VI)}$ (Fig. 5.13a). The seed germination rate of *Vigna radiata* was 100% for sterilized distilled water and fungal treated 100 mg/L of $Cr_{(VI)}$ while 73.5 ± 5.5% was in without fungal treated 100 mg/L of $Cr_{(VI)}$ solution (Fig. S5b). The results revealed that the toxicity of $Cr_{(VI)}$ was successfully detoxified after treating with *A. flavus* CR500.

Table 5.3. The FTIR spectra and assigned functional groups of 100 mg/L of $Cr_{(VI)}$ treated and without $Cr_{(VI)}$ treated biomass *A. flavus* CR500.

Untreated fungal biomass (cm^{-1})	$Cr_{(VI)}$ treated fungal biomass (cm^{-1})	Suggested assignment
3407.5	**3375.6**	─OH Stretching vibration and –NH stretching of protein or acetamide groups of chitin fraction
2925.3	**2927.3**	─CH Stretching vibration of fatty acid in membrane phospholipid
2856.4	─	C─H stretching vibration
2134.8	─	C≡C Stretching
1744.6	─	Stretching of C═O group
1648.9	**1650.5**	Amide I of N-acetyl glucosamine polymer or the protein peptide bond
1554.9	**1549.0**	Amide II of N-Acetyleglucosamine polymer or the protein
─	1409.3	C─N stretching in Amide III
1374.3	─	Amide III band represents to COO^{-} anions
1241.4	1241.0	SO_3 group
1150.3	1150.4	Phosphates group
1076.9	**1078.5**	Phosphate groups
1036.7	1036.9	C─N stretching vibration of the chitin-chitosan and protein
─	888.6	CH_2 out of plane wagging
608.6	**611.0**	C=O in amides

The '─' denote peak not detected and **Bold** values denotes shift in peak when compared to control.

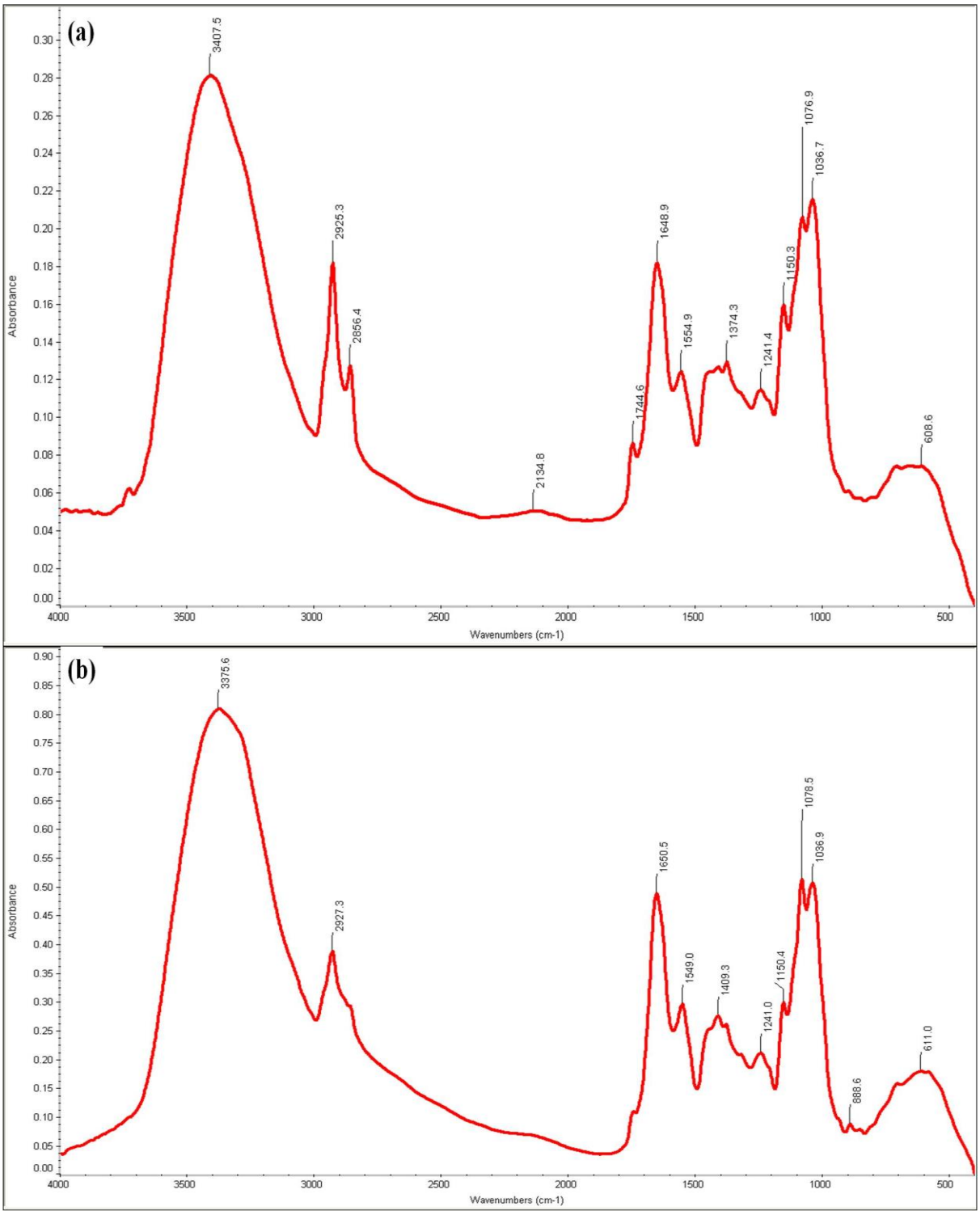

Fig. 5.11. FTIR image of (a) control and (b) treated with 100 mg/L of $Cr_{(VI)}$ fungal biomass of *A. flavus* CR500.

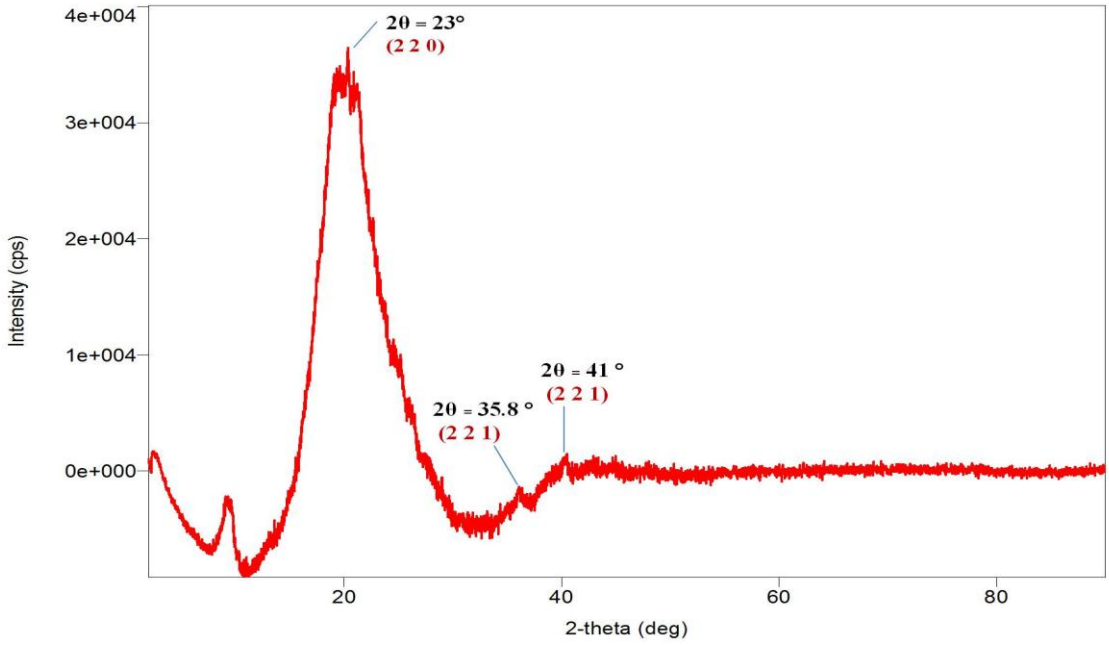

Fig. 5.12. XRD image of 100 mg/L of $Cr_{(VI)}$ treated biomass of *A. flavus* CR500.

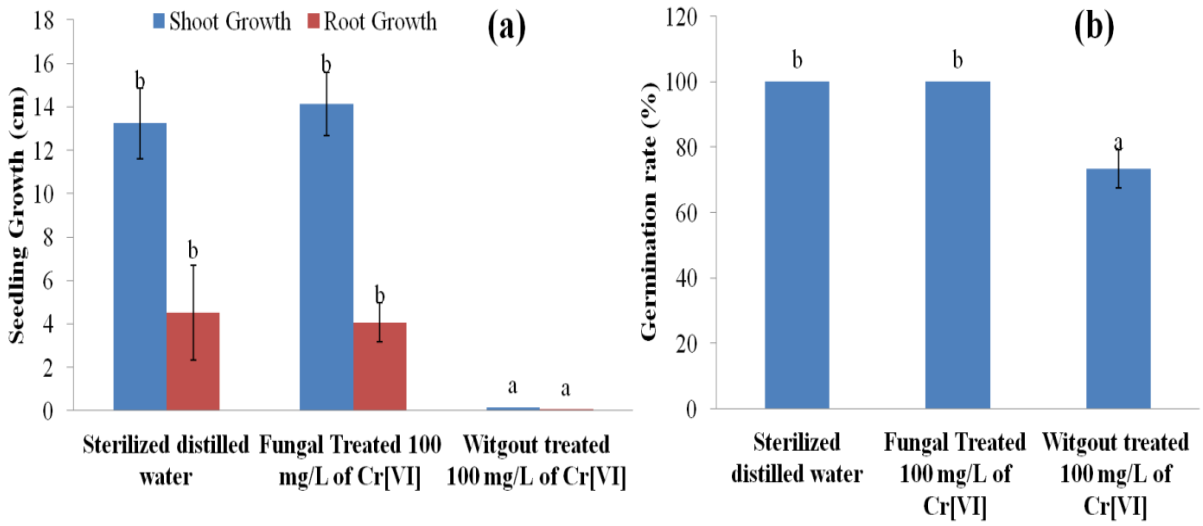

Fig. 5.13. Phytotoxicity test using Mnng bean (*Vigna radiata*) seeds (a) growth of seedling and (b) germination rate in different solution taken for the study (Mean ± standard deviation of three replicates, Value within each column followed by the same letter are not significantly different using $DMRT_{(p < 0.05)}$).

5F. *T. lixii* CR700 and $Cr_{(VI)}$: Reduction, removal and Biochemical analysis

5F.1 Chromium reduction by *T. lixii* CR700

The reduction potential of isolate CR700 was investigated at different concentration ranged from 0 to 200 mg/L of $Cr_{(VI)}$ and the results are shown in Fig. 5.13a. The maximum 99.4% reduction of $Cr_{(VI)}$ into $Cr_{(III)}$ was recorded at the concentration of 50 mg/L which was higher as previously reported 96.6% reduction by *Paecilomyces lilacinus* XLA at 100 mg/L of $Cr_{(VI)}$ concentration (Xu et al., 2017). Chang et al. (2016) investigated reduction potential of *T. asperellum* strain PTN7 and *T. asperellum* strain PTN10 at 10 mg/L of $Cr_{(VI)}$ and reported that 2.70 and 8.35 mg/L of $Cr_{(VI)}$ was reduced into $Cr_{(III)}$ respectively. However, *Arthrobacter* sp. SUK 1201 was able to reduce 62% of $Cr_{(VI)}$ to $Cr_{(III)}$ at the concentration of 2 mmol/L (Dey et al. 2012). In the present study, with increase in the $Cr_{(VI)}$ concentration from 5 to 50 mg/L the reduction percentage of $Cr_{(VI)}$ was increased significantly ($p \leq 0.05$) from 95 to 99.4%, however further increase in the $Cr_{(VI)}$ concentration at 100 and 200 mg/L, the reduction percentage was decreased to 98.9 % and 93.6 % respectively. With increase in the $Cr_{(VI)}$ concentration, decrease in reduction percentage was also recorded by *A. flavus* CR500 (**see section 5E.1**).

The time-dependent reduction potential of isolate CR700 was recorded at 50 mg/L of $Cr_{(VI)}$ (Fig. 5.13b). The results showed that with the increase in the time of exposure, the reduction of $Cr_{(VI)}$ was significantly ($p \leq 0.05$) increased and reached a maximum of 99.4% within 120 hours. Gu et al. (2015) reported 99% reduction of $Cr_{(VI)}$ into $Cr_{(III)}$ by *Aspergillus niger* within 84 hours at the same concentration of $Cr_{(VI)}$, while 90% reduction was recorded within 24 hours by *A. flavus* CR500 (**see section 5E.1**), *Bacillus methylotrophicus* reduces $Cr_{(VI)}$ from 95 µM to 7.14 µM in 48 hours (Mala et al., 2015) and 98.3% reduction was achieved within 52 hours by *Phanerochaete chrysosporium* (Murugavelh, 2013). Moreover, 2.12 ± 0.15 mg/g of dried biomass accumulation and 2.54 ± 0.16 mg/g of dried biomass of total chromium immobilization was recorded by isolate CR700 at 50 mg/L of $Cr_{(VI)}$ after 144 hours of exposure while the surface adsorbed metal concentration was 0.42 ± 0.02 mg/g of dried biomass. The remaining chromium in the supernatant was 4 ± 0.9 mg/L at the same concentration and time duration which revealed that most of the amount of

reduced form of chromium ($Cr_{(III)}$) was adsorbed or precipitated or accumulated by isolate CR700. Long et al. (2018) reported 0.79 mg of Cr per gram of dry biomass accumulation by *Penicillium oxalicum* SL2 and 4.9 mg of Cr per gram of dried biomass was found in *A. flavus* CR500 (**see section 5E.1**).

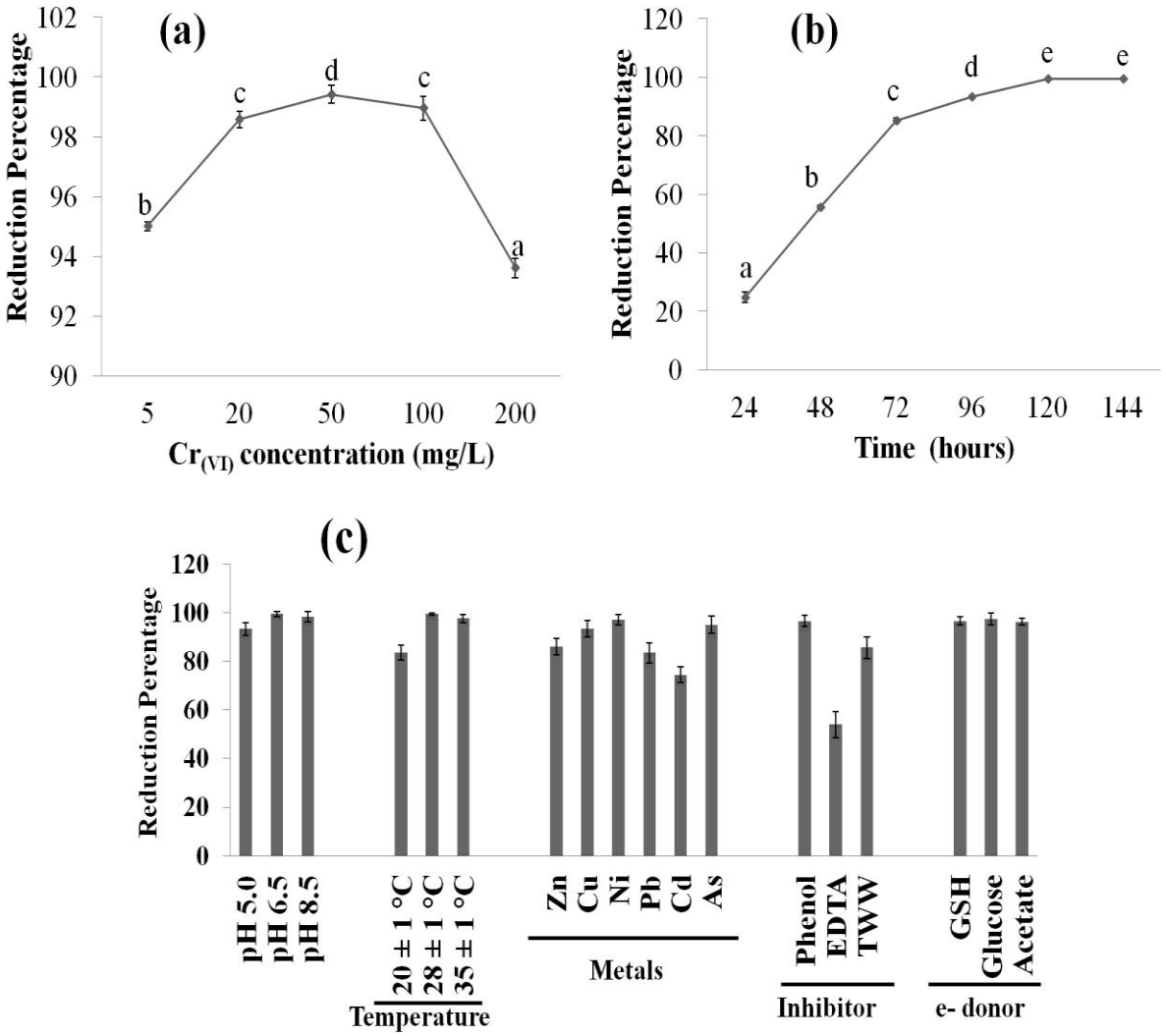

Fig. 5.13. Effect of (a) initial concentration, (b) incubation period on reduction of $Cr_{(VI)}$ by *T. lixii* CR700 (Mean ± standard deviation of three replicates, Value within each column followed by the same letter are not significantly different ($p < 0.05$) using Duncan's Multiple Range Test) and (c) Effect of pH, temperature, different heavy metal, metabolic inhibitor and electron donor on reduction of $Cr_{(VI)}$ by *T. lixii* CR700 (bar above the column denotes standard deviation (n = 2)).

5F.2 Reduction potential of isolate CR700 under different stress conditions

In view of different stress conditions, that generally encountered at natural sites, the reduction potential of the isolate CR700 was evaluated under the different stress conditions (Fig. 5.13c). The isolate CR700 was able to grow and efficiently reduced the $Cr_{(VI)}$ in the range of pH 5.0 to 8.5 and the temperature (20 to 35 °C) (Fig. 5.13c) while optimum pH and temperature was 6.5 and 28 ± 1 °C. Decrease in the reduction percentage above and below the optimum pH and temperature might be due to decrease in the activity of chromate reductase and biomass production (Xu et al., 2017; Das et al., 2014). The isolate CR700 could also reduce the $Cr_{(VI)}$ (74.4 to 97%) under the 10 mg/L of different heavy metal (Zn, Cu, Ni, Pb, Cd and As) (Fig. 5.13c). The EDTA, a metabolic inhibitor negatively affected the growth and reduction capability of isolate CR700, while it could able to reduce $Cr_{(VI)}$ efficiently under the stress of phenol (Fig. 5.13c) (Banerjee et al., 2019). The presence of GSH, glucose and acetate enhanced the reduction ability of isolate CR700 which might be due to their electron donating properties which is helpful in enzymatic $Cr_{(VI)}$ reduction (Banerjee et al., 2019; Mala et al., 2015). Moreover, isolate CR700 could grow in one-fourth diluted sterilized tannery wastewater with PDB medium and 85.7 % externally added 50 mg/L of $Cr_{(VI)}$ was reduced within six days with a slower growth (Fig. 5.13c). Such conditions are stressful to grow for the living organism especially under heavy metals. The ability of isolate CR700 to grow and reduce $Cr_{(VI)}$ under the presence of metals (Zn, Cu, Ni, Pb, Cd and As) metabolic inhibitors and a range of pH and temperature; make it a promising candidate for the bioremediation of $Cr_{(VI)}$.

5F.3 Fungal cell and cell wall response under $Cr_{(VI)}$ stress

The SEM-EDS analysis suggested the tolerance of isolate CR700 towards $Cr_{(VI)}$ associated with sorption and accumulation mechanism (Fig. 5.14). The morphology of isolate CR700 under stress of $Cr_{(VI)}$ was changed, before $Cr_{(VI)}$ treatment smooth and cylindrical mycelia were found (Fig. 5.14a), while with an irregular surface with tightly aggregated and swelled mycelia was found after treatment with $Cr_{(VI)}$ (Fig. 5.14b). Mycelial aggregation under $Cr_{(VI)}$ might be due to detoxification mechanism of isolate CR700 via reducing the surface. Cd tolerance mechanism via mycelial aggregation was also reported for *P. simplicissimum* (Liu et al., 2011). *A. flavus* CR500 also responded towards $Cr_{(VI)}$ by reducing the surface area

via mycelial constriction (**see section 5E.7**). In addition, the presence of chromium (2.52 total effective weight %) was also found in EDS analysis of the 100 mg/L of $Cr_{(VI)}$ treated mycelia surface of isolate CR700 (Fig. 5.14c, d), evidenced to Cr biosorption. Moreover, in the present study it was found that $Cr_{(VI)}$ treated mycelia swelled compared to control, might be due to the accumulation of $Cr_{(VI)}$ via vacuolar compartmentation (Cánovas et al., 2003).

The FTIR analysis of $Cr_{(VI)}$ treated and without treated biomass of isolate CR700 was performed to explore the functional group's contribution in sorption of $Cr_{(VI)}$ on the mycelial surface (Fig. 5.15a, b). The shift in the peaks from 3423.1 (O─H Stretching vibration and N─H stretching of protein or acetamide groups of chitin fraction) to 3425.9 cm^{-1}, 1646.9 (amide I of N-acetyl glucosamine polymer or carbonyl group stretching) to 1645.3 cm^{-1}, 1547.3 (amide II of N-acetylglucosamine polymer or the protein) to 1545.2 cm^{-1}, 1405.5 (C─N stretching in amide III) to 1415.3 and 1076.1 (C─N stretching vibration of amine groups) to 1074.4 cm^{-1} indicates the functional group associated with protein involvement in $Cr_{(VI)}$ biosorption (Chen et al., 2018; Karthik et al., 2017; Rossi et al., 2018). Because, N of N─H (amine) and amide group carry one lone pair (lp) electron and O of O─H and carbonyl group carry two lp electron which indicated the metal-lp interaction in complexation of $Cr_{(VI)}$ (Kumar et al., 2019). However, carbonyl group also indicated the presence of carboxylate anions that may possibly cause electrostatic attraction between carboxylate anion and metal ion (Kumar et al., 2019). The shifted peak from 2916.1 (C─H Stretching vibration of fatty acid in membrane phospholipid) to 2925.6 cm^{-1} indicated the peroxidation of membrane lipid due to increase in H_2O_2 content (Fig. 5.17a, b) under stress of $Cr_{(VI)}$.

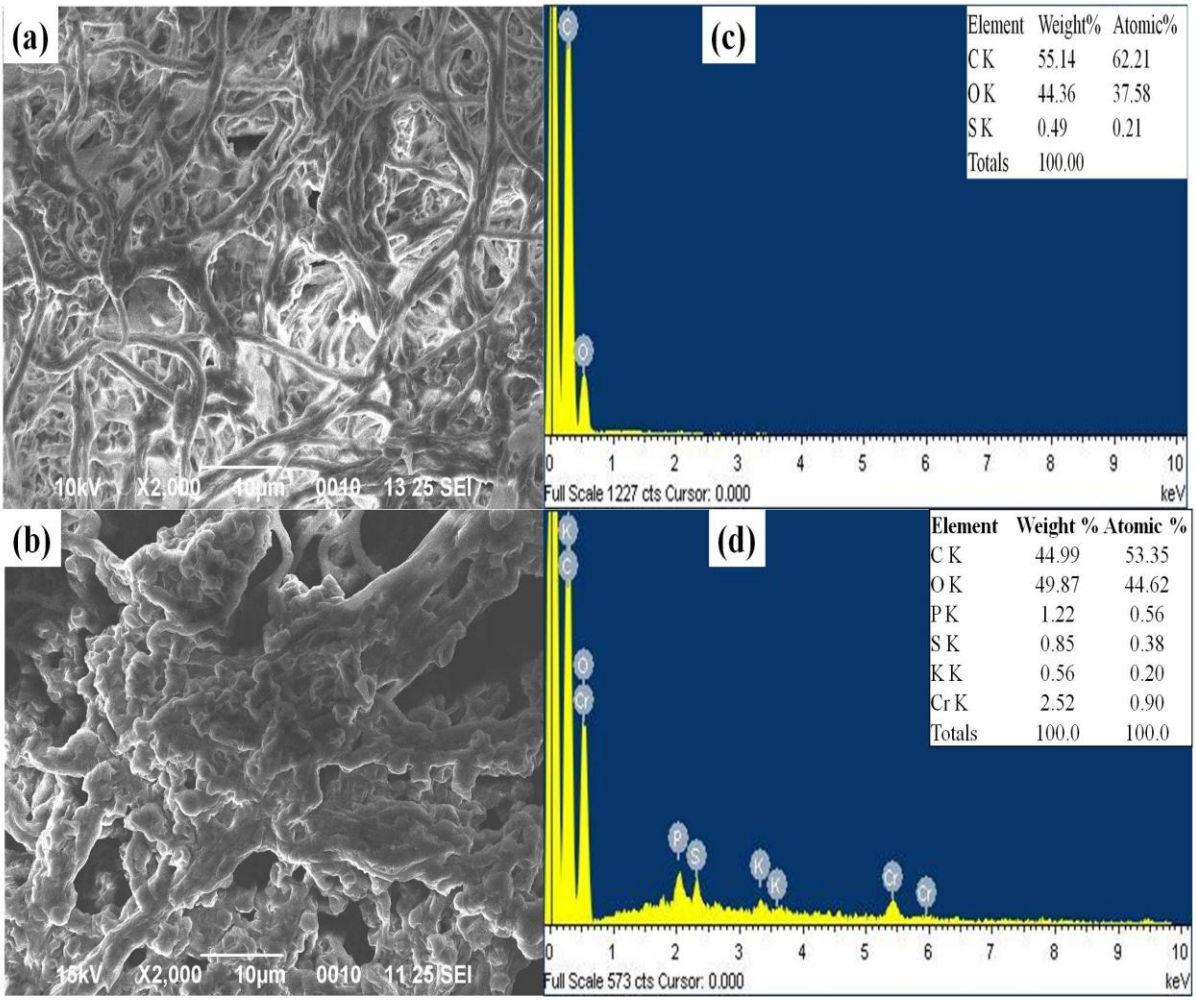

Fig. 5.14. SEM-EDS analysis of without treated (a; showing loosely bound cylindrical mycelia and c; Absence of Cr peak on EDS micrograph) and 100 mg/L of $Cr_{(VI)}$ treated mycelia (b; showing closely aggregated mycelia with irregular morphology and d; presence of Cr peak on EDS micrograph) of *T. lixii* CR700.

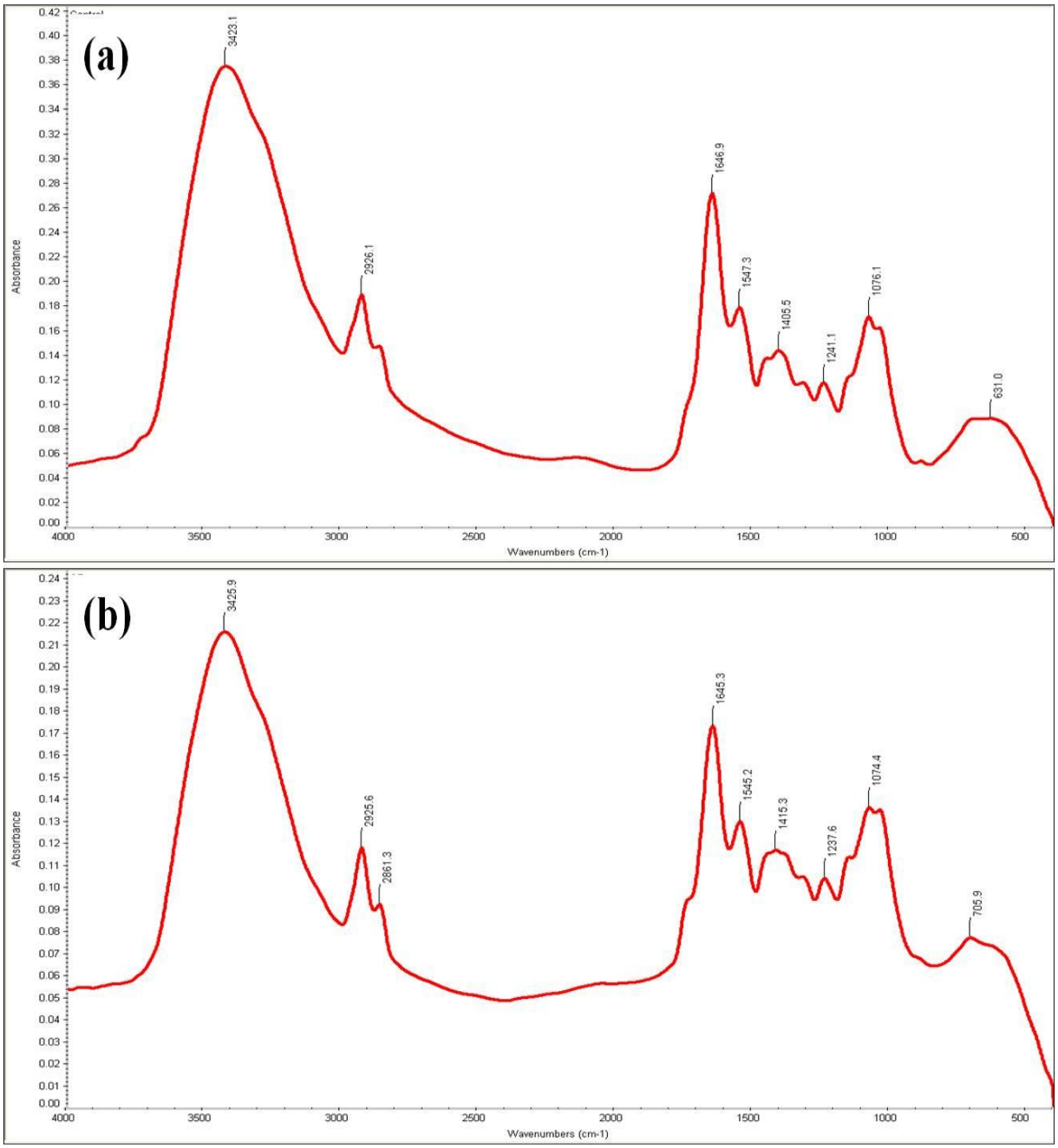

Fig. 5.15. FTIR analysis of control (a) and $Cr_{(VI)}$ treated (b) biomas of *T. lixii* CR700.

The presence of chromium at 100 mg/L of $Cr_{(VI)}$ treated mycelia surface of isolate CR700 was strongly supported by X-ray photoelectron spectroscopic (XPS) analysis. The survey scan of $Cr_{(VI)}$ treated mycelia of isolate CR700 confirmed the presence of chromium on its surface (Fig. 5.16a). The $Cr2p_{3/2}$ peak was found on the high-resolution spectra of Cr2p, which deconvoluted into two peak range 576.1-576.9 eV and 578.4-574.4 eV correspond to $Cr_{(III)}$ and $Cr_{(VI)}$ respectively (Fig. 5.16b) (Shi et al., 2019). The presence of $Cr_{(III)}$ on the mycelia surface confirmed the reduction of $Cr_{(VI)}$ into $Cr_{(III)}$, which might be due $Cr_{(III)}$ precipitation in the form of Cr_2O_3 (Kang et

al., 2015). A similar result was reported on the $Cr_{(VI)}$ reduction and its precipitation in the form Cr_2O_3 by spore of *Aspergillus niger* (Ren et al., 2018). Some other researches also reported the same and reached the same conclusion as found in this study (Kang et al., 2017; Gardea-Torresdey et al., 2000; Kang et al., 2015; Shi et al., 2019).

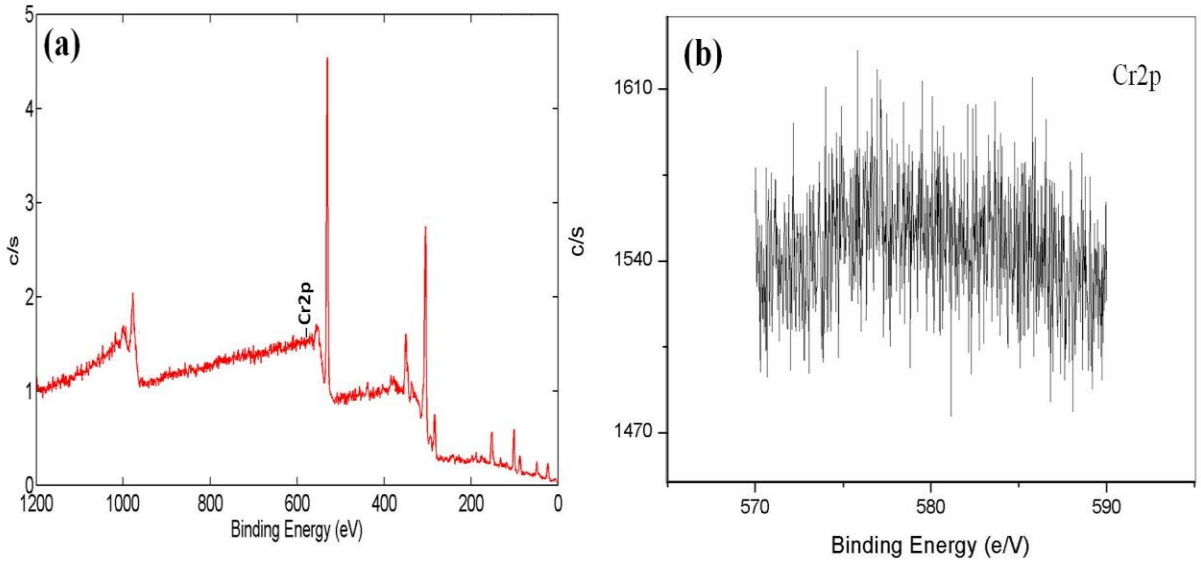

Fig. 5.16. XPS survey scan of $Cr_{(VI)}$ treated mycelia of *T. lixii* CR700 (a) and high resolution spectra of Cr2p (b).

5F.4 Effect of $Cr_{(VI)}$ on Intracellular Protein and Activity of Chromate Reductase (ChrR)

The intracellular protein content in the isolate CR700 was significantly ($p \leq 0.05$) decreased with increase in the concentration of $Cr_{(VI)}$ (Fig. 5.18i). A maximum of 178.6 ± 4.5 µg/g FW of protein content was recorded at concentration of 0 mg/L of $Cr_{(VI)}$ which was decreased by 18.4% at 50 mg/L of $Cr_{(VI)}$ followed by 12.6% and 5.9% at 20 mg/L and 5 mg/L respectively compared to control. The similar result was reported in *Sclerotium rolfsii* (Rafi et al. 2017). In this study, the decrease in the level of intracellular protein with the increase in the $Cr_{(VI)}$ concentration might be due to the increase in the production of reactive oxygen species (H_2O_2; Fig. 5.17a), resulting intracellular oxidative damages and $Cr_{(VI)}$ toxicity (Chakraborty et al., 2014).

The cell free extract (CFE) obtained from culture (isolate CR700) grown in control and 50 mg/L of $Cr_{(VI)}$ treated potato dextrose broth (PDB) medium showed rapid $Cr_{(VI)}$ reduction and the activity of chromate reductase was significantly different in all the sample (Fig. 5.18f). The activity of ChrR was found in both types

of extract however, 174% higher activity was found with the CFE obtained from 50 mg/L of $Cr_{(VI)}$ treated fungal biomass which was significant at the level of $p \leq 0.05$. A small amount of activity of ChrR was also encountered in the supernatant of isolate CR700 treated with 50 mg/L of $Cr_{(VI)}$ amended PDB medium which was 75% less compared to control while no activity was found in the supernatant of control treatment (0 mg/L of $Cr_{(VI)}$). Results suggested that $Cr_{(VI)}$ induces the activity of ChrR in isolate CR700 and ChrR was also extracellularly secreted by isolate CR700 under the exposure of $Cr_{(VI)}$. The increase in the activity of ChrR under the $Cr_{(VI)}$ exposure was also reported in *Cyberlindnera jadinii* M9 and *Wickerhamomyces anomalus* M10, suggested that the $Cr_{(VI)}$ induced ChrR production (Irazusta et al. 2018). $Cr_{(VI)}$ induced ChrR also reported in *A. flavus* CR500, *Bacillus* spp. (Mala et al., 2015; Ontañon et al., 2018). The activity of ChrR in CFE of control fungal biomass suggested that ChrR play role in mechanism other than reduction or some other enzyme also responsible for the reduction of $Cr_{(VI)}$ as secondary function. Similar phenomenon was also reported with *A. flavus* CR500 (**see section 5E.3**). No literature is available over ChrR involvement in mechanism other than the reduction of $Cr_{(VI)}$ into $Cr_{(III)}$, however some studies suggested that enzymes such as Type II nitroreductase (Frm2), flavoprotein wrbA (Ycp4) and putative nitroreductase-like proteins Hbn1 are involved in the $Cr_{(VI)}$ reduction as their secondary function in *Saccharomyces cerevisiae*, *W. anomalus* M10 and *C. jadinii* M9 (de Oliveira et al., 2007; Martorell et al., 2012; Irazusta et al., 2018).

5F.5 Oxidative stress under $Cr_{(VI)}$ exposure

The reactive oxygen species have strong oxidative properties which oxidize unsaturated fatty acid and pigments (multiple biomacromolecules) and thus giving rise many types of damages such as membrane damage, enzyme inactivation and nucleotide damages (Scandalios, 2005; Zhang et al., 2016; Wu et al., 2010). The ROS induction via heavy metal was intensively reported in plants and microbes (Li et al., 2017; Scandalios, 2005; Rafi et al., 2017). The lipid peroxidation was expressed in terms of malondialdehyde (MDA) concentration, a peroxidation product of membrane lipid and this is observed as a stress physiological index (Zhang et al., 2007; Li et al., 2017; Chakraborty et al., 2014). In the present study, with an increase in the concentration of $Cr_{(VI)}$, MDA concentration was significantly ($p \leq 0.05$) increased in isolate CR700 (Fig. 5.17a). At the lower $Cr_{(VI)}$ concentration (5 mg/L) the lipid

peroxidation was neutral and with increase in the $Cr_{(VI)}$ concentration above 20 mg/L, the MDA instantly increased up to 114.75 ± 1.33 mU/mg protein which was 201% more over control. Li et al. (2017) also reported an increase in the MDA and H_2O_2 content in *Pleurotus ostreatus* HAU-2 under the stress of chromium and cadmium. The induction of H_2O_2 via Pb and Cd was found in *Pleurotus ostreatus* HAU-2 and *Fusarium solani* respectively (Zhang et al., 2016; Kumar et al., 2019; Prasad et al., 2018). In this study, the induction of H_2O_2 content was significantly ($p \leq 0.05$) increased in isolate CR700 with an increase in the concentration of $Cr_{(VI)}$ (Fig. 5.17b). The maximum (36.33 ± 1.40 nmol/g FW) H_2O_2 content was recorded at the concentration of 50 mg/L of $Cr_{(VI)}$. The results revealed that $Cr_{(VI)}$ induces the production of reactive oxygen species, the primary cause of $Cr_{(VI)}$ toxicity in hyphae of isolate CR700.

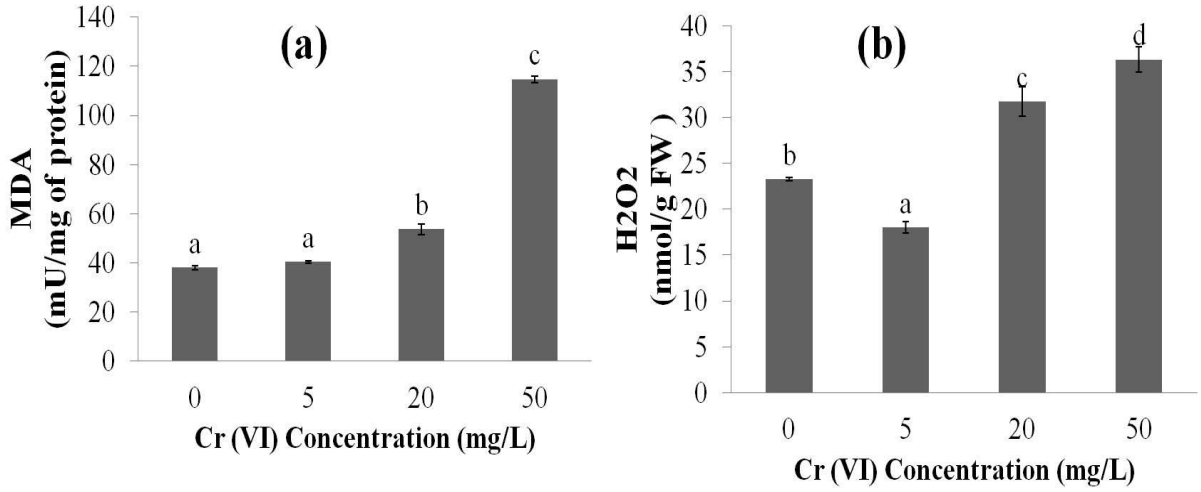

Fig. 5.17. Effect of $Cr_{(VI)}$ on MDA and H_2O_2 content in *T. lixii* CR700 (Mean ± standard deviation of three replicates, Value within each column followed by the same letter are not significantly different ($p < 0.05$) using DMRT).

5F.6 Enzymatic Antioxidants response under $Cr_{(VI)}$ stress

The SOD, POD, CAT and PPO have potential to capture ROS from the cell, and they are the essential components of the cellular immune system and protect the cells against oxidative damages. These compound belong from the group of induced enzymes and are produced in the large amount under the stress of heavy metals as had been reported in various studies (Li et al., 2017; Scandalios, 2005; Zhang et al., 2016; Rafi et al., 2017; Kumar et al., 2019). In this research, it was found that the activity of

CAT decreased by increasing the concentration of $Cr_{(VI)}$ in Isolate CR700 (Fig. 5.18a). The similar result was reported in *P. ostreatus* HAU-2 and *Fusarium solani* under stress of $Cr_{(VI)}$ and Cd respectively (Li et al., 2017; Kumar et al., 2019). The activity of SOD and POD significantly ($p \leq 0.05$) changed as compared to control (Fig. 5.18b, d). The activity of SOD was significantly decreased by 5% at 5 mg/L of $Cr_{(VI)}$ and then increased up to 6% at 20 mg/L and further decreased by 83% at 50 mg/L of $Cr_{(VI)}$ as compared to control and almost similar pattern was recorded in the activity of POD (Fig. 5.18b). The activity of PPO and PAL was significantly increased with the increase in the $Cr_{(VI)}$ concentration (Fig. 5.18c, e). Similar result was reported in *Sclerotium rolfsii* under the exposure of $Cr_{(VI)}$ (Rafi et al., 2017).

The results of this study revealed that 20 mg/L of $Cr_{(VI)}$ induces the activities of POD, CAT and SOD, but with the increase up to 50 mg/L of $Cr_{(VI)}$, the activity of SOD decreased. However, 50 mg/L of $Cr_{(VI)}$ induces the activity of PAL. The activity of PPO, POD and CAT is directly associated with an increase in the lipid peroxidation (MDA concentration) and H_2O_2 content which might be involved in the removal of ROS. The decreased in SOD activity might be due to excess toxicity of $Cr_{(VI)}$ which severely damage the cell, consequently, suppress the SOD activity (Li et al., 2017).

5F.7 Non-enzymatic antioxidants response under $Cr_{(VI)}$ stress

Proline can play the role of electron sink, osmolyte radical scavenger, stabilizer of cell wall components and macromolecules (Matysik et al., 2002; Chakraborty et al., 2014; Hayat et al., 2012; Dubey et al., 2010). Various studies reported Proline production in high content in metal stressed population which may act as antioxidants. Chakraborty et al. (2014) reported that *Aspergillus foetidus* increases the production of proline under the exposure of Cadmium. In the present study, Proline content in isolate CR700 was significantly ($p \leq 0.05$) decreased by treating with increasing concentration of $Cr_{(VI)}$ (Fig. 5.18i). Total phenolic content was significantly ($p \leq 0.05$) changed in isolate CR700 under the exposure of different $Cr_{(VI)}$ concentration. First, with increase in $Cr_{(VI)}$ concentration up to 5 mg/L, the phenolic content significantly ($p \leq 0.05$) increased by 28.1% (Fig. 5.18h) and at 50 mg/L of $Cr_{(VI)}$, the phenolic content was decreased by 18.8% over control. Total phenolic content help to protect the cell from the adverse consequences of heavy metal, belongs from the group of stress-induced non-enzymatic antioxidants (Islam et

al., 2016). It played an important role in scavenging the reactive oxygen species by donating the hydrogen atoms from its hydroxyl group (Hernandez et al., 2009; Tripathi et al., 2012; Posmyk et al., 2009).

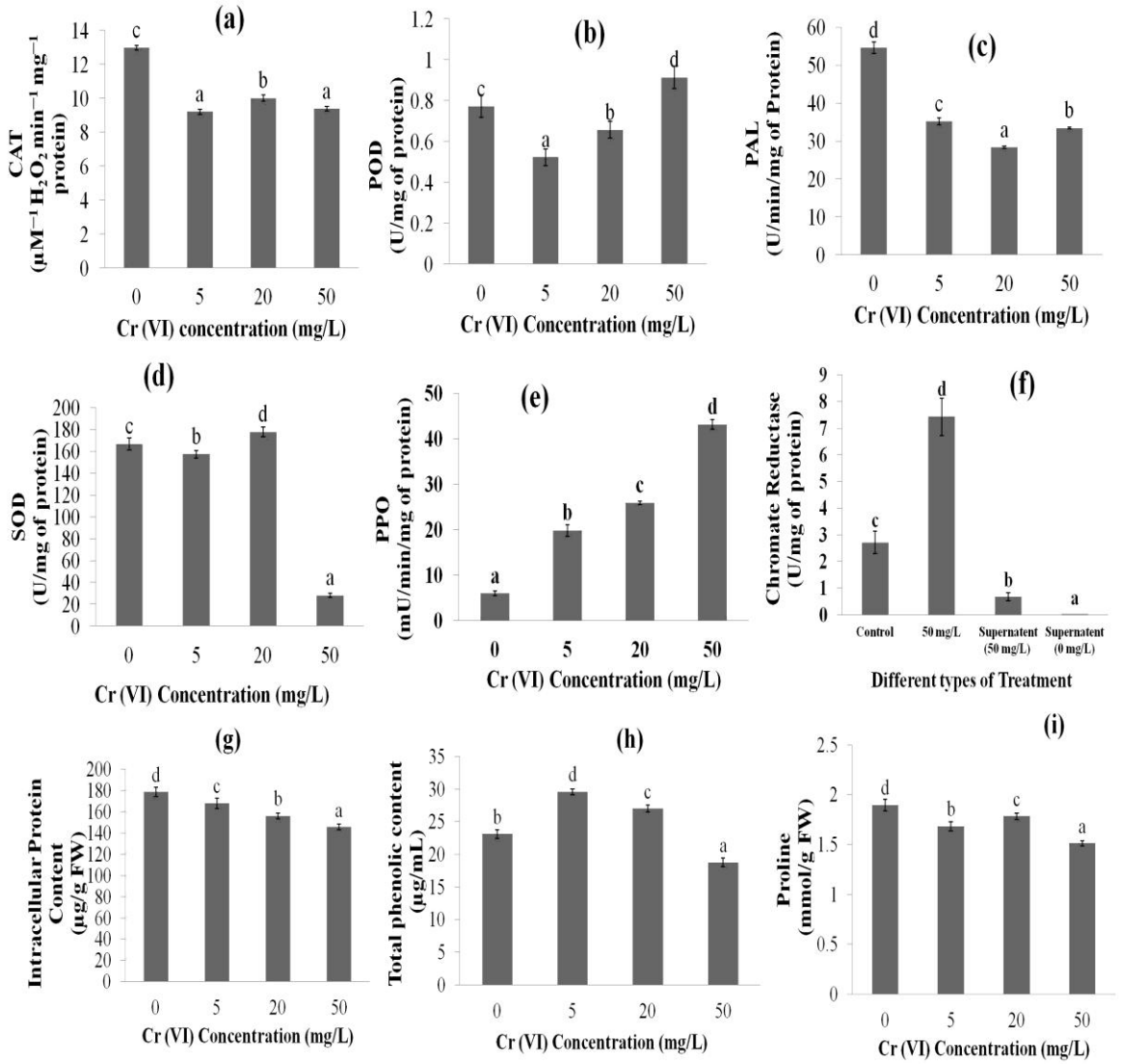

Fig. 5.18. Effect of $Cr_{(VI)}$ on activity of CAT (a), POD (b), PAL (c), SOD (d), PPO (e) and Chromate reductase (f) and the level of protein (g), total phenolic content (h) and proline (i) in *T. lixii* CR700 (Column and bar denote mean of three replicates and standard deviation, Subscripts same letter denotes no significant differences ($p < 0.05$) within the variables using DMRT).

5F.8 Phytotoxicity study

Phytotoxicity studies on *Vigna radiata* and *Cicer arietinum* demonstrated that toxicity of $Cr_{(VI)}$ was successfully reduced through the reduction by *T. lixii* CR700. *V.*

radiata displayed longer shoots and roots with distilled water (shoot 12.3 ± 2.7 and root 4.5 ± 2.1 cm) and fungal treated solution of 100 mg/L of $Cr_{(VI)}$ (shoot 10.8 ± 0.2 cm and roots 3.0 ± 1.0), compared to without treated 100 mg/L of $Cr_{(VI)}$ (0.31 ± 0.02 and 0.0 ± 0.0 cm respectively). The shoots of *C. arietinum* in fungal treated $Cr_{(VI)}$ supernatant was higher (3.2 ± 0.6 cm) compared to distilled water (2.6 ± 0.7) and without treated 100 mg/L of $Cr_{(VI)}$ solution (1.4 ± 0.14). However, the roots were longer in distilled water (5.6 ± 1.7 cm) than treated $Cr_{(VI)}$ supernatant (3.3 ± 1.0) and without treated 100 mg/L of $Cr_{(VI)}$ solution (1.8 ± 0.3) (Fig. 5.19a, b). These results revealed that *T. lixii* CR700 effectively detoxified $Cr_{(VI)}$ by the reduction and removal mechanism (Chen et al., 2019). *A. flavus* CR500 also reduces the toxicity of $Cr_{(VI)}$ (via reduction and removal mechanism) for *V. radiata* (**see section 5E.9**). The germination rate of *V. radiata* and *C. arietinum* seeds were 100% in distilled water and fungal treated $Cr_{(VI)}$ solution compared to without treated 100 mg/L of $Cr_{(VI)}$ solution (*V. radiata*; 76.67 and *C. arietinum*; 96.6%) (Fig. 5.19c) which also confirmed that isolate CR700 successfully detoxified the $Cr_{(VI)}$ solution.

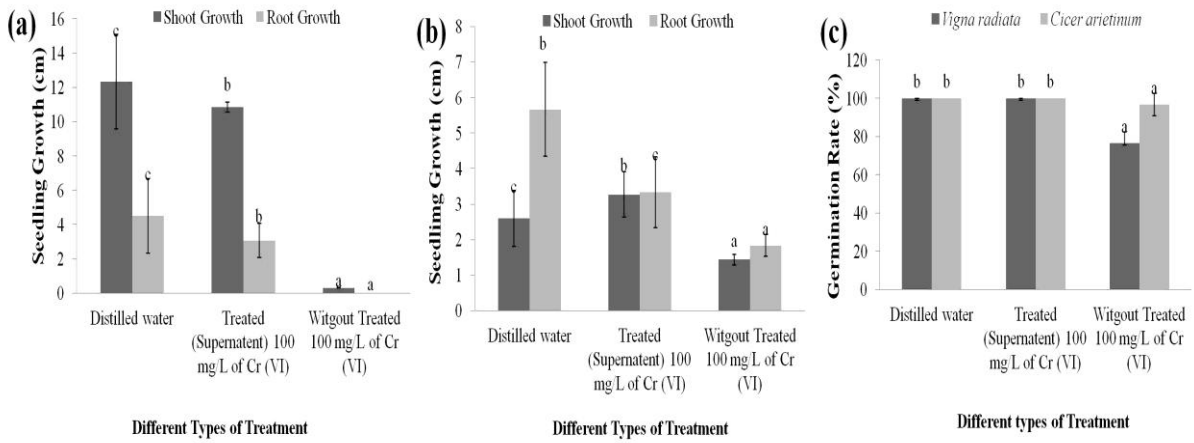

Fig. 5.19. Seedling growth of *Vigna radiata* (a) and *Cicer arietinum* (b) and seeds germination rate *V. radiata* and *C. arietinum* (c) in sterilized distilled water, isolate CR700 treated 100 mg/L of $Cr_{(VI)}$ supernatant and without treated 100 mg/L of $Cr_{(VI)}$ solution (Mean ± standard deviation of three replicates, Value within each column followed by the same letter are not significantly different using $DMRT_{(p < 0.05)}$).

5F.9 $Cr_{(VI)}$ Tolerance and remediation mechanism

Schematic diagram of the $Cr_{(VI)}$ tolerance and remediation mechanism in fungus has been shown in Fig. 5.20. Due to the small size and highly permeable to the

cell wall, $Cr_{(VI)}$ quickly introduced to intracellular space of the fungi. Another way of introduction of $Cr_{(VI)}$ inside the cell is ATP-binding cassette (ABC) transporter, heat shock protein and CHR protein (Bellion et al., 2006; Brunetti et al., 2015; Yung et al., 2014; Díaz-Pérez et al., 2007). The $Cr_{(VI)}$ induced the production of ROS (Fig. 5.17a, b) and caused oxidative stress, migh be a primary cause of its toxicity in isolate CR700. In response of oxidative stress, isolate CR700 increased the activity of enzymatic antioxidant (POD, PAL and PPO; Fig. 5.18b, c, e) and the level of non-enzymatic antioxidant (Proline and phenolic content; Fig. 5.18h, i) which scavenge the ROS and minimizes the impact of oxidative stress. $Cr_{(VI)}$ induced ChrR activity was found in isolate CR700 (Fig. 5.18f) which mainly driven $Cr_{(VI)}$ reduction to $Cr_{(III)}$ (Irazusta et al., 2018; McLean and Beveridge, 2001; Ontañon et al., 2018). The NADH and NADPH might be used as an electron donor for the $Cr_{(VI)}$ reduction into $Cr_{(III)}$ via ChrR activity as previously reported (Martorell et al., 2012; Irazusta et al., 2018). After the reduction of Cr(VI) into Cr(III), the cell might be gone two way. First, effluxed from inside to outside of the cell through efflux pump such as proton motive forces drive the P-type ATPase or CDF protein to transport the heavy metal from the cytoplasm to periplasm or from the periplasm to outside of the cell (Vaccaro et al., 2016; Banerjee et al., 2019). Second, reduced $Cr_{(III)}$ goes to vacuolar compartmentation that leads the accumulation of Cr and accounted up to 2.54 ± 0.16 mg/g of dried biomass by isolate CR700 (Bhatia et al., 2005; Cánovas et al., 2003). One electron transfer mechanism from the substrate (such as organic acid) is another mechanism of $Cr_{(VI)}$ reduction to $Cr_{(III)}$ as suggested by Cui et al. (2011). In one electron transfer mechanism, $Cr_{(VI)}$ transformed into $Cr_{(III)}$ via their intermediate form, pentavalent ($Cr_{(V)}$) and tetravalent ($Cr_{(IV)}$) where substrates are used as an electron donor (Pradhan et al., 2017; Cui et al., 2011). Moreover, EDX analysis confirmed the presence of chromium on the mycelial surface of isolate CR700 (Fig. 5.14c, d) and XPS analysis revealed the oxidation state of adsorbed chromium in the form of $Cr_{(III)}$ (Fig. 5.16a, b) indicated to chromium precipitation as Cr_2O_3. However, the presence of $Cr_{(VI)}$ was also recognized by XPS analysis on the mycelia surface of isolate CR700 which might be due to $Cr_{(VI)}$ complexation as found in FTIR analysis (Fig. 5.15a, b).

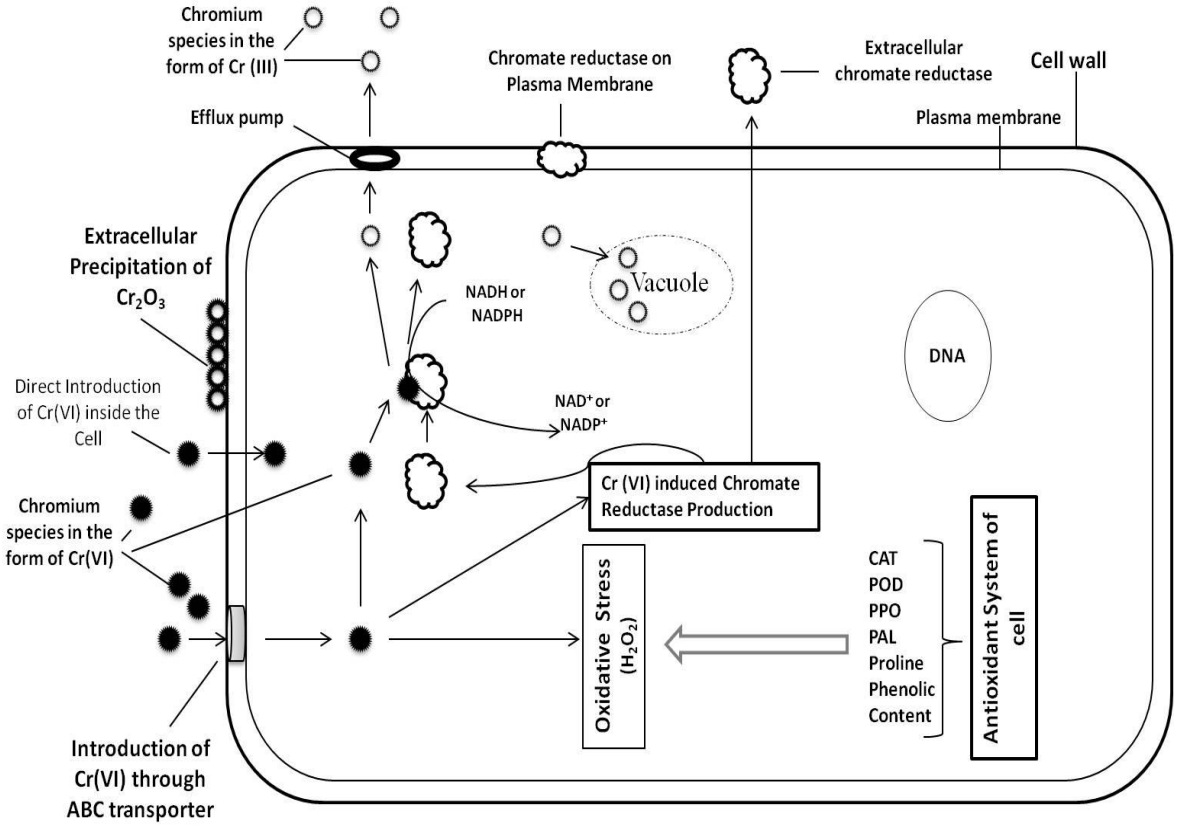

Fig. 5.20. $Cr_{(VI)}$ tolerance and remediation mechanism of *Trichoderma lixii* CR700.

5G. *A. flavus* CR500 and $Ni_{(II)}$: Removal, morphological and Biochemical analysis

5G.1 Effect of initial $Ni_{(II)}$ concentration

The results of the initial $Ni_{(II)}$ concentration on its removal by *A. flavus* CR500 are shown in Fig. 5.21a. Results depicted that with an increase in the $Ni_{(II)}$ concentration the removal rate of $Ni_{(II)}$ by *A. flavus* CR500 was decreased. The maximum removal of $Ni_{(II)}$ was 74.3% at lower concentration (10 mg/L) of $Ni_{(II)}$ and decreased to 14.2 % at 500 mg/L. Rise in the metal concentration also affected the biomass productivity of fungus and was reduced from 6.87 to 3.2 g/L (Fig. 5.21a). These results are in accordance with previous finding (Mishra and Malik, 2012). Reduction in biomass with increase in the $Ni_{(II)}$ concentration indicated its toxicity on *A. flavus* CR500 growth and metabolic process (Gola et al., 2016). As found in the FTIR and metal accumulation adsorption quantification investigation that $Ni_{(II)}$ removal occurred via surface sorption and accumulation mechanisms. So, decrease in the metabolic activity of fungus obstruct the accumulation of $Ni_{(II)}$ inside the cell because accumulation is the metabolic dependent mechanisms (Wu et al., 2015). In addition, the reduction in the growth of the fungus reduce the availability of surface functional groups that leads to decrease in the $Ni_{(II)}$ adsorption on the surface of the fungus (Chen et al., 2019). That's why accumulation and surface adsorption simultaneously affected by the increase in the $Ni_{(II)}$ toxicity under the excess concentration of $Ni_{(II)}$.

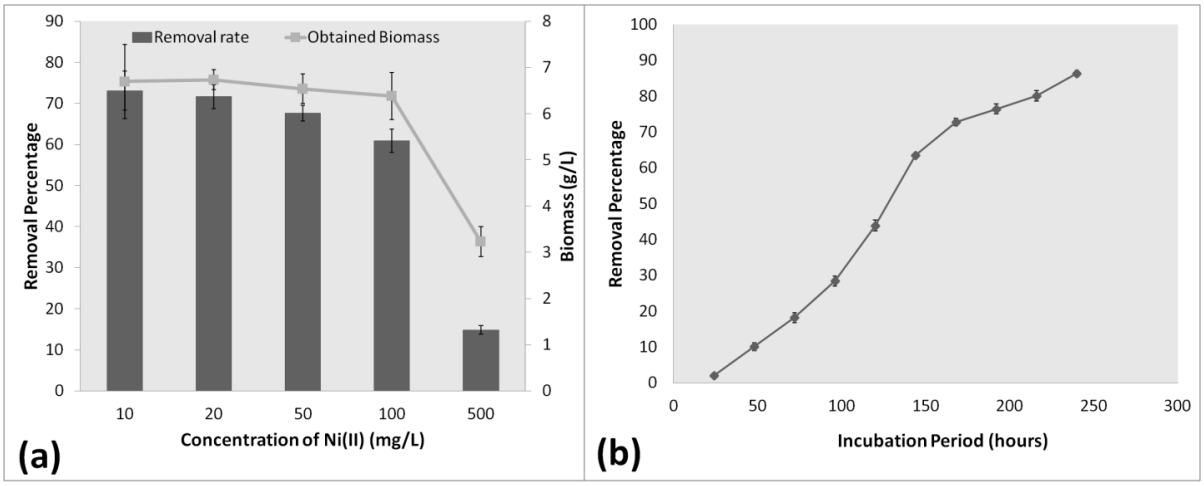

Fig. 5.21. Effect of different initial concentration of $Ni_{(II)}$ (a) and incubation periods (b) on removal of $Ni_{(II)}$ by *A. flavus* CR500 (bar represents standard deviation of three replicates).

5G.2 Effect of incubation periods

Time course is an important factor in bioremediation process for growth of the bioremediation agent and accumulation of the pollutants. In this study, the $Ni_{(II)}$ removal ability of fungus was increased with increase in the incubation period (Fig. 5.21b). The maximum removal of $Ni_{(II)}$ occurred at 192 h of incubation and was 87.8%. In a study, it is reported that *Aspergillus niger* can remove 99% $Ni_{(II)}$ of total $Ni_{(II)}$ from the solution (Magyarosy et al., 2002). Moore et al. (2008) reported 49.7% removal of $Ni_{(II)}$ using fungal isolate in 72h at 21 mg/L of $Ni_{(II)}$ concentration via accumulation. Rise in the incubation periods enhanced the biomass productivity of the fungus and duration of metabolic process that boost the adsorption of Ni(II) on the surface due to high availability of active site and accumulation of $Ni_{(II)}$ inside the cell (Moore et al., 2008). At 192 h of incubation and 50 mg/L of $Ni_{(II)}$ concentration, the accumulation and surface sorption amount of Ni was 4.91 ± 0.161 and 0.12 ± 0.08 mg/g dried biomass of *A. flavus* CR500. A significant amount of $Ni_{(II)}$ accumulation was also reported in several species of fungi such as *Aspergillus niger*, *Phanerochaete chrysosporium*, *Macrolepiota procera* and *Aspergillus* sp. (Congeevaram et al., 2007; Cao et al., 2018; Moore et al., 2008; Magyarosy et al., 2002).

5G.3 Effect of pH

The pH of the medium is the most important aspect for the growth and development of living creatures. Bioremediation utilize living form of potential pollutant in removing organisms that can be greatly influenced by the pH of the solution. In the present study, with change in the pH of the solution biomass productivity of *A. flavus* CR500 was notably affected (Fig. 5.22a). With increase in the pH from 5.0 to 7.0 the biomass productivity was expanded from 4.23 to 6.87 g/L and reduced to 5.41g/L at pH 9.0. The similar trend was recorded for Ni(II) removal of Ni(II) at different pH and maximum removal of Ni(II) by *A. flavus* CR500 was obtained at pH 7.0 which was 72.3% at 100 mg/L of $Ni_{(II)}$ in incubation time of 192h. Congeevaram et al. (2007) reported maximum removal of Ni(II) at pH 5.0 with *Aspergillus* sp. However, in this investigation, $Ni_{(II)}$ removal was higher at pH 9.0 than 7.0 but it was due to occurrence of precipitation of $Ni_{(II)}$ as Nickel hydroxide ($Ni(OH)_2$) due to excess availability of OH^- (hydroxide anion). The neutral pH favour the growth of the fungus as well as removal rate of $Ni_{(II)}$. While, in acidic and basic

conditions the growth of the fungus was reduced that leads to decrease in the metabolic process and biomass productivity (Kumar et al., 2019; Gola et al., 2016). The slower metabolic process cause reduction in accumulation of Ni(II) and low biomass productivity cause less availability of responsible surface functional group for adsorption of $Ni_{(II)}$ on mycelia of fungus (Gola at al., 2016). Another, possible reason for less removal of Ni(II) at lower pH is that in acidic condition, active site on the surface of mycelia occupied by H^+ ions and the surface is positively charged. Because $Ni_{(II)}$ exist as cationic Ni^{2+} so, repulsion occurred between positively charged fungus surface and Ni^{2+} that affected the removal rate (Khalid et al., 2011).

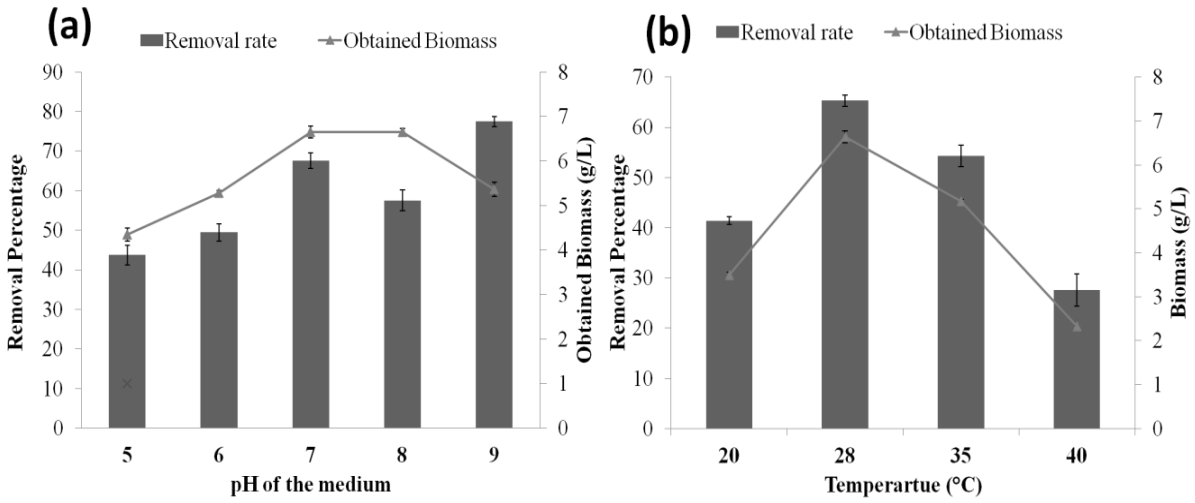

Fig. 5.22. Effect of different pH (a) and temperature (b) on $Ni_{(II)}$ removal and biomass productivity of *A. flavus* CR500 (bar represent standard deviation of three replicates).

5G.4 Effect of Temperature

Temperature is the most influencing parameter that affects the growth of the living organism. It can also affect the bioremediation process by reducing the growth and metabolic process of applied bioremediating agents (Murugavelh and Mohanty, 2013; Kathiravan et al., 2010). The results of $Ni_{(II)}$ removal potential and biomass productivity of *A. flavus* CR500 at different temperature are shown in Fig. 5.22b. It is recorded that with rise in the temperature from 20 to 28 °C the biomass production of *A. flavus* CR500 was raised by 48% but reduced to 3.12 g/L at 40 °C. The trend of $Ni_{(II)}$ removal by *A. flavus* CR500 was parallel to its biomass productivity and was higher (64.4%) at 28 °C (Fig. 5.22b). The optimum temperature for growth of *A.*

flavus CR500 and removal of $Ni_{(II)}$ was 28 °C which is in agreement with previous results (**see section 5E.1, 5F.1**).

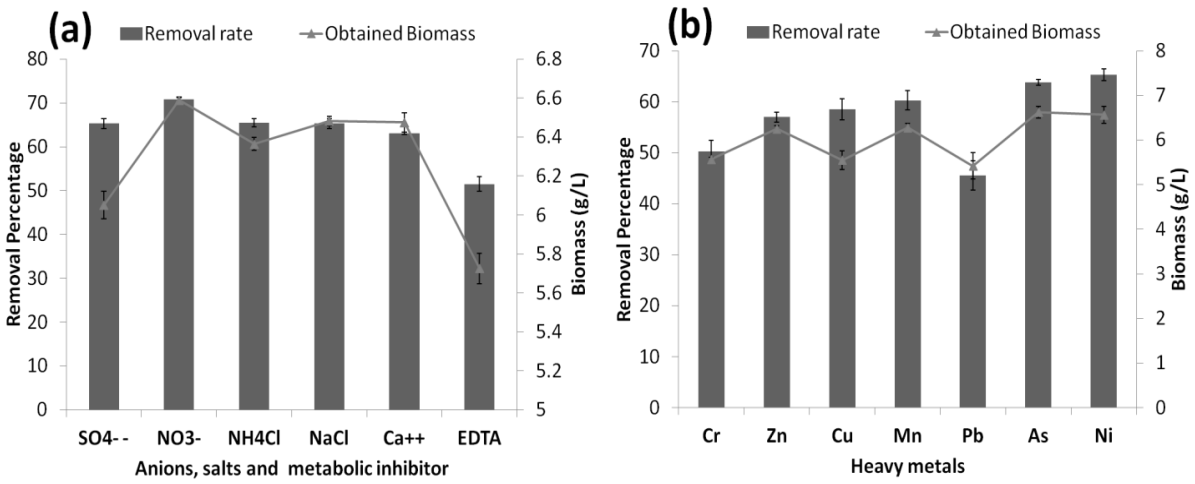

Fig. 5.23. Effect of different mono and divalent anions, cations and salts (a) and Heavy metal (Cr; $K_2Cr_2O_7$, Zn; $ZnSO_4$, Cu; $CuSO_4$, Mn; $MnSO_4$, Pb; $PbSO_4$, As; As_2O_3 and Ni; $NiSO_4$) on removal of $Ni_{(II)}$ by *A. flavus* CR500 and its growth.

5G.5 Effect of different co-occurring contaminant

The co-occurrence of anions, salts and heavy metal in $Ni_{(II)}$ polluted wastewater is commonly reported in the studies. These pollutants can affect the bioremediation potential of microbes and plants by affecting their growth and metabolic process. In view of the effect of these anions, salts and heavy metal, $Ni_{(II)}$ removal potential of *A. flavus* CR500 was investigated in the presence of 10 mg/L of these co-occurring contaminants. Out of selected heavy metal (Cr, Zn, Cu, Mn, Pb and As), Cr and Pb greatly affected the growth of *A. flavus* CR500 as well as removal rate of $Ni_{(II)}$. Even the trend of biomass productivity and $Ni_{(II)}$ removal by *A. flavus* CR500 was parallel with each-other. The $Ni_{(II)}$ removal efficiency of *A. flavus* CR500 was 63.8, 60.3, 58.5, 57.0, 50.2 and 45.5% in the presence of 10 mg/L of As (As_2O_3), Mn ($MnSO_4$), Cu ($CuSO_4$), Zn ($ZnSO_4$), Cr ($K_2Cr_2O_7$) and Pb ($PbSO_4$) (Fig. 5.23b). Toxic effect of Cr, Pb, Cu and As has been reported in many studies for microbes and plants. Oxidative stress caused by heavy metal is one of major cause in the reduction of growth of the fungus (Fig. 5.24; Wu et al., 2010; Scandalios, 2005; Li et al., 2017). However, reduction in the removal of $Ni_{(II)}$ was due to reduction in the growth and metabolic process of fungus that cause lower accumulation of $Ni_{(II)}$ inside the cell and also reduces the availability of surface functional group by reducing the amount of

biomass that is responsible for binding of $Ni_{(II)}$ on mycelia surface (Moore et al., 2008). On another hand, competition may also happen between co-occurring contaminant and $Ni_{(II)}$ for binding with active sites on the mycelia surface that also cause reduction in $Ni_{(II)}$ removal (Gola et al., 2016).

The removal of $Ni_{(II)}$ in presence of NO_3^- was 70.8% which was higher than its absence while the biomass productivity was 6.56 g/L confirm its role in $Ni_{(II)}$ removal. No significant change in the removal and biomass production was observed under the co-occurrence of NaCl, NH_4Cl, SO_4^{2-} and Ca^{2+}. (Fig. 5.23a). EDTA is the metabolic inhibitor, negatively affected the growth of the fungus and $Ni_{(II)}$ removal rate under its presence was 51.5% (Fig. 5.23a) (Banerjee et al., 2019). Reduction in the growth is due to toxicity of the respective agent while reduction in the removal rate of $Ni_{(II)}$ might be due to the reasons that discussed above.

5G.6 Effect of $Ni_{(II)}$ on H_2O_2 and Lipid peroxidation

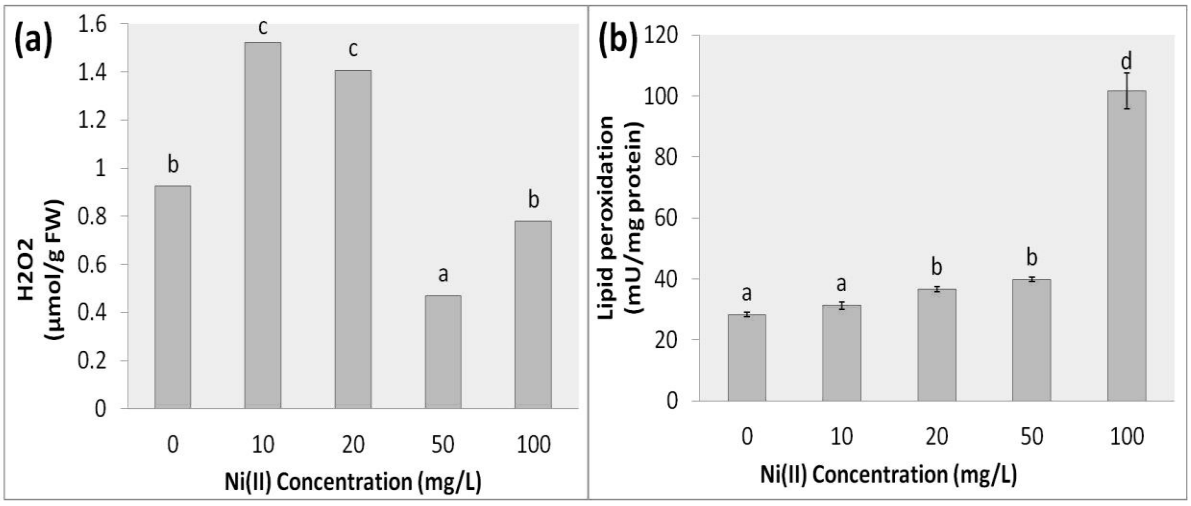

Fig. 5.24. Effect of different concentration of $Ni_{(II)}$ on the level of (a) H_2O_2 and (b) Lipid peroxidation (Bar represent standard deviation of three replicate and different letter above the column denotes significant differences at the level $p<0.05$ followed by DMRT (post hoc test)).

Oxidative stress under the presence of stress conditions such as presence of heavy metal, pesticides, drought, water logging, etc. in microbes and plants have been reported in many studies (Azevedo et al., 2007; Zadrąg-Tęcza et al., 2018; Huang et al., 2017a; Xu et al., 2015). In the present study, to observe the oxidative stress in *A. flavus* CR500 under the presence of different concentration $Ni_{(II)}$ was analyzed by

measuring the level of H_2O_2 content and melandialdehyde (MDA), the end product of lipid membrane peroxidation. The H_2O_2 content was higher at 10 and 20 mg/L of $Ni_{(II)}$ as compared to 0 mg/L but lower at 50 and 100 mg/L of $Ni_{(II)}$ (Fig. 5.24a). However, with rise in the metal concentration from 0 to 100 mg/L the level of MDA was recorded in an increasing order. At 100 mg/L of $Ni_{(II)}$ concentration, MDA content was increased by 316% as compare to control. The changes in level of H_2O_2 and lipid peoxidation confirm the toxicity of $Ni_{(II)}$ on *A. flavus* CR500 is due to oxidative stress (Xu et al., 2012; Mukherjee et al., 2010).

5G.7 Effect of $Ni_{(II)}$ on activity of enzymatic antioxidants

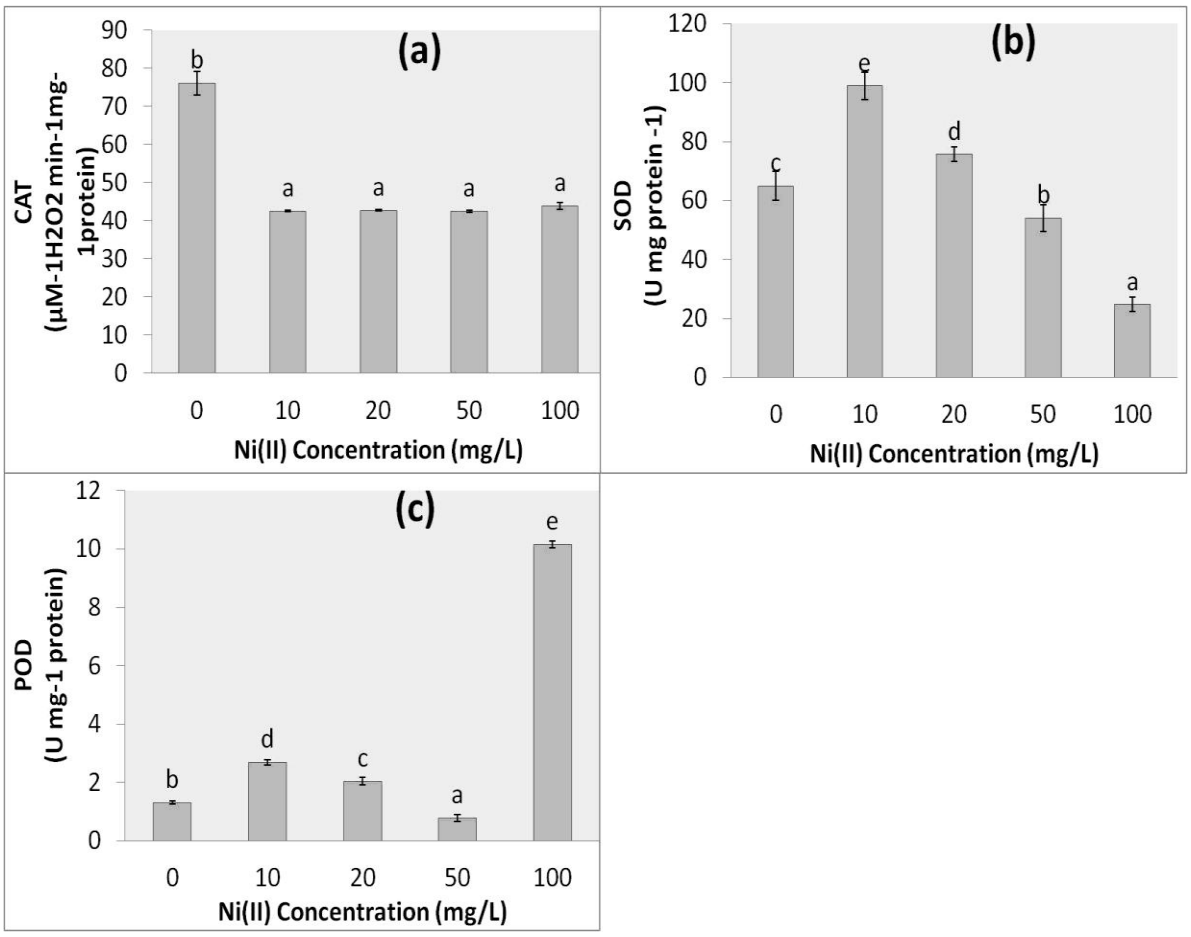

Fig. 5.25. Effect of different concentration of $Ni_{(II)}$ on the activity of (a) CAT, (b) SOD and (c) POD (Bar represent standard deviation of three replicate and different letter above the column denotes significant differences at the level p<0.05 followed by DMRT (post hoc test)).

SOD, POD and CAT play role as reactive oxygen species scavenger and often reported their activity under the oxidative stress conditions caused by stressed

situation such as heavy metal in fungi, bacteria and plants (Huang et al., 2017a; Kumar et al., 2019; Mostofaet al., 2017; Xu etal., 2015). Increased in the SOD, POD and CAT activity was also recorded in *A. flavus* CR500 under the presence of Cr(VI) (**see section 5E.5**). Here, with rise in $Ni_{(II)}$ concentration, the activity of CAT was first reduced at 10 mg/L and after that no significant ($p<0.05$) change was observed (Fig. 5.25a). The activity of SOD was first increased at 10 mg/L than reduced significantly up to the concentration of 100 mg/L (Fig. 5.25b). However, the activity of POD was first increased at 10 mg/L than decreased significantly up to the concentration of 50 mg/L and instantly increased by 7.3 times at 100 mg/L as compared to control (0 mg/L) (Fig. 5.25c). These changes were also observed in the studies under the presence of heavy metal in some fungi *P. chrysosporium, F. solani, A. niger, A. fumigatus* 3_2 (Huang et al., 2017; Kumar et al., 2019; Krumova et al., 2016; Mukherjee et al., 2010).

5G.8 Effect of $Ni_{(II)}$ on level of protein and non-enzymatic antioxidants

Heavy metal toxicity due to oxidative stress is reported in many studies and antioxidants play important role in scavenging the ROS. Induction of proline is sign of stress condition in plants and microbes that play important role in ROS removal (Chakraborty et al., 2014; Mukherjee et al., 2010). In the present study, the level of proline was significantly ($p<0.05$) increased by 1.7 folds as increase in the concentration of $Ni_{(II)}$ from 0 to 50 mg/L, while decreased instantly to 0.29 m mol/g FW at 100 mg/L (Fig. 5.26). The total phenolic content participate in elimination of ROS by dissociating its H^+ ion and donating an electron which is its mechanistic pathway for scavenging of ROS (Hernándezetal., 2009). It is observed in the present investigation that level of total phenolic content was significantly increased with increased in the concentration of $Ni_{(II)}$. The highest level of total phenolic content was found at 100 mg/L which was 1456 % higher as compared to control. These finding confirm the importance of proline and phenolic content in minimization of $Ni_{(II)}$ induced toxicity in *A. flavus* CR500 *via* inducing ROS level (Chakraborty et al., 2014; Mukherjeeetal., 2010).

The metal toxicity can affect the growth and developmental activities of living organisms. Protein is the most essential macromolecules that has significant role in metabolic, growth and developmental activities of bacteria, fungi, plants and other

living organism. Alteration in the level of protein in organisms under the presence of any agents is the sign of its effect of respective agents on the metabolic, growth and developmental activities of the organism. In this study, the level of intracellular protein content significantly reduces the level of intracellular protein content in *A. flavus* CR500. The level of intracellular protein content was first decreased slightly up to 50 mg/L of $Ni_{(II)}$ and increased at 100 mg/L of $Ni_{(II)}$ (0.43 µg/g FW) which lower than control but higher than protein content at 50 mg/L of $Ni_{(II)}$ (Fig. 5.26).

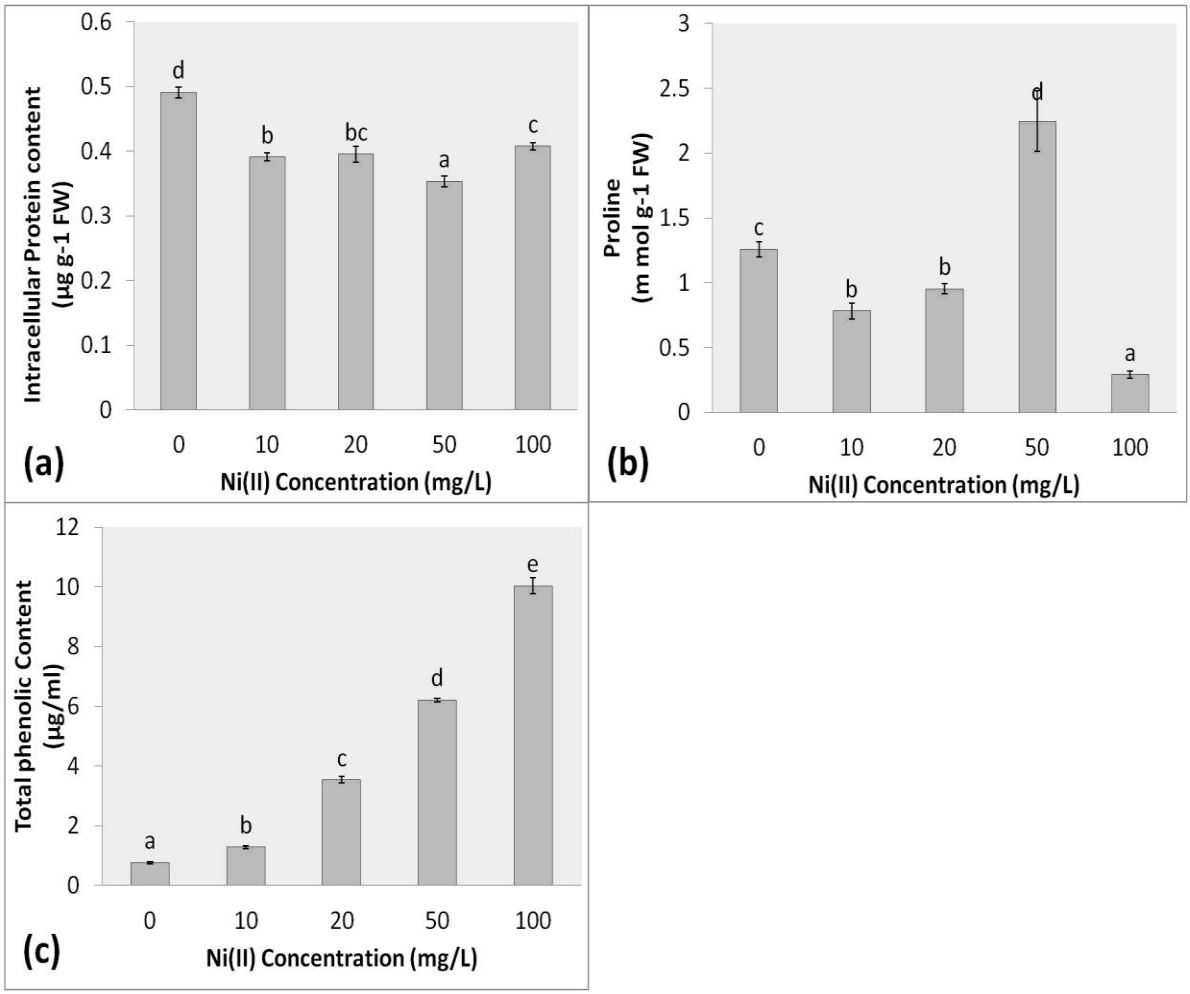

Fig. 5.26. Effect of different $Ni_{(II)}$ concentration on level of (a) intracellular protein content, (b) proline and (c) total phenolic content (Bar represent standard deviation of three replicate and different letter above the column denotes significant differences at the level $p<0.05$ followed by DMRT (post hoc test).

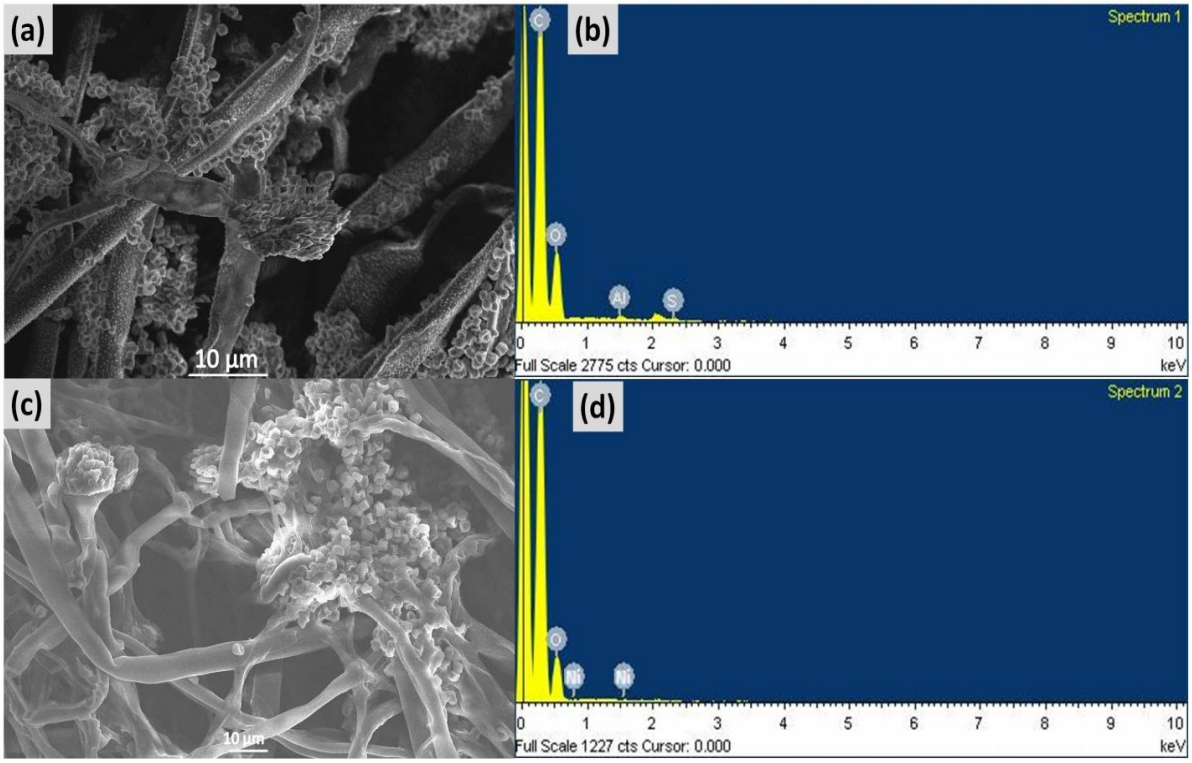

Fig. 5.27. The mycelia surface morphology of *A. flavus* CR500 grown in PDB medium without amended (a) and amended with 100 mg/L of $Ni_{(II)}$ (c) for six days. EDX graph showing (b) absence of Ni representing peak on fungus surface grown in without $Ni_{(II)}$ amended PDB medium and (d) Ni representing peaks on mycelia surface grown in $Ni_{(II)}$ amended PDB medium for six days.

5G.9 Effect of $Ni_{(II)}$ on mycelia morphology of CR500

In stressed environment all the types of organism showed many types of physical responses that may unique for specific types of stress conditions. Similarly, microbes also sowed many of the responses in stress environment such as drought, salinity, heavy metal, pesticides, etc. (Azevedo et al., 2007; Luna et al., 2015; Tu et al., 2020). In the present study, under the presence of $Ni_{(II)}$ hypha surface of *A. flavus* CR500 was smooth, protrusion less and swelled. However, in the absence of $Ni_{(II)}$, hyphae were rough, cylindrical and thin (Fig. 5.27a, c). Changes were observed in the surface morphology might associated with $Ni_{(II)}$ accumulation inside the cell as hyphae are swelled and the toxicicological response as protrusion less mycelia with smooth surface. Similar responses of *A. flavus* CR500 were also observed under stress of Cr(VI) **(see section 5E.7)**. These observed changes are due to toxicity and

accumulation of $Ni_{(II)}$ to the cell of the fungi (Luna et al., 2015; Canovas et al., 2003; Cao et al., 2018; Chen et al., 2019).

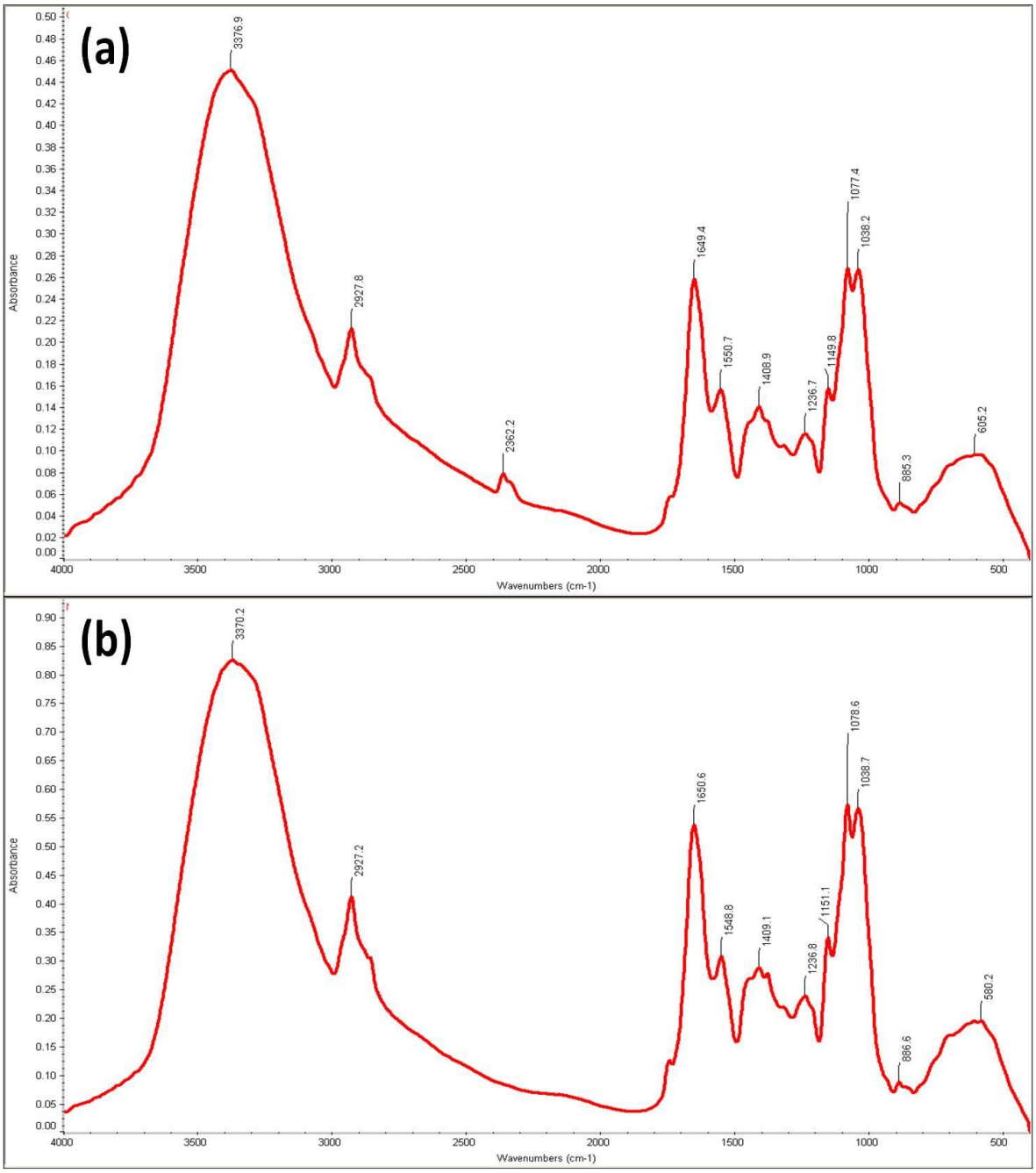

Fig. 5.28. IR graph of fungus grown in (a) normal and (b) 100 mg/L of $Ni_{(II)}$ amended PDB medium for six days.

5G.10 IR analysis

Based on the finding of FTIR analysis hydroxyl (-OH), carbonyl (C=O), amino (NH_2), phosphate group and Nitro groups are the major functional groups

involved in metal biosorption (Fig. 5.28) which also have been previously reported (Yuan et al., 2012; Chen et al., 2019). Treatment of CR700 with Ni causes a strong shift in the peak at 3376.9 cm^{-1}, 1550.7 cm^{-1} and 605.2 and weak shift at 1649.4 cm^{-1}, 1077.4 cm^{-1} (Phosphate group), 1038.2 cm^{-1} and 885.3 cm^{-1} (aromatic C-H stretching). The peak at 1149.8 cm^{-1} representing phosphate group shifted under stress of Ni. The peak at 2362.2 cm^{-1} (C=C stretching) disappeared with the treatment of all metals. The shift in the peak 3376.9 cm^{-1} (─OH and N-H Stretching) and 1149.8 cm^{-1} (phosphates group) on Ni treated biomass suggested the electrostatic attraction between the biomass and positively charged metal ions (Chen et al., 2019). The disappeared peak 2362.2 cm^{-1} (C=C stretching) on Ni treated biomass might be due to the metal─π─bond interaction in biosorption of metals. Amino, hydroxyl and carboxyl group involvement in Pb and As biosorption was reported in *Westerdykella* sp., *Penicillium* sp., *Rhizopus* sp., *Trichoderma* sp. (Velmurugan et al., 2010; Chakraborty et al., 2014).

5H. *T. lixii* CR700 and $Ni_{(II)}$: Removal, morphological and Biochemical Study

5H.1 Removal of $Ni_{(II)}$ by *T. lixii* CR700

The results of the removal of Ni at its different initial concentration by *T. lixii* CR700 is shown in Fig. 5.29b. A maximum removal percentage for Ni was 64.4 % at the 10 mg/L of $Ni_{(II)}$ concentration after 144 h of incubation which was higher than uptake efficiency of 49.7% at 21.5 mgL^{-1} of Ni by a metal tolerant fungus (Moore et al., 2008). A significant amount of Ni removal was also reported by *Aspergillus* sp. and *Phanerochaete chrysosporium* either via accumulation or surface sorption mechanism (Cao et al., 2018; Congeevaram et al., 2007). In this work, with an increase in the concentration of $Ni_{(II)}$ from 10 to 500 mgL^{-1}, the removal rate percent was decreased significantly to 11.7% (Fig. 5.29b). No significant change in the obtained biomass of *T. lixii* CR700 was recorded up to 50 mgL^{-1} of $Ni_{(II)}$ which was almost 7.8 gL^{-1}, while decreased significantly above this concentration (Fig. 5.29b). The data of the obtained biomass is closely associated with the removal rate. Decrease in the removal rate below 50 mgL^{-1} was might be due to limited availability of metal-binding surface functional group as well as accumulation space (vacuoles) and binding agent (thiol content) inside the cell of *T. lixii* CR700 (Canovas et al., 2003; Thorsen et al., 2007; Ilyas and Rehman, 2015) because obtained biomass was not significantly changed up to 50 mgL^{-1}. But, a decrease in removal rate above 50 mgL^{-1} of $Ni_{(II)}$ might be also influenced by the reduction in biomass, possibly due to toxicity of $Ni_{(II)}$ (Brown et al., 2014; Urrialde et al., 2017). Reduction in biomass of *T. lixii* CR700 with increase in the concentration of $Ni_{(II)}$ may be due to increase in the oxidative stress (Fig. 5.32a, b) that ultimately reduces the values of removal rate (Mukherjee et al., 2010; Urrialde et al., 2017).

Change in the duration of the incubation period significantly affected the removal efficiency of the fungi and was increase with an increase in the incubation period (Noormohamadi et al., 2019; Mukherjee et al., 2010; Mohd et al., 2019). The present study, the maximum (67.6%) removal of $Ni_{(II)}$ was recorded at 240 h after incubation at the concentration of 50 mgL^{-1} (Fig. 5.29a). To confirm the contribution of mechanism that is involved in the removal of Ni, at 50 mgL^{-1} and 144 h of incubation period the amount of $Ni_{(II)}$ accumulated and surface adsorbed values were

also investigated. Results showed that accumulation of Ni(II) was 2.42 ± 0.25 mgg^{-1} of dried biomass. In the removal process by *T. lixii* CR700, an amount of 1.12 ± 0.19 mgg^{-1} of dried biomass of $Ni_{(II)}$ was also contributed by surface sorption mechanism at the same concentration and incubation period (Cao et al., 2018). This phenomenon was also confirmed by FTIR investigation as the involvement of the surface functional group in $Ni_{(II)}$ removal (Fig. 5.35; Table 5.4). This investigation confirmed that the removal of $Ni_{(II)}$ was driven by mainly accumulation inside the cell of the CR700.

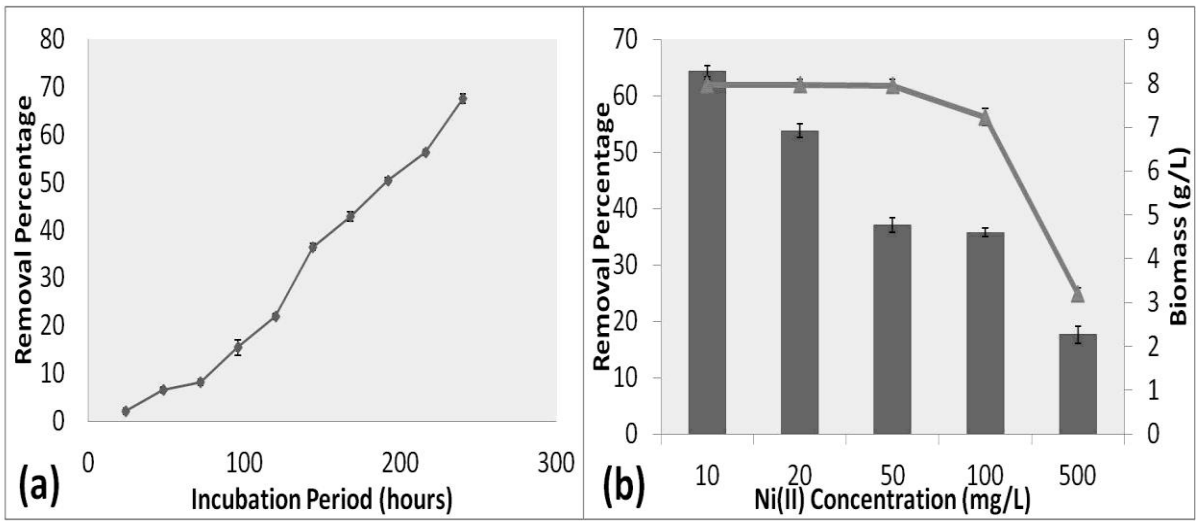

Fig. 5.29. Effect of (a) incubation periods and (b) different initial conetration of $Ni_{(II)}$ on its removal by *T. lixii* CR700.

5H.2 Effect of pH and temperature on removal of $Ni_{(II)}$

Factors such as pH, temperature, presence of other metals, anions, cations and metabolic inhibitors significantly affected the removal ability of the bioremediation agents. In this study, all these factors have been studied to assess their effect on the removal ability of *T. lixii* CR700 in the removal of $Ni_{(II)}$. The pH of the medium significantly affected the removal of Ni by *T. lixii* CR700, and optimum pH for the removal of $Ni_{(II)}$ was slight basic (pH 8.0) where removal percentage was significantly higher than at all the tested pH. The removal percentage by *T. lixii* CR700 at pH 8.0 was 40.9 for Ni at 50 mgL^{-1} and 144 h after incubation (Fig. 5.30a). However, the result of $Ni_{(II)}$ removal by *T. lixii* CR700 was opposite to the previous work studied by Salvadori et al. (2015). They analyzed Ni removal in the pH range from 2.0 to 6.0 and reported maximum removal of Ni at pH 4.0 by live, dried and dead biomass of

Hypocrea lixii possibly due to pH-dependent ionization of surface functional group. In this study, the obtained biomass in the presence of $Ni_{(II)}$ was higher at pH 7.0 as compared to all the tested pH (Fig. 5.30a). Because, the removal of Ni is mainly driven by accumulation, so decrease in the removal percentage below pH 7.0, closely associated with decreased in the obtained biomass which was due to unfavorable condition for the growth, development and metabolic activity of the organism (Kumar et al., 2019; Pundir et al., 2016). Removal was also driven by surface sorption mechanism and a decrease in the pH causes positive charged cell surface of *T. lixii* CR700 due to increase in hydronium (H_3O^+) concentration in the medium (Daoud and Selatnia, 2019; Pundir et al., 2016). This may cause repulsion between the metal ion and positively charged cell wall of the *T. lixii* CR700 that possibly led to decrease in the removal rate of $Ni_{(II)}$. However, above pH 7.0 the phenomenon is reverse to this and causes a negatively charge on the cell surface of the fungi due to OH^- anions which enhanced the electrostatic attraction between the negatively charged surface and metal ions and increases the removal rate at pH 8.0. Above pH 8.0, the decrease in the removal is possibly due to instant decrease in obtained biomass (Fig. 5.30a) that affected the accumulation as well as surface sorption mechanism. Above pH 8.0, Ni also occurs in their hydroxide form [$Ni(OH)_2$] that may also affect its solubility and interferes with its translocation inside the cell (Felmy et al., 1984; Daoud and Selatnia, 2019).

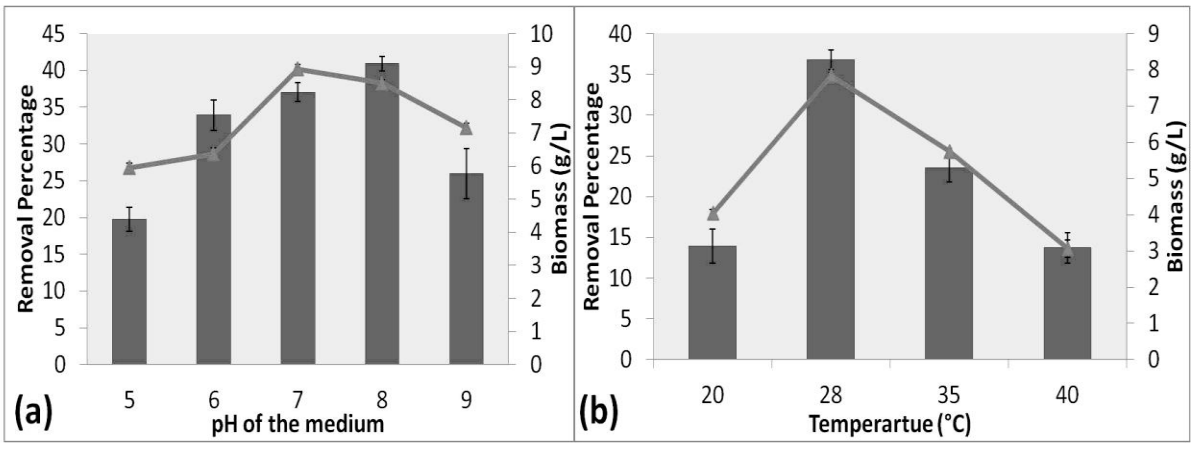

Fig. 5.30. Effect of (a) different pH and (b) Temperature on removal of $Ni_{(II)}$ by *T. lixii* CR700.

The temperature is the most important variable that can affect the removal ability of $Ni_{(II)}$ by altering the growth and metabolic activity of *T. lixii* CR700 (Prasad

et al., 2018; Kumar et al., 2019). It was found in the present study that optimum temperature for removal of $Ni_{(II)}$ by *T. lixii* CR700 was 28 ± 1 °C and the removal percentage was 36.8% for $Ni_{(II)}$ at 50 mgL^{-1} and 144h after incubation (Fig. 5.30b). The temperature is the major variable for growth and development of the living organism. So, the maximum obtained biomass was also recorded at an optimum temperature of 28 ± 1 °C which was 7.84 ± 0.11 gL^{-1} in presence of $Ni_{(II)}$ at the same concentration and incubation periods (Fig. 5.30b). The decrease in the removal percentage with the change in the temperature from their optima was due to a decrease in the biomass that affected the accumulation potential of *T. lixii* CR700 (Pundir et al., 2016; Srivastava et al., 2006). Similar change was observed in previous studies for Cd, Ni and As removal by fungi (Kumar et al., 2019; Congeevaram et al., 2007; Salvadori et al., 2015; Wu et al., 2012). Change in the temperature from optimum also affected the availability of surface functional group due to decrease in the obtained biomass that involve in the removal of $Ni_{(II)}$ (Fig. 5.30b) (Pundir et al., 2016; Prasad et al., 2018).

5H.3 Effect of different anions, cations, salts and EDTA on the removal of As and Ni by CR700

The presence of anions, salts and other contaminants in wastewater are a common phenomenan that can significantly affect the removal ability of the microorganism (Banerjee et al., 2019). The removal ability of $Ni_{(II)}$ by *T. lixii* CR700 was assessed under the presence salts (NaCl and NH_4Cl), anions (NO_3^- and SO_4^{-2}), Ca^{++} and EDTA, a metabolic inhibitor (Banerjee et al., 2019). These variables significantly affected the removal of $Ni_{(II)}$ as compare to their absence at the same concentration of $Ni_{(II)}$. Maximum reduction in removal of $Ni_{(II)}$ was recorded in the presence of SO_4^{2-} and EDTA which was 24.9 and 25.8% respectively (Fig. 5.31a). EDTA might inhibit the removal percentage due to its metabolic inhibiting characteristics as reported in previous studies (Banerjee et al., 2019). The presence of NO_3^- significantly increases the removal of $Ni_{(II)}$ from 36.4 to 41.4%. A significant change in the obtained biomass was also recorded under the presence of these variables which followed the similar pattern as found in the removal of $Ni_{(II)}$ in the presence of these variables (Fig. 5.31a). The presence of different types of cations and anions (NH_4Cl, NO_3^-, Ca^{++} and SO_4^{-2}) affect the metabolic mechanism, development and growth of the fungi that probably affected the obtained biomass as well as

removal percentage. However, some of them (NO_3^-, NaCl and PO_4^{-3}) may be utilizes as nutrients that can improve the removal efficiency of the microbes (Johri et al., 2015; Barua et al., 2012).

5H.4 Effect of different heavy metals on removal of $Ni_{(II)}$ by CR700

The co-occurrence of other heavy metal with Ni(II) in wastewater was encountered in many studies that severely inhibit the growth of the living organism. The removal capability of $Ni_{(II)}$ by CR700 was checked in the presence of Chromium (Cr), Zinc (Zn), Manganese (Mn), Lead (Pb) by using their respective salts $K_2Cr_2O_7$, $ZnCl_2$, $MnCl_2$, $CuCl_2$ and $PbSO_4$ respectively. Results showed that Pb, Cr and As highly affected the removal of $Ni_{(II)}$ and the removal percentage was 10.5, 23.7 and 24.4% respectively (Fig. 5.31a). Most of the heavy metals are toxic and reported to cause oxidative stress in plants and microbes, so their co-occurrence with $Ni_{(II)}$ also affected the obtained biomass of *T. lixii* CR700 (Ye et al., 2018; Ong et al., 2017; Khullar and Reddy, 2017). The results have been shown in Fig. 5.31a which depicted that co-occurrence of Ni-Cu, and Ni-Pb were highly affected the obtained biomass of *T. lixii* CR700. Here, it is to be mentioned that used salts for Pb was $PbSO_4$ where SO_4^{-2} also reduced the obtained biomass and removal rate of $Ni_{(II)}$ (Fig. 5.31b).

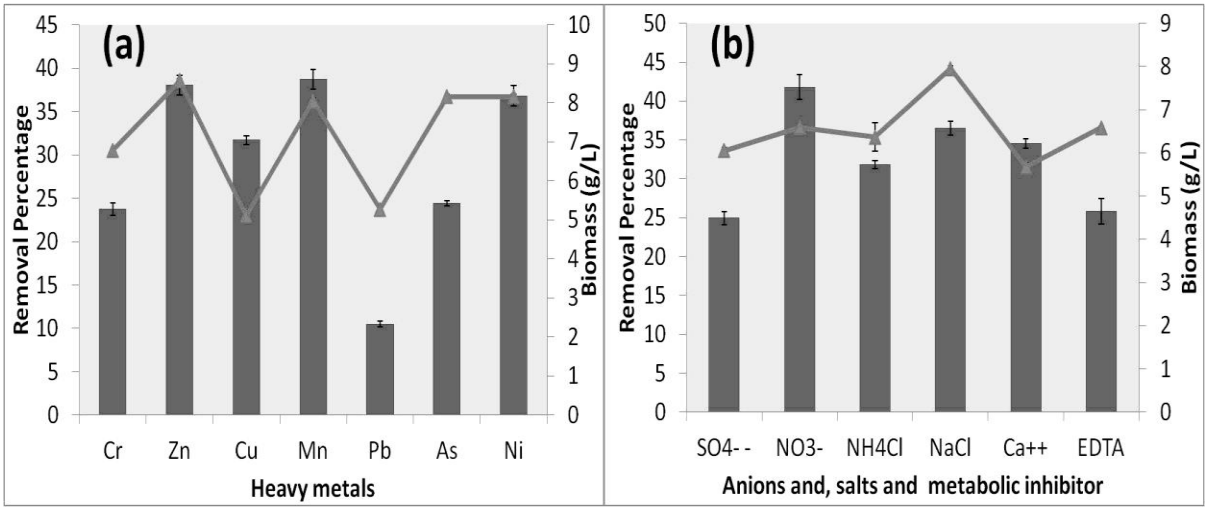

Fig. 5.31. Effect of (a) different heavy metal and (b) anions, cation, salts and EDTA on removal $Ni_{(II)}$ by *T. lixii* CR700.

The effect of $Cr_{(VI)}$ was investigated on *T. lixii* CR700 and found an increase in oxidative stress as well as antioxidants response that may reduces the growth and removal ability of *T. lixii* CR700 for $Ni_{(II)}$ with presence of $Cr_{(VI)}$ (**see section 5F.5**).

Similarly, Pb, Cu and Zn were also reported for their toxicity to other microbes and plants at their elevated concentration that might be affected the growth and removal ability of *T. lixii* CR700 (Ye et al., 2018; Govarthanan et al., 2018; Luna et al., 2015). The simultaneous presence of As and $Ni_{(II)}$ may cause competition between them to bind with thiol content where $Ni_{(II)}$ was failed to bind and its removal rate was reduced from 36.8 to 24.4% while, As make strong relation with GSH and thiol content and its removal rate was increased by *T. lixii* CR700 (Fig. 5.31a) (Canovas et al., 2003; Thorsen et al., 2007). Some of the removed amount of $Ni_{(II)}$ was also contributed by surface sorption mechanism. It was found in FTIR investigation that –OH, ─NH, ─COOH and phosphate group are major functional groups that are probably involved in $Ni_{(II)}$ sorption (Fig. 5.35; Table 5.4) which indicates that these surface functional groups are another site where competition may occur between co-contaminant and $Ni_{(II)}$. Results of the $Ni_{(II)}$ removal (as mentioned above) again favoring the failure of $Ni_{(II)}$ in competition for biosorption on the mycelia surface of isolate CR700. These mechanisms may also occur with $Ni_{(II)}$ removal in presence of other heavy metal (Pb, Cu, Cr and Zn) and other variables (NH_4Cl, NO_3^-, Ca^{++} and SO_4^{-2}) that probably reduces the removal percentage of $Ni_{(II)}$.

5H.5 Effect of $Ni_{(II)}$ on H_2O_2 and Lipid peroxidation in *T. lixii*

Oxidative stress caused by heavy metal including $Ni_{(II)}$ in plant and microbes has been reported in many studies that could cause oxidative damages inside the cell via oxidizing unsaturated fatty acid, protein, membrane lipid, DNA and macromolecules (Scandalios, 2005; Yilmaz and Parlak 2011; Kalita et al. 2018; Pandey and Bhatt 2016; Das and Sarkar 2018). In the present study, lipid peroxidation and H_2O_2 content production in *T. lixii* CR700 under the presence of $Ni_{(II)}$ was demonstrated as a measure of oxidative stress. Results showed that with the increase in the concentration of $Ni_{(II)}$, first the MDA content was significantly decreased at 50 mgL^{-1} of $Ni_{(II)}$ (Fig. 5.32a). However, no significant change was recorded at 100 mgL^{-1}, but at 200 mgL^{-1} of $Ni_{(II)}$, MDA content was significantly increased up to 12.35 nmol g^{-1} FW which was 40% higher than control (Fig. 5.32a). The results of the effect of $Ni_{(II)}$ on H_2O_2 content in *T. lixii* CR700 is shown in Fig. 5.32b. It was found in the results that with an increase in the $Ni_{(II)}$ concentration from 0 to 200 mgL^{-1}, the H_2O_2 content was increased significantly from 22.1 to 34.1 nmol g^{-1} FW (Fig. 5.32b). *T. lixii* CR700 showed a clear response towards increasing concentration

of $Ni_{(II)}$. Previous studies suggested that MDA and H_2O_2 content were increased with an increase in $Ni_{(II)}$ concentration in plant and microbes (Shri et al., 2009; Spagnoletti et al., 2016; Urrialde et al., 2017). These results confirmed that $Ni_{(II)}$ has more toxicity to *T. lixii* CR700 at their elevated concentration, $Ni_{(II)}$ can cause oxidative stress in CR700 (Pandey and Bhatt, 2016; Das and Sarkar, 2018; Shri et al., 2009).

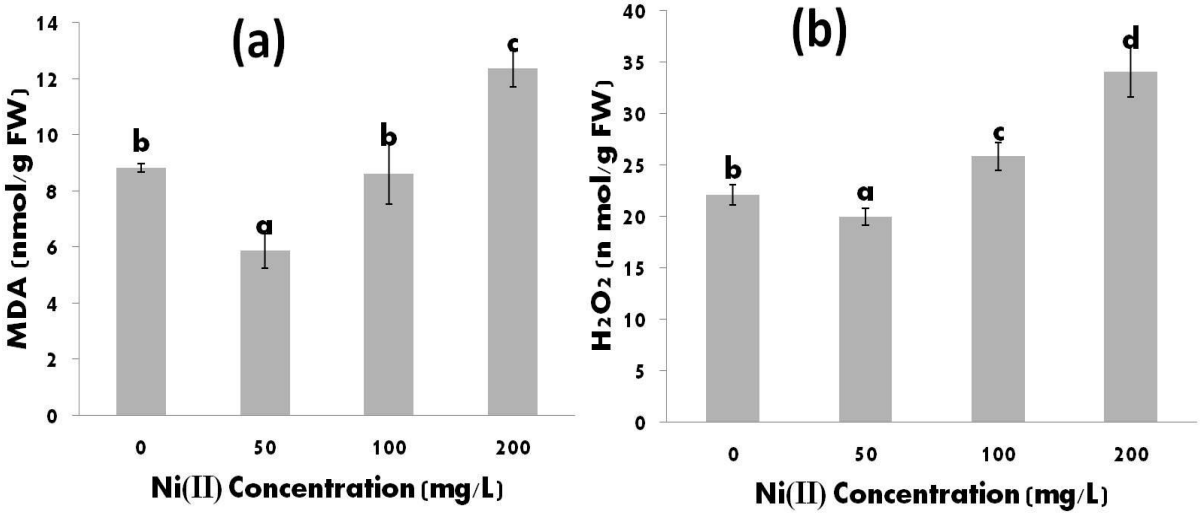

Fig. 5.32. Effect of different $Ni_{(II)}$ concetartion on MDA and H_2O_2 content in *T. lixii* CR700 (bar denotes standard deviation of three replicates and different letter denotes significant differences at the level of $p<0.05$ followed by DMRT).

5H.6 Effect of $Ni_{(II)}$ on enzymatic antioxidants

Enzymatic antioxidant activity has been reported to be increased under the presence of stress conditions in plants and microbes such as drought, salts stress, in presence of heavy metal and other toxicants for scavenging of ROS (Sharma, 2012; Urrialde et al., 2017; Kannaujia et al., 2019; Shri et al., 2009). In this study, the activity of POD was increased with an increase in the concentration of $Ni_{(II)}$ and a maximum of 1.62 Umg^{-1} protein of POD activity was recorded at 200 mgL^{-1} of $Ni_{(II)}$ (Fig. 5.33a). Similarly, the CAT activity was also increased in presence of $Ni_{(II)}$ in *T. lixii* CR700 as an increase in POD was recorded. The maximum CAT activity (41.12 µmol H_2O_2 min^{-1} mg^{-1}) was recorded at 200 mgL^{-1} of $Ni_{(II)}$ which was 169% higher than control (Fig. 5.33b). When, we critically compared the activity pattern of enzymatic antioxidant and level of oxidative (H_2O_2 and MDA) stress in presence of $Ni_{(II)}$, we found that both of them are associated with each-other and their response

was possibly just because of each-other. Results suggested that in *T. lixii* CR700, oxidative stress caused by $Ni_{(II)}$ provoked by different combinations of antioxidants (CAT and POD in presence of $Ni_{(II)}$ Fig. 5.33a, b).

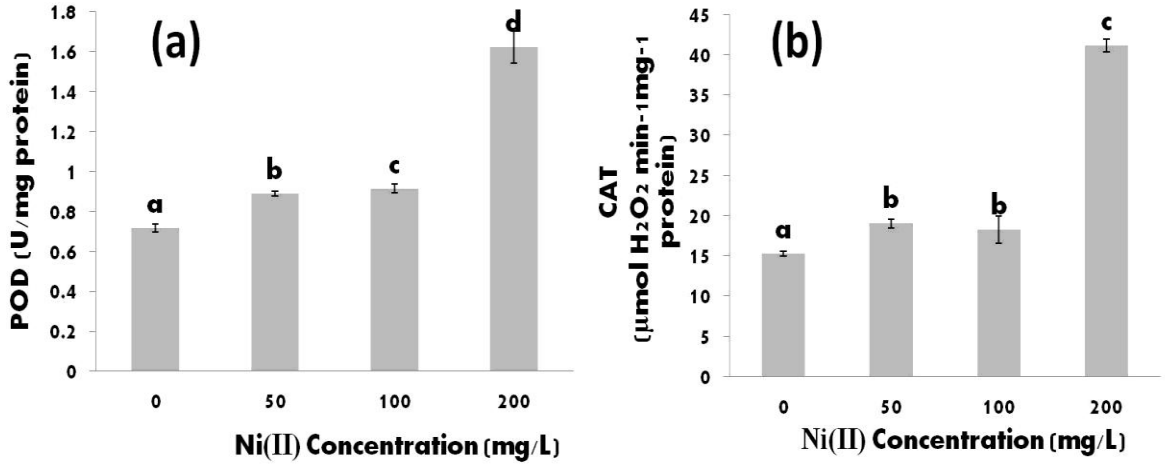

Fig. 5.33. Effect of different concentration of $Ni_{(II)}$ on activity of (a) POD and (b) CAT in *T. lixii* CR700 (bar denotes standard deviation of three replicates and different letter denotes significant differences at the level of $p<0.05$ followed by DMRT).

5H.7 Effect of $Ni_{(II)}$ phenolic content, GSH and Non-protein Thiol content

Results of the total phenolic content, GSH and non-protein thiol content production in *T. lixii* CR700 under the presence of $Ni_{(II)}$ are shown in Fig. 5.34. Results showed that level of phenolic content in *T. lixii* CR700 was first increased by 16% in the presence $Ni_{(II)}$ at 50 mgL^{-1} but as the concentration of $Ni_{(II)}$ was above 50 to 200 mgL^{-1}, the phenolic content production rate was decreased by 38% as compared to control (Fig. 5.34a). Increased in phenolic compound production are reported in stress conditions and causesa oxidative stress in plants and microbes. Total phenolic content plays an important role in scavenging of ROS produced under heavy metal stress via donating their hydrogen ion from the hydroxyl group (Hernandez et al., 2009). Probably it reacts with hydrogen peroxide and superoxide and converts into water and hydrogen peroxide molecules respectively either in presence of enzyme or directly by reacting with these molecules as substrate.

GSH is an important component of immune system of the cell and it has been reported as an antioxidant as well as a good chelating agent for heavy metals inside

the cell (Ilyas and Rehman, 2015; Canovas et al., 2003; Mukherjee et al., 2010; Thorsen et al., 2007). After chelation with the heavy metals, it translocated to vacuoles of the cell and this phenomenon was also reported for non-protein content (Su et al., 2015; Zeng et al., 2015; Rausch and Wachter, 2005; Kumar et al. 2019). However, no significant change in the GSH level was recorded with increase in the concentration of $Ni_{(II)}$ up to 100 mgL^{-1} and was decrease significantly at 200 mgL^{-1} $Ni_{(II)}$. While, the thiol content was increased significantly by increase in the concentration of $Ni_{(II)}$. A maximum of 77.9% increase in the level of thiol content in *T. lixii* was recorded in the presence of 200 mgL^{-1} of $Ni_{(II)}$ as compared to control (Fig. 5.34c). Non-protein thiol content has been reported for their metal chelating properties that could cooperate in accumulation of $Ni_{(II)}$ inside the cell of *T. lixii* CR700 (Rausch and Wachter, 2005; Su et al., 2015; Zeng et al., 2015).

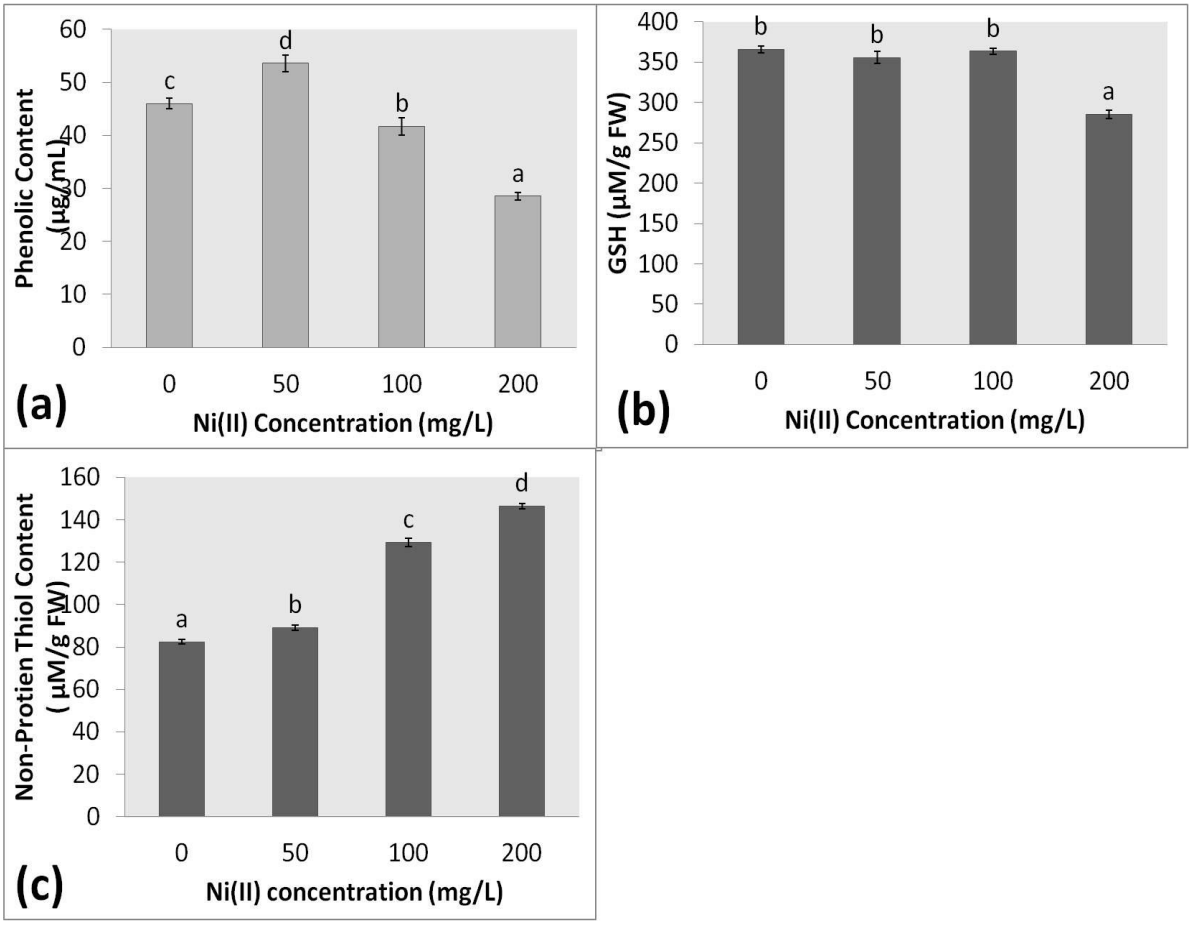

Fig. 5.34. Effect of different $Ni_{(II)}$ concentration on (a) phenolic content, (b) GSH and (c) non-protien thiol content in *T. lixii* CR700 (bar denotes standard deviation of three replicates and different letter denotes significant differences at the level of $p<0.05$ followed by DMRT).

5H.8 FTIR analysis

The changes in the IR band of treated (100 mgL^{-1} of $Ni_{(II)}$) and without treated fungal biomass detected by FTIR investigation and their assignments are shown in Table 5.4 and Fig. 5.35. The minor shift (from 3423.1 to 3425.7 cm^{-1}) was found with the treatment of Ni which represents ─OH and ─NH group stretching (Chen et al., 2019; Li et al., 2019). The atom "O" of -OH contains two lone pair (lp) while "N" of N-H contain one lp electron which suggested the metal-lp electron interaction in $Ni_{(II)}$ biosorption (Kumar et al., 2019). The peak at 1646.9 cm^{-1} shifted to 1650.7 cm^{-1} with the treatment of $Ni_{(II)}$, represent C=O stretching of -COOH and the peak at 1405.5 cm^{-1} shifted to 1412.2 cm^{-1} respectively assigned to C─N stretching (Chen et al., 2019). Two new bands were also recognized at 1384.1 and 1315.7 cm^{-1} that might be assigned to carboxylate anion while these peaks were not detected in control biomass. The shift in C=O of -COOH representing peak and appearance of new COO^{-} assigning peak suggested the involvement of COOH via its dissociation into COO^{-} and H^{+} and simultaneous electrostatic attraction of $Ni_{(II)}$ ions by COO^{-} anions. Phosphate group representing peak at 1076.1 cm^{-1} shifted to 1072.7 cm^{-1} by treating with Ni which also sahow the electrostatic attraction between phosphate anions and positively charged $Ni_{(II)}$ cations (Akar et al., 2012).

The band 1241.1 cm^{-1} was shifted to 1242.4 cm^{-1} with the treatment of $Ni_{(II)}$ that assigned SO_3 group which may have a possible role in $Ni_{(II)}$ biosorption. Interestingly, it was found in the metal quantification experiment that the surface biosorption of $Ni_{(II)}$ was 1.79 ± 0.47 mgg^{-1} of dried biomass. This investigation revealed that the cell wall of *T. lixii* CR700 also participated in the removal of $Ni_{(II)}$ via adsorption with the help of its surface functional groups.

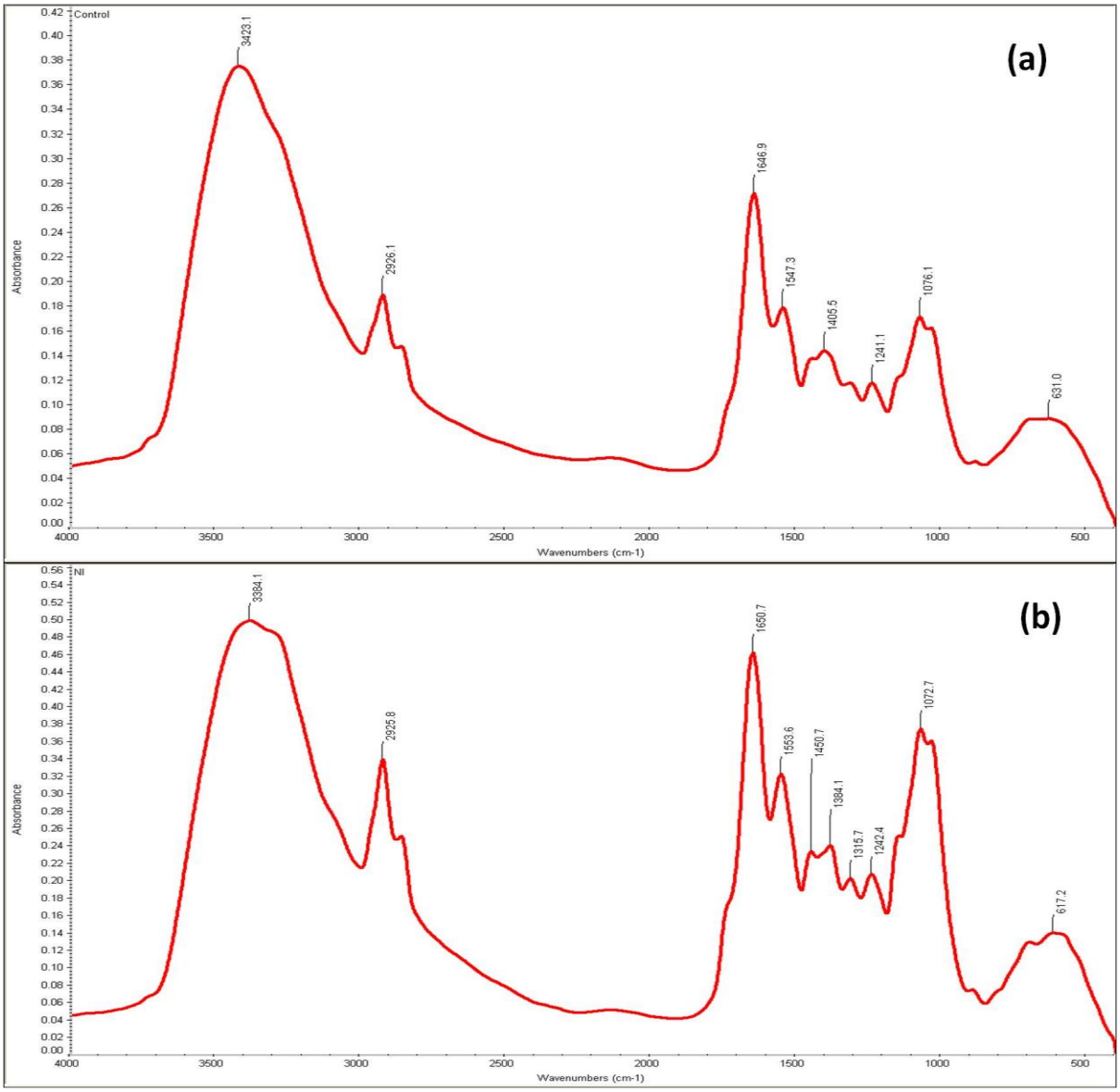

Fig. 5.35. FTIR image of *T. lixii* CR700 biomass grown in (a) control and (b) 100 mg/L $Ni_{(II)}$ amended PDB medium.

Table 5.4. The IR spectra of biomass of *T. lixii* CR700 grown in control and 100 mg/L of Ni and As amended PDB medium and their assigned functional groups.

Control (0 mgL^{-1})	Ni (100 mgL^{-1})	Functional group Assignments
3423.1	**3384.1**	-O─H Stretching vibration and -N─H stretching of protein or acetamide groups of chitin fraction
2926.1	2925.8	-C─H Stretching vibration of fatty acid in membrane phospholipid

1646.9	1650.7*	C=O group in Amide I of N-acetyl glucosamine polymer or the protein peptide bond or Carboxylic acid group
1547.3	**1553.6**	Amide II of N-Acetyleglucosamine polymer or the protein
1405.5	**1450.7**	C─N stretching in Amide III
-	1384.1	Amide III band represents to COO^- anions
-	1315.7	Amide III band represents to COO^- anions
1241.1	1242.4*	SO_3 group
1076.1	**1072.7**	Phosphate group of glycoprotein
631.0	**617.2**	

The "-" denotes no peaks were detected, **Bolded** values denotes major shift in the peak and "*****" denotes minor shift in the peaks as compared to control.

5H.9 Scanning electron microscopic (SEM) analysis

In scanning electron microscopic analysis, dense, aggregated, swelled and irregular surface mycelia of *T. lixii* CR700 were observed under the presence of 100 mgL^{-1} of $Ni_{(II)}$ (Fig. 5.36b, c) that is different from control treatment which was cylindrical with smooth surface mycelia (Fig. 5.36a). These morphological responses of *T. lixii* CR700 was also found under the presence of Cr(VI), a sign of tolerance and removal mechanism of Cr(VI) (**see section 5F.3**). Fungi possess many types of morphological responses when coming under the stress condition such as heavy metal, organic pollutants, pesticides, drought and other stress conditions. These responses are the basically tolerance mechanisms of the fungi that deal with stress condition and provide the tolerance ability to fungi to adopt in the adverse conditions. $Ni_{(II)}$ is the toxic metal that can affect the growth and its removal efficiency of fungi. Dense and aggregated mycelia of *P. chrysosporium* and *Hypocrea lixii* was reported under the presence of Ni (Pakshirajan et al., 2013). Swell and aggregated mycelia of *Aspergillus* sp. was reported in the presence of As (Cánovas et al., 2003). They found that mycelium swelling is basically due to As-thiol compound vacuolar compartmentation. In another report, it was found that *Phanerochaete chrysosporium* produces extracellular polymeric substances in the presence of Ni (Cao et al., 2018) that possibly lead mycelial aggregation and helpful to protect the cell from the toxicity of the $Ni_{(II)}$ via adsorption on its surface and impaired the way of introduction of Ni inside the cell. In the present study, dense/aggregated, comparatively, swell and irregular surface mycelia are the tolerance mechanisms of *T. lixii* CR700 and vacuolar

compartmentation of $Ni_{(II)}$ inside the cell of *T. lixii* CR700 (Cánovas et al., 2003; Cao et al., 2018).

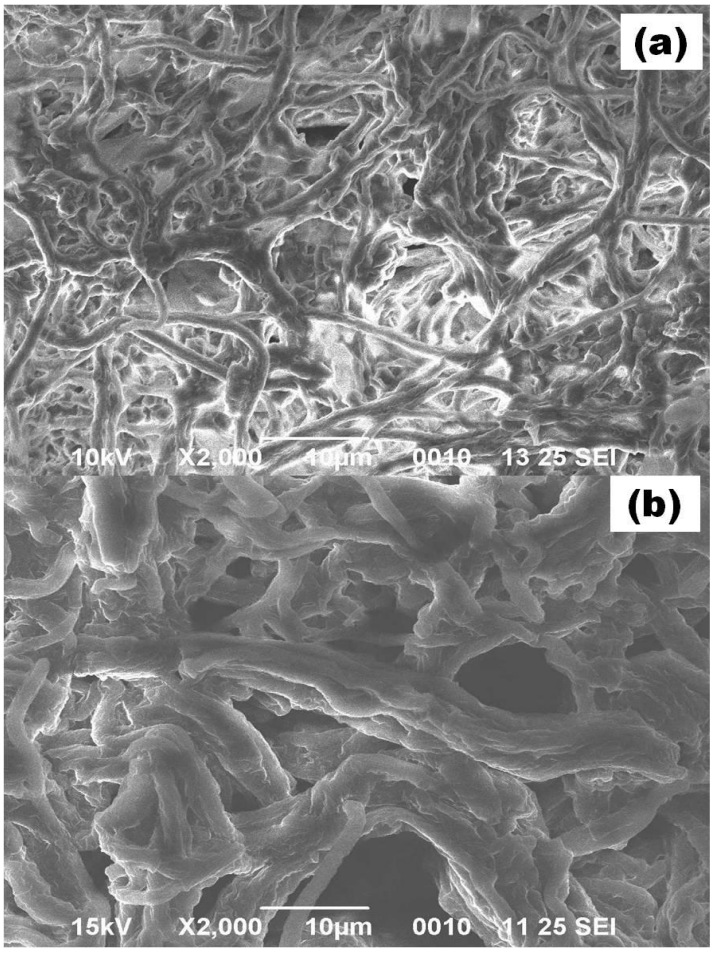

Fig. 5.36. Scanning electron microscopic image of *T. lixii* CR700 biomass grown in control and 100 mg/L of $Ni_{(II)}$ amended potato dextrose broth medium.

5H.10 Ecotoxicological assessment

Results of the phytotoxicity test on *Vigna radiata* confirmed that the toxicity of 100 mgL^{-1} of $Ni_{(II)}$ solution was reduced after getting treated with *T. ixii* CR700. The roots and shoots length of *V. radiata* in fungal-treated (f-treated) $Ni_{(II)}$ was 1.48 ± 0.25 and 4.94 ± 1.05 cm respectively which was higher than without fungal-treated Ni (0.44 ± 0.19 and 1.32 ± 0.13 cm respectively) but lower than control (4.96 ± 1.15 and 9.12 ± 1.92 cm respectively) (Table 5.5). These results showed that *T. lixii* not only removed Ni(II) from the solution but also biotransform from toxic to non/less-toxic (Chen et al., 2019). However, growth of *V. radiata* was higher in control than the fungal treated $Ni_{(II)}$ solution which might be due to remaining concentration of $Ni_{(II)}$ in

solution (at 100 mgL^{-1}), the removal percentage of $Ni_{(II)}$ was not recorded to 100% (Das and Sarkar, 2018). Seed germination rate of *V. radiata* was 100% for control and f-treated $Ni_{(II)}$. These results are also the agreement that *T. lixii* CR700 has the ability to reduce the toxicity of $Ni_{(II)}$ via accumulation, adsorption and biotransformation mechanisms.

Table 5.5. Phytotoxicity assay of fungal treated and without fungal treated 100 mgL^{-1} of Ni(II) solution on *Vigana radiata* seeds in terms of seed germination rate and shoot and root length.

Types of Treatment	Shoot Length (cm)	Root Length (cm)	Germination rate (%)
Control	9.12 ± 1.92	4.96 ± 1.15	100.0 ± 0.0
Without treated $Ni_{(II)}$	1.32 ± 0.13	0.44 ± 0.19	80.0 ± 10.0
Fungal Treated $Ni_{(II)}$	4.94 ± 1.05	1.48 ± 0.25	100.0 ± 0.0

The values are mean of three replicates ± Standard deviation.

5I. Multiple metal removal from Simmulated wastewaster (SWW) by *A. flavus* CR500

5I.1 Metal Removal from SWW

Increase in the metal concentration in SWW from 5 to 20 mg/L of mixture of each metal the biomass production was reduced by 22% (Fig. 5.37). However, efficient metal removal potential of *A. flavus* CR500 was also recorded in SWW (Fig. 5.37). *A. flavus* CR500 could remove 97.5% of As followed by 93.3, 82.2, 46.6% of Pb, Cr, and Ni from SWW containing 5 mg/L of each metal respectively. By increase in the metal concentration from 5-20 mg/L in the SWW, the removal percentage of As, Ni, and Cr significantly decreased which was similar as decreased in metal removal from single metal exposure (Fig. 5.37). However, a significant increase (93.3-95.1%) in the Pb removal was recorded (Fig. 5.37). Similar to our results, an increase in removal of Cu from three metal combinations than individual Cu was reported in *Trichoderma atroviride* (Errasquın and Vázquez, 2003). While the decrease in the removal of As, Cr and Ni was similar to the observation of Açikel and Alp (2009). The authors observed that due to antagonistic nature, the removal of Cu and Ni was decreased with increase in the multimetal concentration in comparison to single metal by *Rhizopus delemar*. In this work, the removal of metal from SWW was low as compared to the individual metal which might be due to competition that occur between metal ions for the adsorption on the surface functional groups as found in FTIR investigation (Gola et al., 2016). Another possible explanation might be the multimetal toxicity to the cell of the fungi, as discussed above that Pb increases the level of H_2O_2 and MDA content and similar phenomenon was recorded in the presence of Cr (**see section 5E.4**). That's why simultaneous presence of these metal may resultant into multimetal toxicity for CR500 and decreases the metabolic activity, biomass production (22.3%; Fig. 5.37) as well as metal removal rate. Moore et al. (2008) reported the inhibitory effect of Ni and Cu causes a decrease in the production of biomass.

5I.2 Effect of pH on Growth and multimetal removal from SWW

The biomass production of fungus was negatively affected by the change in the pH of the medium (Fig. 5.38). At neutral pH (7.0) of SWW, the obtained biomass

was 6.2 g/L and with an increase in the pH to 9.0, the obtained biomass was reduced to 4.2 g/L (Fig. 5.38). Similarly, with decrease in the pH to 5.0, the obtained biomass was 4.1 g/L. The results revealed that with influence in the pH of the medium, biomass production was negatively affected. *A. flavus* CR500 could remove 83-94.8% of As, 80-93% of Pb, 53-75% of Cr and 24-43.6% of Ni at different pH (5.0-9.0) from SWW containing 10 mg/L of each metal while optimum pH was 7.0 (Fig. 5.38). The lower pH (5.0) highly reduces the metal removal ability of *A. flavus* CR500 than higher pH (9.0) (Fig. 5.38). At lower pH, the association between hydronium ion and fungal cell wall may causes positive charge on the surface of the fungi and create repulsive forces between metal ions and fungal cell wall (Khalid et al., 2011). A similar trend of effect of pH was reported for *Beauveria bassiana* and *Metarhizium anisopliaein* in the removal of Cd, Pb, Ni, Cr, Zn and Cu from the single as well as multimetal contaminated medium (Khalid et al., 2011; Gola et al., 2016). However, higher pH (8.0), increased the level of hydroxyl anions cause negative charge on the surface of fungal biomass and may favour the maximum removal of metal via electrostatic attraction between negatively charged cell surface and positively charged metal ions (Rawat et al., 2020; Kumar et al., 2019). In the present study, it was found that metal removal was mainly occurred due to accumulation while change in the pH of the SWW, biomass production was reduced which results into decrease in the metal removal (Gola et al., 2016).

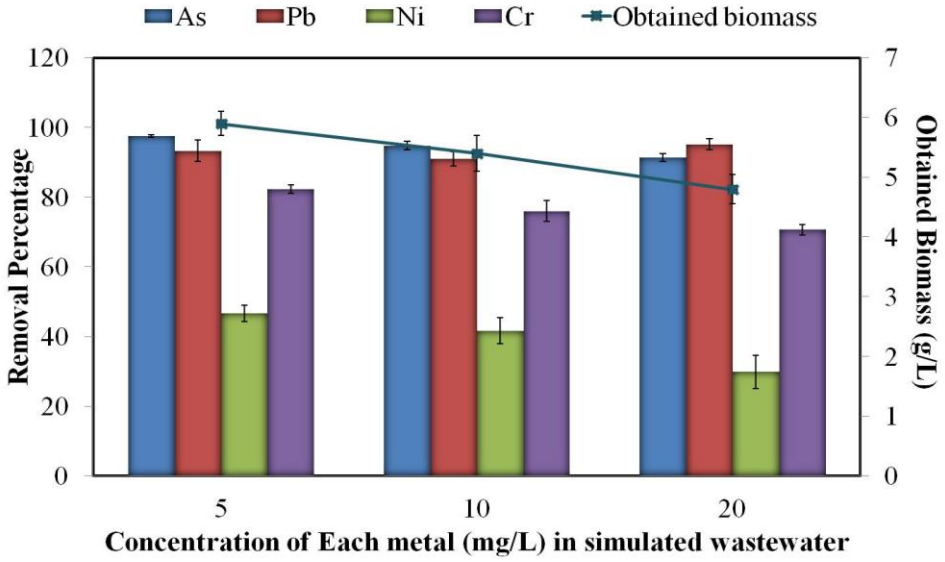

Fig. 5.37. Metal removal by *A. flavus* CR500 from different metal contaminated simulated wastewater at different concentration.

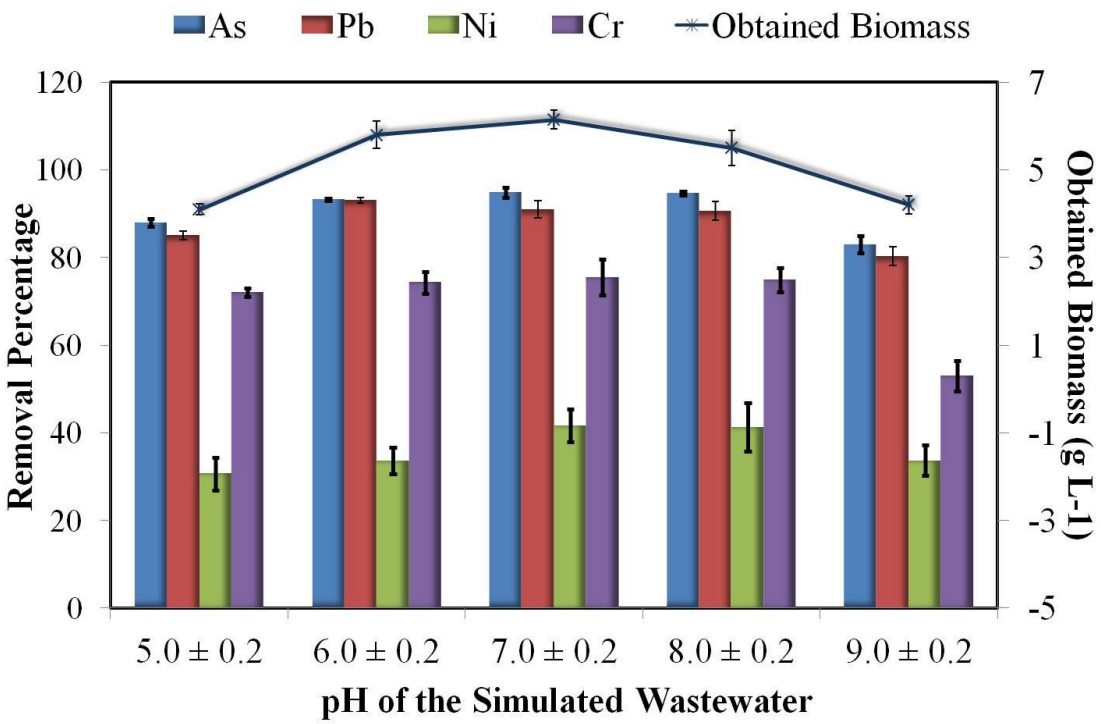

Fig. 5.38. Effect of pH on multiple metal removal efficiency of Heavy metal by fungus *A. flavus* CR500.

5I.3 Growth and multimetal removal in TWW

The physicochemical characteristics of the tannery wastewater are listed in Table 5.6. In without metal and PDB supplemented TWW, no growth of CR500 was observed and after supplementation of TWW with PDB and metal the growth of the CR500 was 2.73 g/L which was comparatively higher than growth in SWW. Slow growth of *A. flavus* CR500 in TWW might be due to presence of different types of other recalcitrant organic compounds as found in a study in TWW collected from the same site (Bharagava et al., 2018). The similar result was recorded in the biomass production of *A. lentulus* in undiluted and growth medium supplemented electroplating effluents (Mishra and Malik, 2012). CR500 showed efficient removal potential from diluted TWW in a ratio of 1:2 and supplemented with metal and PDB and could remove 76.8% of externally added Pb followed by 61.2, 58.2 and 38.6% of externally added Cr, As, Ni respectively and the obtained biomass was 3.7 g/L which was 70% higher than undiluted TWW (Fig. 5.39). At the dilution in the ratio of 1:4 of TWW, the obtained biomass was increased by 32% as compared to 1:2 diluted TWW and this much increase in the biomass led to significant increase in the metal removal rate (Fig. 5.39). Mishra and Malik (2012) investigated the removal capability *A.*

lentulus in electroplating effluents with supplementation of growth medium glucose and Yeast extract, maximum removal was recorded for Cr and Pb. The results of the present study revealed that due to complexity and toxicity of undiluted TWW (Bharagava et al., 2018), the growth of the fungus was inhibited while after the dilution of TWW in the ratio of 1:2 and 1:4 the toxicity of TWW was decreased that favoured the fungus growth and its metal removal efficiency.

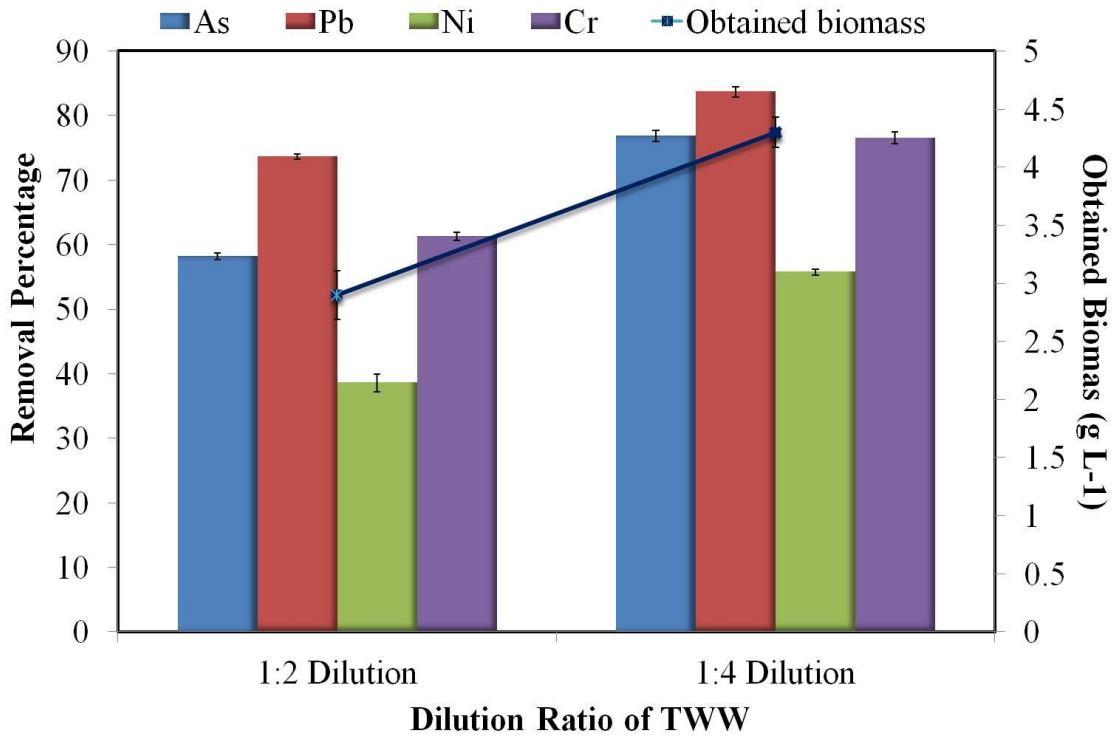

Fig. 5.39. Growth and Multiple metal removal effieciecny of *A. flavus* CR500 from real tannery wastewater (TWW).

Table 5.6. Physicochemical characteristics of tannery wastewater (TWW).

S. N.	Physicochemical Parameters	Recorded values*
1	pH	8.49 ± 0.012
2	Electrical Conductivity (mS cm^{-1})	21.60 ± 0.03
3	BOD (mg L^{-1})	860.00 ± 5.65
4	COD (mg L^{-1})	1730.0 ± 6.12
5	Total Solid (mg L^{-1})	5631.65 ± 8.13
6	Cr (mg L^{-1})	18.84 ± 0.09
7	Cd(mg L^{-1})	0.43 ± 0.002
8	Cu (mg L^{-1})	0.76 ± 0.02
9	Ni (mg L^{-1})	0.10 ± 0.002

10	Pb (mg L^{-1})	0.63 ± 0.002
11	As (mg L^{-1})	0.11 ± 0.007

*The values are mean of tow replicates ± standard deviation.

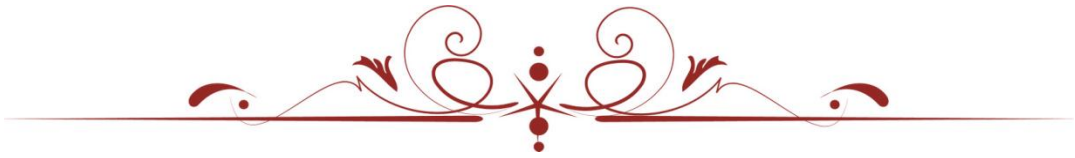

Chapter-6

Summary

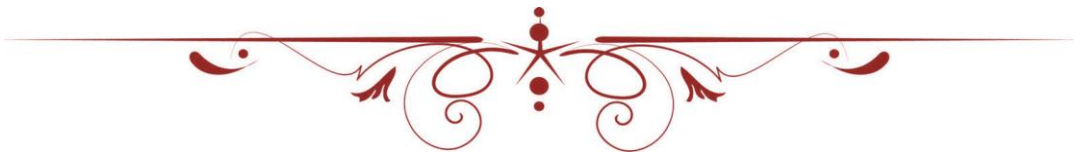

Chapter-6 Summary

Heavy metal pollution has magnetized the public concern due to negative consequences on human health and the environment. $Cr_{(VI)}$ and $Ni_{(II)}$ are two heavy metals have serious issues. These both metals are generated from different types of industrial and commercial activities such as electroplating, tannery, mining, paper-pulp, paint and pigment, etc. and discharged into the natural water bodies with their generating effluents without proper treatment. Discharged $Cr_{(VI)}$ and $Ni_{(II)}$ containing effluents disrupt the aquatic life by making number of alteration in their metabolic and physiological processes and get accumulated inside them as well as in plants too. Discharged effluents also contaminate the ground water through percolation from the discharged sites. Consumption of contaminated water and food is the way by which human being come in exposure of $Cr_{(VI)}$ and $Ni_{(II)}$. $Cr_{(VI)}$ and $Ni_{(II)}$ are toxic, carcinogenic and mutagenic and causes eye and skin irritation, severe diarrhoea, corrosion of skin and respiratory tract, kidney dysfunction, and probably lung carcinoma in human after coming in exposure via ingestion, inhalation and consumption.

Many physicochemical treatment systems are being used for the remediation of heavy metal contaminated water including $Cr_{(VI)}$ and $Ni_{(II)}$. But, their cost, insufficient treatment potency, generation of huge amount of sludge as a secondary pollutant, high energy and skilled man power requirement are the disadvantages that possess a need of new and advance treatment system for remediation of heavy metal polluted wastewater. Biological treatment system utilizes microbes and plants and can remove the disadvantages of the existing systems and may become more appropriate system for treatment purpose. In this regards many work has been done and several species of microbes and plants have been explored for the treatment perspective. Fungi possess several features such as easy in handle and use, adopted to stress environment such drought, saline, heavy metal, etc. They can be cultivated with low graded material and applied on sites as well engineered treatment systems without making hard efforts. Because, heavy metals are very toxic for living organisms, so only adopted fungi to heavy metal can be applied in the treatment system for the treatment of heavy metal polluted wastewater. The

electroplating wastewater often contains different type of heavy metal such as Cr, Ni, Pb, Cu, Mn, etc. The electroplating wastewater discharged site is contaminated with many metals. The microbes (bacteria and fungi) present in these contaminated sites may highly adopted to heavy metal including $Cr_{(VI)}$ and $Ni_{(II)}$ contaminated environment and may have high potency for reduction and removal of Cr(VI) as well as $Ni_{(II)}$. These heavy metals adopted organism which have the ability for reduction and removal of $Cr_{(VI)}$ and $Ni_{(II)}$ can be alternative for the bioremediation of heavy metal polluted wastewater. However, the tolerance and remediation mechanism of $Cr_{(VI)}$ and $Ni_{(II)}$ also not well explored presently in fungi and this is major gap to resolve for better applicability of fungi in remediation process. Keeping into mind these hypotheses, this work has been performed and some key finding of the entire study after critical evaluation and elucidation of the experimental data are as follows:

6.1. Physicochemical characterization of electroplating wastewater

- The electroplating wastewater was collected from the electroplating industrial area of Faridabad, India. This area is highly dense and clustered with different types of electroplating factories.
- The electroplating wastewater was highly laden with different types of heavy metal (Ni, Cr, Pb and Cu) and other pollutant which are presented in Table 6.1.

Table 6.1. Physicochemical characteristics of electroplating wastewater.

S. N.	Physicochemical Parameters	Recorded values*
1	pH	9.49 ± 0.12
2	Electrical Conductivity (mS/cm)	39.60 ± 3.3
3	BOD (mg/L)	670.00 ± 6.6
4	COD (mg/L)	1130.0 ± 11.12
5	Total Solid (mg/L)	3830.6 ± 13.13
6	Cr (mg/L)	54.84 ± 2.09
7	Cd (mg/L)	2.43 ± 1.20

8	Cu (mg/L)	23.76 ± 0.02
9	Ni (mg/L)	140.21 ± 1.2
10	Pb (mg/L)	0.83 ± 0.04
11	As (mg/L)	0.11 ± 0.02

*Values are mean of three replicates.

6.2. Isolation fungal isolate from electroplating wastewater

- Chromium tolerant fungal isolates were isolated on 50 mg/L of $Cr_{(VI)}$ amended potato dextrose agar plate.
- At 50 mg/L of $Cr_{(VI)}$ amended PDA plate four morphologically distinct microbes were recorded, that were further purified on PDA plate.

6.3. Screening of Heavy metal tolerance of isolated fungi

- First, the isolated fungal species were tested for their tolerance towards different concentration of $Cr_{(VI)}$ only two (isolate A and C) of them were able to grow above 300 mg/L of $Cr_{(VI)}$. That's why only two species were selected for further study (as per the plan of wok).
- Isolate A was able to tolerate 800 mg/L of $Cr_{(VI)}$, while isolate C was able to tolerate 1000 mg/L of $Cr_{(VI)}$.
- Isolate A was renamed as isolate CR500 and isolate C as isolate CR700.
- The metal tolerance ability of both the isolates toward different concentration of some co-occurring metal contaminant was investigated.
- Isolate CR500 able to tolerate As(2000 mg/L), Mn(1600 mg/L), Ni (1600 mg/L), Pb (1200 mg/L), Cr(800 mg/L), Cu (200 mg/L) and Cd (100 mg/L).
- Isolate CR700 showed its tolerance towards As (2000 mg/L), Ni (1500 mg/L), Zn (1200 mg/L), Cu (1200 mg/L), Cr (1000 mg/L), and 100 mg/L of Pb and Cd.

6.4. Molecular Identification of fugal isolates

- For molecular identification, internal transcribed spacer region sequencing was done. For identification, blast tool, NCBI database was used to identify the fungal species using sequenced data.
- Isolate CR500 showed maximum similarities with *Aspergillus flavus* species.

- Isolate CR700 showed maximum similarities with *Trichoderma lixii* species.

6.5. *Aspergillus flvaus* CR500 and $Cr_{(VI)}$: Reduction, removal and biochemical response analysis

- For the reduction of $Cr_{(VI)}$ using *A. flavus* CR500, batch study was conducted and *A. flavus* CR500 showed high efficiency (almost 100%) for the reduction of $Cr_{(VI)}$ up to the concentration of 100 mg/L of $Cr_{(VI)}$. At lower $Cr_{(VI)}$ concentration, removal ability of $Cr_{(VI)}$ was also higher.
- Fungus also showed significant $Cr_{(VI)}$ reduction efficiency in the pH ranges from 6.0 to 8.0, temperature (28-35 °C) and under the presence of co-occurring different salts, anions, cations, metabolic inhibitor and heavy metal (Ni, Pb, Cu, Mn, Cd, As, etc.). The fungus also showed high $Cr_{(VI)}$ reduction efficiency in the Tannery wastewater.
- Intracellular Chromate reductase activity was recorded in the presence of $Cr_{(VI)}$ in *A. flavus* CR500 that played important role in intracellular reduction of $Cr_{(VI)}$ to $Cr_{(III)}$, while reduce form $Cr_{(III)}$ may exported to outside of the cell or accumulated inside the cell. Some amount of $Cr_{(III)}$ was also precipitated as Cr_2O_3 on the surface of cell wall.
- The removal of $Cr_{(VI)}$ happen through reduction, accumulation, adsorption and precipitation mechanism as explored in FTIR, SEM-EDX, XPS and Cr removal and adsorption experimentation.
- SEM results showed that in $Cr_{(VI)}$ exposure fungus showed different types of morphological responses (swelling in mycelia, protrusion less, ruptured, constricted mycelia). The functional group such as COO^{-}, O─H, N─H and C≡C are participated in adsorption of $Cr_{(VI)}$ on the surface of *A. flavus* CR500 evinced from FTIR analysis.
- $Cr_{(VI)}$ induced oxidative stress has been found which might reduce the growth of the fungus at higher concentration of $Cr_{(VI)}$.
- Enzymatic (CAT, SOD, POD, PPO and PAL) and non-enzymatic (total phenolic content, Proline, GSH and non-protein thiol content) antioxidants might play role in alleviation of ROS in *A. flavus* CR500 demonstrated from their increased activity and level under the presence of $Cr_{(VI)}$ in *A. flavus* CR500.

- In the phytoxicity assessment, *Vigna radiata* seeds showed good germination and shoot/root growth in fungal 100 mg/L of $Cr_{(VI)}$ solution as compared to without fungal treated 100 mg/L of $Cr_{(VI)}$ solution confirming the reduction in the toxicity of $Cr_{(VI)}$ solution.

6.6. *Trichoderma lixii* CR700 and $Cr_{(VI)}$: reduction, removal and biochemical response

- In batch study, *T. lixii* CR700 showed 99% reduction of $Cr_{(VI)}$ to $Cr_{(III)}$ up to the concentration of 100 mg/L of $Cr_{(VI)}$.
- *T. lixii* CR700 also showed efficient $Cr_{(VI)}$ reduction capacity in the temperature of 28-35 °C and pH (6.0 to 8.0), under the presence of different heavy metal (Cr, As, Ni, Pb, Cu and Mn), salts, anions and metabolic inhibitor (EDTA) and showed efficient $Cr_{(VI)}$ reduction capability in tannery wastewater.
- Under the presence of hexavalent chromium, the activity of intracellular as well as extracellular chromate reductase enzyme was recorded in *T. lixii* CR700 that possibly involved in reduction of Chromium.
- *T. lixii* CR700 removed $Cr_{(VI)}$ via reduction, accumulation, surface adsorption and precipitation mechanism evinced from different investigation (SEM-EDX, XRD, FTIR, etc.).
- Elevated concentration of $Cr_{(VI)}$ induces ROS production in *T. lixii* CR700 that might be due the toxicity of $Cr_{(VI)}$ to fungus and is the possible cause for the reduction growth and biomass productivity of the fungus.
- At higher concentration of $Cr_{(VI)}$, activity of antioxidants enzyme (CAT, POD and SOD) and the level of non-enzymatic antioxidants (proline, total phenolic content, non-protein thiol content) was increased.
- Reduction in the toxicity of $Cr_{(VI)}$ solution was confirmed from good germination rate and shoot/root growth of *Cicer arietinum* and *Vigna radiata* in *T. lixii* CR700 treated $Cr_{(VI)}$ solution.

6.7. *A. flavus* CR500 and $Ni_{(II)}$: Removal, biochemical and morphological analysis

- *A. flavus* CR500 has high $Ni_{(II)}$ removal potential. The maximum removal (73 %) potential of *A. flavus* CR500 was recorded at lower concentration (10 mg/L) of $Ni_{(II)}$.
- *A. flavus* also exhibited removal efficiency under the presence of different salts, anions, metabolic inhibitor and co-occurring heavy metal contaminant of electroplating wastewater.
- SEM analysis revealed that morphology of the mycelia of *A. flavus* CR500 was changed from protrusion full, straight and cylindrical to protrusion less and swollen mycelia that might be due to toxicity response of fungi or due to accumulation of $Ni_{(II)}$ inside the cell of the fungus that results into swollen mycelia.
- FTIR study suggested the involvement of surface functional group in adsorption of $Ni_{(II)}$ ion the surface of fungal mycelia. However, removal $Ni_{(II)}$ is mostly driven by accumulation of $Ni_{(II)}$ inside the cell of the fungus as observed from determination of accumulation and adsorption study.
- Due to toxicity, $Ni_{(II)}$ induced ROS production was recorded that possibly reduces the growth of the fungus at elevated concentration.
- Increased SOD, CAT, POD activity and level of total phenolic content and proline was recorded in *A. flavus* CR500 in the response of $Ni_{(II)}$ that possibly reduces the effect of ROS and maintain the cellular homeostasis.
- *Vigna radiata* seeds showed high germination rate and shoot and root growth in fungal (*A. flavus* CR500) treated $Ni_{(II)}$ solution compared to without fungal treated solution in phytotoxicty test.

6.8. *T. lixii* CR700 and $NI_{(II)}$: Biochemical, morphological and $Ni_{(II)}$ removal investigation

- *T. lixii* CR700 has potential for effective removal of $Ni_{(II)}$. It has been investigated under the different stress condition and was able to remove $Ni_{(II)}$ under the presence of other co-occurring pollutants such heavy metal, mono and bi-anions and salts. The removal efficiency of *T. lixii* CR700 was high at low concentration of $Ni_{(II)}$ and was 64 % at 10 mg/L of $Ni_{(II)}$.

- The removal happen via surface adsorption and accumulation mechanism, confirmed from metal accumulation and surface sorption investigation. The electrostatic attraction and hydrogen bond were the major mechanism of the surface functional group such as COO, OH, NH, etc. that played role in adsorption of $Ni_{(II)}$ onto the mycelia surface of the fungus.
- $Ni_{(II)}$ stress induces the ROS production that possibly diminished the fungal growth via causing oxidative damages. Increased CAT and POD activity and level of total phenolic content and proline may be participated in ROS reduction.
- In SEM investigation, it was found that mycelia surface of *T. lixii* CR700 after $Ni_{(II)}$ exposure swelled and enhanced than unexposed mycelia of *T. lixii* CR700 that might indicated the $Ni_{(II)}$ adsorption on the surface of mycelia as well as production extracellular polymeric substances.
- The toxicity of fungal treated $Ni_{(II)}$ solution was reduced as confirmed from high germination rate and growth of shoot/root in *T. lixii* CR700 treated $Ni_{(II)}$ as compared to untreated $Ni_{(II)}$ solution.

6.9. Multiple metal removal by *A. flavus* CR500 from simulated wastewater (SWW)

- The multiple removal ability of *A. flavus* CR500 was investigated in batch study. *A. flavus* CR500 was able to remove 97.5% of As followed by 93.3, 82.2, 46.6% of Pb, Cr, and Ni from SWW containing 5 mg/L of each metal respectively. Increasing metal concentration up to 20 mg/L of each in SWW significantly reduces the biomass and metal removal potential of *A. flavus* CR500.

- The pH of the medium was also optimized for multiple metal removal from SWW using 5 mg/L of each metal. *A. flavus* CR500 exhibited high metal removal efficiency at pH 7.0.
- The removal of efficiency of *A. flavus* CR500 was also investigated in real tannery wastewater to assess its applicability for real wastewater treatment. *A. flavus* could remove 76.8% of externally added Pb followed by 61.2, 58.2 and

38.6% of externally added Cr, As, Ni respectively from diluted tannery wastewater (in ratio of 1:2; v:v) and amended with PDB.

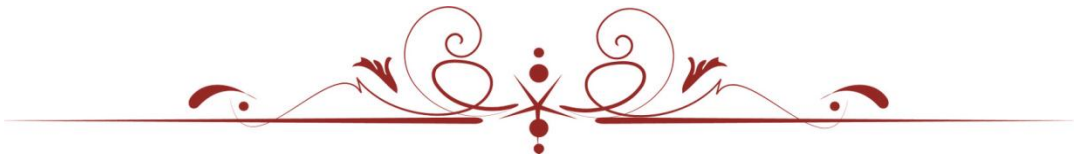

Chapter-7

Conclusion

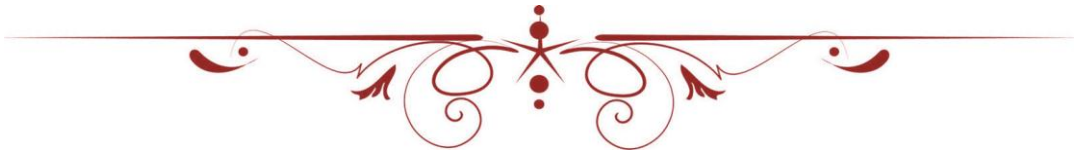

Chapter-7 Conclusion

In this study, four morphologically distinct fungal isolate was isolated from electroplating wastewater. Two of them showed high tolerance potential towards heavy metal including $Cr_{(VI)}$ and $Ni_{(II)}$ and were identified as *Aspergillus flavus* CR500 and *Trichoderma lixii* CR700 based on ITS region sequencing. Both of the isolates showed high efficiency (99 %) in reduction of $Cr_{(VI)}$ up to the concentration of 100 mg/L of $Cr_{(VI)}$ and also showed high $Ni_{(II)}$ removal potential. The proficient $Cr_{(VI)}$ reduction and $Ni_{(II)}$ removal ability was also recorded in the pH ranges from 6.0 to 8.0, temperature 28-35 °C and under the presence of co-contaminant such as salts, mono and bidentate anions, cations, metabolic inhibitor and in the presence different heavy metal (Pb, Cu, Ni, Mn, As etc.) even both the isolate showed distinct $Cr_{(VI)}$ reduction efficiency in real tannery wastewater. *A. flavus* CR500 also exhibited multiple metal removal efficiency from simulated as well as real tannery wastewater which can be exploited for treatment of multiple-metal contaminated wastewater. In the removal process both fungi uses enzyme catalyzed reduction (for $Cr_{(VI)}$), accumulation, precipitation and surface sorption mechanism in remediation of $Cr_{(VI)}$ and $Ni_{(II)}$ contaminated water. In fungi, $Cr_{(VI)}$ and $Ni_{(II)}$ induced oxidative stress diminished by enzymatic (CAT, POD and SOD) and non-enzymatic antioxidants (proline, GSH, phenolic content). While, fungal treated $Cr_{(VI)}$ and $Ni_{(II)}$ solution showed no/less toxicity as compared to their pure solution, observed from good germination rate and growth of plant seeds (*Vigna radiata*). Therefore, both can become possible candidates for the treatment of $Cr_{(VI)}$ and $Ni_{(II)}$ contaminated wastewater in ecofriendly, safe and economical way. However, all the data recorded in this study are from the experiments that were run in controlled condition. So, the field experiment data may differ from the results obtained in this study. While, to get better reduction and removal efficiency with *A. flavus* CR500 and *T. lixii* CR700 for $Cr_{(VI)}$ and $Ni_{(II)}$ from wastewater, the reduction and removal ability of the fungi should be analyzed with used growth medium, applied wastewater and experimental conditions should be optimized before large scale application of both isolates.

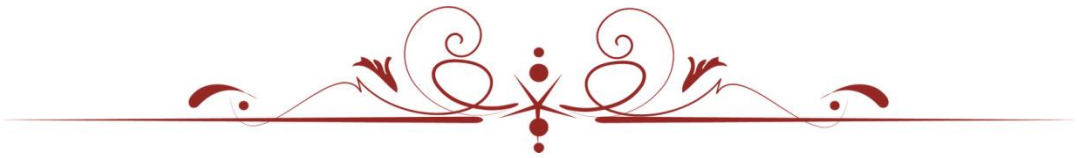

References

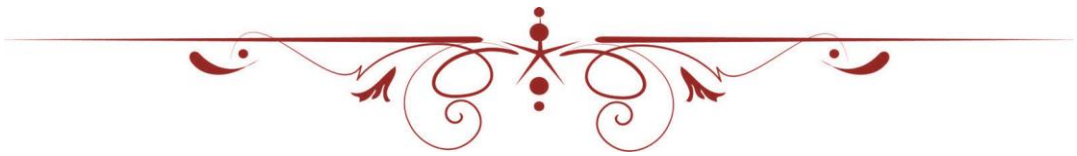

References

Abbasi, P., McKevitt, B., Dreisinger, D. B. 2018. The kinetics of nickel recovery from ferrous containing solutions using an Iminodiacetic acid ion exchange resin. Hydrometallurgy 175, 333-339.

ABC (American Biogenics Corporation), 1998. Ninety day gavage study in albino rats using nickel. Final report submitted to U.S. Environmental Protection Agency, Office of Solid Waste. Study 410-2520. Submitted by Research Triangle Institute and Ameri -can Biogenics Corporation, NY.

Abdullahi, T., Harun, Z., Othman, M. H. D. 2017. A review on sustainable synthesis of zeolite from kaolinite resources via hydrothermal process. Advanced Powder Technology 28(8), 1827-1840.

Abigail, E.A., Samuel, M.S., Chidambvaram, R., 2014. Hexavalent chromium Biosorption studies using *Penicillium griseofulvum* MSR1 a novel isolate from tannery effluent site: Box Behnken optimization, equilibrium, kinetics and thermodynamic studies. J. Taiwan Inst. Chem. Eng. 49, 156–164. https://doi.org/10.1016/j.jtice.2014.11.026

Acevedo-Aguilar, F.J., Espino-Saldana, A.E., Leon-Rodriguez, I.L., Rivera-Cano, M.E., vila-Rodriguez, M., Wrobel, K., Lappe, P., Ulloa, M., Gutierrez-Corona, J.F., 2006. Hexavalent chromium removal in vitro and from industrial wastes, using chromate-resistant strains of filamentous fungi indigenous to contaminated wastes. Can. J. Microbiol. 52 (9), 809 –815.

Açıkel, Ü., Alp, T. 2009. A study on the inhibition kinetics of bioaccumulation of Cu (II) and Ni (II) ions using *Rhizopus delemar*. Journal of hazardous materials 168(2-3), 1449-1458.

Adebiyi, Adeyinka, K., 2017. Bioremediation of Heavy Metals in the Soil by *Pseudomonas aeruginosa* and *Trichoderma harzianum* Using *Solanum lycopersicum* as Test Plant. Adeyinka. AJSSPN, 2(2), 1-13. DOI:10.9734/AJSSPN/2017/36868

Adeli, M., Yamini, Y., Faraji, M. 2017. Removal of copper, nickel and zinc by sodium dodecyl sulphate coated magnetite nanoparticles from water and wastewater samples. Arabian Journal of Chemistry 10, S514-S521.

Adriaensen, K., Vangronsveld, J., and Colpaert, J.V., 2006. Zinc-tolerant *Suillus bovinus* improves growth of Zn-exposed *Pinus sylvestris* seedlings. Mycorriza 16(8), 553-558. doi: 10.1007/s00572-006-0072-7

Aftab, K., Akhtar, K., Jabbar, A., 2014. Batch and column study for Pb-II remediation from industrial effluents using glutaraldehyde–alginate–fungi biocomposites. Ecological Engineering 73, 319–325.

Ahmad, M.S.A., Hussain, M., Ijaz, S., Alvi, A.K., 2008. Photosynthetic performance of two mung bean (*Vigna radiata*) cultivars under lead and copper stress. Int. J. Agri. Biol. 10, 167-172.

Ajayan, K. V., Harilal, C. C., Selvaraju, M. 2018. Phycoremediation resultant lipid production and antioxidant changes in green microalgae Chlorella Sp. International journal of phytoremediation 20(11): 1144-1151.

Ajayan, K.V., Selvaraju, M., Unnikannan, P., Sruthi, P. 2015. Phycoremediation of Tannery Wastewater Using Microalgae *Scenedesmus* Species. International Journal of Phytoremediation 17(10): 907-916. DOI: 10.1080/15226514.2014.989313.

Ajmal, M., Rao, R.A., Ahmad, R., Ahmad, J., Rao, L.A. 2001. Removal and recovery of heavy metals from electroplating wastewater by using Kyanite as an adsorbent. J. Hazard. Mater. 87(1-3), 127-137. https://doi.org/10.1016/S0304-3894(01)00234-5

Akar T., Celik S., Ari A.G., Akar, S.T. 2012. Nickel removal characteristics of an immobilized macro fungus: equilibrium, kinetic and mechanism analysis of the biosorption. J. Chem. Technol. Biotechnol. 88(4), 680-689. https://doi.org/10.1002/jctb.3886.

Akbal, F., Camcı, S., 2011. Copper, chromium and nickel removal from metal plating wastewater by electrocoagulation. Desalination 269(1-3), 214-222.

Algarra, M., Jiménez, M.V., Rodríguez-Castellón, E., Jiménez-López, A., Jiménez-Jiménez, J., 2005. Heavy metals removal from electroplating wastewater by aminopropyl-Si MCM-41. Chemosphere 59(6), 779-786. doi.org/10.1016/j.chemosphere.2004.11.023

Al-Homaidan, A. A., Al-Qahtani, H. S., Al-Ghanayem, A. A., Ameen, F., Ibraheem, I. B. 2018. Potential use of green algae as a biosorbent for hexavalent chromium removal from aqueous solutions. Saudi journal of biological sciences 25(8): 1733-1738.

Ali, Z., Malik, R., Shinwari, Z. Qadir, A., 2015. Enrichment, risk assessment, and statistical apportionment of heavy metals in tannery-affected areas. Int. J. Environ. Sc. Technol. 12 (2), 537-550.

Alimohammadi, M., Saeedi, Z., Akbarpour, B., Rasoulzadeh, H., Yetilmezsoy, K., Al-Ghouti, M.A., Khraisheh, M., McKay, G., 2017. Adsorptive removal of arsenic and mercury from aqueous solutions by eucalyptus leaves. Water, Air, & Soil Pollution. 228, 429. https://doi.org/10.1007/s11270-017-3607-y.

Al-Qodah Z (2006) Biosorption of heavy metal ions from aqueous solutions by activated sludge. *Desalination*, *196*(1-3), 164-176.

Al-Qodah, Z., Al-Shannag, M. 2017. Heavy metal ions removal from wastewater using electrocoagulation processes: a comprehensive review. Separation Science and Technology 52(17): 2649-2676.

Amin, F., Talpur, F. N., Balouch, A., Chandio, Z. A., Surhio, M. A., Afridi, H. I., 2016. Biosorption of mercury (II) from aqueous solution by fungal biomass *Pleurotus eryngii*: isotherm, kinetic, and thermodynamic studies. Environmental Progress & Sustainable Energy 35(5), 1274-1282.

An, Q., Jiang, Y. Q., Nan, H. Y., Yu, Y., Jiang, J. N. 2019. Unraveling sorption of nickel from aqueous solution by KMnO4 and KOH-modified peanut shell biochar: Implicit mechanism. Chemosphere 214: 846-854.

Andrewes, P., Cullen, W.R., Polishchuk, E., Reimer, K.J., 2001. Antimony biomethylation by the wood rotting fungus *Phaeolus schweinitzii*. Applied organometallic chemistry 15(6), 473-480.

Angelin, J.A., Jones, R.S., Das, S.S.M. 2015. Investigation of acute toxicity and the effect of chrome plating industry effluent on behavior of the guppy (Poecilia reticulata). European Journal of Biotechnology and Bioscience. 1-5.

Anjum, S.A., Farooq, M., Xie, X.Y., Liu, X.J., Ljaz, M.F., 2012. Antioxidant defense system and proline accumulation enables hot pepper to perform better

under drought. Sci. Hortic. 140, 66–73. https://doi.org/10.1016/j.scienta.2012.03.028

Ao, W., Fu, J., Mao, X., Kang, Q., Ran, C., Liu, Y., ... Dai, J. 2018. Microwave assisted preparation of activated carbon from biomass: A review. Renewable and Sustainable Energy Reviews 92: 958-979.

APHA., 1992. Standard method for the examination of water and waste water. American public health association. 8th ed. Washington: American Water Works Association and Water Environment Federation 981.

Appenroth, K.J. 2010. Definition of "Heavy Metals" and Their Role in Biological Systems. In: Soil Heavy Metals. Soil Biology, vol 19. Springer, Berlin, Heidelberg. https://doi.org/10.1007/978-3-642-02436-8_2

Arán, D. S., Harguinteguy, C. A., Fernandez-Cirelli, A., Pignata, M. L. 2017. Phytoextraction of Pb, Cr, Ni, and Zn using the aquatic plant *Limnobium laevigatum* and its potential use in the treatment of wastewater. Environmental Science and Pollution Research 24(22): 18295-18308.

Arévalo-Rangel, D. L., Cárdenas-González, J. F., Martínez-Juárez, V. M., Acosta-Rodríguez, I. 2013. Hexavalent Chromate Reductase Activity in Cell Free Extracts of *Penicillium* sp. Bioinorganic chemistry and applications, 2013.

Ashraf, M., Foolad, M., 2007. Roles of glycine betaine and proline in improving plant abiotic stress resistance. Environ. Exp. Bot. 59(2), 206–216. doi.org/10.1016/j.envexpbot.2005.12.006

Awasthi, A. K., Pandey, A. K., Khan, J., 2017. Potential of fungus *Trichoderma harzianum* for toxicity reduction in municipal solid waste leachate. International Journal of Environmental Science and Technology 14(9), 2015-2022. https://doi.org/10.1007/s13762-017-1271-9.

Ayangbenro, A. S., Babalola, O. O. 2017. A New Strategy for Heavy Metal Polluted Environments: A Review of Microbial Biosorbents. Int. J. Environ. Res. Public Health 14(1), 94. doi:10.3390/ijerph14010094

Azevedo, M. M., Carvalho, A., Pascoal, C., Rodrigues, F., Cássio, F. 2007. Responses of antioxidant defenses to Cu and Zn stress in two aquatic fungi. Science of the total environment 377(2-3), 233-243.

Babu, D. J., Kalyani, G., Rao, H. J., Kumar, Y. P., King, P., 2012. Biosorption characteristics of lead onto bentonite clay, as low-cost natural biosorbent. Int. J. Sci. Eng. Res. 3, 1–6.

Bachofen R (1990) Microorganisms in nuclear waste disposal. Part I. *Experientia*, *46*(8), 777-851.

Baerlocher C., McCusker L.B., Olson D.H. 2007. Atlas of Zeolite Framework Types, 944 Elsevier.

Bai, Y.-N., Lu, Y.-Z., Shen, N., Lau, T.-C., Zeng, R.J., 2018. Investigation of Cr(VI) reduction potential and mechanism by *Caldicellulosiruptor saccharolyticus* under glucose fermentation Condition. J. Hazard. Mater. 344, 585–592. doi.org/10.1016/j.jhazmat.2017.10.059

Bakti, F., Sasse, C., Heinekamp, T., Pócsi, I., Braus, G. H., 2018. Heavy metal-induced expression of PcaA provides cadmium tolerance to *Aspergillus fumigatus* and supports its virulence in the *Galleria mellonella* model. Frontiers in microbiology 9, 744.

Balabaskaran, S., Tilakavati, K., Das, V.K. 1987. Studies on the phytotoxic effects of some organotin (IV) compounds on the germination of the mung bean seed, Phaseolus aureus. Appl Organometal Chem 1(4):347-353. DOI: 10.1002/aoc.590010408

Baldrian, P., 2003. Interactions of heavy metals with white-rot fungi. Enzyme Microb. Technol. 32, 78–91.

Bandehali, S., Parvizian, F., Moghadassi, A. R., Hosseini, S. M., Shen, J. N. 2020. Fabrication of thin film-PEI nanofiltration membrane with promoted separation performances: Cr, Pb and Cu ions removal from water. Journal of Polymer Research 27(4): 1-10.

Banerjee, S., Misra, A ., Chaudhury, S., Dam, B., 2019. A *Bacillus* strain TCL isolated from Jharia coalmine with remarkable stress responses, chromium reduction capability and bioremediation potential. J. Hazard. Mater. 367, 215-223. https://doi.org/10.1016/j.jhazmat.2018.12.038.

Bannister, J. V., Bannister, W. H., Rotillo, G., 1987. Aspects of the structure, function, and applications of superoxide dismutase. Crit. Rev. Biochem. 22(2), 111-80.

Bano A, Hussain J, Akbar A, Mehmood K, Anwar M, Hasni MS ... Ali I (2018) Biosorption of heavy metals by obligate halophilic fungi. Chemosphere, 199, 218-222.

Barakat, M.A., 2011. "New trends in removing heavy metals from industrial waste water." Arab. J. Chem. 4(4), 361–377. https://doi.org/10.1016/j.arabjc.2010.07.019

Barrera-Díaz, C. E., Lugo-Lugo, V., Bilyeu, B. 2012. A review of chemical, electrochemical and biological methods for aqueous Cr (VI) reduction. Journal of hazardous materials 223, 1-12.

Barrera-Díaz, C. E., Lugo-Lugo, V., Bilyeu, B. 2012. A review of chemical, electrochemical and biological methods for aqueous Cr (VI) reduction. Journal of hazardous materials 223, 1-12.

Basaran, G., Kavak, D., Dizge, N., Asci, Y., Solener, M., Ozbey, B. 2016. Comparative study of the removal of nickel (II) and chromium (VI) heavy metals from metal plating wastewater by two nanofiltration membranes. Desalination and Water Treatment 57(46): 21870-21880.

Basta, A.H., Fierro, V., El-Saied, H., Celzard, A., 2009. 2-Steps KOH activation of rice straw: an efficient method for preparing high-performance activated carbons. Bioresour. Technol. 100 (17): 3941e3947.

Bazrafshan, E., Zarei, A. A., Mostafapour, F. K., 2015. Biosorption of cadmium from aqueous solutions by *Trichoderma* fungus: kinetic, thermodynamic, and equilibrium study. Desalination and Water Treatment, 14598-14608. DOI: 10.1080/19443994.2015.1065764.

Beheshti, H., Irani, M., Hosseini, L., Rahimi, A., Aliabadi, M. 2016. Removal of Cr (VI) from aqueous solutions using chitosan/MWCNT/Fe3O4 composite nanofibers-batch and column studies. Chemical Engineering Journal 284, 557-564.

Bellion A, Baudoin JP, Alvarez C, Bornens M, Métin C (2005) Nucleokinesis in tangentially migrating neurons comprises two alternating phases: forward migration of the Golgi/centrosome associated with centrosome splitting and myosin contraction at the rear. *Journal of Neuroscience*, *25*(24), 5691-5699.

Bellion, M., Courbot, M., Jacob, C., and Blaudez, C.M. 2006. Extracellular and cellular mechanisms sustaining metal tolerance in ectomycorrhizal fungi-a mini review. FEMS Microbiol. Lett. 254:173–181.

Bello, A. O., Tawabini, B. S., Khalil, A. B., Boland, C. R., Saleh, T. A. 2018. Phytoremediation of cadmium-, lead-and nickel-contaminated water by Phragmites australis in hydroponic systems. Ecological engineering 120: 126-133.

Bennett, R. M., Cordero, P.R.F., Bautista, G.S., Dedeles, G.R., 2013. Reduction of hexavalent chromium using fungi and bacteria isolated from contaminated soil and water samples. Chem. Ecol. 29(4), 320-328. DOI:10.1080/02757540.2013.770478

Bentley SD, Chater KF, Cerdeño-Tárraga AM, Challis GL, Thomson NR, James KD, ... Bateman A (2002) Complete genome sequence of the model actinomycete Streptomyces coelicolor A3 (2). *Nature*, *417*(6885), 141-147.

Berger, L.R. R., Stamford, T.C.M., Oliveira K.A.R., Pessoa, A.M.P., Lima M.A.B., Pintado, M.M.E., Camara, M.P.S., Franco, L.O., Magnani, M., Souza, E.L., 2018. Chitosan produced from Mucorales fungi using agroindustrial by-products and its efficacy to inhibit *Colletotrichum* species. Int. J. Biolog. Macromol. 108, 635-641. https://doi.org/10.1016/j.ijbiomac.2017.11.178

Bhainsa, K.C., Syed, K., Yadav, J.S., 2014. Factors Alleviating Cadmium Toxicity in White Rot Fungus. J. Bioremediat. Biodegrad. S18: 005. https://doi.org/10.4172/2155-6199.s18-005.

Bhanoori, M., Venkateswerlu, G., 2000. In vivo chitin-cadmium complexation in cell wall of *Neurospora crassa*. Biochim. Biophys. Acta 1;1523(1), 21-8.

Bharagava, R. N., Saxena, G., Mulla, S. I., Patel, D. K. 2018. Characterization and identification of recalcitrant organic pollutants (ROPs) in tannery wastewater

and its phytotoxicity evaluation for environmental safety. Archives of environmental contamination and toxicology 75(2), 259-272.

Bhateria, R., Dhaka, R. 2017. Impact of electroplating effluent on growth of Triticum aestivum and Hordeum vulgare. Environ Technol Innovat 8:389-398. https://doi.org/10.1016/j.eti.2017.09.005

Bhatia, N.P., Walsh, K. B., Baker, A. J. M., 2005. Detection and quantification of ligands involved in nickel detoxification in a herbaceous Ni hyperaccumulator *Stackhousia tryonii* Bailey. Journal of Experimental Botany 56(415), 1343–1349. https://doi.org/10.1093/jxb/eri135

Bibaj, E., Lysigaki, K., Nolan, J. W., Seyedsalehi, M., Deliyanni, E. A., Mitropoulos, A. C., Kyzas, G. Z. (2019). Activated carbons from banana peels for the removal of nickel ions. International Journal of Environmental Science and Technology 16(2), 667-680.

Binet, M. T., Adams, M. S., Gissi, F., Golding, L. A., Schlekat, C. E., Garman, E. R., ... Stauber, J. L. 2018. Toxicity of nickel to tropical freshwater and sediment biota: A critical literature review and gap analysis. Environmental toxicology and chemistry 37(2), 293-317.

Bingöl, N. A., Özmal, F., Akın, B. 2017. Phytoremediation and Biosorption Potential of Lythrum salicaria L. for Nickel Removal from Aqueous Solutions. Polish Journal of Environmental Studies 26(6).

Birch, L., Bachofen, R., 1990. Complexing agents from microorganisms. Experientia 46, 827-834.

Bisheh, M. G., Ghorbani, M., Peyravi, M., Jahanshahi, M. 2020. Static and dynamic filtration of nickel and lead ions by adsorptive membrane induced by POP via layer by layer technique. Chemical Engineering Research and Design, 153, 829-838.

Biswas, S., Meikap, B. C., Sen, T. K. 2019. Adsorptive Removal of Aqueous Phase Copper (Cu 2+) and Nickel (Ni 2+) Metal Ions by Synthesized Biochar–Biopolymeric Hybrid Adsorbents and Process Optimization by Response Surface Methodology (RSM). Water, Air, & Soil Pollution 230(8), 197.

Blaudez D, Botton B, Chalot M (2000). Cadmium uptake and subcellular compartmentation in the ectomycorrhizal fungus Paxillus involutus. *Microbiology*, *146*(5), 1109-1117.

Blaudez, D., Chalot, M., 2011. Characterization of the ER-located zinc transporter ZnT1 and identification of a vesicular zinc storage compartment in *Hebeloma cylindrosporum*. Fungal Genet. Biol. 48, 496–503. DOI:10.1016/j.fgb.2010.11.007

Bogusz, A., Nowak, K., Stefaniuk, M., Dobrowolski, R., Oleszczuk, P. 2017. Synthesis of biochar from residues after biogas production with respect to cadmium and nickel removal from wastewater. Journal of Environmental Management 201: 268-276.

Boratyn, G.M., Camacho, C., Cooper, P.S., Coulouris, G., Fong, A., Ma, N., Madden, T.L., Matten, W.T., McGinnis, S.D., Merezhuk, Y., Raytselis, Y., Sayers, E.W., Tao, T., Ye, J., Zaretskaya, I., 2013. BLAST: a more efficient report with usability improvements. Nucleic Acids Res. 41, W29-W33. doi: 10.1093/nar/gkt282

Borgia, V.F., Thatheyus, A.J. 2015. Acute Toxicity of Effluent from Electroplating Industry to the Common Carp, Cyprinus Carpio Linn. International Journal of Research Studies in Zoology 1(1):10-14.

Borgia, V.F., Thatheyus, A.J., Murugesan, A.G., Alexander, S.C.P., Geetha, I. 2018. Effects of effluent from electoplating industry on the immune response in the freshwater fish, *Cyprinus carpio*. Fish & shellfish immunology 79, 86-92. https://doi.org/10.1016/j.fsi.2018.05.010

Boriová, K., Cerňanský, S., Matúš, P., Bujdoš, M., Simonovičová, A., 2014. Bioaccumulation and biovolatilization of various elements using filamentous fungus *Scopulariopsis brevicaulis*. Lett. Appl. Microbiol. 59(2), 217-223. doi:10.1111/lam.12266

Borovaya, M., Pirko, Y., Krupodorova, T., Naumenko, A., Blume, Y., Yemets, A., 2015. Biosynthesis of cadmium sulphide quantum dots by using *Pleurotus ostreatus* (Jacq.) P. Kumm. Biotechnology & Biotechnological Equipment, 29(6), 1156-1163. DOI: 10.1080/13102818.2015.1064264.

Bowman, S.M., Free, S.J., 2006. The structure and synthesis of the fungal cell wall. BioEssays 28, 799 –808. DOI:10.1002/bies.20441

Boyd, E.S., Barkay, T., 2012. The mercury resistance operon: from an origin in a geothermal environment to an efficient detoxification machine. Front. Microbiol. 3, 349.

Braud, A., Jezequel, K., Bazot, S., Lebeau, T., 2009. Enhanced phytoextraction an agricultural Cr- and Pb-contaminated soil by bioaugmentation with siderophore-producing bacteria. Chemosphere 74(2), 280-286. 10.1016/j.chemosphere.2008.09.013

Brown, A. J., Budge, S., Kaloriti, D., Tillmann, A., Jacobsen, M. D., Yin, Z., ... Potrykus, J., 2014. Stress adaptation in a pathogenic fungus. Journal of Experimental Biology, 217(1), 144-155. doi: 10.1242/jeb.088930

Bruins, M.R., Kapil, S., Oehme, F.W., 2000. Microbial resistance to metal in the environment, Ecotox. Environ. Safe. 45, 198-207. doi:10.1006/eesa.1999.1860.

Brunetti, P., Zanella, L., De Paolis, A., Di Litta, D., Cecchetti, V., Falasca, G., ... Cardarelli, M., 2015. Cadmium-inducible expression of the ABC-type transporter AtABCC3 increases phytochelatin-mediated cadmium tolerance in Arabidopsis. J. Experiment. Bot. 66(13), 3815-3829.

Bučková, M., Godočíková, J., Polek, B., 2007. Responses in the mycelial growth of *Aspergillus niger* isolates to arsenic contaminated environments and their resistance to exogenic metal stress. Journal of Basic Microbiology 47, 295–300. DOI:10.1002/jobm.200610299

Butler, M. J., and Day, A.W. 1998. Fungal melanins: A review. Can. J. Microbiol. 44(12):1115–1136. https://doi.org/10.1139/w98-119

Butt, M.I., Chauhan, D., Shahnawaz, M., Shehzad, F., Trak, T.H., Sahay, S., Collection, 2017. Isolation and Screening of Fungal Isolates with Potential to Degrade Chromium. Trends in Biosciences 10(42), 8875-8882.

Cai, C., Zhao, M., Yu, Z., Rong, H., Zhang, C. 2019. Utilization of nanomaterials for in-situ remediation of heavy metal (loid) contaminated sediments: a review. Science of the Total Environment 662: 205-217.

Cai, C.X., Xu, J., Deng, N.F., Dong, X.W., Tang, H., Liang, Y., Fan, X.W., Li, Y.Z., 2016. A novel approach of utilization of the fungal conidia biomass to remove heavy metals from the aqueous solution through immobilization. Scientific Reports 6, 36546. DOI: 10.1038/srep36546

Cai, W. F., Geng, D. L., Wang, Y. H. 2016. Assessment of cathode materials for Ni (ii) reduction in microbial electrolysis cells. RSC advances 6(38): 31732-31738.

Canning, W. 1982. The Canning Handbook of Electroplating, 23rd ed., W. Canning & Co. Ltd, Birmingham, UK and Spon, NY, 1982.

Canning, W. 1982. The Canning Handbook of Electroplating, 23rd ed., W. Canning & Co. Ltd, Birmingham, UK and Spon, NY, 1982.

Cánovas, D., Mukhopadhyay, R., Rosen, B.P., De Lorenzo, V., 2003. Arsenate transport and reduction in the hyper-tolerant fungus *Aspergillus* sp. P37. Environ. Microbial. 5(11), 1087-1093. doi:10.1046/j.1462-2920.2003.00508.x

Cao, F., Bourven, I., Guibaud, G., Rene, E. R., Lens, P. N., Pechaud, Y., van Hullebusch, E. D., 2018. Alteration of the characteristics of extracellular polymeric substances (EPS) extracted from the fungus Phanerochaete chrysosporium when exposed to sub-toxic concentrations of nickel (II). International Biodeterioration & Biodegradation 129, 179-188.

Cappellaro, C., Baldermann, C., Rachel, R., Tanner, W., 1994. Mating type-specific cell-cell recognition of *Saccharomyces cerevisiae*: cell wall attachment and active sites of a- and alpha-agglutinin. EMBO J. 13(20), 4737-4744.

Castro-González, I., Rojas-Verde, G., Quintero-Zapata, I., Almaguer-Cantú, V., 2017. A Comparative Study on Removal Efficiency of Cr(VI) in Aqueous Solution by *Fusarium* sp. and *Myrothecium* sp. Water Air Soil Pollut. 228, 301. DOI 10.1007/s11270-017-3476-4

Cecchi, G., Roccotiello, E., Di Piazza, S., Riggi, A., Mariotti, M. G., Zotti, M. 2017. Assessment of Ni accumulation capability by fungi for a possible approach to remove metals from soils and waters. Journal of Environmental Science and Health, Part B 52(3): 166-170.

Çelik, S., Akar, S.T., Solener, M., Akar, T., 2017. Anionically reinforced hydrogel network entrapped fungal cells for retention of cadmium in the contaminated aquatic media. J. Environ. Manage. 204, 583-593. doi: 10.1016/j.jenvman.2017.08.049.

Chakraborty, S., Mukherjee, A., Khuda-Bukhsh, A. R., Das, T.K., 2014. Cadmium-induced oxidative stress tolerance in cadmium resistant *Aspergillus foetidus*: its possible role in cadmium bioremediation. Ecotox. Environ. Safe. 106, 47–53. doi: 10.1016/j.ecoenv.2014.04.007.

Chakraborty, V., Sengupta, S., Chaudhuri, P., Das, P., 2018. Assessment on removal efficiency of chromium by the isolated manglicolous fungi from Indian Sundarban mangrove forest: Removal and optimization using response surface methodology. Environ. Technol. Inno. 10, 335-344. https://doi.org/10.1016/j.eti.2018.04.007

Challacombe, J.F., Hesse, C.N., Bramer, L.M., McCue, L.A., Lipton, M., Purvine, S., ... Kuske, C.R. 2019. Genomes and secretomes of Ascomycota fungi reveal diverse functions in plant biomass decomposition and pathogenesis. BMC genomics 20(1), 976.

Challenger, F., 1945. Biological Methylation Chem. Rev. 36, 315–361.

Chang, L., Zhang, Y., Liu, H., Peng, R., Yu, X., Zhao, Y., Zhang, J. 2020. Migration and identification of mercury species in wet flue gas desulfurization system using temperature programmed decomposition. Journal of Cleaner Production 276, 124211.

Chang, F., Tian, C., Liu, S., Ni, J., 2016. Discrepant hexavalent chromium tolerance and detoxification by two strains of *Trichoderma asperellum* with high homology. Chem. Eng. J. 298(15), 75–81. https://doi.org/10.1016/j.cej.2016.04.023

Chang, J., Shi, Y., Si, G., Yang, Q., Dong, J., Chen, J., 2020. The bioremediation potentials and mercury (II)-resistant mechanisms of a novel fungus *Penicillium* spp. DC-F11 isolated from contaminated soil. Journal of Hazardous Materials 122638.

Chaudhary, E., Sharma, P. 2019. Chromium and cadmium removal from wastewater using duckweed-*Lemna gibba* L. and ultrastructural deformation due to metal toxicity. International journal of phytoremediation 21(3), 279-286.

Chen S.H., Ng S.L., Yuen, L.C., Ting, A.S.Y., 2017. A novel study based on adaptive metal tolerance behavior in fungi and SEM-EDX analysis. J. Hazard. Mater. 15(334),132-141. http://dx.doi.org/10.1016/j.jhazmat.2017.04.004.

Chen, G., Zhou, Y., Zeng, G., Liu, H., Yan, M., Chen, A., Guan, S., Shang, C., Li, H., He, J. 2015. Alteration of culture fluid proteins by cadmium induction in *Phanerochaete chrysosporium*. J. Basic Microbiol. 55, 141–147. https://doi.org/10.1002/jobm.201300398

Chen, S., Yue, Q., Gao, B., Li, Q., Xu, X., Fu, K., 2012. Adsorption of hexavalent chromium from aqueous solution by modified corn stalk: a fixed-bed column study. Bioresour. Technol. 113, 114–120.

Chen, S.H., Cheow, Y.L., Ng, S.L., Ting, A .S.Y., 2019. Mechanisms for metal removal established via electron microscopy and spectroscopy: a case study on metal tolerant fungi *Penicillium simplicissimum*. J. Hazard. Mater. 362, 394 e 402. https://doi.org/10.1016/j.jhazmat.2018.08.077.

Chen, Y., An, D., Sun, S., Gao, J., Qian, L. 2018. Reduction and removal of chromium VI in water by powdered activated carbon. Materials 11(2): 269.

Cheng, W., Ding, C., Wang, X., Wu, Z., Sun, Y., Yu, S., ... Wang, X. 2016. Competitive sorption of As (V) and Cr (VI) on carbonaceous nanofibers. Chemical Engineering Journal 293; 311-318.

Choi, A., Wang, S., Lee, M. 2009. Biosorption of cadmium, copper, and lead ions from aqueous solutions by *Ralstonia* sp. and *Bacillus* sp. isolated from diesel and heavy metal contaminated soil. Geosci. J. 13: 331–341.

Choi, K., Meier, P.G. 2001. Toxicity evaluation of metal plating wastewater employing the Microtox® assay: a comparison with cladocerans and fish. Environmental Toxicology: An International Journal 16(2), 136-141. DOI:10.1002/tox.1017

Choudhary, T.R., Amin, M.N., Quraishi, S.B., et al. 2014. Adsorption, desorption and kinetic study on hexavalent chromium removal from aqueous solution using groundnut shell. Res. J. Eng. Appl. Sci. 3(1), 1–6.

Christoforidis, A.K., Orfanidis, S., Papageorgiou, S.K., Lazaridou, A.N., Favvas, E.P., Mitropoulos, A.C., 2015. Study of Cu(II) removal by *Cystoseira crinitophylla* biomass in batch and continuous flow Biosorption. Chem. Eng. J. 277, 334–340.

Cima, F. 2011. Tin: environmental pollution and health effects. Encyclopedia of Environmental Health. Burlington: Elsevier 351-9.

Çimen, A., Kılıçel, F. Arslan, G. 2014. Removal of chromium ions from waste waters using reverse osmosis AG and SWHR membranes. Russ. J. Phys. Chem. 88**:** 845–850. https://doi.org/10.1134/S0036024414050045

Collins, F., Rozhkovskaya, A., Outram, J. G., Millar, G. J. 2020. A critical review of waste resources, synthesis, and applications for Zeolite LTA. Microporous and Mesoporous Materials 291, 109667.

Coman, V., Robotin, B., Ilea, P. 2013. Nickel recovery/removal from industrial wastes: A review. Resources Conservation and Recycling 73, 229-238.

Coman, V., Robotin, B., Ilea, P. 2013. Nickel recovery/removal from industrial wastes: A review. Resources Conservation and Recycling 73, 229-238.

Congeevaram, S., Dhanarani, S., Park, J., Dexilin, M., Thamaraiselvi, K., 2007. Biosorption of chromium and nickel by heavy metal resistant fungal and bacterial isolates. J. Hazard. Mater. 146: 270–277. DOI:10.1016/j.jhazmat.2006.12.017

Coreno-Alonso A ., Sole A., Diestra E., Esteve I., Gutierrez-Corona J.F., Lopez G.R., Tomasini A. 2014. Mechanisms of interaction of chromium with Aspergillus niger var tubingensis strain Ed8. Bioresour. Technol. 158, 188-192. https://doi.org/10.1016/j.biortech.2014.02.036

Coreño-Alonso, A., Acevedo-Aguilar, F. J., Reyna-López, G. E., Tomasini-Campocosio, A., Fernandez-Perrino, F.J., Wrobel, K., Wrobel, K., Gutiérrez-Corona, J. F., 2009. Cr(VI) reduction by an *Aspergillus tubingensis* strain: role of carboxylic acids and implications for natural attenuation and biotreatment of Cr(VI) contamination. Chemosphere 76, 43–47. doi: 10.1016/j.chemosphere.2009.02.031.

Costa, F., Tavares, T., 2017. Bioremoval of Ni and Cd in the presence of diethylketone by fungi and by bacteria, A comparative study. Int. Biodeteriorat. Biodegrad. 120, 115-123. https://doi.org/10.1016/j.ibiod.2017.02.018

Courbot, M., Diez, L., Ruotolo, R., Chalot, M., Leroy, P., 2004. Cadmium Responsive Thiols in the Ectomycorrhizal Fungus *Paxillus involutus*. App. Environ. Microbiol. 70(12), 7413–7417. DOI: 10.1128/AEM.70.12.7413–7417.2004.

CPCB 2007. Comprehensive Industry Document on Electroplating Industries: Central Pollution Control Board. COINDS 70/2007.

Cui, H., Fu, M., Yu, S., Wang, M.K., 2011. Reduction and removal of Cr (VI) from aqueous solutions using modified byproducts of beer production. J. Hazard. Mater. 186(2-3), 1625-1631. doi: 10.1016/j.jhazmat.2010.12.050

Cui, H., Li, F., Ren, B., Xue, C., Cui, C., Wang, J.-Y., 2018. Biosorption of aquatic Pb^{2+}, Hg^{2+}, and Cd^{2+} using a combined biosorbent—*Aspergillus niger*-Treated Rice Straw. Separation Science and Technol. 53(4), 626-635. DOI: 10.1080/01496395.2017.1412463.

Cui, J., Wang, X., Yuan, Y., Guo, X., Gu, X., Jian, L. 2014. Combined ozone oxidation and biological aerated filter processes for treatment of cyanide containing electroplating wastewater. Chem Eng J 241:184-189. https://doi.org/10.1016/j.cej.2013.09.003

Cunha, M.M.L., Franzen, A.J., Seabra, S. H., Herbst, M. H., Vugman, N. V., Borba, L. P., Souza, W., Rozental, S., 2010. Melanin in *Fonsecaea pedrosoi*: A trap for oxidative radicals. BMC Microbiol 10(1), 1–9. doi: 10.1186/1471-2180-10-80.

Damodaran, D., Balakrishnan, R.M., Shetty, V.K., 2013. The uptake mechanism of Cd(II), Cr(VI), Cu(II), Pb(II), and Zn(II) by mycelia and fruiting bodies of *Galerina vittiformis*, Biomed. Res. Int. 149120. https://doi.org/10.1155/2013/149120.

Dang, C., Yang, Z., Liu, W., Du, P., Cui, F., He, K., 2018. Role of extracellular polymeric substances in biosorption of Pb2+ by a high metal ion tolerant fungal strain *Aspergillus niger* PTN31. Journal of Environmental Chemical Engineering 6(2), 2733-2742.

Daoud, N., Selatnia, A., 2019. Taguchi Optimization Method for Nickel Removal from Aqueous Solutions Using Non-living *Pleurotus mutilus*. Arabian Journal for Science and Engineering, 44(12), 10067-10077. https://doi.org/10.1007/s13369-019-04108-x.

Daraei H., Mittal A., Mittal J., Kamali H., 2013. Optimization of Cr(VI) removal onto biosorbent eggshell membrane: experimental & theoretical approaches. Desalination and Water Treatmen 1307-1315.

Das, D., Chakraborty, A., Santra, S.C., 2017. Characteristics of metabolic changes and antioxidative response in a potential zinc tolerant fungal strain, *Aspergillus terreus*. Proc. Natl Acad. Sci. India Sec. B: Biol. Sci. 87(2), 571-578. DOIhttps://doi.org/10.1007/s40011-015-0639-1

Das, J., Sarkar, P., 2018. Remediation of arsenic in mung bean (*Vigna radiata*) with growth enhancement by unique arsenic-resistant bacterium *Acinetobacter lwoffii*. Science of the Total Environment 624, 1106–1118. doi: 10.1016/j.scitotenv.2017.12.157.

Das, P. K., Das, B. P., Dash, P. 2020. Chromite mining pollution, environmental impact, toxicity and phytoremediation: a review. Environmental Chemistry Letters, 1-13.

Das, P., Barua, S., Sarkar, S., Chatterjee, S. K., Mukherjee, S., Goswami, L., ... Bhattacharya, S. S. 2018. Mechanism of toxicity and transformation of silver nanoparticles: Inclusive assessment in earthworm-microbe-soil-plant system. Geoderma 314, 73-84.

Das, S., Mishra, J., Das, S.K., Pandey, S., Rao, D.S., Chakraborty, A., Sudarshan, M., Das, N., Thatoi, H., 2014. Investigation on mechanism of Cr(VI) reduction and removal by *Bacillus amyloliquefaciens*, a novel chromate tolerant bacterium isolated from chromite mine soil. Chemosphere 96, 112-21. 10.1016/j.chemosphere.2013.08.080

Daylan, B., Ciliz, N., Mammodov, A. 2013. Hazardous process chemical and water consumption reduction through cleaner production application for a zinc electroplating industry in Istanbul. Resour Conser Recy 81:1-7. https://doi.org/10.1016/j.resconrec.2013.09.002

de Almeida, E. A., Miyamoto, S., Bainy, A. C. D., de Medeiros, M. H. G., Di Mascio, P., 2004. Protective effect of phospholipid hydroperoxide glutathione peroxidase (PHGPx) against lipid peroxidation in mussels Perna perna exposed to different metals. Mar. Pollut. Bull. 49, 386-392.

de Oliveira, I.M., Henriques, J.A., Bonatto, D., 2007. Insilico identification of a new group of specific bacterial and fungal nitroreductases like proteins. Biochem. Biophys. Res. Commun. 355, 919–925. Doi.10.1016/j.bbrc.2007.02.049

Delalande, O., Desvaux, H., Godat, E., et al., 2010. Cadmium-glutathione solution structures provide new insights into heavy metal detoxification. FEBS J. 277, 5086–5096. doi: 10.1111/j.1742-4658.2010.07913.x.

Demirbas A. 2009. Agricultural based activated carbons for the removal of dyes from aqueous solutions: a review. J. Hazard. Mater. 167(1-3), 1-9. doi:10.1016/j.jhazmat.2008.12.114

Deng, S., Ting, Y., 2005. Polyethylenimine-Modified Fungal Biomass as a High-Capacity Biosorbent for Cr(VI) Anions: Sorption Capacity and Uptake Mechanisms. Environ. Sci. Technol. 39, 8490-8496. DOI: 10.1021/es050697u

Deng, X., Chai, L., Yang, Z., Tang, C., Wang, Y., Shi, Y., 2013. Bioleaching mechanism of heavy metals in the mixture of contaminated soil and slag by using indigenous *Penicillium chrysogenum* strain F1. J. Hazard. Mater. 248-249, 107–114. https://doi.org/10.1016/j.jhazmat.2012.12.051

Deng, Y., Huang, S., Laird, D. A., Wang, X., Meng, Z. 2019. Adsorption behaviour and mechanisms of cadmium and nickel on rice straw biochars in single-and binary-metal systems. Chemosphere 218, 308-318.

Devi, S.S., Sreenivasulu, Y., Rao, K.V.B., 2017. Protective role of *Trichoderma logibrachiatum* (WT2) on Lead induced oxidative stress in Helianthus annus L. Ind. J. of Exep. Biol., 55, 235-241.

Dey, P., Golaa, D., Mishra, A., Malik, A., Singh, D. K., Patel, N., Bergend, M., Jehmlich, N., 2016. Comparative performance evaluation of multi-metal resistant fungal strains for simultaneous removal of multiple hazardous metals. Journal of Hazardous Materials 318, 679–685. doi: 10.1016/j.jhazmat.2016.07.025.

Dey, S., Paul, A. K. 2012. Optimization of cultural conditions for growth associated chromate reduction by Arthrobacter sp. SUK 1201 isolated from chromite mine overburden. J. Hazard. Mater. 213, 200-206.

Dhal, B., Abhilash, Pandey, B., 2018. Mechanism elucidation and adsorbent characterization for removal of Cr(VI) by native fungal adsorbent. Sustainable Environment Research 28(6), 289-297. https://doi.org/10.1016/j.serj.2018.05.002

Dhal, B., Thatoi, H. N., Das, N. N., Pandey, B. D. 2013. Chemical and microbial remediation of hexavalent chromium from contaminated soil and mining/metallurgical solid waste: a review. Journal of hazardous materials 250, 272-291.

Dhami, N. K., Quirin, M. E. C., Mukherjee, A., 2017. Carbonate biomineralization and heavy metal remediation by calcifying fungi isolated from karstic caves. Ecol. Eng. 103, 106–117. https://doi.org/10.1016/j.ecoleng.2017.03.007

Dhankhar. R., Hooda, A., 2011. Fungal biosorption – an alternative to meet the challenges of heavy metal pollution in aqueous solutions. Environ. Technol. 32(5), 467-491. https://doi.org/10.1080/09593330.2011.572922

Dhar, R. K., Zheng Y., Rubenstone J., Geen A.V. 2004. A rapid colorimetric method for measuring arsenic concentrations in groundwater. Analytica Chimica Acta, 526, 203-209. https://doi.org/10.1016/j.aca.2004.09.045

Díaz-Pérez, C., Cervantes, C., Campos-García, J., Julián-Sánchez, A., & Riveros-Rosas, H. 2007. Phylogenetic analysis of the chromate ion transporter (CHR) superfamily. *The FEBS journal*, *274*(23), 6215-6227.

Dickerson, D.P., Pascholati, S.F., Hagerman, A.E., Butler, L.G., Nicholson, R.L., 1984. Phenylalanine ammonia-lyase and hydroxycinnamate: CoA ligase in maize mesocotyls inoculated with *Helminthos poriummaydis* or *Helminthosporium carbonum*. Physiol. Plant Pathol. 25, 111–123. http://dx.doi.org/10.4236/ajps.2012.32031

Diels, L. S., Roy, V., Taghavi, S., Houdt, R. V., 2009. From industrial sites to environmental applications with Cupriavidus metallidurans. Antonie Van Leeuwenhoek 96(2), 247-258. doi: 10.1007/s10482-009-9361-4.

Dimkpa, C. O., Merten, D., Svatoš, A., Büchel, G., Kothe, E., 2009. Siderophores mediate reduced and increased uptake of cadmium by *Streptomyces tendae* F4 and sunflower (*Helianthus annuus*), respectively. J. Appl. Microbiol. 107, 1687. doi: 10.1111/j.1365-2672.2009.04355.x.

Dixit, R., Malaviya, D., Pandiyan, K., Singh, U. B., Sahu, A., Shukla, R., Singh, B.P., Rai, J.P., Sharma, P.K., Lade, H., 2015. Bioremediation of heavy metals from soil and aquatic environment: an overview of principles and criteria of fundamental processes. Sustainability 7(2), 2189-2212. https://doi.org/10.3390/su7022189

Dönmez, G., Aksu, Z. 2001. Bioaccumulation of copper (II) and nickel (II) by the non-adapted and adapted growing *Candida* sp. *Water Research*, *35*(6), 1425-1434.

dos Santos, C. S. L., Reis, M. H. M., Cardoso, V. L., de Resende, M. M. 2019. Electrodialysis for removal of chromium (VI) from effluent: Analysis of concentrated solution saturation. Journal of Environmental Chemical Engineering 7(5), 103380.

Doyle, F. M., Liu, Z. 2003. The effect of triethylenetetraamine (Trien) on the ion flotation of Cu2+ and Ni2+. Journal of colloid and interface science 258(2), 396-403.

Drewnowska, M., Hanć, A., Barałkiewicz, D., Falandysz, J., 2017. Pickling of chanterelle *Cantharellus cibarius* mushrooms highly reduce cadmium contamination. Environ. Sci. Pollut. Res. 24, 21733–21738.

Dubey, S., Misra, P., Dwivedi, S., Chatterjee, S., Bag, S.K., Mantri, S., et al. 2010. Transcriptomic and 566 metabolomic shifts in rice roots in response to Cr (VI) stress. BMC Genomics 11, 648.

Dubois, M., Gilles, K.A., Hamilton, J.K., Rebers, P.T., Smith, F., 1956. Colorimetric method for determination of sugars and related substances. Anal. Chem. 28, 350-356. https://doi.org/10.1021/ac60111a017

Dzyazko Y.S., Belyakov V.N. 2004. Purification of a diluted nickel solution containing nickel by a process combining ion exchange and electrodialysis. Desalination 162, 179-189.

Eide, D. J., 2006. Zinc transporters and the cellular trafficking of zinc. Biochim. Biophys. Acta 176(3), 711–722. doi: 10.1016/j.bbamcr.2006.03.005

Eisenman, H.C., Casadevall, A., 2012. Synthesis and assembly of fungal melanin. Appl. Microbiol. Biotechnol. 93(3), 931–940. doi: 10.1007/s00253-011-3777-2.

Eisler, R. 1989. Tin Hazards to Fish, Wildlife, and Invertebrates: A Synoptic Review (No. FWS-85/1.15). PATUXENT WILDLIFE RESEARCH CENTER LAUREL MD.

Elabbas, S., Ouazzani, N., Mandi, L., Berrekhis, F., Perdicakis, M., Pontvianne, S., ... Leclerc, J. P. (2016). Treatment of highly concentrated tannery wastewater using electrocoagulation: influence of the quality of aluminium used for the electrode. *Journal of hazardous materials*, *319*, 69-77.

Errasquın, E. L., Vazquez, C. 2003. Tolerance and uptake of heavy metals by Trichoderma atroviride isolated from sludge. Chemosphere 50(1), 137-143.

Ertugay, N., Bayhan, Y. K., 2010. The removal of copper (II) ion by using mushroom biomass (*Agaricus bisporus*) and kinetic modeling. Desalination 255(1–3), 137-142. doi.org/10.1016/j.desal.2010.01.002

Esfahani, R. N., Khaghani, S., Azizi, A., Mortazaeinezhad, F., Gomarian, M. 2020. Facile and eco-friendly synthesis of TiO 2 NPs using extracts of *Verbascum thapsus* plant: an efficient photocatalyst for reduction of Cr (VI) ions in the aqueous solution. Journal of the Iranian Chemical Society 17(1), 205-213.

Faisal, M., Hasnain, S., 2004. Microbial conversion of Cr (VI) in to Cr (III) in industrial effluent. African Journal of Biotechnology 3(11), 610-617.

Fan, Z., Zhang, Q., Gao, B., Li, M., Liu, C., Qiu, Y. 2019. Removal of hexavalent chromium by biochar supported nZVI composite: batch and fixed-bed column evaluations, mechanisms, and secondary contamination prevention. Chemosphere 217, 85-94.

Fang W, Jiang X, Luo H, Geng J. Synthesis of graphene/SiO2@polypyrrole nanocomposites and their application for Cr(VI) removal in aqueous solution. Chemosphere. 2018 Apr;197:594-602. DOI: 10.1016/j.chemosphere.2017.12.163.

Felmy AR, Girvin DC, Jenne EA. 1984. MINTEQ—Un programme informatique pour calculer les équilibres géochimiques aqueux EPA-600/3-84-031 US Environmental Protection Agency, Athens, GA; French

Feng Su, J., Gao, J., lin Huang, T., ming Zhang, Y. 2020. Simultaneous nitrate, nickel ions and phosphorus removal in a bioreactor containing a novel composite material. Bioresource Technology, 123081.

Feng, X., Xu, J., Liang, Y., Chen, G.-L., Fan, X.-W., Li, Y.-Z., 2017. A proteomic-based investigation of potential copper-responsive biomarkers: Proteins, conceptual networks, and metabolic pathways featuring *Penicillium janthinellum* from a heavy metal-polluted ecological niche. MicrobiologyOpen 00:e485. https://doi.org/10.1002/mbo3.485

Fernández, P. M., Cruz, E. L., Viñarta, S. C., De Figueroa, L. I. C. 2017. Optimization of culture conditions for growth associated with Cr (VI) removal by Wickerhamomyces anomalus M10. Bulletin of environmental contamination and toxicology 98(3), 400-406.

Fischer, R.G., Rapsomanikis, S., Andreae, M. O., Baldi, F., 1995. Bioaccumulation of methylmercury and transformation of inorganic mercury by macrofungi. Environmental science & technology 29(4), 993-999.

Flores-Alvarez, L. J., Corrales-Escobosa, A. R., Cortés-Penagos, C., Martínez-Pacheco, M., Wrobel-Zasada, K., Wrobel-Kaczmarczyk, K., ... Gutiérrez-Corona, F., 2012. The *Neurospora crassa* chr-1 gene is up-regulated by chromate and its encoded CHR-1 protein causes chromate sensitivity and chromium accumulation. Current genetics 58(5-6), 281-290.

Fomina, M., Bowen, A. D., Charnock, J. M., Podgorsky, V., Gadd, G. M., 2017. Biogeochemical spatio-temporal transformation of copper in *Aspergillus niger* colonies grown on malachite with different inorganic nitrogen sources. Wiley-Blackwell Soci. App. Microbiol. doi: 10.1111/1462-2920.13664.

Freitas, J.H.E.S., Mahnke, L.C., Alves, M.H.M.E., Santana, K.V., Campos-Takaki, G.M. Nascimento, A.E., 2015. Evaluation of the Potential Biotechnological Removal of the Ion Cd(II) by *Rhizopus arrhizus* UCP 402. Int. J. Curr. Microbiol. App. Sci 4(8), 157-166.

Fu, F., Wang, Q. 2011. "Removal of heavy metal ions from wastewaters: A review." J. Environ. Manage. 92(3), 407–418. https://doi.org/10.1016/j.jenvman.2010.11.011

Gabli, M., Smara, A., Mecibah, W., Djellabi, R. 2020. Intensification of nickel recovery from water using an electrically driven hybrid process: continuous electropermutation. Environmental Technology 41(15), 2003-2012.

Gadd, G. M., 2007. Geomycology: biogeochemical transformations of rocks, minerals, metals and radionuclides by fungi, bioweathering and bioremediation. Mycol. Res. 111, 3–49. DOI:10.1016/j.mycres.2006.12.001

Gaikwad, M. S., Balomajumder, C. 2017. Simultaneous rejection of chromium (VI) and fluoride [Cr (VI) and F] by nanofiltration: Membranes characterizations and estimations of membrane transport parameters by CFSK model. Journal of environmental chemical engineering 5(1), 45-53.

Gaikwad, M. S., Balomajumder, C. 2017. Simultaneous rejection of chromium (VI) and fluoride [Cr (VI) and F] by nanofiltration: Membranes characterizations and estimations of membrane transport parameters by CFSK model. Journal of environmental chemical engineering, 5(1), 45-53.

Gan, M., Li, J., Sun, S., Cao, Y., Zheng, Z., Zhu, J., ... Qiu, G. 2018. The enhanced effect of Acidithiobacillus ferrooxidans on pyrite based Cr (VI) reduction. Chemical Engineering Journal 341, 27-36.

Gao P., Chen X., Shen F., Chen G., 2005. Removal of chromium(VI) from wastewater by combined electrocoagulation–electroflotation without a filter. Separaation Science and Technology. 43(2) 117-123.

Gardea-Torresdey, J. L., Tiemann, K. J., Armendariz, V., Bess-Oberto, L., Chianelli, R. R., Rios, J., Parsons, J.G., Gamez, G., 2000. Characterization of Cr (VI) binding and reduction to Cr (III) by the agricultural by products of Avena monida (Oat) biomass. J. Hazard. Mater. 80(1-3), 175-188.

Gardea-Torresdey, J. L., Tiemann, K. J., Armendariz, V., Bess-Oberto, L., Chianelli, R. R., Rios, J., ... Gamez, G. 2000. Characterization of Cr (VI) binding and reduction to Cr (III) by the agricultural byproducts of *Avena monida* (Oat) biomass. Journal of Hazardous Materials 80(1-3), 175-188.

Gazi, M., Oladipo, A. A., Azalok, K. A. 2018. Highly efficient and magnetically separable palm seed-based biochar for the removal of nickel. Separation Science and Technology 53(7), 1124-1131.

Gebru, K. A., & Das, C. 2018. Removal of chromium (VI) ions from aqueous solutions using amine-impregnated TiO2 nanoparticles modified cellulose acetate membranes. Chemosphere 191, 673-684.

Georgieva, V. G., Gonsalvesh, L., Tavlieva, M. P. 2020. Thermodynamics and kinetics of the removal of nickel (II) ions from aqueous solutions by biochar adsorbent made from agro-waste walnut shells. Journal of Molecular Liquids, 112788.

Ghaedi, M., Hajati, S., Karimi, F., Barazesh, B., Ghezelbash, G., 2013. Equilibrium, kinetic and isotherm of some metal ion Biosorption. J. Ind. Eng. Chem. 19, 987–992.

Gheethi, A. A., Efaq, A. N., Mohamed, R. M., Abdel-Monem, M. O., Hashim, M. A. 2017. Bio-removal of Nickel ions by Sporosarcina pasteurii and Bacillus megaterium, A Comparative Study. In *IOP Conference Series: Materials Science and Engineering* (Vol. 226, No. 1, p. 012044). IOP Publishing.

Ghosh, A., Dastidar, M. G., Sreekrishnan, T. R., 2016. Bioremediation of a chromium complex dye using *Aspergillus flavus* and *Aspergillus tamarii*. Chem. Eng. Technol. 39(9), 1636–1644.

Ghosh, S., Paul, A. K., 2016. Bioleaching of nickel by *Aspergillus humicola* SKP102 isolated from Indian lateritic overburden. J. Sust. Mining 15(3), 108-114.

Gibb, H.J., Lees, P.S., Pinsky, P.F., Rooney, B.C. 2000. Lung cancer among workers in chromium chemical production. Am J Ind Med. 38(2), 115-26. doi: 10.1002/1097-0274(200008)38:2<115::aid-ajim1>3.0.co;2-y.

Giovanella, P., Cabral, L., Bento, F.M., Gianello, C. Camargo, F.A., 2016. Mercury (II) removal by resistant bacterial isolates and mercuric (II) reductase activity in a new strain of *Pseudomonas* sp. B50A. N. Biotechnol. 33, 216-223.

Godet, F., Babut, M., Burnel, D., Veber, A.M., Vasseur, P. 1996. The genotoxicity of iron and chromium in electroplating effluents. Mutat. Res-Gen. Toxicol. 370(1):19-28. https://doi.org/10.1016/S0165-1218(96)90123-8

Godlewska-Zyłkiewicz, B., 2006. Microorganisms in inorganic chemical analysis. Anal. Bioanal. Chem. 384, 114–123.

Gola, D., Kaushik, P., Mishra, A., Malik, A. 2018. Production and shelf life evaluation of three different formulations of Beauveria bassiana in terms of multimetal removal. *Biotechnology Research and Innovation*, *3*(2), 242-251.

Gola, D., Dey, P., Bhattacharya, A., Mishra, A., Malik, A., Namburath, M., Ahammad, S.Z. 2016. Multiple heavy metal removal using an entomopathogenic fungi *Beauveria bassiana*. Bioresour. Technol. 218, 388–396. doi: 10.1016/j.biortech.2016.06.096.

Golovanova, I.L. 2008. Effects of heavy metals on the physiological and biochemical status of fishes and aquatic invertebrates. Inland Water Biol 1(1):93. https://doi.org/10.1007/s12212-008-1014-1

Gonçalves, R.C.R., Lisboa, H.C.F., Pombeiro-Sponchiado, S.R., 2012. Characterization of melanin pigment produced by *Aspergillus nidulans*. World J. Microbiol. Biotechnol. 28(4), 1467–1474. doi: 10.1007/s11274-011-0948-3.

González-Guerrero, M., Benabdellah, K., Valderas, A., Azcón-Aguilar, C., Ferrol, N., 2010. GintABC1 encodes a putative ABC transporter of the MRP subfamily induced by Cu, Cd, and oxidative stress in *Glomus intraradices*. Mycorrhiza 20(2), 137-146.

Gopinath K.P., Madhav N.V., Krishnan A., Malolan R, Rangarajan G. 2020. Present applications of titanium dioxide for the photocatalytic removal of pollutants from water: A review. Journal of Environmental Management 270, 110906.

Goutam, S. P., Saxena, G., Singh, V., Yadav, A. K., Bharagava, R. N., Thapa, K. B. 2018. Green synthesis of TiO2 nanoparticles using leaf extract of Jatropha curcas L. for photocatalytic degradation of tannery wastewater. Chemical Engineering Journal 336, 386-396.

Govarthanan, M., Mythili, R., Selvankumar, T., Kamala-Kannan, S., Kim, H., 2018. Myco-phytoremediation of arsenic-and lead-contaminated soils by *Helianthus annuus* and wood rot fungi, *Trichoderma* sp. isolated from decayed wood. Ecotoxicology and environmental safety 151, 279-284. doi: 10.1016/j.ecoenv.2018.01.020.

GracePavithra, K., Jaikumar, V., Kumar, P. S., SundarRajan, P. 2019. A review on cleaner strategies for chromium industrial wastewater: present research and future perspective. Journal of Cleaner Production 228, 580-593.

Gratao, P.L., Monteiro, C.C., Antunes, A.M., Peres, L.E.P., Azevedo, R.A., 2008. Acquired tolerance of tomato (*Lycopersicon esculentum* cv. Micro-Tom) plants to cadmium-induced stress. Ann. Appl. Biol. 153, 321–333. https://doi.org/10.1111/j.1744-7348.2008.00299.x

Gratão, P.L., Monteiro, C.C., Carvalho, R.F., Tezotto, T., Piotto, F.A., Peres, L.E., Azevedo, R.A., 2012. Biochemical dissection of diageotropica and Never ripe tomato mutants to Cd-stressful conditions. Plant Physiology and Biochemistry, 56, 79-96.

Grill, E., Löffler, S., Winnacker, E.-L., Zenk, M. H., 1989. Phytochelatins, the heavy-metal binding peptides of plants, are synthesized from glutathione by specific γ-glutamylcys-teine dipeptidyl transpeptidase (phytochelatin synthase). Proc. Natl. Acad. Sci. USA 86, 6838–6842.

Gu, Y., Xu, W., Liu, Y., Zeng, G., Huang, J., Tan, X., Jian, H., Hu, X., Li, F., Wang, D., 2015. Mechanism of Cr(VI) reduction by *Aspergillus niger* : enzymatic characteristic, oxidative stress response, and reduction product. Environ. Sci. Pollut. Res. 22, 6271–6279. DOI 10.1007/s11356014-3856-x

Guarín-Romero, J. R., Rodríguez-Estupiñán, P., Giraldo, L., Moreno-Piraján, J. C. 2019. Simple and Competitive Adsorption Study of Nickel (II) and Chromium (III) on the Surface of the Brown Algae Durvillaea antarctica Biomass. ACS omega, 4(19), 18147-18158.

Guimarães, L.H.S., Segura, F.R., Tonani, L., von-Zeska-Kress, M.R., Rodrigues, J.L., Calixto, L. A., ... Batista, B. L., 2019. Arsenic volatilization by *Aspergillus* sp. and *Penicillium* sp. isolated from rice rhizosphere as a promising eco-safe tool for arsenic mitigation. J. Environ. Manage. 237, 170-179.

Gururajan, K., Belur, P. D. 2018. Screening and selection of indigenous metal tolerant fungal isolates for heavy metal removal. Environmental Technology & Innovation 9, 91-99.

Haas, H., Eisendle, M., Turgeon, B.G. 2008. Siderophores in fungal physiology and virulence. *Annu. Rev. Phytopathol.*, *46*, 149-187.

Hackbarth, F.V., Maass, D., de Souza, A.A.U., Vilar, V.J.P., de Souza, S.M.A. 2016. Removal of Hexavalent Chromium from Electroplating Wastewaters using Marine Macroalga *Pelvetia canaliculata* as Natural Electron Donor. Chem. Eng. J. 290, 477-489. https://doi.org/10.1016/j.cej.2016.01.070

Hadad, H. R., de las Mercedes Mufarrege, M., Di Luca, G. A., Maine, M. A. 2018. Long-term study of Cr, Ni, Zn, and P distribution in Typha domingensis growing in a constructed wetland. Environmental Science and Pollution Research 25(18), 18130-18137.

Hajahmadi, Z., Younesi, H., Bahramifar, N., Khakpour, H., Pirzadeh, K., 2015. Multi component isotherm for Biosorption of Zn (II), Co(II) and Cd(II) from ternary mixture on top retreated dried *Aspergillus niger* biomass. Water Resour. Ind. 11, 71–80.

Halliwell B (2006) Reactive species and antioxidants. Redox biology is a fundamental theme of aerobic life. *Plant physiology*, *141*(2), 312-322.

Halliwell, B., Gutteridge, J.M., 1984. Oxygen toxicity, oxygen radicals, transition metals and disease. Biochem. J. 19(1), 1–14. doi: 10.1042/bj2190001

Han, H. X., Shi, C., Zhang, N., Yuan, L., Sheng, G. P. 2018. Visible-light-enhanced Cr (VI) reduction at Pd-decorated silicon nanowire photocathode in photoelectrocatalytic microbial fuel cell. Science of The Total Environment 639, 1512-1519.

Hartmann, L.M., Craig, P.J., Jenkins, R. O., 2003. Influence of arsenic on antimony methylation by the aerobic yeast *Cryptococcus humicolus*. Archives of microbiology 180(5), 347-352.

Haselwandter, K., Häninger, G., Ganzera, M., Haas, H., Nicholson, G., Winkelmann, G. 2013. *Linear fusigen* as the major hydroxamate siderophore of the ectomycorrhizal Basidiomycota *Laccaria laccata* and *Laccaria bicolor*. Biometals 26(6), 969-979.

Hassan, S. H., Koutb, M., Nafady, N. A., Hassan, E. A. 2018. Potentiality of Neopestalotiopsis clavispora ASU1 in biosorption of cadmium and zinc. Chemosphere 202, 750-756.

Hassan, S. H., Koutb, M., Nafady, N. A., Hassan, E. A., 2018. Potentiality of *Neopestalotiopsis clavispora* ASU1 in biosorption of cadmium and zinc. Chemosphere 202, 750-756.

Hassett, R., Kosman, D. J., 1995. Evidence for Cu (II) reduction as a component of copper uptake by *Saccharomyces cerevisiae*. J. Biol. Chem. 270, 128–134. doi: 10.1074/jbc.270.1.128

Hattori, T., Hisamori, H., Suzuki, S., Umezawa, T., Yoshimura, T., Sakai, H., 2015. Rapid copper transfer and precipitation by wood-rotting fungi can effect copper removal from copper sulfate-treated wood blocks during solid-state fungal treatment. Int. Biodeterior. Biodegradation 97, 195-201. https://doi.org/10.1016/j.ibiod.2014.11.011

Have, T. R., and Teunissen, P. J.M., 2001. "Oxidative mechanisms involved in lignin degradation by white-rot fung." Chemical Reviews 101(11), 3397–3413. DOI: 10.1021/cr000115l

Hayat, S., Hayat, Q., Alyemeni, M. N., Wani, A. S., Pichtel, J., Ahmad, A., 2012. Role of proline under changing environments: a review. Plant signaling & behavior, 7(11), 1456-1466.

Haynes, W.M. CRC Handbook of Chemistry and Physics, 95th ed., CRC Press, Taylor and Francis, 2014– 2015.

Heidmann I., Calmano W., 2008. Removal of Zn(II), Cu(II), Ni(II), Ag(I) and Cr(VI) present in aqueous solutions by aluminium electrocoagulation. Journal of Hazardous Materials 152(3), 934-941.

Herath, H.M.L.I., Rajapaksha, A.U., Vithanage, M., Seneviratne, G., 2014. Developed fungal–bacterial biofilms as a novel tool for bioremoval of hexavelant chromium from wastewater. Chem. Ecol. 30(5), 418-427. DOI: 10.1080/02757540.2013.861828

Hernandez, I., Alegre, L., Van, Breusegem, F., Munne-Bosch, S., 2009. How relevant are flavonoids as antioxidants in plants? Trends Plant Sci. 14, 125-132. https://doi.org/10.1016/j.tplants.20 08.12.003

Hernández, I., Alegre, L., Van, Breusegem, F., Munné-Bosch, S., 2009. How relevant are flavonoids as antioxidants in plants? Trends Plant Sci. 14, 125-132. doi: 10.1016/j.tplants.2008.12.003

Hider, R. C., Kong, X., 2010. Chemistry and biology of siderophores. Nat. Prod. Rep. 27, 637-657. doi:10.1039/b906679a.

Hirata, K., Tsuji, N., Miyamoto, K., 2005. Biosynthetic Regulation of Phytochelatins, Heavy Metal-Binding Peptides. J. Biosci. BioEng. 100(6), 593–599. DOI: 10.1263/jbb.100.593

Hložková, K., Matěnová, M., Žáčková, P., Strnad, H., Hršelová, H., Hroudová, M., Kotrba, P., 2016. Characterization of three distinct metallothionein genes of the Ag-hyperaccumulating ectomycorrhizal fungus *Amanita strobiliformis*. Fungal biology 120(3), 358-369.

Holda, A., Mlynarczykowska, A., 2016. Use of dead and living fungal biomass for removal of hexavalent chromium. Physicochem. Probl. Miner. Process 52(2), 551−563. DOI: 10.5277/ppmp160203

Hoogduijn, M. J., Cemeli, E., Anderson, D., Wood, J. M., Thody, A. J., 2003. Melanin protects against Ho-induced DNA strand breaks through its ability to bind Ca. Br. J. Dermatol. 148(4), 867. DOI: 10.1016/j.yexcr.2003.11.007

Hoseinzadeh, S., Shahabivand, S., Aliloo, A. A. 2017. Toxic metals accumulation in Trichoderma asperellum and T. harzianum. Microbiology 86(6), 728-736.

Hossain, M. A., Piyatida, P., da Silva, J. A. T., Fujita, M., 2012. Molecular mechanism of heavy metal toxicity and tolerance in plants: central role of glutathione in detoxification of reactive oxygen species and methylglyoxal and in heavy metal chelation. J. Bot., 872875. doi: 10.1155/2012/872875

Hosseini, S. S., Nazif, A., Shahmirzadi, M. A. A., Ortiz, I. 2017. Fabrication, tuning and optimization of poly (acrilonitryle) nanofiltration membranes for effective nickel and chromium removal from electroplating wastewater. Separation and Purification Technology 187, 46-59.

Howe, R., Evans, R. L., Ketteridge, S. W. 1997. Copper-Binding Proteins in Ectomycorrhizal Fungi. New Phytologist 135(1), 123-131. http://www.jstor.org/stable/2558663

Hu, Y., Zhu, J., Liu, Y. 2017. Removal of chromium (VI) from aqueous solutions by electrochemical reduction–precipitation. International Journal of Electrochemical Science 12, 11387-11396.

Huang B., Gu L., He H., Xu Z., Paan X., 2016. Enhanced biotic and abiotic transformation of Cr(VI) by quinone-reducing bacteria/dissolved organic matters/Fe(III) in anaerobic environment. **Environ. Sci.: Processes 18**, 1185-1192

Huang, C., Lai, C., Xu, P., Zeng, G., Huang, D. et al. 2017. Lead-induced oxidative stress and antioxidant response provide insight into the tolerance of *Phanerochaete chrysosporium* to lead exposure. Chemosphere 187, 70-77. doi: 10.1016/j.chemosphere.2017.08.104.

Huang, W., Nie, X., Dong, F., Ding, C., Huang, R., Qin, Y., Liu, M., Sun, S., 2017. Kinetics and pH dependent uranium bioprecipitation by *Shewanella putrefaciens* under aerobic conditions. J. Radioanal. Nucl. Chem. 312, 531–541. DOI 10.1007/s10967-017-5261-7

Huang, X., Wang, L., Zhu, S., Ho, S.-H., Wu, J., Kalita, P. K., Ma, F., 2018. Unraveling the effects of arbuscular mycorrhizal fungus on uptake, translocation, and distribution of cadmium in *Phragmites australis* (Cav.) Trin. ex Steud. Ecotoxicol. Environ. Safe. 149, 43–50. doi: 10.1016/j.ecoenv.2017.11.011

Huang, Y., Lee, X., Macazo, F. C., Grattieri, M., Cai, R., Minteer, S. D. 2018. Fast and efficient removal of chromium (VI) anionic species by a reusable chitosan-modified multi-walled carbon nanotube composite. Chemical Engineering Journal 339, 259-267.

Huang, Z., Kuang, X., Chen, Z., Fang, Z., Wang, S., Shi, P. 2013. Comparative Studies of Tri- and Hexavalent Chromium Cytotoxicity and Their Effects on Oxidative State of Saccharomyces cerevisiae Cells. Current Microbiology 68, 448-456.

Ilyas, S., Rehman, A., 2015. Oxidative stress, glutathione level and antioxidant response to heavy metals in multi-resistant pathogen, *Candida*

tropicalis. Environmental monitoring and assessment, 187(1), 4115. https://doi.org/10.1007/s10661-014-4115-9.

Ipek, U. 2005. Removal of Ni(II) and Zn(II) from an aqueous solutionby reverse osmosis. Desalination 174, 161-169.

Iram, S., Sumera, A., 2015. Biosorption of Copper and Lead by Heavy Metal Resistant Fungal Isolates. Int. J. of Sci. Res. Pub. 5(1), 1-5.

Irazusta, V., Bernal, A. R., Estévez, M. C., de Figueroa, L. I. 2018. Proteomic and enzymatic response under Cr (VI) overload in yeast isolated from textile-dye industry effluent. Ecotoxicology and environmental safety 148, 490-500.

Irazusta, V., Bernal, A.R., Estévez, M. C., de Figueroa, L. I. C. 2018. Proteomic and enzymatic response under Cr(VI) overload in yeast isolated from textile-dye industry effluent. Ecotoxicol. Environ. Safe. 148, 490–500. http://dx.doi.org/10.1016/j.ecoenv.2017.10.076

Irazusta, V., Cabiscol, E., Reverter-Branchat, G., Ros, J., Tamarit, J., 2006. Manganese is the link between frataxin and iron–sulfur deficiency in the yeast model of Friedreich ataxia. J. Biol. Chem. 281, 12227–12232. DOI:10.1074/jbc.M511649200

Isaza-Pérez, F., Ramírez-Carmona, M., Rendón-Castrillón, L., Ocampo-López, C., 2020. Potential of residual fungal biomass: a review. Environmental Science and Pollution Research 1-13.

Islam, F., Yasmeen, T., Ali, Q., Mubin, M., Ali, S., Arif, M. S., Abbas, F., 2016. Copper-resistant bacteria reduces oxidative stress and uptake of copper in lentil plants: potential for bacterial bioremediation. Environ. Sc. Pol. Res. 23(1), 220-233. doi: 10.1007/s11356-015-5354-1

Jacob, C., Courbot, M., Martin, F., Brun, A., Chalot, M., 2004. Transcriptomic responses to cadmium in the ectomycorrhizal fungus *Paxillus involutus*. FEBS Lett. 576, 423–427. https://doi.org/10.1016/j.febslet.2004.09.028

Jacob, J. M., Sharma, S., Balakrishnan, R.M., 2016. Exploring the fungal protein cadre in the biosynthesis of Pb Sequantum dots. J. Hazard. Mater. 15;324, 54-61. doi: 10.1016/j.jhazmat.2015.12.056

Jacobs, J., Hardison, R. L., Rose, J. V. 2001. In-situ remediation of heavy metals using sulfur-based treatment technologies. Hydrovisions 10(2), 1-4.

Jacobs, J., Hardison, R. L., Rose, J. V. 2001. In-situ remediation of heavy metals using sulfur-based treatment technologies. Hydrovisions 10(2), 1-4.

Jadhav, U., Hong, H., 2014. Use of *Aspergillus niger* 34770 culture supernatant for tin metal removal. Corrosion Science 82, 248–254.

Jamali, M. K., Kazi, T. G., Arain, M. B., Afridi, H. I., Jalbani, N., Menon, A.R., 2007. Heavy metal contents of vegetables grown in soil, irrigated with mixtures of wastewater and sewage sludge in Pakistan, using ultrasonic assisted pseudo-digestion. J. Agron. Crop. Sci. 193(3), 218. https://doi.org/10.1111/j.1439-037X.2007.00261.x

Jensen, L. T., Howard, W. R., Strain, J. J., Winge, D.R., Culotta, V. C., 1996. Enhanced effectiveness of copper ion buffering by CUP1 metallothionein compared with CRS5 metallothionein in *Saccharomyces cerevisiae*. J. Biol. Chem. 271, 18514–18519.

Jigami, Y., Odani, T., 1999. Mannosylphosphate transfer to yeast mannan. Biochim. Biophys. Acta 1426, 335-345.

Jin, X., Jiang, M., Du, J., Chen, Z. 2014. Removal of Cr (VI) from aqueous solution by surfactant-modified kaolinite. Journal of Industrial and Engineering Chemistry 20(5), 3025-3032.

Jobby, R., Jha, P., Yadav, A. K., Desai, N. 2018. Biosorption and biotransformation of hexavalent chromium [Cr (VI)]: a comprehensive review. Chemosphere 207, 255-266.

Jobby, R., Jha, P., Yadav, A. K., Desai, N. 2018. Biosorption and biotransformation of hexavalent chromium [Cr (VI)]: a comprehensive review. Chemosphere 207, 255-266.

Johri, A. K., Oelmüller, R., Dua, M., Yadav, V., Kumar, M., Tuteja, N., ... et al., 2015. Fungal association and utilization of phosphate by plants: success, limitations, and future prospects. Frontiers in microbiology 6, 984. doi: 10.3389/fmicb.2015.00984.

Joshi, B.H., 2014. Evaluation and Characterization of Heavy Metal Resistant Fungi for their Prospects in Bioremediation. J. of Envir. Res. and Dev. 8(4), 876-882.

Kadota, I, Kurita M. 1995. Hyperglycemia and islet cell damage caused by nickel chloride. Metabolism 4, 337–42.

Kadukova, J., Vircikova., 2005. Comparison of differences between copper bioaccumulation and biosorption. Environ. Int. 31, 227-232.

Kaewdoung, B., Sutjaritvorakul. T., Gadd, G.M., Whalley, A.J.S., Sihanonth, P., 2016. Heavy Metal Tolerance and Biotransformation of Toxic Metal Compounds by New Isolates of Wood-Rotting Fungi from Thailand. Geomicrobiol. J. 33(3-4), 283-288. DOI: 10.1080/01490451.2015.1048394

Kafi lzadeh, F., Saberifard, S., 2016. Isolation and identi fi cation of chromium (VI)-Resistant bacteria from Soltan Abad river sediments (Shiraz-Iran) Jundishapur. J. Health Sci. 8, 533-576

Kalita, J., Pradhan, A.K., Shandilya, Z.M., Tanti, B., 2018. Arsenic Stress Responses and Tolerance in Rice: Physiological, Cellular and Molecular Approaches. Rice Science 25(5), 235−249. https://doi.org/10.1016/j.rsci.2018.06.007

Kalyani, P., Lakshmi, B. K. M., Dinesh Reddy, G., Hemalatha, K. P. J. 2018. Green synthesis of silver nanoparticles by using aspergillus fumigatus and their antibacterial activity. International Journal of Current Research in Life Sciences 7(01), 788-791.

Kamaraj, M., Srinivasan, N. R., Assefa, G., Adugna, A. T., Kebede, M. 2020. Facile development of sunlit ZnO nanoparticles-activated carbon hybrid from pernicious weed as an operative nano-adsorbent for removal of methylene blue and chromium from aqueous solution: Extended application in tannery industrial wastewater. Environmental Technology & Innovation 17, 100540.

Kan, S.-H., Sun, B.-Y., Xu, F., Song, Q.-X., Zhang, S.-F., 2015. Biosorption of aquatic copper (II) by mushroom biomass *Pleurotus eryngii*: kinetic and isotherm studies. Water Sci. Technol. 71(2), 383-288. doi: 10.2166/wst.2014.511

Kan, Y., Yue, Q., Li, D., Wu, Y., Gao, B. 2017. Preparation and characterization of activated carbons from waste tea by H3PO4 activation in different atmospheres

for oxytetracycline removal. Journal of the Taiwan Institute of Chemical Engineers 71, 494-500.

Kanai, T., Uzumaki, T., Kawase, Y., 1996. Simulation of airlift bioreactors: steady-state performance of continuous culture processes. Computers & chemical engineering, 20(9), 1089-1099.

Kanaujiya, D., Kumar, V., Dwivedi, S. K., Prasad, G. 2020. Photobiosynthesis of Silver Nanoparticle Using Extract of Aspergillus flavus CR500: Its Characterization, Antifungal Activity and Mechanism Against *Sclerotium rolfsii* and *Rhizoctonia solani*. *Journal of Cluster Science*, 1-10. https://doi.org/10.1007/s10876-019-01709-2.

Kang, C., Wu, P., Li, L., Yu, L., Ruan, B., Gong, B., Zhu, N., 2017. Cr(VI) reduction and Cr (III) immobilization by resting cells of *Pseudomonas aeruginosa* CCTCC AB93066: spectroscopic, microscopic, and mass balance analysis. Environ. Sci. Pollut. R. 24(6), 5949-5963.

Kang, C., Wu, P., Li, Y., Ruan, B., Li, L., Tran, L., Zhu N. & Dang, Z., 2015. Understanding the role of clay minerals in the chromium (VI) bioremoval by *Pseudomonas aeruginosa* CCTCC AB93066 under growth condition: microscopic, spectroscopic and kinetic analysis. World J. Microb. Biotech 31(11), 1765-1779.

Kang, X., Kirui, A., Muszyński, A., Widanage, M. C.D., Chen, A., Azadi, P., Wang, P., Mentink-Vigier, F., Wang, T., 2018. Molecular architecture of fungal cell walls revealed by solid-state NMR. Nature Communications DOI: 10.1038/s41467-018-05199-0

Kannan, A. Upreti, R.K. 2008. Influence of distillery effluent on germination and growth of mung bean (*Vigna radiata*) seeds. J. Hazard. Mater. 153, 609-615. https://doi.org/10.1016/j.jhazmat.2007.09.004

Kantarci, N., Borak, F., Ulgen, K.O., 2005. Bubble column reactors. Proc. Biochem. 40, 2263-2283.

Karigar, C.S., Rao, S.S., 2011. Role of microbial enzymes in the bioremediation of pollutants: a review. Enzyme Res. doi:10.4061/2011/805187

Kariuki, Z., Kiptoo, J., Onyancha, D., 2017. Biosorption studies of lead and copper using rogers mushroom biomass '*Lepiota hystrix*'. South African Journal of chemical engineering 23, 62-70. https://doi.org/10.1016/j.sajce.2017.02.001

Karthik, C., Barathi, S., Pugazhendhi, A., Ramkumar, V. S., Thi, N.B.D., Arulselvi, P. I., 2017. Evaluation of Cr (VI) reduction mechanism and removal by *Cellulosimicrobium funkei* strain AR8, a novel haloalkaliphilic bacterium. J. Hazard. Mater. 333, 42-53. https://doi.org/10.1016/j.jhazmat.2017.03.037

Karunasekera, H., Terziev, N., Daniel, G., 2017. Does copper tolerance provide a competitive advantage for degrading copper treated wood by soft rot fungi? Int. Biodeterior. Biodegradation 117, 105-114. doi.org/10.1016/j.ibiod.2016.12.006

Kathiravan, M.N., Rani, R.K., Karthick, R., Muthukumar, K. 2010. Mass transfer studies on the reduction of Cr(VI) using calcium alginate immobilized *Bacillus* sp. in packed bed reactor. Bioresour. Technol. 101(3), 853-858. https://doi.org/10.1016/j.biortech.2009.08.088

Kaushik, A., Kansal, A., Santosh, Meena, Kumari, S., Kaushik, C.P., 2009. Heavy metal contamination of river Yamuna, Haryana, India: Assessment by Metal Enrichment Factor of the Sediments. J. Hazard. Mater. 164, 265–270. doi: 10.1016/j.jhazmat.2008.08.031

Kerfoot, D.G.E. 2005. Nickel. In: Ullmann's encyclopedia of industrial chemistry. Wiley-VCH Verlag GmbH & Co. KGaA.

Keunen, E., Remans, T., Bohler, S., Vangronsveld, J., Cuypers, A., 2011. Metal-induced oxidative stress and plant mitochondria.Int. J. Mol. Sci.12, 6894–6918. doi: 10.3390/ijms12106894

Khadiga, A. A., Abou-Taleb, Wed, E., Eweda, and Mira, H. I. 2017. Optimization of Chromium and Copper Ions Uptake by *Aspergillus terreus* Strain Using Different Techniques. A.F.S. E. 1(1): doi.org/10.22606/afse.2017.11005

Khadim, H. J., Ammar, S. H., & Ebrahim, S. E. 2019. Biomineralization based remediation of cadmium and nickel contaminated wastewater by ureolytic bacteria isolated from barn horses soil. Environmental Technology & Innovation 14, 100315.

Khajavian, M., Wood, D. A., Hallajsani, A., Majidian, N. 2019. Simultaneous biosorption of nickel and cadmium by the brown algae *Cystoseria indica*

characterized by isotherm and kinetic models. Applied Biological Chemistry 62(1), 1-12.

Khalid, S., Shahid, M., Niazi, N.K., Rafiq, M., Bakhat, H.F., Imran, M., Abbas, T., Bibi, I., Dumat, C., 2017. Arsenic behaviour in soil-plant system: Biogeochemical reactions and chemical speciation influences. In Enhancing Cleanup of Environmental Pollutants; Springer: Berlin, Germany 97–140.

Khelifa A., Aoudj S., Moulay S., Petris-Wery M. D. 2013. A one-step electrochlorination/electroflotation process for the treatment of heavy metals wastewater in presence of EDTA. Chemical Engineering and Processing: Process Intensification 70, 110-116

Khosravi, R., Ehrampoush, M. H., Moussavi, G., Ghaneian, M. T., Barikbin, B., Ebrahimi, A. A., Sharifzadeh, G. 2019. Facile green synthesis of zinc oxide nanoparticles using Thymus vulgaris extract, characterization, and mechanism of chromium photocatalytic reduction. Materials Research Express 6(11), 115093.

Khouja, H. R., Abbà, S., Lacercat-Didie, L., Daghino, S., Doillon, D., et al. 2013. OmZnT1 and OmFET, two metal transporters from the metal-tolerant strain Zn of the ericoid mycorrhizal fungus *Oidiodendron maius*, confer zinc tolerance in yeast. Fungal Genet. Biol. 52, 53-64. https://doi.org/10.1016/j.fgb.2012.11.004

Khullar, S., Sudhakara Reddy, M., 2019. Cadmium and arsenic responses in the ectomycorrhizal fungus *Laccaria bicolor*: glutathione metabolism and its role in metal (loid) homeostasis. Environmental microbiology reports 11(2), 53-61. https://doi.org/10.1111/1758-2229.12712.

Kimbrough, D. E., Cohen, Y., Winer, A. M., Creelman, L., Mabuni, C. 1999. A critical assessment of chromium in the environment. Critical reviews in environmental science and technology 29(1), 1-46.

Kiptoo, J. K., Ngila, J. C., Sawula, G. M. 2004. Speciation studies of nickel and chromium in wastewater from an electroplating plant. Talanta 64(1), 54-59.

Kneer R, Zenk MH (1992) Phytochelatins protect plant enzymes from heavy metal poisoning. *Phytochemistry*, *31*(8), 2663-2667.

Kolesnikov, A. V., Achkasov, M. G., Kandelaki, G. I., Kovalenko, V. S., Kolesnikov, V. A. 2018. Raising the Efficiency of Electroflotation Extraction of Metals in Multicomponent Systems from Aqueous Media. Russian Journal of Applied Chemistry 91(6), 915-919.

Kolesnikov, A.V., Kuznetsov, V.V., Kolesnikov, V.A. *et al.* 2015. The role of surfactants in the electroflotation extraction of copper, nickel, and zinc hydroxides and phosphates. *Theor Found Chem Eng* 49**,** 1–9. https://doi.org/10.1134/S0040579515010042

Kovacec, E., Regvar, M., Elteren, J.T., Arcon, I., Papp, T., Makovec, D., Vogel-Mikus, K., 2017. Biotransformation of copper oxide nanoparticles by the pathogenic fungus *Botrytis cinerea*. Chemosphere 180, 178-185.

Kretschmer, I., Senn, A. M., Meichtry, J. M., Custo, G., Halac, E. B., Dillert, R., ... Litter, M. I. 2019. Photocatalytic reduction of Cr (VI) on hematite nanoparticles in the presence of oxalate and citrate. Applied Catalysis B: Environmental *242*, 218-226.

Krishnan, K. A., Sreejalekshmi, K. G., Baiju, R. S. 2011. Nickel (II) adsorption onto biomass based activated carbon obtained from sugarcane bagasse pith. Bioresource technology, 102(22), 10239-10247.

Krumova, K., Cosa, G. 2016. Overview of reactive oxygen species. in *Singlet Oxygen: Applications in Biosciences and Nanosciences 1*, 1-21.

Kumar V., Singh, S., Singh, G., Dwivedi, S.K., 2019. Exploring the Cadmium Tolerance and Removal capability of a filamentous fungus *Fusarium solani*. Geomicrobiol. J. DOI. 10.1080/1490451.2019.1627443

Kumar, P., Kaur, R., Celestin, D., Kumar, P. 2020. Chromium removal efficiency of plant, microbe and media in experimental VSSF constructed wetlands under monocropped and co-cropped conditions. Environmental Science and Pollution Research 27(2), 2071-2086.

Kumar, R., Bhatia, D., Singh, R., Rani, S., Bishnoi, N.R., 2011. Sorption of heavy metals from electroplating effluent using immobilized biomass *Trichoderma*

viride in a continuous packed-bed column. Int. Biodeter. Biodegradation 65, 1133–1139.

Kumar, S., Stecher, G., Li, M., Knyaz, C., Tamura, K., 2018. MEGA X: Molecular Evolutionary Genetics Analysis across computing platforms. Mol. Biol. Evol. 35:1547-1549.

Kumar, V., & Dwivedi, S. K. (2020). Multimetal tolerant fungus *Aspergillus flavus* CR500 with remarkable stress response, simultaneous multiple metal/loid removal ability and bioremediation potential of wastewater. Environmental Technology & Innovation 20, 101075.

Kumar, V., Singh, S., Singh, G., Dwivedi, S.K., 2019. Exploring the Cadmium Tolerance and Removal Capability of a Filamentous Fungus *Fusarium solani*. Gemicrobiol. J., 36(9), 782-791. https://doi.org/10.1080/01490451.2019.1627443

Kurniati, E., Arfarita, N., Imai, T., Higuchi, T., Kanno, A., Yamamoto, K., Sekine, M., 2014. Potential bioremediation of mercury-contaminated substrate using filamentous fungi isolated from forest soil. J. Environ. Sci. 26, 1223–1231. doi: 10.1016/S1001-0742(13)60592-6

Kurniawan, T. A., Chan, G. Y., Lo, W. H., Babel, S. 2006. Physico–chemical treatment techniques for wastewater laden with heavy metals. Chemical engineering journal 118(1-2), 83-98.

Kurniawan, T. A., Chan, G. Y., Lo, W. H., Babel, S. 2006. Physico–chemical treatment techniques for wastewater laden with heavy metals. Chemical engineering journal 118(1-2), 83-98.

Kurth, C., Kage, H., Nett, M., 2016. Siderophores as molecular tools in medical and environmental applications. Org. Biomol. Chem. DOI: 10.1039/C6OB01400C.

Kushwaha, D., Saha, S., Dutta, S. 2014. Enhanced Biomass Recovery During Phycoremediation of Cr(VI) Using Cyanobacteria and Prospect of Biofuel Production. *Industrial & Engineering Chemistry Research, 53*, 19754-19764.

Kwak, Y.H., Lee, D.S., Kim, H.B., 2003. *Vibrio harveyi* nitroreductase is also a chromate reductase. Appl. Environ. Microbiol. 69, 4390 –4395. doi: 10.1128/AEM.69.8.4390-4395.2003

Labied, R., Benturki, O., Eddine Hamitouche, A. Y., Donnot, A. 2018. Adsorption of hexavalent chromium by activated carbon obtained from a waste lignocellulosic material (*Ziziphus jujuba cores*): Kinetic, equilibrium, and thermodynamic study. Adsorption Science & Technology 36(3-4), 1066-1099.

Lakshmipathiraj, P., Raju, G. B., Basariya, M. R., Parvathy, S., Prabhakar, S. 2008. Removal of Cr (VI) by electrochemical reduction. Separation and Purification Technology 60(1), 96-102.

Langård, S. 1990. One hundred years of chromium and cancer: a review of epidemiological evidence and selected case reports. Am. J. Ind. Med. 17(2), 189-215. doi: 10.1002/ajim.4700170205.

Ledin, M., 2000. Accumulation of metals by microorganisms – processes and importance for soil systems. Earth-Sci. Rev. 51, 1–31. https://doi.org/10.1016/S0012-8252(00)00008-8

Leong, Y. K., Chang, J. S. 2020. Bioremediation of heavy metals using microalgae: Recent advances and mechanisms. Bioresource technology 303, 122886.

Lerch, K., 1980. Copper metallothionein, a copper-binding protein from *Neurospora crassa*. Nature 27;284(5754), 368-70.

Li, J., Du, Z., Zou, C.B., Dai, Z., Du, D., Yan, C., 2018. The mutual restraint effect between the expansion of *Alternanthera philoxeroides* (Mart.) Griseb and cadmium mobility in aquatic environment. Ecotoxicol. Environ. Safe. 148, 237–243. doi: 10.1016/j.ecoenv.2017.10.032

Li, J., Sun, Y., Jiang, X., Chen, B., Zhang, X., 2018. Arbuscular mycorrhizal fungi alleviate arsenic toxicity to *Medicago sativa* by influencing arsenic speciation and partitioning. Ecotoxicology and Environmental safety 157, 235-243.

Li, L., Chen, O.S., Mc, V., Ward, D., Kaplan, J., 2001. CCC1 is a transporter that mediates vacuolar iron storage in yeast. J. Biol. Chem. 276, 29515–29519. doi: 10.1074/jbc.M103944200.

Li, M., Wang, R., Tian, H., Gao, Y. 2018. Transcriptome responses in wheat roots to colonization by the arbuscular mycorrhizal fungus *Rhizophagus irregularis*. Mycorrhiza *28*(8), 747-759.

Li, Q., Csetenyi, L., Paton, G.I., Gadd, G.M., 2015. CaCO3 and SrCO3 bioprecipitation by fungi isolated from calcareous soil. Environ. Microbiol. 17(8), 3082–3097 doi:10.1111/1462-2920.12954

Li, Q., Huang, W., Xiong, C., Zhao, J., 2018. Transcriptome analysis reveals the role of nitric oxide in *Pleurotus eryngii* responses to Cd2+ stress. Chemosphere 201, 294-302.

Li, S., Huang, H., Li, Z., Li, Z., He, Z., Liang, H. 2017. Chromium removal capability and photosynthetic characteristics of Cyperus alternifolius and Coix lacryma-jobi L. in vertical flow constructed wetland treated with hexavalent chromium bearing domestic sewage. Water Science and Technology 76(8), 2203-2212.

Li, T., Zhang, W., Zhai, S., Gao, G., Ding, J., Zhang, W., ... Lv, L. 2018. Efficient removal of nickel (II) from high salinity wastewater by a novel PAA/ZIF-8/PVDF hybrid ultrafiltration membrane. Water research 143, 87-98.

Li, X., Wang, J., Tan, Z., Ma, L., Lu, D., Li, W., Wang, J., 2018. Cd resistant characterization of mutant strain irradiated by carbon-ion beam. J. Hazard. Mater. 353, 1-8. https://doi.org/10.1016/j.jhazmat.2018.03.036

Li, X., Wang, Y., Pan, Y., Yu, H., Zhang, X., Shen, Y., ... Zhang, S. 2017c. Mechanisms of Cd and Cr removal and tolerance by macrofungus Pleurotus ostreatus HAU-2. Journal of hazardous materials 330, 1-8.

Li, X., Wang, Y., Pan, Y., Yu, H., Zhang, X., Shen, Y., Jiao, S., Wu, K., La, G., Yuan, Y., Zhang, S., 2017. Mechanisms of Cd and Cr removal and tolerance by macrofungus *Pleurotus ostreatus* HAU-2. J. Hazard. Mater. 15(330), 1-18. doi: 10.1016/j.jhazmat.2017.01.047

Li, Z., Liu, Y., Wang, B., Lang, Q., Tan, M., Lee, M., ... Zhang, Y. 2020. Insights into the facilitated transport mechanisms of Cr (VI) in ionic liquid-based polymer inclusion membrane-electrodialysis (PIM-ED) process. Chemical Engineering Journal 125324.

Li, Z., Lu, Y., Zhen, R., Szczypka, M., Thiele, D.J., Rea, P.A., 1997. A new pathway for vacuolar cadmium sequestration in *Saccharomyces cerevisiae*; YCF1-catalyzed transport of bis (glutathionato) cadmium. Proceedings of the National

Academy of Sciences of the United States of America 94, 42–47. doi:10.1073/pnas.94.1.42.

Lian, G., Wang, B., Lee, X., Li, L., Liu, T., Lyu, W. 2019. Enhanced removal of hexavalent chromium by engineered biochar composite fabricated from phosphogypsum and distillers grains. Science of the Total Environment 697, 134119.

Liang, X., Csetenyi, L., Gadd, G.M. 2016. Uranium bioprecipitation mediated by yeasts utilizing organic phosphorus substrates. Appl. Microbiol. Biotechnol. 100, 5141–5151. DOI 10.1007/s00253-016-7327-9

Liang, X., Csetenyi, L., Gadd, G.M., 2015. Lead Bioprecipitation by Yeasts Utilizing Organic Phosphorus Substrates. Geomicrobiol. J. 33(3-4), 294-307. DOI:10.1080/01490451.2015.1051639

Liu, J., Zhang, X.H., Tran, H., Wang, D.Q., Zhu, Y.N. 2011. Heavy metal contamination and risk assessment in water, paddy soil, and rice around an electroplating plant. Environ. Sci. Pollut.\ Res. 18(9), 1623. https://doi.org/10.1007/s11356-011-0523-3

Liu, S., Ye, X., He, K., Chen, Y., Hu, Y. 2017a. Simultaneous removal of Ni (II) and fluoride from a real flue gas desulfurization wastewater by electrocoagulation using Fe/C/Al electrode. Journal of Water Reuse and Desalination 7(3), 288-297.

Liu, T., Li, H., Li, Z., Xiano, X., Cheng, L., Deng, L., 2007. Removal of hexavalent chromium by fungal biomass of *Mucor racemosus*: influencing factors and removal mechanisms. World J. Microbiol. Biotechnol. 23, 1685–1693. doi: 10.1007/s11274-007-9416-5

Liu, T.F., Wang, T., Sun, C., Wang, Y.M., 2009. Single and joint toxicity of Cypermethrin and Copper on Chinese cabbage (Pakchoi) seeds. J. Hazard. Mater. 163, 344–348.

Liu, Y., Wang, G., Luo, Q., Li, X., Wang, Z. 2018. The thermodynamics and kinetics for the removal of copper and nickel ions by the zeolite Y synthesized from fly ash. Materials Research Express 6(2), 025001.

Liu, Y., Wang, G., Wang, L., Li, X., Luo, Q., Na, P. 2019. Zeolite P synthesis based on fly ash and its removal of Cu (II) and Ni (II) ions. Chinese Journal of Chemical Engineering 27(2), 341-348.

Liu, Y., Xin, S., Jiang, B. 2018. The enhanced effect of oxalic acid on the electroreduction of Cr (VI) via formation of intermediate Cr (VI)-oxalate complex. *Environmental technology*.

Liu, Z.F., Zeng, G.M., Zhong, H., Yuan, X.Z., Jiang, L.L., Fu, H.Y., ... Zhang, J.C., 2011. Effect of saponins on cell surface properties of *Penicillium simplicissimum*: Performance on adsorption of cadmium (II). Colloids Surf. B Biointerfaces 86(2), 364-369. doi: 10.1016/j.colsurfb.2011.04.021

Loebus, J., Leitenmaier, B., Meissner, D., Braha, B., Krauss, G.-J., Dobritzsch, D., Freisinger, E., 2013. The major function of a metallothionein fro m the aquatic fungus *Heliscus lugdunensis* is cadmium detoxification. Journal of Inorganic Biochemistry 127 : 253-260.

Long, B., Ye, B., Liu, Q., Zhang, S., Ye, J., Zou, L., Shi, J., 2018. Characterization of *Penicillium oxalicum* SL2 isolated from indoor air and its application to the removal of hexavalent chromium. PLoSONE 13(1): e0191484. https://doi.org/10.1371/journal.pone. 0191484

Long, B., Ye, J., Ye, Z., He, J., Luo, Y., Zhao, Y., Shi, J. 2020. Cr (VI) removal by Penicillium oxalicum SL2: Reduction with acidic metabolites and form transformation in the mycelium. Chemosphere 126731.

Lopez-Fernandez, M., Romero-Gonzalez, M., Günther, A., Solari, P.L., Merroun, M.L., 2018. Effect of U(VI) aqueous speciation on the binding of uranium by the cell surface of *Rhodotorula mucilaginosa*, a natural yeast isolate from bentonites. Chemosphere 199, 351-360. doi: 10.1016/j.chemosphere.2018.02.055

Lotlikar, N.P., Damare, S.R., Meena, R.M., Linsy, P., Mascarenhas, B., 2018. Potential of Marine-Derived Fungi to Remove Hexavalent Chromium Pollutant from Culture Broth. Indian J. Microbiol. 58(2), 182–192. https://doi.org/10.1007/s12088-018-0719-z

Loukidou, M. X., Matisa, K. A., Zouboulisa, A. I., Liakopoulou-Kyriakidou, M., 2003. Removal of As (V) from wastewaters by chemically modified fungal biomass. Water Res. 37, 4544–4552. https://doi.org/10.1016/S0043-1354(03)00415-9

Lowry, O.H., Rosebrough, N.J., Farr, A.L., Randall, R.J., 1951. Protein measurement with 600 the foliar phenol reagent. J. Biol. Chem. 193, 265–275.

Lu, H., Wang Y., Wang J. 2015. Recovery of Ni2+ and pure water from electroplating rinse wastewater by an integrated two-stage electrodeionization process. Journal of Cleaner Production 92 (1) 257-266.

Lu, J., Liu, Z., Wu, Z., Liu, W., Yang, C. 2020. Synergistic effects of binary surfactant mixtures in the removal of Cr (VI) from its aqueous solution by foam fractionation. Separation and Purification Technology 237, 116346.

Lu, J., Wang, Z. R., Liu, Y. L., Tang, Q. 2016. Removal of Cr ions from aqueous solution using batch electrocoagulation: Cr removal mechanism and utilization rate of in situ generated metal ions. Process Safety and Environmental Protection 104, 436-443.

Lu, W., Li, J., Sheng, Y., Zhang, X., You, J., Chen, L. 2017. One-pot synthesis of magnetic iron oxide nanoparticle-multiwalled carbon nanotube composites for enhanced removal of Cr (VI) from aqueous solution. Journal of colloid and interface science 505, 1134-1146.

Luna, C., Marcos, A., Rodrigues Vieira, E., Okada, K., Campos-Takaki, G. M., do Nascimento, A. E., 2015. Copper-induced adaptation, oxidative stress and its tolerance in *Aspergillus niger* UCP1261. Electronic journal of biotechnology, 18(6), 418-427. https://doi.org/10.1016/j.ejbt.2015.09.006.

Luo, C., Cao, C., & Jiang, L. (2016). The endosomal sorting complex required for transport (ESCRT) is required for the sensitivity of yeast cells to nickel ions in Saccharomyces cerevisiae. FEMS yeast research, 16(3).

Lynn, S., Shiung, J. N., Gurr, J. R., Jan, K. Y. 1998. Arsenite stimulates poly (ADP-ribosylation) by generation of nitric oxide. Free Radical Biology and Medicine 24(3), 442-449.

Lytras, G., Lytras, C., Argyropoulou, D., Dimopoulos, N., Malavetas, G., Lyberatos, G. 2017. A novel two-phase bioreactor for microbial hexavalent chromium removal from wastewater. Journal of hazardous materials 336, 41-51.

Ma, X., K., ling, Wu, L., Fam, H., 2014. Heavy metal ions affecting the removal of polycyclic aromatic hydrocarbons by fungi with heavy-metal resistance. App. Microbiol. Biotechnol. 98(23), 9817-9827.

Machado, M.D., Soares, E.V., Soares, H.M. 2010a. Removal of heavy metals using a brewer's yeast strain of *Saccharomyces cerevisiae*: Chemical speciation as a tool in the prediction and improving of treatment efficiency of real electroplating effluents. J Hazard Mater 180(1-3), 347-353. https://doi.org/10.1016/j.jhazmat.2010.04.037

Machado, M.D., Soares, H.M., Soares, E.V. 2010b. Removal of chromium, copper, and nickel from an electroplating effluent using a flocculent brewer's yeast strain of *Saccharomyces cerevisiae*. Water Air Soil Pollut 212(1-4), 199-204. https://doi.org/10.1007/s11270-010-0332-1

Machado, R.M., Monteggia, L.O., Arenzon, A., Curia, A.C. 2016. Assessment of the toxicity of wastewater from the metalworking industry treated using a conventional physico-chemical process. Environ Monit Assess 188(6):373. https://doi.org/10.1007/s10661-016-5361-9

Madera-Parra C. A., Peña-Salamanca E. J., Peña M. R., Rousseau D. P. L. Lens P. N. L. 2015. Phytoremediation of Landfill Leachate with *Colocasia esculenta, Gynerum sagittatum* and *Heliconia psittacorum* in Constructed Wetlands, International Journal of Phytoremediation 17:1, 16-24, DOI: 10.1080/15226514.2013.828014

Magyarosy, A., Laidlaw, R.D., Kilaas, R., Echer, C., Clark, D.S., Keasling, J.D., 2002. Nickel accumulation and nickel oxalate precipitation by *Aspergillus niger*. Appl. Microbiol. Biotechnol. 59, 382–388. DOI 10.1007/s00253-002-1020-x

Mahdi, Z., El Hanandeh, A., Yu, Q. J. 2019. Preparation, characterization and application of surface modified biochar from date seed for improved lead, copper, and nickel removal from aqueous solutions. Journal of Environmental Chemical Engineering 7(5), 103379.

Mahdi, Z., Qiming, J. Y., El Hanandeh, A., 2018. Removal of lead (II) from aqueous solution using date seed-derived biochar: batch and column studies. Applied Water Science 8(6), 181.

Mahmoud, Y. A., 2004. Uptake of radionuclides by some fungi. Mycobiology 32(3), 110–114.

Maisa, M., Amin, I., Elaassy, E., Mohamed, G., El-Feky, N.A., Kawady, M. S. T., Abdelsattar, M. S., 2018. Recovery of uranium from low-grade ore using microorganism isolated from uraniferous rock sample. Separat. Sci. Technol. DOI:10.1080/01496395.2018.1437182

Majumdar, S. S., Dasb, S. K., Saha, T., Panda, G. C., Bandyopadhyoy, T., Guha, A. K., 2008. Adsorption behavior of copper ions on *Mucor rouxii* biomass through microscopic and FTIR analysis. Colloids and Surfaces B: Biointerfaces 63, 138–145. doi: 10.1016/j.colsurfb.2007.11.022

Majumder, R., Sheikh, L., Naskar, A., Vineeta, Mukherjee, M., Tripathy, S., 2017. Depletion of Cr(VI) from aqueous solution by heat dried biomass of a newly isolated fungus *Arthrinium malaysianum*: A mechanistic approach. Scientific reports. https://doi.org/10.1038/s41598-017-10160-0

Mala, J.G.S., Sujatha, D., Rose, C., 2015. Inducible chromate reductase exhibiting extracellular activity in Bacillus methylotrophicus for chromium bioremediation. Microbiological research, 170, 235-241.

Malaviya, P., Singh, A. 2016. Bioremediation of chromium solutions and chromium containing wastewaters. Crit. Rev. Microbiol. 607-33. doi: 10.3109/1040841X.2014.974501.

Maneechakr, P., Karnjanakom, S. 2017. Adsorption behaviour of Fe (II) and Cr (VI) on activated carbon: Surface chemistry, isotherm, kinetic and thermodynamic studies. The Journal of Chemical Thermodynamics 106, 104-112.

Manorama, B. A., Sucharita, P. S., Aradhana, B., Kumar, D. N., 2016. Kinetics and Surface studies on Biosorption of Cr (VI) by using dead Fungal Biomass from Chromium Mine Waste, Sukinda, India. Research Journal of Chemistry and Environment 20, 12.

Martín-Lara, M.A., Blázquez, G., Trujillo, M.C., Pérez, A., Calero, M. 2014. New treatment of real electroplating wastewater containing heavy metal ions by adsorption onto olive stone. J Clean Prod 81:120-129. https://doi.org/10.1016/j.jclepro.2014.06.036

Martorell, M.M., Fernández, P.M., Fariña, J.I., C. Figueroa, L.I., 2012. Cr(VI) reduction by cell-free extracts of *Pichia jadinii* and *Pichia anomala* isolated from textile-dye factory effluents. Int. Biodeter. Biodegrad. 71, 80–85. https://doi.org/10.1016/j.ibiod.2012.04.007

Matysik, J., Alia, Bhalu, B., Mohanty, P., 2002. Molecular mechanisms of quenching of reactive oxygen species by proline under stress in plants. Current Science 82(5), 525-532.

Mayer, A.M., Harel, E., Shaul, R.B., 1965. Assay of catechol oxidase: a critical comparison of methods. Phytochemistry 5, 783–789. https://doi.org/10.1016/S0031-9422(00)83660-2

McLean, J., Beveridge, T.J., 2001. Chromate reduction by a pseudomonad isolated from a site contaminated with chromated copper arsenate. Appl. Environ. Microbiol. 67, 1076 –1084. DOI: 10.1128/AEM.67.3.1076-1084.2001

Mehra, R. K., Winge, D.R., 1991. Metal-ion resistance in fungi: molecular mechanisms and their regulated expression. J. Cell Biochem. 45, 30–40. DOI:10.1002/jcb.240450109

Melvin, S.S., Evy A.A.M., Ramalingam, C., 2015. Isotherm Modelling, Kinetic Study and Optimization of Batch Parameters Using Response Surface Methodology for Effective Removal of Cr(VI) Using Fungal Biomass. PLoS ONE, 10(3), 0116884. doi:10.1371/journal.pone.0116884

Merchuk, J.C., Gluz, M. 1991. Bioreactors, air-lift reactors. In: Flickinger MC, Drew SW, (Eds.). Encyclopedia of Bioprocess Technology. John Wiley & Sons, New York, 320-350.

Merroun, M. L., Omar, N. B., Alonso, E., Arias, J. M., GonzÁlez-MuÑoz, M. T., 2001. Silver sorption to *Myxococcus xanthus* biomass. Geomicrobiol. J. 18, 183–192. https://doi.org/10.1080/01490450117323

Mestrot, A., Planer-Friedrich, B., Feldmann, J., 2013. Biovolatilisation: a poorly studied pathway of the arsenic biogeochemical cycle. Environ. Sci. Process Impact 15,1639–1651.

Migahed, F., Abdelrazak, A., Fawzy, G. 2017. Batch and continuous removal of heavy metals from industrial effluents using microbial consortia. *International Journal of Environmental Science and Technology*, *14*(6), 1169-1180.

Migahed, F., Abdelrazak, A., Fawzy, G., 2017. Batch and continuous removal of heavy metals from industrial effluents using microbial consortia. Int. J. Environ. Sci. Technol. 14, 1169–1180. DOI 10.1007/s13762-016-1229-3.

Mirazimi, S. M. J., Abbasalipour, Z., Rashchi, F., 2015. Vanadium removal from LD converter slag using bacteria and fungi. J. Env. Manag. 153, 144-151. https://doi.org/10.1016/j.jenvman.2015.02.008

Mishra, A., Malik, A. 2012. Simultaneous bioaccumulation of multiple metals from electroplating effluent using Aspergillus lentulus. *water research*, *46*(16), 4991-4998.

Miyata, N. et al. 2004. Enzymatic formation of manganese oxides by an Acremonium-like hyphomycete fungus, strain KR21-2. FEMS Microbiol. Ecol. 47, 101–109. DOI: 10.1016/S0168-6496(03)00251-4

Mohammadian, E., Ahari, A.B., Arzanlou, M., Oustan, S., Khazaei, S.H., 2017. Tolerance to heavy metals in filamentous fungi isolated from contaminated mining soils in the Zanjan Province, Iran. Chemosphere 185, 290-296. DOI: 10.1016/j.chemosphere.2017.07.022

Mohanty, S., Ghosh, S., Nayak, S., Das, A.P., 2016. Bioleaching of manganese by *Aspergillus oryzae* isolated from mining deposits. Chemosphere 172, 302-309. doi: 10.1016/j.chemosphere.2016.12.136

Mohd, S., Kushwaha, A. S., Shukla, J., Mandrah, K., Shankar, J., Arjaria, N., ...et al., 2019. Fungal mediated biotransformation reduces toxicity of arsenic to soil dwelling microorganism and plant. Ecotoxicology and environmental safety 176, 108-118. doi: 10.1016/j.ecoenv.2019.03.053.

Mohsenzadeh, Shahrokhi, 2014. Biological removing of Cadmium from contaminated media by fungal biomass of *Trichoderma* species. J. Environ. Health Sci. Eng. 12, 102. doi:10.1186/2052-336X-12-102

Mokhtari, M., Keshtkar, A. R. 2016. Removal of Th (IV), Ni (II) and Fe (II) from aqueous solutions by a novel PAN–TiO 2 nanofiber adsorbent modified with aminopropyltriethoxysilane. Research on Chemical Intermediates *42*(5), 4055-4076.

Mondal, N.K., Samanta, A., Dutta, S., Chattoraj, S., 2017. Optimization of Cr(VI) biosorption onto *Aspergillus niger* using 3-level Box-Behnken design: Equilibrium, kinetic, thermodynamic and regeneration studies. J. Genet. Eng. Biotechnol. 15, 151–160. https://doi.org/10.1016/j.jgeb.2017.01.006

Moore, B.A., Duncan, J.R., Burgess, J.E., 2008. Fungal bioaccumulation of copper, nickel, gold and platinum. Minerals Engineering 21, 55–60. https://doi.org/10.1016/j.mineng.2007.08.005

Moran, L. K., Gutteridge, J. M. C., Quinlan G.-J. 2001. Thiols in cellular redox signaling and control. Curr. Med. Chem. 8, 763–772.

Moreira, M.T., Feijoo, G., Lema, J.M., 2003. Fungal bioreactors: Applications to white-rot fungi. Rev. Environ. Sci. Biotechnol. 2, 247-259.

Mortazavian, S., Saber, A., Hong, J., Bae, J. H., Chun, D., Wong, N., ... Moon, J. 2019. Synthesis, characterization, and kinetic study of activated carbon modified by polysulfide rubber coating for aqueous hexavalent chromium removal. Journal of industrial and engineering chemistry 69; 196-210.

Mostofa, M. G., Hossain, M. A., Siddiqui, M. N., Fujita, M., Tran, L. S. P. 2017. Phenotypical, physiological and biochemical analyses provide insight into selenium-induced phytotoxicity in rice plants. Chemosphere 178, 212-223.

Moukadiri, I., Jaafar, L., Zueco, J., 1999. Identification of two mannoproteins released from cell walls of a *Saccharomyces cerevisiae* mnn1 mnn9 double mutant by reducing agents. J. Bacteriol. 181, 4741-4745.

Moulick, D., Ghosh, D., Santra, S.C., 2016. Evaluation of effectiveness of seed priming with selenium in rice during germination under arsenic stress. Plant Physiology and Biochemistry 109, 571-578. doi: 10.1016/j.plaphy.2016.11.004.

Moussa, I. D. B., Athmouni, K., Chtourou, H., Ayadi, H., Sayadi, S., Dhouib, A. 2018. Phycoremediation potential, physiological, and biochemical response of

Amphora subtropica and Dunaliella sp. to nickel pollution. Journal of Applied Phycology 30(2), 931-941.

MRR. (2017) Electroplating Market: Automotive and Electrical & Electronics End Use Industry Segments Estimated to Hold About 65% of the Total Market Value Share by 2026 End: Global Industry Analysis and Opportunity Assessment, 2016-2026. Future Market Insights. Report ID: 4715257.

Murugavelh, S., Mohanty, K., 2013. Bioreduction of Cr(VI) using live and immobilized Phanerochaete chrysosporium. Desalin. Water Treat. 51, 3482–3488. DOI: 10.1080/19443994.2012.749371

Nadeem, S.G., Fatima, A., Hakim S.T., 2015. Effect of Cadmium Levels on the Growth Curve of *Candida albicans*. World J. Clin. Pharmacol. Microbiol.Toxicol. 1(1), 45-48.

Nayak, A.K., Panda, S.S., Basu, A., Dhal, N. K., 2018. Enhancement of toxic Cr (VI), Fe, and other heavy metals phytoremediation by the synergistic combination of native *Bacillus cereus* strain and *Vetiveria zizanioides* L. Inter. J. Phyto. 20, 682-691. https://doi.org/10.1080/15226514.2017.1413332

Negi, B. B., Sinharoy, A., Pakshirajan, K., 2020. Selenite removal from wastewater using fungal pelleted airlift bioreactor. Environmental Science and Pollution Research 27(1), 992-1003.

Netpae, T., Suckley, S., Phalaraksh, C., 2015. Cadmium tolerance fungi isolated from polluted sites in the Mae Tao creek, Thailand. Adv. Stud. Biol. 7, 29–37.

Neu, T.R., Lawrence, J.R., 2010. Extracellular polymeric substances in microbial biofilms. In: Holst, O., Brennan, P.J., Itzstein, M. (Eds.), Microbial Glycobiology. Academic Press, San Diego, 733–758 (Chapter 37).

Niazi, L., Lashanizadegan, A., Sharififard, H. 2018. Chestnut oak shells activated carbon: Preparation, characterization and application for Cr (VI) removal from dilute aqueous solutions. Journal of cleaner production 185, 554-561.

Nishida, S., Mizuno, T., Obata, H., 2008. Involvement of histidine-rich domain of ZIP family transporter TjZNT1 in metal ion specificity. Plant Physiol. Biochem. 46, 601–606. doi: 10.1016/j.plaphy.2008.02.011.

Noormohamadi, H. R., Fat'hi, M. R., Ghaedi, M., Ghezelbash, G. R. 2019. Potentiality of white-rot fungi in biosorption of nickel and cadmium: Modeling optimization and kinetics study. Chemosphere *216*, 124-130.

Noreen, S., Bhatti, H.N., Nausheen, S., Sadaf, S., Ashfaq, M., 2013. Batch and fixed bed adsorption study for the removal of Drimarine Black CL-B dye from aqueous solution using a lignocellulosic waste: a cost affective adsorbent. Ind. Crops Product. 50, 568–579.

Oladipo, O.G., Awotoye, O.O., Olayinka, A., Bezuidenhout, C.C., Maboeta, M. S., 2018. Heavy metal tolerance traits of filamentous fungi isolated from gold and gemstone mining sites. Braz. J. Microbiol. 49(1), 29-37.

Olubunmi, O. A., Bernard, O. E., 2016. Removal of Cr (VI) from tannery effluents with mixed cultures of bacteria and fungi isolated from soils contaminated with tropical tannery effluents. IJEWM. 17(1), 60-70. https://doi.org/10.1504/IJEWM.2016.076431

Ong, G. H., Ho, X. H., Shamkeeva, S., Manasha Savithri Fernando, A. S., Wong, L. S., 2017. Biosorption study of potential fungi for copper remediation from Peninsular Malaysia. Remediation Journal 27(4), 59-63. DOI: 10.1002/rem.21531

Ontañon, O.M., Fernandez, M., Agostini, E., González, P.S., 2018. Identification of the main mechanisms involved in the tolerance and bioremediation of Cr (VI) by *Bacillus* sp. SFC 500-1E. Environ. Sci. Pollut. Res. 25(16), 1611-16120. doi: 10.1007/s11356-018-1764-1

Onundi, Y. B., Mamun, A. A., Al Khatib, M. F., Ahmed, Y. M. 2010. Adsorption of copper, nickel and lead ions from synthetic semiconductor industrial wastewater by palm shell activated carbon. International Journal of Environmental Science & Technology 7(4), 751-758.

Osumi, M., 1998. The ultrastructure of yeast: cell wall structure and formation. Micron 29(2-3), 207-233. https://doi.org/10.1016/S0968-4328(97)00072-3

Otero-Fernández, A., Otero, J. A., Maroto, A., Carmona, J., Palacio, L., Prádanos, P., Hernández, A. 2017. Concentration-polarization in nanofiltration of low

concentration Cr (VI) aqueous solutions. Effect of operative conditions on retention. Journal of Cleaner Production, 150, 243-252.

Ott, T., Fritz, E., Polle, A., Schützendübel, A., 2002. Characterisation of antioxidative systems in the ectomycorrhiza-building basidiomycete *Paxillus involutus* (Bartsch) Fr. and its reaction to cadmium. *FEMS Microbiol. Ecol.* 42(3), 359–366. https://doi.org/10.1111/j.1574-6941.2002.tb01025.x

Oztürk, A. 2007. Removal of nickel from aqueous solution by the bacterium Bacillus thuringiensis. Journal of Hazardous Materials.147(1-2), 518-523. DOI: 10.1016/j.jhazmat.2007.01.047.

Padhi, D. K., Panigrahi, T. K., Parida, K., Singh, S. K., Mishra, P. M. 2017. Green synthesis of Fe3O4/RGO nanocomposite with enhanced photocatalytic performance for Cr (VI) reduction, phenol degradation, and antibacterial activity. ACS Sustainable Chemistry & Engineering 5(11), 10551-10562.

Pagana A.E., Sklari S.D., Kikkinides E.S., Zaspalis V.T. 2008. Microporous ceramic membrane technology for the removal of arsenic and chromium ions from contaminated water. Microporous and Mesoporous Materials 150-156.

Pahlavanzadeh, H., Motamedi M. 2020. Frameworks‐8 Microspheres Adsorption of Nickel, Ni(II), in Aqueous Solution by Modified Zeolite as a Cation-Exchange Adsorbent. Journal of Chemical & Engineering Data 2020 *65* (1), 185-197. DOI: 10.1021/acs.jced.9b00868

Pakshirajan, K., Izquierdo, M., Lens, P. N., 2013. Arsenic (III) removal at low concentrations by biosorption using *Phanerochaete chrysosporium* pellets. Separation Science and Technology, 48(7), 1111-1122. https://doi.org/10.1080/01496395.2012.723102

Palacios, Ò., Espart, A., Espín, J., Ding, C., Thiele, D. J., Atrian, S., Capdevila, M., 2014. Full characterization of the Cu-, Zn-, and Cd-binding properties of CnMT1 and CnMT2, two metallothioneins of the pathogenic fungus *Cryptococcus neoformans* acting as virulence factors. Metallomics 6(2), 279-291.

Palmieri, G., Giardina, P., Bianco, C., Fontanella, B., Sannia, G., 2000. Copper induction of laccase isoenzymes in the ligninolytic fungus *Pleurotus ostreatus*. Appl. Environ. Microbiol. 66, 920–924.

Panda, S.S., Sahoo, K., Muduli, S.D., Sahoo, G., Ahemad, M.D.J., Nayak, B.B., Dhal, N.K., 2014. Chromium tolerant indigenous fungal strains from Industrial Effluents of Anugul District, Odisha, India. Biolife 2(2), 634-640.

Pandey, N., Bhatt, R., 2016. Role of soil associated Exiguobacterium in reducing arsenic toxicity and promoting plant growth in *Vigna radiata*. European journal of soil biology 75, 142-150. https://doi.org/10.1016/j.ejsobi.2016.05.007

Pani, B.K., 2010. Optimal Invitro Environmental Conditions for the Growth of White Summer Mushroom (*Calocybe indica*). Res. J. Agric. Sci. 3, 280–281.

Peng, C., Meng, H., Song, S., Lu, S., Lopez-Valdivieso, A. 2005. Elimination of Cr (VI) from electroplating wastewater by electrodialysis following chemical precipitation. Sep Sci Technol 39(7), 1501-1517. https://doi.org/10.1081/SS-120030788

Perfil'eva, A. V., Brodskii, V. A., Il'in, V. I., Kolesnikov, V. A. 2016. Effect of the composition of the medium and electroflotation processing parameters on extraction efficiency of chromium (III) dispersed phase from aqueous solutions. Russian Journal of Applied Chemistry 89(3), 388-393.

Pócsi, I., Prade, R. A., Penninckx, J., 2004. Glutathione, altruistic metabolite in fungi. Adv. Microb. Physiol. 49, 1–76. doi: 10.1016/S0065-2911(04)49001-8.

Posmyk, M. M., Kontek, R., Janas, K. M., 2009. Antioxidant enzymes activity and phenolic compounds content in red cabbage seedlings exposed to copper stress. Ecotoxicol. Environ. Safe. 72(2), 596-602.

Pradhan, D., Shukla, L.B., Sawyer, M., Rahman, P.K.S.M., 2017. Recent bioreduction of hexavalent chromium in wastewater treatment: A review. J. Ind. Eng. Chem. 55, 1-20. http://dx.doi.org/10.1016/j.jiec.2017.0 6.0 40

Prasad, G., Kumar, V., Dwivedi, S.K. 2018. Antifungal activity of some selected medicinal plants against *Fusarium solani* causing wilt and rot in Pearl

millet. Asian Journal of Bio Science, 13, 21-27. DOI : 10.15740/HAS/AJBS/13.1/21-27.

Puig, S.,Thiele, D.J. 2002. Molecular mechanisms of copper uptake and distribution. *Current opinion in chemical biology*, *6*(2), 171-180.

Pundir, R., Dastidar, M.G. 2015. Feasibility of cheese whey as an energy source for the growth of Aspergillus sp. and for the removal of heavy metals in batch reactor. *Desalination and Water Treatment*, *57*(33), 15467-15474.

Pundir, R., and Dastidar, M. G. 2015. Feasibility of cheese whey as an energy source for the growth of *Aspergillus sp.* and for the removal of heavy metals in batch reactor. Desalinat. Water Treat. DOI: 10.1080/19443994.2015.1084950.

Pundir, R., Chary, G.H.V.C., Dastdar, M.G., 2018. Application of Taguchi method for optimizing the process parameters for the removal of copper and nickel by growing *Aspergillus sp.* Water Resour. Ind. http://dx.doi.org/10.1016/j. wri.2016.05.001

Qamar, M., Gondal, M. A., Yamani, Z. H., 2011. Synthesis of Nanostructured NiO and Its Application in Laser-Induced Photocatalytic Reduction of Cr(VI) from Water. J. Mol. Catal. A: Chem. 341, 83–88. DOI:10.1016/j.molcata.2011.03.029

Qayyum, S., Khan, I., Meng, K., Zang , X., Zhoa, Y., Gu, Q., Peng, C., 2016. Bioaccumulation of heavy metals from aqueous solution using indigenous fungal isolates. Indian journal of Geo-Marine Science 45(4), 499-507.

Qian, X., Fang, C., Huang, M., Achal, V., 2017. Characterization of fungal-mediated carbonate precipitation in the biomineralization of chromate and lead from an aqueous solution and soil. J. Clean. Product. 164, 198-208. doi: 10.1016/j.jclepro.2017.06.195.

Qin, S. Zhi, H.Y. Xiao, R.W. Ming, H.W., 2007. Cadmium hyper accumulation leads to anincrease of glutathione rather than phytochelatins in the cadmium hyperaccumulator *Sedum alfredii*. J. Plant Physiol. 164, 1489-1498. https://doi.org/10.1016/j.jplph.2006.10.001

Qiu, M., Xie, R. S., Shi, Y., Zhang, H., Chen, H. M., 2010. Isolation and identification of two flavonoid-producing endophytic fungi from *Ginkgo biloba* L. Ann. Microbiol. 60(1), 143-150. https://doi.org/10.1007/s13213-010-0016-5

Qu, J., Wang, Y., Tian, X., Jiang, Z., Deng, F., Tao, Y., ... Zhang, Y. 2020. KOH-activated porous biochar with high specific surface area for adsorptive removal of chromium (VI) and naphthalene from water: Affecting factors, mechanisms and reusability exploration. Journal of Hazardous Materials 401, 123292.

Radisky, D., Kaplan, J. 1999. Regulation of transition metal transport across the yeast plasma membrane. J. Biol. Chem. 274, 4481–4484. doi: 10.1074/jbc.274.8.4481

Rafi, S., Shoaib, A., Awan, Z. A., Rizvi, N. B., Nafisa, Shafiq, M., 2017. Chromium tolerance, oxidative stress response, morphological characteristics, and FTIR studies of phytopathogenic fungus *Sclerotium rolfsii*. Folia Microbiol. 62, 207–219. DOI 10.1007/s12223-016-0489-0

Rajput, S., Pittman Jr, C. U., Mohan, D. 2016. Magnetic magnetite (Fe3O4) nanoparticle synthesis and applications for lead (Pb^{2+}) and chromium (Cr^{6+}) removal from water. Journal of colloid and interface science 468, 334-346.

Ramadoss, R., Subramaniam, D. 2019. Removal of divalent nickel from aqueous solution using blue-green marine algae: adsorption modeling and applicability of various isotherm models. Separation Science and Technology 54(6), 943-961.

Ramesh, G., Podila, G.K., Gay, G., Marmeisse, R., Reddy, M.S., 2009. Different patterns of regulatio n for the copper and cadmium metallothioneins of the ectomycor rhizal fungus *Hebeloma cylindrosporum*. Applied and Environment al Microb iology75: 2266-2274.

Ramırez-Ramırez, R., Calvo-Mendez, C., Avila-Rodrıguez, M., Lappe, P., Ulloa, M., Vazquez, J. R., Gutierrez-Corona, J. F., 2004. Cr(VI) reduction in a chromate-resistant strain of Candida maltose isolated from the leather industry. Antonie van Leeuwenhoek 85, 63–68. DOI:10.1023/B:ANTO.0000020151.22858.7f

Ramrakhiani, L., Majumder, R., Khowala, S., 2011. Removal of hexavalent chromium by heat inactivated fungal biomass of *Termitomyces clypeatus*: Surface characterization and mechanism of Biosorption. Chem. Eng. J. 171, 1060–1068. https://doi.org/10.1016/j.cej.2011.05.002

Rana-Madaria, P., Nagarajan, M., Rajagopal, C., Garg, B.S. 2005. Removal of chro-mium from aqueous solutions by treatment with carbon aerogel electrodes using response surface methodology. Ind. Eng. Chem. Res. 44 (17), 6549 e6559.

Rashid, A., Bhatti, H. N., Iqbal, M., Noreen, S., 2016. Fungal biomass composite with bentonite efficiency for nickel and zinc adsorption: a mechanistic study. Ecological engineering 91, 459-471.

Rausch, T., Wachter, A., 2005. Sulfur metabolism: a versatile platform for launching defence operations. Trends Plant Sci. 10, 503–509. 10.1016/j.tplants.2005.08.006

Ravikumar, K. V. G., Argulwar, S., Sudakaran, S. V., Pulimi, M., Chandrasekaran, N., Mukherjee, A. 2018. Nano-Bio sequential removal of hexavalent chromium using polymer-nZVI composite film and sulfate reducing bacteria under anaerobic condition. Environmental Technology & Innovation 9, 122-133.

Rawat, A.P., Kumar, V., Singh, D.P., 2019. A combined effect of adsorption and reduction potential of biochar derived from Mentha plant waste on removal of methylene blue dye from aqueous solution. Sep. Sci. and Technol. https://doi.org/10.1080/01496395.2019.1580732

Raza, M.A., Kanwal, Z., Riaz, S., Naseem, S., 2016. Antibacterial performance of chromium nanoparticles against *Escherichia coli*, and *Pseudomonas aeruginosa*. In World Congress on Advances in Civil, Environmental and Materials Research (ACEM'16).

Reddy, M.S., Prasanna, L., Marmeisse, R., Fraissinet-Tachet, L., 2014. Differential expression of metallothioneins in response to heavy metals and their involvement in metal tolerance in the symbiotic basidiomycete *Laccaria bicolor*. Microbiology 160 : 2235-2242.

Reese, R. N., Mehra, R. K., Tarbet, B. E., Winge, D. R.,, 1980. Studies on the gamma-glutamyl Cu-binding peptide from *Schizosaccharomyces pombe*. J. Biol. Chem. 25;263(9), 4186-4192.

Regnell, O., Watras, C. J. 2018. Microbial mercury methylation in aquatic environments: a critical review of published field and laboratory studies. Environmental science & technology 53(1), 4-19.

Rehman, A., Anjum, M.S. 2010. Cadmium uptake by yeast, Candida tropicalis, isolated from industrial effluents and its potential use in wastewater clean-up

operations. Water Air Soil Pollut. 205 (1e4), 149. https://doi.org/10.10 07/s11270-0 09-0 062- 4.

Rehman, A ., Anjum, M.S., 2010. Cadmium uptake by yeast,*Candida tropicalis*, isolated from industrial effluents and its potential use in wastewater clean-up operations. Water Air Soil Pollut. 205 (1-4), 149. https://doi.org/10.10 07/s11270-0 09-0 062- 4.

Rehman, A., Anjum, M. S. 2010. Cadmium uptake by yeast, Candida tropicalis, isolated from industrial effluents and its potential use in wastewater clean-up operations. Water, Air, and Soil Pollution 205(1-4), 149.

Ren, B., Zhang, Q., Zhang, X., Zhao, L., Li, H., 2018. Biosorption of Cr (VI) from aqueous solution using dormant spores of *Aspergillus niger*. RSC Advances, 8(67), 38157-38165.

Ren, W. X., Li, P. J., Geng, Y., Li, X. J., 2009. Biological leaching of heavy metals from a contaminated soil by *Aspergillus niger*. J. Hazard. Mater. 167, 164–169. https://doi.org/10.1016/j.jhazmat.2008.12.104

Reynolds, T. B., Fink, G. R., 2001. Bakers'yeast, a model for fungal biofilm formation. Science 291, 878-881. DOI:10.1126/science.291.5505.878

Rhee Y.J., Hillier S., Gadd, G.M., 2016. A New Lead Hydroxycarbonate Produced During Transformation of Lead Metal by the Soil Fungus *Paecilomyces javanicus*. Geomicrobiol. J. 33(3-4), 250-260. DOI: 10.1080/01490451.2015.1076544.

Rhee,Y. J., Hillier, S., Pendlowski, H., Gadd, G.M., 2014. Fungal transformation of metallic lead to pyromorphite in liquid medium. Chemosphere 113, 17–21. http://dx.doi.org/10.1016/j.chemosphere.2014.03.085

Romero-Gonzalez, M., Nwaobi, B. C., Hufton, J. M., Gilmour, D. J., 2016. Ex-situ bioremediation of U (VI) from contaminated mine water using *Acidithiobacillus ferrooxidans* strains. Front. Environ. Sci. 4, 39. https://doi.org/10.3389/fenvs.2016.00039

Romo-Rodríguez, P., Acevedo-Aguilar, F. J., Lopez-Torresm, A., Wrobel, K., Wrobel, K., Gutiérrez-Corona, J. F., 2015. Cr (VI) reduction by gluconolactone and hydrogen peroxide, the reaction products of fungal glucose oxidase: Cooperative interaction with organic acids in the biotransformation of

Cr(VI). Chemosphere 134, 563-570. http://dx.doi.org/10.1016/j.chemosphere.2014.12.009

Rossi, A.D., Rigon M.R., Zaparoli, M., Braido, R.D., Colla, L.M., Dotto, G.L., Piccin, J. S., 2018. Chromium (VI) biosorption by *Saccharomyces cerevisiae* subjected to chemical and thermal treatments. Environ. Sci. Pollut. R. 25, 19179–19186.

Ruta, L. L., Lin, Y.-F., Kissen, R., Nicolau, I., Neagoe, A. D., Ghenea, S. et al. 2017. Anchoring plant metallothioneins to the inner face of the plasma membrane of *Saccharomyces cerevisiae* cells leads to heavy metal accumulation. PLoS ONE 12(5), e0178393. https://doi.org/10.1371/journal.

Sadyrbaeva, T. Z. 2015. Separation of cobalt (II) from nickel (II) by a hybrid liquid membrane–electrodialysis process using anion exchange carriers. Desalination 365, 167-175.

Saha, P., Shinde, O., Sarkar, S. 2017. Phytoremediation of industrial mines wastewater using water hyacinth. International journal of phytoremediation 19(1), 87-96.

Saini, D., Kaushik, J., Garg, A. K., Dalal, C., Sonkar, S. K. 2020. N, S-codoped Carbon Dots for Nontoxic Cell Imaging and As a Sunlight-Active Photocatalytic Material for the Removal of Chromium. ACS Applied Bio Materials.

Saitou, N., Nei, M. 1987. The neighbor-joining method: a new method for reconstructing phylogenetic trees. Molecular biology and evolution 4(4), 406-425.

Sakthivel, M., Ayyasamy P.M., Hemalatha, N., 2016. Biotransformation of chromium (Cr-VI to Cr III) from tannery effluent using bacteria and fungi. Int. J. Adv. Res. Biol. Sci. 3(11), 68-79. DOI: http://dx.doi.org/10.22192/ijarbs.2016.03.11.008

Salvadori, M. R., Ando, R. A., Oller, N. C. A., Corrêa, B., 2015. Extra and Intracellular Synthesis of Nickel Oxide Nanoparticles Mediated by Dead Fungal Biomass. PLoS ONE 10(6), 0129799. doi:10.1371/journal.pone.0129799

Salvadori, M. R., Ando, R.A.C., Nascimento, A. O. D., Corrêa, B., 2014. Bioremediation from wastewater and extracellular synthesis of copper

nanoparticles by the fungus *Trichoderma koningiopsis*. J. Environ. Sci. Health, Part A 49(11), 1286-1295. DOI: 10.1080/10934529.2014.910067

Samadi, S., Karimi, K., Behnam, S., 2017. Simultaneous biosorption and bioethanol production from lead-contaminated media by *Mucor indicus*. Biofuel Res. J. 13, 545-555. DOI: 10.18331/BRJ2017.4.1.4

Sambrook, J., Fritsch, E.F., Maniatis, T., 1989. Molecular Cloning a laboratory manual. New York: Cold Spring Harbor Laboratory Press.

Samuel, M. S., Bhattacharya, J., Raj, S., Santhanam, N., Singh, H., Singh, N. P. 2019. Efficient removal of Chromium (VI) from aqueous solution using chitosan grafted graphene oxide (CS-GO) nanocomposite. International journal of biological macromolecules 121, 285-292.

Sandra, R., Pombeiro-Sponchiado, Gabriela, S. S., Jazmina, C. R., Andrade, Helen, F., Lisboa, Rita, C. R., Gonçalves, 2017. Production of Melanin Pigment by Fungi and Its Biotechnological Applications. Intech Open Science http://dx.doi.org/10.5772/67375

Sani, A., Nagam, V., Netala, V.R., Tartte, V., 2017. Characterization of Heavy Metal Resitant Endophytic Fungi from Boswellia Ovalifoliolata. Imperial Journal of Interdisciplinary Research 3(2), 1072-1076.

Santos, G. D. O. S., de Salles Pupo, M. M., Vasconcelos, V. M., Eguiluz, K. I. B., Banda, G. R. S. 2018. Electroflotation. In *Electrochemical Water and Wastewater Treatment* , 77-118. Butterworth-Heinemann.

Saravanan, A., Senthil, P.K., Preetha, B., 2015. Optimization of process parameters for the removal of chromium(VI) and nickel(II) from aqueous solutions by mixed biosorbents (custard apple seeds and *Aspergillus niger*) using response surface methodology. Desalinat. Water Treat. DOI: 10.1080/19443994.2015.1064034.

Sathvika, T., Manasi, Rajesh, V., Rajesh, N., 2015. Prospective application of *Aspergillus* species immobilized in sodium montmorillonite to remove toxic hexavalent chromium from wastewater. RSC Adv. 5: 107031-107044. doi.10.1039/C5RA22778J

Scandalios, J.G., 2005. Oxidative stress: molecular perception and transduction of signals triggering antioxidant gene defenses. Braz. J. med. Biol. Res. 38, 995-1014. Doi. S0100-879X2005000700003

Schlosser, D., Hofer, C., 2002. Laccas e-catalyzed oxidation of Mn2 Cin the p resence of natural Mn3C chelators as a novel source of extra cellular H2O2 production and its impact on manganese peroxidase. Appl. Environ. Microbiol. 68, 3514 3521.

Selvaraj, R., Santhanam, M., Selvamani, V., Sundaramoorthy, S., Sundaram, M. 2018. A membrane electroflotation process for recovery of recyclable chromium (III) from tannery spent liquor effluent. Journal of hazardous materials 346, 133-139.

Sen, S., Dutta, S., Guhathakurata, S., Chakrabarty, J., Nandi, S., Dutta, A. 2017. Removal of Cr (VI) using a cyanobacterial consortium and assessment of biofuel production. International Biodeterioration & Biodegradation 119, 211-224..

Sepehr, M. N., Zarrabi, M., Amrane, A., 2014. Effect of medium nutrients on Cr(III) removal by *Phanerochaete chrysosporium*, *Aspergillus Niger* and *Aspergillus Oryzae*. Environ. Eng. Mana. J. 13(4), 827-834.

Seyedmousavi, S., Badali, H., Chlebicki, A., Zhao, J., Prenafeta-Boldu, F. X., De Hoog, G. S. 2011. *Exophiala sideris*, a novel black yeast isolated from environments polluted with toxic alkyl benzenes and arsenic. Fungal biology 115(10), 1030-1037.

Shahid, M., Dumat, C., Khalid, S., Schreck, E., Xiong, T., Niazi, N.K., 2017. Foliar heavy metal uptake, toxicity and detoxification in plants: A comparison of foliar and root metal uptake. J. Hazard. Mater. 325, 36–58. https://doi.org/10.1016/j.jhazmat.2016.11.063

Shahrak, M. N., Ghahramaninezhad, M., Eydifarash, M. 2017. Zeolitic imidazolate framework-8 for efficient adsorption and removal of Cr (VI) ions from aqueous solution. Environmental Science and Pollution Research 24(10), 9624-9634.

Shahverdi, F., Ahmadi, M., Avazmoghadam, S., 2016. Isotherm models for the nickel (II) biosorption using dead fungal biomass of *Aspergillus awamori*:

comparison of various error functions. Desalination and Water Treatment 57(42), 19846-19856.

Shakya, A., Núñez-Delgado, A., Agarwal, T. 2019. Biochar synthesis from sweet lime peel for hexavalent chromium remediation from aqueous solution. Journal of environmental management 251; 109570.

Shao, Z., Huang, C., Wu, Q., Zhao, Y., Xu, W., Liu, Y., ... Hou, H. 2019. Ion exchange collaborating coordination substitution: more efficient Cr (VI) removal performance of a water-stable CuII-MOF material. Journal of hazardous materials 378, 120719.

Shao-Hong, Y., Xue-Hong, Z., Jie, L., Yi-Nian, Z., Chen, G., 2014. Feasibility of constructed wetland planted with Leersia hexandra Swartz for removing Cr, Cu and Ni from electroplating wastewater. Environmental Technology 35(2), 187–194. Doi. 10.1080/09593330.2013.822006

Sharma, M., Joshi, M., Nigam, S., Shree, S., Avasthi, D. K., Adelung, R., ... Mishra, Y. K. 2019. ZnO tetrapods and activated carbon based hybrid composite: Adsorbents for enhanced decontamination of hexavalent chromium from aqueous solution. Chemical Engineering Journal 358; 540-551.

Sharma, S., Malaviya, P., 2016. Bioremediation of tannery wastewater by chromium resistant novel fungal consortium. Ecol. Eng. 91, 419–425. http://dx.doi.org/10.1016/j.ecoleng.2016.03.005

Sharma, S., Pathak, H., 2017. Physico-chemical properties of petroleum contaminated soil Collected from arid region of rajasthan (churu). Int. J. Pharm. Bio. Sci. 8(2)(B), 926-932. DOI: http://dx.doi.org/10.22376/ijpbs.2017.8.2.b926-932

Sharma, S., Tiwari, K. L., Jadhav, S. K. 2018. Diversity of fungal endophytes in Typha latifolia (L.) and their lead biosorption activity. Euro-Mediterranean Journal for Environmental Integration 3(1), 4.

Sharma, S., Tiwari, K. L., Jadhav, S. K., 2018. Diversity of fungal endophytes in *Typha latifolia* (L.) and their lead biosorption activity. Euro-Mediterr J. Environ. Integr. 3(4). DOI 10.1007/s41207-017-0041-x

Sharma, S.S., Dietz, K.J. 2009. The relationship between metal toxicity and cellular redox imbalance. *Trends in plant science*, *14*(1), 43-50.

Shen, L., Saky, S.A., Yang, Z., Ho, S.-H., Chen, C., Qin, L., Zhang, G., Wang, Y., Lu, Y., 2019. The critical utilization of active heterotrophic microalgae for bioremoval of Cr(VI) in organics co-contaminated wastewater, Chemosphere 228, 536-544. doi: https://doi.org/10.1016/j.chemosphere.2019.04.152.

Shen, M., Zhao, D. K., Qiao, Q., Liu, L., Wang, J. L., Cao, G. H., ... Zhao, Z.W., 2015. Identification of glutathione S-transferase (GST) genes from a dark septate endophytic fungus (*Exophiala pisciphila*) and their expression patterns under varied metals stress. PloS one 10(4), e0123418.Stress

Sheng, G.-P., Yu, H.-Q., Li, X.-Y., 2010. Extracellular polymeric substances (EPS) of microbial aggregates in biological wastewater treatment systems: a review. Biotechnol. Adv. 28, 882–894. https://doi.org/10.1016/j.biotechadv.2010.08.001

Shi, J., Fan, X., Tsang, D. C., Wang, F., Shen, Z., Hou, D., Alessi, D. S. 2019. Removal of lead by rice husk biochars produced at different temperatures and implications for their environmental utilizations. Chemosphere 235, 825-831.

Shi, J., Zhang, B., Qiu, R., Lai, C., Jiang, Y., He, C., Guo, J. 2019. Microbial chromate reduction coupled to anaerobic oxidation of elemental sulfur or zerovalent iron. Environmental science & technology 53(6), 3198-3207.

Shi, L., Xue, J., Liu, B., Dong, P., Wen, Z., Shen, Z., Chen, Y., 2018. Hydrogen ions and organic acids secreted by ectomycorrhizal fungi, *Pisolithus* sp1, are involved in the efficient removal of hexavalent chromium from waste water. Ecotoxicol. Environ. Safe. 161, 430–436. https ://doi.org/10.1016/j.ecoenv.2018.06.004

Shi, Z., Shen,W., Yang, K., Zheng, N., Jiang, X., Liu, L., Yang, D., Zhang, L., Ai, Z., Xie, B., 2019. Hexavalent chromium removal by a new composite system of dissimilatory iron reduction bacteria *Aeromonas hydrophila* and nanoscale zero-valent iron. Chem. Eng. J. 352, 63-70.

Shih, Y. J., Lin, C. P., Huang, Y. H. 2013. Application of Fered-Fenton and chemical precipitation process for the treatment of electroless nickel plating wastewater. Separation and Purification Technology 104, 100-105.

Shoaib, A., Akhtar, S., Akhtar, N., 2015. Copper tolerance, protein and catalytic activity in phytopathogenic fungus *Alternaria alternata*. Global Nest. J. 17, 664–672.

Shoaib, A., Aslam, N., Athar, M.M., Akhtar, Nafisa, S. Khurshid, S., 2013. Removal of Cr(III) through bread mold fungus. Pol. J. Environ. Stud. 22, 1171-1176.

Shokoohi, R., Salari, M., Molla Mahmoudi, M., Azizi, S., Ghiasian, S. A., Faradmal, J., Faraji, H., 2020. The sorption of cationic and anionic heavy metal species on the biosorbent of *Aspergillus terreus*: Isotherm, kinetics studies. Environmental Progress & Sustainable Energy 39(2), e13309.

Shri, M., Kumar, S., Chakrabarty, D., Trivedi, P.K., Mallick, S., Misra, P., Shukla, D., Mishra, S., Srivastava,S., Tripathi, R.D., Tuli, R., 2009. Effect of arsenic on growth, oxidative stress, and antioxidant system in rice seedlings. Ecotoxicology and Environmental Safety 72, 1102–1110. https://doi.org/10.1007/978-981-13-1292-2_4

Shroff, K.A., Vaidya, V.K., 2011. Kinetics and equilibrium studies on biosorption of nickel from aqueous solution by dead fungal biomass of *Mucor hiemalis*. Chem. Eng. J. 171, 1234–1245.

Siegel, S. M., 1987. Fungal biosorption: A comparative study of metal uptake by *Penicillium* and *Cladosporil'h*. Met Speciat Sep Recover 1, 339.

Singh, P., Chowdhuri, D. K. 2017. Environmental presence of hexavalent but not trivalent chromium causes neurotoxicity in exposed Drosophila melanogaster. Molecular neurobiology 54(5), 3368-3387.

Singh, R., Bishnoi, N.R., 2015. Biotransformation dynamics of chromium (VI) detoxification using Aspergillus flavus system. Ecological Engineering 75, 103-109.

Singh, S., Parihar, P., Singh, R., Singh, V. P., Prasad, S. M. 2016. Heavy metal tolerance in plants: role of transcriptomics, proteomics, metabolomics, and ionomics. Frontiers in plant science 6, 1143.

Singhal, R. K., Anderson, M. E., Meister, A., 1987. Glutathione, a first line of defense against cadmium toxicity. The FASEB J. 1, 220–223.

Sochacki, A., Surmacz-Gorska, J., Faure, O., Guy, B. 2014. Polishing of synthetic electroplating wastewater in microcosm upflow constructed wetlands: Effect of operating conditions. Chem Eng J 237:250-258. https://doi.org/10.1016/j.cej.2013.10.015

Song, J., He, Q., Hu, X., Zhang, W., Wang, C., Chen, R., ... Mosa, A., 2019. Highly efficient removal of Cr (VI) and Cu (II) by biochar derived from *Artemisia argyi* stem. Environmental Science and Pollution Research 26(13), 13221-13234.

Spagnoletti, F. N., Balestrasse, K., Lavado, R. S., Giacometti, R., 2016. Arbuscular mycorrhiza detoxifying response against arsenic and pathogenic fungus in soybean. Ecotoxicology and environmental safety 133, 47-56. doi: 10.1016/j.ecoenv.2016.06.012.

Sriharsha, D. V., Lokesh, K. R., Savitha, J., 2017. Immobilized fungi on *Luffa cylindrica* : An effective biosorbent for the removal of lead. J. Taiwan Inst. Chem. Eng. 80, 589–595. https://doi.org/10.1016/j.jtice.2017.08.032

Sriram, S., Nambi, I. M., Chetty, R. 2018. Electrochemical reduction of hexavalent chromium on titania nanotubes with urea as an anolyte additive. Electrochimica Acta 284, 427-435.

Srivastava, S., Agrawal, S. B., Mondal, M. K., 2015. Biosorption isotherms and kinetics on removal of Cr(VI) using native and chemically modified *Lagerstroemia speciosa* bark. Ecological Engineering 85, 56–66.

Srivastava, S., Thakur, I.S., 2006. Isolation and process parameter optimization of *Aspergillus sp.* for removal of chromium from tannery effluent. Bioresour. Technol. 97, 1167–1173.

Su, P., Zhang, J., Tang, J., Zhang, C. 2019. Preparation of nitric acid modified powder activated carbon to remove trace amount of Ni (II) in aqueous solution. Water Science and Technology 80(1); 86-97.

Sugasini, A., Rajagopal, K., 2015. Hexavalent chromium removal from aqueous solution using *Trichoderma viride*. Int. J. Pharm. Bio Sci. 6(1)(B), 485–495.

Sun, X.F., Wang, S.G., Zhang, X.M., Chen, J.P., Li, X.M., Gao, B.Y., Ma, Y. 2009. Spectroscopic study of Zn2+ and Co2+ binding to extracellular polymeric

substances (EPS) from aerobic granules. J. Colloid Interface Sci. 2009; 335(1), 11-18.

Sundararaju, S., Manjula, A., Kumaravel, V., Muneeswaran, T., Vennila, T. 2020. Biosorption of nickel ions using fungal biomass Penicillium sp. MRF1 for the treatment of nickel electroplating industrial effluent. *Biomass Conversion and Biorefinery*, 1-10.

Sunderman, J, F. W., Coulston, F., Eichhorn, G. L., FELLOWS, J., MAS-TROMATTEO, E., RENO, H., SAMITZ, M. 1975. Nickel. Washington DC. In *National Academy of Science* (pp. 97-143).

Sutherland, D. E., Stillman, M. J., 2014. Challenging conventional wisdom: single domain metallothioneins. Metallomics 6, 702–728. doi: 10.1039/c3mt00216k

Sutjaritvorakul, T., Gadd, G. M., Whalley, A. J.S., Suntornvongsagul, K., Sihanonth, P., 2016. Zinc Oxalate Crystal Formation by *Aspergillus nomius*. Geomicrobiol. J. 33(3-4), 289-293. DOI: 10.1080/01490451.2015.1048395

Tabatabaei, S., Rad, B. F., Baghdadi, M. 2020. Semicontinuous enhanced electroreduction of Cr (VI) in wastewater by cathode constructed of copper rods coated with palladium nanoparticles followed by adsorption. Chemosphere 251, 126309.

Taha, A.A., Wu, Y.N., Wang, H., Li, F. 2012. Preparation and application of functionalized cellulose acetate/silica composite nanofibrous membrane via electrospinning for Cr(VI) ion removal from aqueous solution. J Environ Manage. 112, 10-16. doi:10.1016/j.jenvman.2012.05.031

Tahir, A., Lateef, Z., Abdel-Megeed, A., Sholkamy, E. N., Mostafa, A. A., 2017. In vitro compatibility of fungi for the biosorption of zinc(II) and copper(II) from electroplating effluent. Current Science 112(4), 839-844. DOI: 10.18520/cs/v112/i04/839-844

Talukdar, D., 2013. Arsenic-induced changes in growth and antioxidant metabolism of fenugreek. Russ. J. Plant Physiol. 60, 652–660.

Talukdar, D., Jasrotia, T., Sharma, R., Jaglan, S., Kumar, R., Vats, R., ... Umar, A. 2020. Evaluation of novel indigenous fungal consortia for enhanced

bioremediation of heavy metals from contaminated sites. Environmental Technology & Innovation 101050.

Tamayo, E., Gómez-Gallego, T., Azcón-Aguilar, C, Ferrol, N. 2014. Genome-wide analysis of copper, iron and zinc transporters in the arbuscular mycorrhizal fungus Rhizophagus irregularis. *Frontiers in plant science*, *5*, 547.

Tamayo, E., Gómez-Gallego, T., Azcón-Aguilar, C., Ferrol, N., 2014. Genome-wide Analysis of copper, iron and zinc transporters in the arbuscular mycorrhizal fungus *Rhizophagus irregularis* 5, 547. https://doi.org/10.3389/fpls.2014.00547

Tamura, K., Nei, M., Kumar, S. 2004. Prospects for inferring very large phylogenies by using the neighbor-joining method. Proceedings of the National Academy of Sciences, 101(30), 11030-11035.

Tangsombatvichit, P., Semkiv, M.V., Sibirny, A.A., Jensen, L.T., Ratanakhanokchai, K., Soontorngun, N. 2015. Zinc cluster protein Znf1, a novel transcription factor of non-fermentative metabolism in Saccharomyces cerevisiae. *FEMS yeast research*, *15*(2).

Tangsombatvichit, P., Semkiv, M. V., Sibirny, A. A., Jensen, L. T., Ratanakhanokchai, K., Soontorngun, N. 2015. Zinc cluster protein Znf1, a novel transcription factor of non-fermentative metabolism in *Saccharomyces cerevisiae*. FEMS yeast research *15*(2).

Teng Y, Du X, Wang T, Mi C, Yu H, Zou L (2017) Isolation of a fungus Pencicillium sp. with zinc tolerance and its mechanism of resistance. *Archives of microbiology*, *200*(1), 159-169.

Thanh, D. N., Novák, P., Vejpravova, J., Vu, H. N., Lederer, J., Munshi, T. 2018. Removal of copper and nickel from water using nanocomposite of magnetic hydroxyapatite nanorods. Journal of magnetism and magnetic materials 456, 451-460.

Thorsen, M., Lagniel, G., Kristiansson, E., Junot, C., Nerman, O., Labarre, J., Tamás, M. J. 2007. Quantitative transcriptome, proteome, and sulfur metabolite profiling of the *Saccharomyces cerevisiae* response to arsenite. Physiological genomics, 30(1), 35-43. https://doi.org/10.1152/physiolgenomics.00236.2006

Tripathi, D.K., Singh, V.P., Kumar, D., Chauhan, D.K., 2012. Impact of exogenous silicon addition on chromium uptake, growth, mineral elements, oxidative stress, antioxidant capacity, and leaf and root structures in rice seedlings exposed to hexavalent chromium. Acta physiologiae plantarum 34(1), 279-289.

Tu, B., Wen, R., Wang, K., Cheng, Y., Deng, Y., Cao, W., ... Tao, H. 2020. Efficient removal of aqueous hexavalent chromium by activated carbon derived from Bermuda grass. Journal of colloid and interface science 560, 649-658.

Un, U. T., Onpeker, S. E., Ozel, E. 2017. The treatment of chromium containing wastewater using electrocoagulation and the production of ceramic pigments from the resulting sludge. Journal of Environmental Management 200, 196-203.

Urík, M., Hlodák, M., Mikušová, P. et al., 2014. Potential of Microscopic Fungi Isolated from Mercury Contaminated Soils to Accumulate and Volatilize Mercury(II). Water Air Soil Pollut. 225**,** 2219. https://doi.org/10.1007/s11270-014-2219-z

Urrialde,V., Alburquerque, B., Guirao-Abad, J.P., Pla, J., Argüelles, J.C., Alonso-Monge, R., 2017. Arsenic inorganic compounds cause oxidative stress mediated by the transcription factor PHO4 in *Candida albicans*. Microbiological Research 203, 10–18. DOI: 10.1016/j.micres.2017.06.004

US EPA (United State Environmental Protection Agencies) 2016. Preliminary Study of the Metal Finishing Category: 2015 Status Report, U.S. Environmental Protection Agency Office of Water (4303T) 1200 Pennsylvania Avenue, NW Washington, DC 20460. EPA-821-R-16–004.

USEPA (United States Environmental Protection Agency), 1998. Toxicological Review of Trivalent Chromium, CAS No. 160 65-83-1.

Vaccaro, B. J., Lancaster, W. A., Thorgersen, M. P., Zane, G. M., Younkin, A. D., Kazakov, A. E., Wetmore, K. M., Deutschbauer, A., Arkin, A. P., Novichkov, P. S., Wall, J. D., and Adams, W. W., 2016. Novel Metal Cation Resistance Systems from Mutant Fitness Analysis of Denitrifying *Pseudomonas Stutzeri*. Appl. Environ. Microbiol. 82, 6046–6056. http://dx.doi.org/10.1128/AEM.01845-16

Vaseem, H., Singh,V.K., Singh, M.P., 2017. Heavy metal pollution due to coal washery effluent and its decontamination using a macrofungus, *Pleurotus ostreatus*. Ecotoxicol. Environ. Safe. 145, 42–49.

Velasco, G., Gutiérrez-Granados, S., De León, C. P., Alatorre, A., Walsh, F. C., Rodríguez-Torres, I. 2016. The electrochemical reduction of Cr (VI) ions in acid solution at titanium and graphite electrodes. Journal of environmental chemical engineering 4(3), 3610-3617.

Velikova, V., Yordanov, I., Edreva, A., 2000. Oxidative stress and some antioxidant systems in acid rain-treated bean plants: protective role of exogenous polyamines. Plant science 151(1), 59-66. https://doi.org/10.1016/S0168-9452(99)00197-1

Velma, V., Vutukuru, S. S., Tchounwou, P. B., 2009. Ecotoxicology of hexavalent chromium in freshwater fish: a critical review. Reviews on environmental health, 24(2), 129-146.

Velmurugan, P., Shim, J., You, Y., Choia, S., Kamala-Kannana S., Lee, K-J., Oh B-T., 2010. Removal of zinc by live, dead, and dried biomass of *Fusarium* spp. isolated from the abandoned-metal mine in South Korea and its perspective of producing nanocrystals. J. Hazard. Mater. 182(1–3), 317-324. DOI.org/10.1016/j.jhazmat.2010.06.032

Verhalen, B., Dastvan, R., Thangapandian, S., Peskova, Y., Koteiche, H. A., Nakamoto, R. K., Tajkhorshid, E., Mchaourab, H. S., 2017. Energy transduction and alternating access of the mammalian ABC transporter P-glycoprotein. Nature 543, 738–741. doi: 10.1038/nature21414

Visioli, G., and Marmiroli, N. 2013. The proteomics of heavy metal hyper accumulation by plants. Journal of Proteomics 79, 133-145. https://doi.org/10.1016/j.jprot.2012.12.006

Viti, C., Marchi, E., Decorosi, F., Giovannetti, L. 2014. Molecular mechanisms of Cr (VI) resistance in bacteria and fungi. FEMS microbiology reviews 38(4), 633-659.

Vutukuru, S., 2005. Acute effects of hexavalent chromium on survival, oxygen consumption, hematological parameters and some biochemical profiles of the

Indian major carp, Labeo rohita. International Journal of Environmental Research and Public Health, 2(3), 456-462.

Wallwork, G. R. 1976. The oxidation of alloys. Reports on Progress in Physics 39(5), 401.

Wang, J.T., Zhang, L., Kang, Y., Chen, G., Jiang, F. 2018. Long-term feeding of elemental sulfur alters microbial community structure and eliminates mercury methylation potential in sulfate-reducing bacteria abundant activated sludge. *Environmental science & technology*, *52*(8), 4746-4753.

Wang, B., Li, Z., Lang, Q., Tan, M., Ratanatamskul, C., Lee, M., ... Zhang, Y. 2020. A comprehensive investigation on the components in ionic liquid-based polymer inclusion membrane for Cr (VI) transport during electrodialysis. *Journal of Membrane Science*, 118016.

Wang, H., He, Z., Luo, L., Zhao, X., Lu, Z., Luo, T., Li, M., Zhang, Y., 2018. An aldo-keto reductase, Bbakr1, is involved in stress response and detoxification of heavy metal chromium but not required for virulence in the insect fungal pathogen, *Beauveria bassiana*. Fungal Genet. Biol. 111, 7-15. https://doi.org/10.1016/j.fgb.2018.01.001

Wang, J., Chen, C., 2006. Biosorption of heavy metals by *Saccharomyces cerevisiae*: a review. Biotechnol. Adv. 24, 427–451. https://doi.org/10.1016/j.biotechadv.2006.03.001

Wang, P., Sun, G., Jia, Y., Meharg, A.A., Zhu, Y., 2014. A review on completing arsenic biogeochemical cycle: microbial volatilization of arsines in environment. J. Environ. Sci. 26, 371–381.

Wang, X., Liu, W., Fu, H., Yi, X. H., Wang, P., Zhao, C., ... Zheng, W. 2019. Simultaneous Cr (VI) reduction and Cr (III) removal of bifunctional MOF/Titanate nanotube composites. Environmental pollution 249, 502-511.

Wani, P.A., Wani, J.A., Wahid, S., 2018. Recent advances in the mechanism of detoxification of genotoxic and cytotoxic Cr(VI) by microbes. J. Environ. Chem. Eng. 6(4), 3798-3804. https://doi.org/10.1016/j.jece.2018.05.042

Waschke, A., Sieh, D., Tamasloukht, M., Fischer, K., Mann, P., Franken, P., 2006. Identification of heavy metal-induced genes encoding glutathione S-transferases in the arbuscular mycorrhizal fungus *Glomus intraradices*. Mycorrhiza 17(1), 1-10.

WBG (World Bank Group), & World Health Organization (1999). *Pollution Prevention and Abatement Handbook, 1998: Toward Cleaner Production*. World Bank Publications.

White, J.H., Wise, A., Main, M.J., Green, A., Frasae N.J., Disney, G.H., Barnes, A.A., Emosan, P., Foord, S.M., Marshall, S.H., 1998. Heterodimerization is required for the formation of a functional GABAb receptor. Nature 396, 679–682. Doi. 10.1038/25354

WHO (World Health Organization) 2017. Guidelines for drinking-water quality: first addendum to the fourth edition.

WHO, 2017. Guidelines for drinking-water quality: fourth edition incorporating the first addendum. Geneva: World Health Organization; Licence: CC BY-NC-SA 3.0 IGO

Wierzba, S. 2017. Biosorption of nickel (II) and zinc (II) from aqueous solutions by the biomass of yeast Yarrowia lipolytica. Polish Journal of Chemical Technology 19(1), 1-10.

Wong, S., Ngadi, N., Inuwa, I. M., Hassan, O. 2018. Recent advances in applications of activated carbon from biowaste for wastewater treatment: a short review. Journal of Cleaner Production 175, 361-375.

Wu, S., Zhang, X., Sun, Y., Wu, Z., Li, T., Hu, Y., Su, D., Lv, J., Li, G., Zhang, Z., Zheng, L., Zhang, J., Chen, B. 2015 Transformation and immobilization of chromium by arbuscular mycorrhizal fungi as revealed by SEM-EDS, TEM-EDS and XAFS. Environ. Sci. Technol. 4 9 (24), 14036-14047. https://doi.org/10.1021/acs.est.5b03659.

Wu, G., L., Cui, J., Tao, L., Yang, H., 2010. Fluroxypyr triggers oxidative damage by producing superoxide and hydrogen peroxide in rice (*Oryza sativa*). Ecotoxicology 19(1), 124. doi: 10.1007/s10646-009-0396-0

Wu, Y., Wen, Y., Zhou, J., Dai, Q., Wu, Y., 2012. The characteristics of waste *Saccharomyces cerevisiae* biosorption of arsenic (III). Environmental Science and Pollution Research 19(8), 3371-3379. https://doi.org/10.1007/s11356-012-0861-9

Xafenias, N., Zhang, Y., Banks, C.J., 2013. Enhanced performance of hexavalent chromium reducing cathodes in the presence of *Shewanella oneidensis* MR-1 and lactate. Environ. Sci. Technol. 47(9), 4512-4520. doi: 10.1021/es304606u

Xiang, C., Oliver, D. J., 1998. Glutathione metabolic genes coordinately respond to heavy metals and jasmonic acid in *Arabidopsi*s. Plant Cell 10, 1539–1550. DOI: https://doi.org/10.1105/tpc.10.9.1539

Xie, Y., Luo, H., Dua, Z., Hua, L., Fu, J., 2014. Identification of cadmium-resistant fungi related to Cd transportation in bermudagrass [*Cynodon dactylon* (L.) Pers.]. Chemosphere 117, 786–792. DOI:10.1016/j.chemosphere.2014.10.037

Xing Y., Chen X., Wang D. 2009. Variable effects on the performance of continuous electrodeionization for the removal of Cr(VI) from wastewater. Separation and Purification Technology 68(3), 357-362.

Xu R., Pang W., Yu J., Huo Q., Chen J., 2008. Chemistry of zeolites and related porous materials: synthesis and structure, Environ. Eng. Manage. 7, 73–75.

Xu, J., 2010. Nitric oxide is associated with long-term zinc tolerance in *Solanum nigrum*. Plant Physiol. 154, 1319-1334. DOI: https://doi.org/10.1104/pp.110.162982

Xu, J., Zhu, Y. Y., Ge, Q., Li, Y. L., Sun, J. H., Zhang, Y., Liu, X. J., 2012. Comparative physiological responses of *Solanum nigrum* and *Solanum torvum* to cadmium stress. New Phytologist 196, 125-138. doi: 10.1111/j.1469-8137.2012.04236.x

Xu, W., Jian, H., Liu, Y., Zeng, G., Li X., Gu Y., Tan X., 2015. Removal of Chromium (VI) from Aqueous Solution Using Mycelial Pellets of *Penicillium simplicissimum* Impregnated with Powdered Biochar. Bioremediation J. 19(4), 259-268.

Xu, X., Xia, L., Chen, W., Huang, Q., 2017a. Detoxification of hexavalent chromate by growing *Paecilomyces lilacinus* XLA. Environ. Pollut. 225, 47-54.

Xu, X., Zhang, Z., Huang, Q., Chen, W., 2017. Biosorption performance of multi-metal resistant fungus *Penicillium chrysogenum* XJ-1 for removal of Cu2+ and Cr6+ from aqueous solutions. Geomicrobiol. J. 35, 40-49. DOI: 10.1080/01490451.2017.1310331

Yakout, A. A., Shaker, M. A., Albishri, H. M. 2016. Application of bifunctional Mangifera indica L.-loaded Saccharomyces cerevisiae as efficacious biosorbent for bivalent cobalt and nickel cations from different wastewaters: equilibrium and kinetic studies. Desalination and Water Treatment *57*(19), 8967-8980.

Yang, X., Guo, M., Wu, Y., Wu, Q., Zhang, R., 2014. Removal of Emulsified Oil from Water by Fruiting Bodies of Macro-Fungus (*Auricularia polytricha*). PLoS ONE 9(4), e95162.

Yang, X., Li, L., 2011. miRDeep-P: a computational tool for analyzing the microRNA transcriptome in plants. Bioinformatics 27(18), 2614-2615. doi: 10.1093/bioinformatics/btr430

Yannai, S., Berdicevsky, I., Duek, L., 1991. Transformations of inorganic mercury by *Candida albicans* and *Saccharomyces cerevisiae*. Applied and environmental microbiology 57(1), 245–247.

Yao, F., Jia, M., Yang, Q., Luo, K., Chen, F., Zhong, Y., ... Li, X. 2020. Electrochemical Cr (VI) removal from aqueous media using titanium as anode: Simultaneous indirect electrochemical reduction of Cr (VI) and in-situ precipitation of Cr (III). Chemosphere 127537.

Yao, Q., Yang, R., Long, L., Zhu, H., 2013. Phosphate application enhances the resistance of arbuscular mycorrhizae in clover plants to cadmium *via* polyphosphate accumulation in fungal hyphae. Environ. Experiment. Bot. doi. org/10.1016/j.envexpbot.2013.11.007

Ye, B., Luo, Y., He, J., Sun, L., Long, B., Liu, Q., ...et al., 2018. Investigation of lead bioimmobilization and transformation by *Penicillium oxalicum* SL2. Bioresource technology 264, 206-210. DOI: 10.1016/j.biortech.2018.05.066

Ye, X., Zhang, J., Zhang, Y., Lv, Y., Dou, R., Wen, S., ... Hu, Y. 2016. Treatment of Ni-EDTA containing wastewater by electrocoagulation using iron scraps packed-bed anode. Chemosphere *164*, 304-313.

Ye, Z., Yin, X., Chen, L., He, X., Lin, Z., Liu, C., ... Wei, Y. 2019. An integrated process for removal and recovery of Cr (VI) from electroplating wastewater by ion exchange and reduction–precipitation based on a silica-supported pyridine resin. Journal of Cleaner Production 236, 117631.

Yilmaz, D. D., Parlak, K. U., 2011. Nickel-induced changes in lipid peroxidation, antioxidative enzymes, and metal accumulation in *Lemna gibba*. International journal of phytoremediation 13(8), 805-817. DOI: 10.1080/15226514.2010.525563

Yin, Y., Hu, Y., & Xiong, F., 2011. Sorption of Cu (II) and Cd (II) by extracellular polymeric substances (EPS) from Aspergillus fumigatus. International biodeterioration & biodegradation 65(7), 1012-1018.

Ying, W. C., Bonk, R. R., Tucker, M. E. 1988. Precipitation treatment of spent electroless nickel plating baths. Journal of hazardous materials 18(1), 69-89.

Yu, J., Zhang, J., Song, S., Liu, H., Guo, Z., Zhang, C. 2019. Removal of Ni (II) from aqueous solutions using activated carbon with manganese formate hydrate in-situ modification. Colloids and Surfaces A: Physicochemical and Engineering Aspects 560, 84-91.

Yun, C.-W., Bauler, M., Moore, R. E., Klebba, P. E., Philpott, C. C., 2001. The role of the FRE family of plasma membrane reductases in the uptake of siderophore-iron in *Saccharomyces cerevisiae.* J. Biol. Chem. 276, 10218–10223. DOI:10.1074/jbc.M010065200

Yuncu, B., Sanin, F. D., Yetis, U., 2006. An investigation of heavy metal biosorption in relation to C/N ratio of activated sludge. J. Hazard. Mater. 137, 990–997. DOI:10.1016/j.jhazmat.2006.03.020

Yung, M.C., Ma, J., Salemi, M. R., Phinney, B. S., Bowman, G. R., Jiao, Y., 2014. Shotgun proteomic analysis unveils survival and detoxification strategies by *Caulobacter crescentus* during exposure to uranium, chromium, and cadmium. Journal of proteome research, 13(4), 1833-1847.

Zadrąg-Tęcza, R., Maślanka, R., Bednarska, S., Kwolek-Mirek, M. 2018. Response Mechanisms to Oxidative Stress in Yeast and Filamentous Fungi. In *Stress Response Mechanisms in Fungi* (pp. 1-34). Springer, Cham.

Zahmatkesh, M., Spanjers, H., Toran, M.J., Blánquez, P., Lier, J.B., 2016. Bioremoval of humic acid from water by white rot fungi: exploring the removal mechanisms. AMB Expr. 6, 118. doi 10.1186/s13568-016-0293-x

Zang, T., Cheng, Z., Lu, L., Jin, Y., Xu, X., Ding, W., Qu, J., 2017. Removal of Cr(VI) by modified and immobilized *Auricularia auriculaspent* substrate in a fixed-bed column. Ecol. Eng. 99, 358–365.

Zapana-Huarache SV, Romero-Sánchez CK, Gonza AD, Torres-Huaco FD, Rivera AL (2020) Chromium (VI) bioremediation potential of filamentous fungi isolated from Peruvian tannery industry effluents. *Brazilian Journal of Microbiology*, *51*(1), 271-278.

Zare, M.R., Fatehizadeh, A., Amin, M.M., Bina, B., Rahmani, A., Rahmani, H., Asadi, A. 2015. Effect of metal plating industry effluents on biological wastewater treatment. Int. J. Env. Health Eng. 4(1):39. DOI: 10.4103/2277-9183.170706

Zeng, X., Su, S., Feng, Q., Wang, X., Zhang, Y., Zhang, L., ... Wu, C., 2015. Arsenic speciation transformation and arsenite influx and efflux across the cell membrane of fungi investigated using HPLC–HG–AFS and in-situ XANES. Chemosphere 119, 1163-1168. https://doi.org/10.1016/j.chemosphere.2014.10.034

Zhang Z., Liba D., Alvarado L., Chen A. 2014. Separation and recovery of Cr(III) and Cr(VI) using electrodeionization as an efficient approach. Separation and Purification Technology 137, 86-93.

Zhang, S. M., Zhang, X. L., Chang, C., Yuan, Z. Y., Wang, T., Zhao, Y., Yang, X. T., Zhang, Y. T., La, G. X., Wu, K., Zhang, Z. M., Li, X. Z., 2016. Improvement of tolerance to lead by filamentous fungus *Pleurotus ostreatus* HAU-2 and its oxidative responses. Chemosphere 150, 33-39. doi: 10.1016/j.chemosphere.2016.02.003

Zhang, C., Xu, Y., Zhao, M., Rong, H., Zhang, K., 2018. Influence of inoculating white-rot fungi on organic matter transformations and mobility of heavy metals in sewage sludge based composting. J. Hazard. Mater. 344, 163–168.

Zhang, F.Q., Wang, Y.S., Lou, Z.P., Dong, J.D., 2007. Effect of heavy metal stress on antioxidative enzymes and lipid peroxidation in leaves and roots of two

mangrove plant seedlings (*Kandelia candel* and *Bruguiera gymnorrhiza*). Chemosphere 67(1), 44-50. Doi.10.1016/j.chemosphere.2006.10.007

Zhang, F.Q., Wang, Y.S., Lou, Z.P., Dong, J.D., 2007. Effect of heavy metal stress on antioxidative enzymes and lipid peroxidation in leaves and roots of two mangrove plant seedlings (*Kandelia candel* and *Bruguiera gymnorrhiza*). Chemosphere 67(1), 44-50.

Zhang, H., Li, Q., Lu, Y., Sun, D., Lin, X., Deng, X., He, N., Zheng, S., 2005. Biosorption and bioreduction of diamine silver complex by Corynebacterium. J. Chem. Technol. Biotechnol. 80, 285–290. doi:10.1002/jctb.1191.

Zhang, S., Lyu, H., Tang, J., Song, B., Zhen, M., Liu, X. 2019. A novel biochar supported CMC stabilized nano zero-valent iron composite for hexavalent chromium removal from water. Chemosphere 217, 686-694.

Zhitkovich, A. 2011. Chromium in drinking water: sources, metabolism, and cancer risks. Chemical research in toxicology *24*(10), 1617-1629.

Zhu, K., Chen, C., Xu, H., Gao, Y., Tan, X., Alsaedi, A., Hayat, T. 2017. Cr (VI) reduction and immobilization by core-double-shell structured magnetic polydopamine@ zeolitic idazolate frameworks-8 microspheres. ACS Sustainable Chemistry & Engineering, 5(8), 6795-6802.

Zhu, Z.J., Wei, G., Li, J., Qian, Q.O., Yu, J.Q., 2004. Silicon alleviates salt stress and increases antioxidant enzymes activity in leaves of salt-stressed cucumber (*Cucumis sativus* L.). Plant Sci. 167, 527-533. https://doi.org/10.1016/j.plantsci.2004.04.020

Zinicovscaia, I., Safonov, A., Boldyrev, K., Gundorina, S., Yushin, N., Petuhov, O., Popova, N. 2020. Selective metal removal from chromium-containing synthetic effluents using Shewanella xiamenensis biofilm supported on zeolite. Environmental Science and Pollution Research 1-11.

Zischka, H., Lichtmannegger, J., 2014. Pathological mitochondrial copper overload in livers of Wilson's disease patients and related animal models. Ann. N. Y. Acad. Sci. 1315(1), 6-15. doi: 10.1111/nyas.12347

Zongo I., Leclerc J.-P., Maïga H.A., Wéthé J., Lapicque F., 2009. Removal of hexavalent chromium from industrial wastewater by electrocoagulation: A comprehensive comparison of aluminium and iron electrodes. Separation and Purification Technology 66 (1), 159-166.

Zou, H., Huang, J. C., Zhou, C., He, S., Zhou, W. 2020. Mutual effects of selenium and chromium on their removal by *Chlorella vulgaris* and associated toxicity. Science of The Total Environment 724, 138219.

Zuo,Y., Chen, G., Zeng, G., Li, Z., Yan, M., Chen, A., Guo, Z., Huang, Z., Tan, Q., 2015. Transport, fate, and stimulating impact of silver nanoparticles on the removal of Cd(II) by *Phanerochaete chrysosporium* in aqueous solutions. J. Hazard. Mater. 285, 236–244.

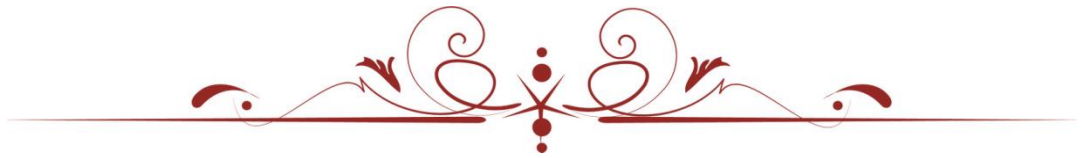

Appendix

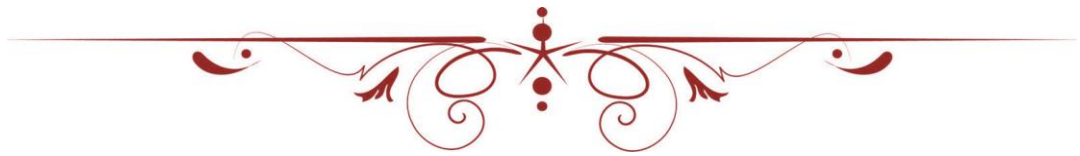

Appendix - I List of Publications

1. **Kumar, V**., & Dwivedi S. K. (2021). A review on accessible techniques for removal of hexavalent Chromium and divalent Nickel from industrial wastewater: Recent research and future outlook. Journal of Cleaner Production, 126229. https://doi.org/10.1016/j.jclepro.2021.126229. **($IF_{(2019)}$ 7.24)**

2. **Kumar, V**., & Dwivedi S. K. (2021). Mycoremediation of heavy metals: processes, mechanisms, and affecting factors. *Environmental Science and Pollution Research.* DOI: 10.1007/s11356-020-11491-8. **($IF_{(2019)}$ 3.05)**

3. **Kumar, V.,** & Dwivedi, S. K. (2021). Bioremediation mechanism and potential of copper by actively growing fungus Trichoderma lixii CR700 isolated from electroplating wastewater. *Journal of Environmental Management, 277*, 111370. **($IF_{(2019)}$ 5.64)**

4. **Kumar, V.,** & Dwivedi, S. K. (2020). Multimetal tolerant fungus *Aspergillus flavus* CR500 with remarkable stress response, Simultaneous multiple metal/loid removal ability and bioremediation potential of wastewater. *Environmental Technology and Innovation*. 101075. **($IF_{(2019)}$ 3.35)**

5. **Kumar, V.,** & Dwivedi, S. K. (2019). Hexavalent chromium stress response, reduction capability and bioremediation potential of *Trichoderma* sp. isolated from electroplating wastewater. *Ecotoxicology and Environmental Safety*, *185*, 109734. **($IF_{(2019)}$ 4.87)**

6. **Kumar, V.**, & Dwivedi, S. K. (2019). Hexavalent chromium reduction ability and bioremediation potential of *Aspergillus flavus* CR500 isolated from electroplating wastewater. *Chemosphere*, *237*, 124567. **($IF_{(2019)}$ 5.77)**

7. Kanaujiya, D., **Kumar, V.**, Dwivedi, S. K., & Prasad, G. (2019). Photobiosynthesis of Silver Nanoparticle Using Extract of Aspergillus flavus CR500: Its Characterization, Antifungal Activity and Mechanism Against

Sclerotium rolfsii and *Rhizoctonia solani*. *Journal of Cluster Science*, 1-10. **(IF$_{(2019)}$ 1.73)**

8. **Kumar, V.**, Singh, S., Singh, G., & Dwivedi, S. K. (2019). Exploring the Cadmium Tolerance and Removal Capability of a Filamentous Fungus *Fusarium solani*. *Geomicrobiology Journal*, 36(9), 782-791. **(IF$_{(2019)}$ 1.989)**

9. Rawat, A. P., **Kumar, V.**, & Singh, D. P. (2019). A combined effect of adsorption and reduction potential of biochar derived from Mentha plant waste on removal of methylene blue dye from aqueous solution. *Separation Science and Technology*, 1-15. **(IF$_{(2019)}$ 1.71)**

10. Prasad, G., **Kumar, V.**, & Dwivedi, S. K. (2018). Antifungal activity of some selected medicinal plants against *Fusarium solani* causing wilt and rot in Pearl millet. *AJBS*, *13*(1), 21-27.

Journal of Cleaner Production 295 (2021) 126229

Contents lists available at ScienceDirect

Journal of Cleaner Production

journal homepage: www.elsevier.com/locate/jclepro

Review

A review on accessible techniques for removal of hexavalent Chromium and divalent Nickel from industrial wastewater: Recent research and future outlook

Vinay Kumar*, S.K. Dwivedi*

Department of Environmental Science, School for Environmental Sciences, Babasaheb Bhimrao Ambedkar University, Lucknow, 226025, India

ARTICLE INFO

Article history:
Received 8 October 2020
Received in revised form
27 January 2021
Accepted 30 January 2021
Available online 10 February 2021

Handling editor: Dr Sandra Caeiro

Keywords:
Chromium
Nickel
Bioremediation
Electrochemical remediation
Integrated technique
Wastewater

ABSTRACT

The present era is seeking our attention on the dilemma caused by the contamination of the aquatic system with chromium (Cr) and nickel (Ni). Amid Ni and Cr oxidation states, hexavalent Cr (Cr(VI)) and divalent Ni (Ni(II)) often found in the contaminated water body with prominent toxicity on flora and fauna. The negative consequences of the Cr and Ni are strongly connected with human health. The effluents discharged by ventures such as plating, tannery, battery, mining, coloring, material, paint, metal processing etc. industries also bring Cr and Ni into the water body. The removal of Cr and Ni from waste/industrial water faced the difficulties owing to inappropriate selection of technologies in aspects of cost, technique, efficiency and sustainability. Thus, in this review we discussed the chemistry and toxicity of Cr(VI) and Ni(II) and have bring together all the possible methods that can be effectively exploited for the treatment of Cr(VI) and Ni(II) contaminated water. We have also focused on the recent advances in integration/combination of biological or natural processes with other existing methods that have high scope for future research and have great opportunity in treatment of Cr and Ni contaminated water in ecofriendly and sustainable way in upcoming days.

Contents

* Corresponding authors.
E-mail addresses: vinaysahubbau@gmail.com, vinaykmr.rs@bbau.ac.in (V. Kumar), skd_es@bbau.ac.in, skdwivedibbau@gmail.com (S.K. Dwivedi).

https://doi.org/10.1016/j.jclepro.2021.126229
0959-6526/

Environmental Science and Pollution Research (2021) 28:10375–10412
https://doi.org/10.1007/s11356-020-11491-8

REVIEW ARTICLE

Mycoremediation of heavy metals: processes, mechanisms, and affecting factors

Vinay Kumar[1] · Shiv Kumar Dwivedi[1]

Received: 31 January 2020 / Accepted: 30 October 2020 / Published online: 6 January 2021

Abstract

Industrial processes and mining of coal and metal ores are generating a number of threats by polluting natural water bodies. Contamination of heavy metals (HMs) in water and soil is the most serious problem caused by industrial and mining processes and other anthropogenic activities. The available literature suggests that existing conventional technologies are costly and generated hazardous waste that necessitates disposal. So, there is a need for cheap and green approaches for the treatment of such contaminated wastewater. Bioremediation is considered a sustainable way where fungi seem to be good bioremediation agents to treat HM-polluted wastewater. Fungi have high adsorption and accumulation capacity of HMs and can be potentially utilized. The most important biomechanisms which are involved in HM tolerance and removal by fungi are bioaccumulation, bioadsorption, biosynthesis, biomineralisation, bioreduction, bio-oxidation, extracellular precipitation, intracellular precipitation, surface sorption, etc. which vary from species to species. However, the time, pH, temperature, concentration of HMs, the dose of fungal biomass, and shaking rate are the most influencing factors that affect the bioremediation of HMs and vary with characteristics of the fungi and nature of the HMs. In this review, we have discussed the application of fungi, involved tolerance and removal strategies in fungi, and factors affecting the removal of HMs.

Keywords Metal tolerance · Molecular mechanism · Heavy metal · Reactive oxygen species · Bioprecipitation · Bioremediation

Introduction

The present scenario of industrial and developmental activities is altering the natural flow of the materials and introducing foreign compounds into the environment (Faisal and Hasnain 2004). Environmental pollutants including halogenated solvents, petroleum hydrocarbons, explosives, agrochemicals, heavy metal/loids, and radionuclides are a serious problem to the environment. Out of these pollutants, heavy metals (HMs) (cadmium; Cd, copper; Cu, mercury; Hg, lead; Pb, manganese; Mn, arsenic; As, nickel; Ni, zinc; Zn, iron; Fe, etc.) are extensively used in different types of industries and released in high amount with their disposing effluents. These contaminants directly or indirectly come into the environment.

Responsible Editor: Elena Maestri

✉ Vinay Kumar
vinaysahubbau@gmail.com; vinaykmr.rs@bbau.ac.in

[1] Department of Environmental Science, Babasaheb Bhimrao Ambedkar University, Lucknow 226025, India

A few numbers of metals including Fe, Mg, Cu, Mn, Co, and Zn are the micronutrients for most of the organisms, while not for all living organisms, and increasing concentration from their limit causes toxicity (Manorama et al. 2016; Singh et al. 2016). HMs as micronutrients may play an essential role in metabolic activity, e.g., metalloenzyme (Tahir et al. 2017). Because of the high solubility of HMs in the aquatic medium, they can be easily absorbed or taken by the organisms. On the other hand, being metal, they are non-biodegradable and have multiple threats to living organisms due to their persistence in nature, high-toxicity characteristics, and long half-lives after coming into the food chain (Ali et al. 2015; Jamali et al. 2007; Mondal et al. 2017). They have multiple ways to come into the food chain such as by seeping in groundwater from wastewater, by drinking of water from the polluted water bodies, crop irrigation by wastewater, etc. (Jamali et al. 2007). After accumulation into the living organism, they cause multiple threats to humans (Table 1) as well as other living organisms. So, due to extensive use and toxicity, heavy metal has a rising number of environmental and health issues and has become a serious concern to resolve at present (Dhankhar and Hooda 2011; Mishra and Malik 2012).

Journal of Environmental Management 277 (2021) 111370

Contents lists available at ScienceDirect

Journal of Environmental Management

journal homepage: http://www.elsevier.com/locate/jenvman

Research article

Bioremediation mechanism and potential of copper by actively growing fungus *Trichoderma lixii* CR700 isolated from electroplating wastewater

Vinay Kumar, S.K. Dwivedi *

Department of Environmental Science, School of Environmental Sciences, Babasaheb Bhimrao Ambedkar University, Lucknow, 226025, India

ARTICLE INFO

Keywords:
Copper
Fungi
Mechanism
Accumulation
Bioremediation
Wastewater

ABSTRACT

Present study investigated the Cu^{2+} removal potential of *Trichoderma lixii* CR700, isolated from enormously heavy metal polluted electroplating wastewater. In the batch study, actively growing CR700 was able to remove 84.6% of Cu^{2+} at the concentration 10 mg/L of Cu^{2+} within 120 h after incubation and the accumulated and surface adsorbed amount of Cu was 0.51 and 0.47 mg/g of dry biomass respectively. *T. lixii* CR700 also showed efficient Cu^{2+} removal potential in the pH ranges from 5.0 to 8.0, in the presence of other co-occurring contaminant such as heavy metal, anions and metabolic inhibitor as well from real tannery wastewater. Alteration on cell surface of Cu^{2+} treated mycelia of *T. lixii* CR700 was analyzed using scanning electron microscope. Fourier transform infrared spectroscopic analysis was performed to identify the role of surface functional group in Cu^{2+} adsorption which revealed that COO^{-} functional group lead Cu^{2+} adsorption onto the surface of *T. lixii* CR700. Thus, *T. lixii* CR700 uses simultaneous surface sorption and accumulation mechanism in Cu^{2+} removal and can be potentially applied for bioremediation of Cu^{2+} contaminated wastewater in ecofriendly, safe and sustainable way.

1. Introduction

Heavy metal pollution in an aquatic ecosystem is the worldwide (especially developing countries) issues at the present, caused by industrial, developmental and modern agricultural practices (Cui et al., 2012; Ma et al., 2017). Industries associated with mining, battery, fertilizer and metal plating generating huge amount of effluent containing high concentration heavy metal including Cu that was mostly discharged into the aquatic environment (Pathak et al., 2017; Fage et al., 2014; Ong et al., 2017; Angelin et al., 2015). Runoff from irrigation and agricultural soil containing pesticide and fertilizer also contribute to metal pollution in aquatic bodies (Kaushik et al., 2009). Thus, Copper (Cu) is the heavy metal widely spread in aquatic bodies. Most of the organism uses Cu^{2+} as an essential element for their growth and development (Serra et al., 2009). However, excess intake of Cu^{2+} will mean adverse health issues to humans as well as environment (Ong et al., 2017; Dubey et al., 2014). The liver and kidney damage are the chronic effects of copper intake in excess in humans (Karabulut et al., 2000; Luk et al., 2017). As per the World Health Organization (WHO) guideline, the upper limit of Cu^{2+} intake should not exceed 2 mg/L (Luk et al., 2017).

The physical and chemical methods such as ion exchange, membrane filtration technologies, adsorption on biochar or activated carbon, electrochemical treatment and precipitation have been developed to remove heavy metal pollution including Cu from wastewater (Fu and Wang, 2011; Fage et al., 2014; Serra et al., 2009). These technologies have several demerits such as low efficiency, high cost and produces huge amount of toxic sludge as a secondary pollutant, these methods cannot be used to treat heavy metal polluted wastewater at large scale (Das et al., 2008; Pathak et al., 2017; Jobby et al., 2018). Biological method is an alternative approach of physicochemical methods, uses bacteria, fungi, algae and plants to treat polluted wastewater and aquatic environment (Malik, 2004; Das et al., 2008; Kumar and Dwivedi, 2020). Many species of bacteria, fungi and plants have been reported for their efficient bioremediation potential to treat heavy metal contaminated sites. Microbial bioremediation has their own merits such as high efficiency, easy to handle, cost-effective etc. make it more prominent for wastewater treatment (Malik et al., 2004; Soares and Soares, 2012). Active cell (growing form) utilization in bioremediation has self-replenishment ability and has great potential application for bioremediation in batch and continuous mode for treatment of wastewater which is another merit of microbial bioremediation (Malik, 2004).

* Corresponding author.
E-mail address: skdwivedibbau@gmail.com (S.K. Dwivedi).

https://doi.org/10.1016/j.jenvman.2020.111370
Received 1 August 2020; Received in revised form 5 September 2020; Accepted 7 September 2020

Environmental Technology & Innovation 20 (2020) 101075

Contents lists available at ScienceDirect

Environmental Technology & Innovation

journal homepage: www.elsevier.com/locate/eti

Multimetal tolerant fungus *Aspergillus flavus* CR500 with remarkable stress response, simultaneous multiple metal/loid removal ability and bioremediation potential of wastewater

Vinay Kumar *, S.K. Dwivedi

Department of Environmental Science, Babasaheb Bhimrao Ambedkar University, Lucknow 226025, India

ARTICLE INFO

Article history:
Received 22 January 2020
Received in revised form 22 July 2020
Accepted 26 July 2020
Available online 28 July 2020

Keywords:
Multimetal
Oxidative stress
Antioxidants response
Phytotoxicity
Bioremediation
Simulated wastewater

ABSTRACT

Microbial bioremediation of multimetal contaminated wastewater can mitigate its environmental toxicity and human health risk. A multimetal tolerating fungus *Aspergillus flvaus* CR500, able to tolerate As (2000 mg/L), Ni (1600 mg/L), Mn (1600 mg/L), Pb (1200 mg/L), Cr (800 mg/L), Cu (200 mg/L) and Cd (100 mg/L), evident by the tolerance index of 0.22, 0.16, 0.19, 0.09, 0.15, 0.12 and 0.29 respectively *A. flavus* CR500 adopted multifarious biochemical (enzymatic and non-enzymatic) and morphological strategies (observed by scanning electron microscopic analysis) to deals with As, Pb and Ni toxicity. During the batch study, isolate CR500 could able to remove 99.0, 97.7 and 73.1% of As, Pb and Ni respectively from individual metal contaminated potato dextrose broth (PDB) medium via bioaccumulation and surface adsorption mechanism. *A. flavus* CR500 also exhibited excellent multimetal (As, Ni, Pb and Cr) removal potential from simulated wastewater (SWW) and Tannery wastewater (TWW) with a high amount of biomass production rate. The removal from 5 mg/L of each metal amended SWW was 97.5, 93.3, 82.2 and 46.6% for As, Pb, Cr and Ni respectively. The toxicity of fungal treated metal solution was reduced, observed from good germination rate and growth of *Vigna radiata* seeds. Thus *A. flavus* CR500 has single as well as multimetal removal ability and can be used for ecofriendly treatment of multimetal contaminated wastewater.

1. Introduction

The present scenario of industrial and developmental activities and modern agriculture practices are introducing heavy metal/loid laden wastewater in huge amount into the environment Bhattacharya et al., 2015; Gupta et al., 2014. Lead, cadmium, nickel, copper, arsenic and chromium have a number of applications in metal plating, battery, paint, fertilizers, pesticides, automobiles, leather tanning, and petrochemicals processing Kumar and Dwivedi, 2019a,b; Shao-Hong et al., 2014; Sudarsan et al., 2015; Acikel and Alp, 2009. Due to toxic, carcinogenic, corrosive, accumulative and non-biodegradable/persistence properties, heavy metal/loid causes number of issues to the environment and human health. As reported, many serious diseases such as autoimmune disorder, heart disorders, digestive disorder, liver, kidney and stomach and lung cancer are associated with exposure of these toxic metals (Gola et al., 2016; Huang et al., 2017; Velmurugan et al., 2010; Ayangbenro and Babalola, 2017). Hence, heavy metals must be removed from wastewater before discharging into the environment or crop irrigation. Conventionally, the physicochemical processes are used for removing

* Corresponding author.
E-mail addresses: vinaykmr.rs@bbau.ac.in, vinaysahubbau@gmail.com (V. Kumar).

https://doi.org/10.1016/j.eti.2020.101075
2352-1864/

Ecotoxicology and Environmental Safety 185 (2019) 109734

Contents lists available at ScienceDirect

Ecotoxicology and Environmental Safety

journal homepage: www.elsevier.com/locate/ecoenv

Hexavalent chromium stress response, reduction capability and bioremediation potential of *Trichoderma* sp. isolated from electroplating wastewater

Vinay Kumar*, S.K. Dwivedi

Department of Environmental Science, Babasaheb Bhimarao Ambedkar University, Lucknow, 226025, India

ARTICLE INFO

Keywords:
Hexavalent chromium
Stress response
Chromate reductase
Bioremediation potential
Phytotoxicity
Trichoderma lixii CR700

ABSTRACT

In the present study we are investigating the $Cr_{(VI)}$ reduction potential of a multi-metal tolerant fungus (isolate CR700); isolated from electroplating wastewater. Based on the ITS region sequencing, the isolate was identified as *Trichoderma lixii* isolate CR700 and able to tolerate As(2000 mg/L), Ni(1500 mg/L), Zn(1200 mg/L), Cu (1200 mg/L), Cr(1000 mg/L), and 100 mg/L of Pb and Cd evident from tolerance assay. $Cr_{(VI)}$ reduction experiment was conducted in Erlenmeyer flasks containing different concentration of $Cr_{(VI)}$ (0–200 mg/L) amended potato dextrose broth medium followed by inoculating with a disk (0.5 cm diameter) of 7 days grown isolate CR700, and achieved a maximum of 99.4% within 120 h at 50 mg/L of $Cr_{(VI)}$. However, the accumulation of total Cr by isolate CR700 was 2.12 ± 0.15 mg/g of dried biomass at the same concentration after 144 h of exposure. Isolate CR700 showed the capability to reduce $Cr_{(VI)}$ at different physicochemical stress conditions such as pH, temperature, heavy metals, metabolic inhibitor and also in tannery wastewater. Fungus exhibited multifarious morphological and biochemical response under the exposure of $Cr_{(VI)}$; the scanning electron microscopic analysis revealed that $Cr_{(VI)}$ treated mycelia of isolate CR700 comparatively irregular, aggregated and swelled than without treated mycelia which might be due to the tolerance mechanism and vacuolar compartmentation of chromium. Moreover, energy dispersive spectroscopy and x-ray photoelectron spectroscopic analysis exposed the $Cr_{(III)}$ precipitation on the mycelia surface of isolate CR700 and Fourier-transform infrared spectroscopic analysis suggested the contribution of the protein associated functional group in the complexation of $Cr_{(VI)}$. The phytotoxicity test of fungal treated 100 mg/L of $Cr_{(VI)}$ supernatant on *Vigna radiata* and *Cicer arietinum* revealed the successful detoxification/remediation of $Cr_{(VI)}$.

1. Introduction

The electroplating processes basically applied the metal on the material surface to provide resistance against corrosion (Arshad et al., 2014; Hackbarth et al., 2016). The wastewater generated from electroplating industries has potential risk for livings organisms and the environment due to containing a very high concentration of heavy metals (nickel, chromium, lead, cadmium, zinc, arsenic and copper) (Shao-Hong et al., 2014; Sudarsan et al., 2015). Out of heavy metals, chromium is common environmental contaminant due to its extensive use in different other types of anthropogenic activities such as leather tanning and mining and are generating a considerable amount of Cr contaminated wastewater and disposed-off into the natural water bodies or used in crop irrigation (Tian et al., 2019; Coreño-Alonso et al., 2014; Angelin et al., 2015; Hang et al., 2009; Kaushik et al., 2009). The $Cr_{(VI)}$ (hexavalent) and $Cr_{(III)}$ (trivalent) form of chromium are the most common species which are predominant in wastewater (Mala et al., 2015; Gu et al., 2015). $Cr_{(VI)}$ is highly soluble, carcinogenic and 100 times more toxic than the trivalent form of chromium (Fernandes et al., 2002; Dey and Paul, 2012; Kaushik et al., 2009). $Cr_{(VI)}$ produces reactive oxygen species and causes oxidative damages inside the cell which is the major cause of its toxicity to living organisms (Wu et al., 2010; Li et al., 2017; Halliwell and Gutteridge, 1984). $Cr_{(VI)}$ has number of problems to human health including bronchopneumonia, chronic bronchitis, diarrhea, emphysema, headache, irritation of the skin, itching of respiratory tract, liver diseases, lung cancer, nausea, renal failure, reproductive toxicity, vomiting (Coreño-Alonso et al., 2014; Rafi et al., 2017; Ayangbenro and Babalola, 2017). It has also prominent toxicity to plants causes chlorosis, delayed senescence, wilting, biochemical lesions, reduced germination, stunted growth, and

* Corresponding author.
E-mail addresses: vinaysahubbau@gmail.com, vinaykmr.rs@bbau.ac.in (V. Kumar).

https://doi.org/10.1016/j.ecoenv.2019.109734
Received 10 June 2019; Received in revised form 23 September 2019; Accepted 24 September 2019

Chemosphere 237 (2019) 124567

Contents lists available at ScienceDirect

Chemosphere

journal homepage: www.elsevier.com/locate/chemosphere

Hexavalent chromium reduction ability and bioremediation potential of *Aspergillus flavus* CR500 isolated from electroplating wastewater

Vinay Kumar*, S.K. Dwivedi

Department of Environmental Science, Babasaheb Bhimrao Ambedkar University, Lucknow, 226025, India

HIGHLIGHTS

- *A. flavus* CR500 show multifarious biochemical and morphological response to deals with $Cr_{[VI]}$ toxicity.
- $Cr_{[VI]}$ induced chromate reductase play a major role in the reduction of $Cr_{[VI]}$ to $Cr_{[III]}$.
- Accumulation, precipitation and adsorption mechanism involve in Cr removal by isolate CR500.
- Isolate CR500 has excellent $Cr_{[VI]}$ bioremediation potential.

GRAPHICAL ABSTRACT

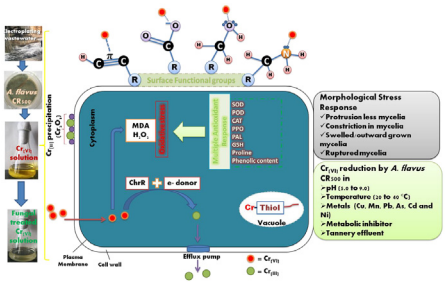

ARTICLE INFO

Article history:
Received 3 June 2019
Received in revised form
8 August 2019
Accepted 9 August 2019
Available online 10 August 2019

Handling Editor: Lena Q. Ma

Keywords:
Antioxidant
Hexavalent chromium
Chromate reductase
Bioremediation
Phytotoxicity

ABSTRACT

Hexavalent chromium reduction by microbes can mitigate the chromium toxicity to the environment. In the present study $Cr_{[VI]}$ tolerant fungal isolate (CR500) was isolated from electroplating wastewater, was able to tolerate 800 mg/L of $Cr_{[VI}$. Based on the ITS region sequencing, the isolate was identified as *Aspergillus flavus* CR500, showed multifarious biochemical (reactive oxygen species, antioxidants response and non-protein thiol) and morphological (protrusion less, constriction and swelling/outwards growth in mycelia) response under $Cr_{[VI]}$ stress. Batch experiment was conducted at different $Cr_{[VI]}$ concentration (0–200 mg/L) to optimize the $Cr_{[VI]}$ reduction and removal ability of isolate CR500; results showed 89.1% reduction of $Cr_{[VI]}$ to $Cr_{[III]}$ within 24 h and 4.9 ± 0.12 mg of Cr per gram of dried biomass accumulation within 144 h at the concentration of 50 mg/L of $Cr_{[VI]}$. However, a maximum of 79.4% removal of Cr was recorded at 5 mg/L within 144 h. Fourier-transform infrared spectroscopy, energy dispersive x-ray spectroscopy and X-ray diffraction analysis revealed that chromium removal also happened via adsorption/precipitation on the mycelia surface. Fungus treated and without treated 100 mg/L of $Cr_{[VI]}$ solution was subjected to phytotoxicity test using *Vigna radiata* seeds and result revealed that *A. flavus* CR500 successfully detoxified the $Cr_{[VI]}$ via reduction and removal mechanisms. Isolate CR500 also exhibited efficient bioreduction potential at different temperature (20–40 °C), pH (5.0–9.0), heavy metals (As, Cd, Cu, Mn, Ni and Pb), metabolic inhibitors (phenol and EDTA) and in sterilized tannery effluent that make it a potential candidate for $Cr_{[VI]}$ bioremediation.

1. Introduction

Multiple metals are used in electroplating processes in metal plating industries (Arshad et al., 2014; Hackbarth et al., 2016) thus, generated wastewater contain metals such as chromium (Cr),

* Corresponding author.
E-mail address: vinaysahubbau@gmail.com (V. Kumar).

https://doi.org/10.1016/j.chemosphere.2019.124567
0045-6535/

Journal of Cluster Science (2020) 31:1041–1050
https://doi.org/10.1007/s10876-019-01709-2

ORIGINAL PAPER

Photobiosynthesis of Silver Nanoparticle Using Extract of *Aspergillus flavus* CR500: Its Characterization, Antifungal Activity and Mechanism Against *Sclerotium rolfsii* and *Rhizoctonia solani*

Deepa Kanaujiya[1] · Vinay Kumar[1] · S. K. Dwivedi[1] · Ganesh Prasad[1]

Received: 14 September 2019 / Published online: 5 November 2019

Abstract
Newly biosynthesized metallic nanoparticle with antimicrobial characteristic attracted its demand in the field of disease management. The present study deals with the synthesis of silver nanoparticle using the extract *Aspergillus flavus* CR500 under the presence of sunlight. The characterization via scanning and transmission electron microscope revealed their size distribution ranges from 60 to 130 nm with a high content of Ag, confirmed by energy dispersive X-ray spectroscopic analysis. X-ray diffraction and Fourier transform infrared analysis exposed the crystalline nature and active functional group availability on silver nanoparticle (AgNPs). Photobiosynthesized AgNPs have high antimicrobial property and completely inhibited the growth of plant pathogenic fungi *Rhizoctonia solani* GPB and *Sclerotium rolfsii* at the concentration of 150 and 300 µg/L respectively. AgNPs exposure increases the lipid peroxidation (via reactive oxygen species production) in *R. solani* and *S. rolfsii*, might be a primary cause of AgNPs toxicity to fungal cell. However, fungal cell responded to oxidative stress caused by AgNPs by increasing the catalase and peroxidase activity. In order to assess the AgNPs applicability in seed protection and its impact on germination, growth and development of the crop, *Cicer arietinum* and *Vigna radiata* seeds were used for growth and germination assay under AgNPs exposure.

Keywords Nanoparticle · Shape and size of AgNPs, Antifungal mechanism · Oxidative stress · Antioxidants

Introduction

In recent year, the demand of newly synthesized silver nanoparticles (AgNPs) has been significantly increased for the application in the agricultural and industrial sectors. The antimicrobial (antibacterial, antifungal and antiviral activity) property of AgNPs is major cause of considerable attraction for its potential use in controlling the bacterial, fungal and viral pathogen in medical, industrial and agriculture field [1–4]. These days agriculture being challenged due to insect and pathogen (fungi and bacteria) attack [5] and the ability to adopt the stress conditions, the pathogens adopted resistance against traditional pesticides resulting spectacular crop loss [6, 7]. Chemical pesticide is also eco-destructive, persistent in nature, affect to soil micro-biota and causes number of human health issues. In this regards, there is need of novel strategies to control the pathogen and improve agriculture productivity. The implementation of nanoparticle in the agriculture sector is believed as navel strategies to deal with plant pathogen that will transform agricultural performance and help to improve crop productivity [5].

The chemical based synthesis of metallic nanoparticle is associated with number of disadvantages at all the stages due to applying toxic chemically originated organic solvents, reducing agents, and stabilizers, consequently are not environmental friendly [3, 8]. However, the green synthesis of nanoparticle can remove the disadvantages. The biologically originated bioactive materials from various sources such as microbes (bacteria and fungi) and plant (plant extract) are being utilized for synthesis of AgNPs, having potential antimicrobial activity [4, 9–12]. Fungal mediated synthesis of metallic nanoparticle is described to be more compensation than using bacteria in the processes

Deepa Kanaujiya and Vinay Kumar contributed for first author.

✉ S. K. Dwivedi
skdwivedibbau@gmail.com

[1] Department of Environmental Science, Babasaheb Bhimrao Ambedkar University, Lucknow 226025, India

GEOMICROBIOLOGY JOURNAL
2019, VOL. 36, NO. 9, 782–791
https://doi.org/10.1080/01490451.2019.1627443

Exploring the Cadmium Tolerance and Removal Capability of a Filamentous Fungus *Fusarium solani*

Vinay Kumar, Saumya Singh, Garima Singh, and S. K. Dwivedi

Department of Environmental Science, Babasaheb Bhimarao Ambedkar University, Lucknow, India

ABSTRACT

Cadmium is one of the most toxic contaminant causing many problems to human health and the environment. These days the world is moving toward ecofriendly and efficient techniques to remove the pollutant from the wastewater. The present study aims to investigate the tolerance of *Fusarium solani* toward cadmium (Cd), nickel (Ni), and lead (Pb). Maximum tolerance was observed with Cd. Cadmium removal ability of *F. solani* was examined from contaminated PDB medium. pH, initial concentration and time optimization for maximum removal of Cd by *F. solani* was also studied. The maximum removal (92.4%) was recorded at initial concentration of 50 mg/L after 144 h of incubation. Cadmium exposure increased the level of glutathione (GSH) and oxidized glutathione (GSSG) contents and the activity of catalase (CAT) in *F. solani*. Fourier-transform infrared spectroscopy (FTIR) analysis indicated the involvement of the different surface functional group in biosorption of Cd while Scanning Electron Microscopy coupled with Energy Dispersive Spectroscopy (SEM-EDS) analysis revealed the presence of Cd on the surface of fungal cell. The changes observed in compositions of S, P, and Cd using EDS analysis on biomass surface indicated the precipitation of Cd as CdS and $Cd_3(PO_4)_2$. The XRD analysis revealed the presence of $Cd_3(PO_4)_2$ on mycelia surface of *F. solani*.

ARTICLE HISTORY
Received 3 March 2019
Accepted 30 May 2019

KEYWORDS
Tolerance index; glutathione; catalase; biosorption; bioprecipitation

Introduction

Unmanaged exploitation of heavy metal due to wide application alters the natural flow of environment and threats to human health and the environment (Chen et al. 2008). Among the heavy metals, cadmium is highly toxic because of its high transfer potential from soil and water to plant tissues with strong bio-toxicity even at low concentrations (Chen et al. 2015; Goswami et al. 2016; Yadanaparthi et al. 2009). Many metabolic disorder such as hypertension, renal damage, testicular atrophy, emphysema and itai-itai disease caused by cadmium exposure (Çelik et al. 2017), and it is also identified as B_1 Carcinogen by Environmental Protection Agency (EPA). Cadmium-loaded effluents arise from many industrial processes such as metal coating and production, nickel-cadmium batteries, pigments, alloys, stabilizers, solar cells, and also from mining activities (Singh et al. 2006; Su et al. 2017).

Conventional technologies such as chemical precipitation, electrochemical treatment, and reduction using ion exchange, filtration and flocculation are used for the removal of heavy metal to minimizes the impact (Chen et al. 2015; Fu and Wang 2011). But, these conventional methods have considerable disadvantages including incomplete metal removal, requirements for expensive equipment and monitoring systems, high reagent and energy requirements and generation of toxic sludge or other waste products that necessitate disposal (Huang et al. 2017; Rojjanateeranaj et al. 2017) while, biological treatment offers the advantages of low operating costs, fewer waste products, high efficiency, and convenience of operation (Akar et al. 2013; Elwakeel and Guibal 2015; Munagapati et al. 2010). However, excess metal ions may negatively affect and reduce the efficiency of biological treatment systems (Taboski et al. 2005; Li et al. 2018). Microorganisms possess a number of mechanisms to tolerate heavy metals such as intra and extra-cellular chelation using metal chelating ligands like metallothioneins and gluthione, enhanced efflux, subcellular compartmentation, enzymatic oxidation-reduction, etc. (Bellion et al. 2006; Borut et al. 2010). In the midst of various bioremediator (bacteria, fungi, algae, and others), fungi are very striking options due to their easy and immense growth with the economical substrate in processes of wastewater treatment (Abdolali et al. 2006; Vilar et al. 2009). Several studies suggested that many species of fungi are proficient for removing heavy metals from wastewater such as *Phanerochaete chrysosporium, Aspegillus awamori, Aspegillus flavus*, and *Trichoderma viride*. They able to remove Cd, Pb, Cr, and Ni up to 400 mg/L of heavy metal contaminated liquid media (Tabosk et al. 2005; Abdolali et al. 2006; Mohsenzadeh and Shahrokhi 2014; Paria et al. 2018). Luo et al. (2010) reported the biosorption of cadmium on the surface of *Rhizopus cohnil*. The efficient removal of Cd^{2+} ions

CONTACT S. K. Dwivedi skdwivedibbau@gmail.com Department of Environmental Science, Babasaheb Bhimarao Ambedkar University, Lucknow 226025, India

SEPARATION SCIENCE AND TECHNOLOGY
2020, VOL. 55, NO. 5, 907–921
https://doi.org/10.1080/01496395.2019.1580732

A combined effect of adsorption and reduction potential of biochar derived from Mentha plant waste on removal of methylene blue dye from aqueous solution

Abhay Prakash Rawat, Vinay Kumar, and Devendra Pratap Singh

Department of Environmental Science, Babasaheb Bhimrao Ambedkar University, Lucknow, Uttar Pradesh, India

ABSTRACT

Plant biochars were prepared by slow pyrolysis of Mentha plant waste to remove cationic dye methylene blue (MB) from aqueous solution. The biochars were characterized by X-Ray diffraction, IR-spectroscopy, thermogravimetric analysis, scanning electron microscope, cyclic voltammetry (CV), Brunauer-Emmett-Teller analysis, and zeta potential analyzer. Adsorption isotherms and kinetics applied on the MB dye removal by biochars showed monolayer chemisorption of MB dye. Present investigation revealed that removal of MB dye was due to synergistic action of chemisorption coupled with reductive electron transfer mechanisms. CV test showed a reversible, coupled redox reaction at interface of MB dye and biochar particles.

ARTICLE HISTORY
Received 27 February 2018
Accepted 6 February 2019

KEYWORDS
Mentha plant waste; biochar; methylene blue; decolorization; electrochemical reduction

Introduction

Food, textiles, dyeing, and printing industries are the key sources for release of dye containing waste water into natural water bodies. Synthetic dyestuffs are the major water pollutants discharged by the paper industry, dye houses, textile, and printing industries[1,2] which contribute to environmental contamination and serious health problems due to their extensive application.[3] Most of the organic dyes used in various industrial processes are found to be more stable against photobleaching and remain unaffected by aerobic digestion because of their large molecular size and complexity of their structure.[4] Methylene blue (MB), a basic cationic dye, has been extensively applied for dyeing of wool, silk, jute, and leather due to its low price and easy availability.[5] MB dye has chemical properties which contribute to its mutagenic and carcinogenic properties in a wide range of living beings including humans. Therefore, a complete elimination of these dyes from the dye-laden industrial effluents is desirable before its discharge into the water bodies.

During the last few years, several physico-chemical methods have been employed for dye removal from aqueous media, including photo-catalytic degradation,[6] coagulation and ultrafiltration,[7] electrochemical,[8] oxidative degradation,[9] adsorption,[10] and other electrochemical methods.[11,12] Among these methods, dye removal by using different biosorbents is considered to be more economical and effective method. Since the adsorption potential of many biosorbent materials depend upon their physico-chemical properties and selection of an efficient adsorbent is, therefore a prime concern for treatment of dye-laden waste water.

Applicability of different adsorbents for treatment of waste water is limited as they are usually prepared from non-renewable materials and are also found to be expensive. In recent years, different types of biomaterials have been applied for removal of dyes and heavy metals from waste water due to their low cost and enhanced adsorption potential.[13] This has led many researchers to find some cheaper and efficient alternative materials for treatment of waste water. The biochar is a carbon-rich biomass derived from biomaterials by slow pyrolysis under oxygen-limited condition. Biochar has been considered as an efficient adsorbent comparable to activated charcoal in removal of organic and inorganic toxicants from industrial waste water due to its porous structure, surface active binding ligands, and large surface area.[14]

In order to reduce the material cost of adsorbents, low price agro-waste materials including crop residues, animal maures, forestry, and many food materials are being used for biochar production. The post-distillation Mentha plant residues is a by-product of Mentha distillation industry with no further application. India is the main producer of post-distillation Mentha plant

CONTACT Devendra Pratap Singh dpsinghbbau1959@gmail.com
Color versions of one or more of the figures in the article can be found online at www.tandfonline.com/lsst.

➔DOI : 10.15740/HAS/AJBS/13.1/21-27
e ISSN-0976-8343 | ■ Visit us : *www.researchjournal.co.in*
ASIAN JOURNAL OF BIO SCIENCE
Volume **13** | Issue 1 | Apr., 2018 | 21-27

RESEARCH **P**APER

Antifungal activity of some selected medicinal plants against *Fusarium solani* causing wilt and rot in Pearl millet

Ganesh Prasad, Vinay Kumar **and S.K. Dwivedi**

Department of Environmental Science, Babasaheb Bhimrao Ambedkar (A Central) University, Vidya Vihar, Raebareli Road, Lucknow (U.P.) India
Email : *skdwivedibbau@gmail.com, ganeshat86@gmail.com, vinaysahubbau@gmail.com

Article Info : Received : 24.01.2018; Revised : 07.03.2018; Accepted : 22.03.2018

Fusarium solani is a soil-borne fungus which causes wilt and rot disease in pearl millet. Pearl millet belongs to family Poaceae, contains carbohydrates, vitamins, protein and high amount in minerals *i.e.* iron, zinc, calcium and other minerals. It maintains human health. To control the soil-borne diseases in Pearl millet with the use of chemicals under in field condition is hazardous, loss of soil fertility and causes serious environmental pollution, thus use of plant extract as an ecofriendly means is needed. *Fusarium solani* treated with *Allium sativum, Zingiber officinale, Momordica charantina, Mentha arvensis, Allium cepa* and *Capsicum annum* using poisoned food technique at 10%, 25%, 50% and 75% concentration on 3rd, 5th, 7th day incubation period under *in vitro* condition. The selected plant extracts were significantly ($P \leq 0.05$) effective against *F. solani* but *Allium sativum* was most effective compared to others. *Allium sativum* inhibited 100% mycelial growth of *F. solani* at 10% concentration on 3rd day of incubation period. *Zingiber officinale* and *Capsicum annum* inhibited 71.2% and 75.7% mycelial growth of *F. solani* under *in vitro* condition respectively.

Key words : Pearl millet, *Fusarium solani*, Soil-borne, Wilt and rot, Plants extract

How to cite this paper : Prasad, Ganesh, Kumar, Vinay and Dwivedi, S.K. (2018). Antifungal activity of some selected medicinal plants against *Fusarium solani* causing wilt and rot in Pearl millet. *Asian J. Bio. Sci.*, **13** (1) : 21-27.**DOI : 10.15740/HAS/AJBS/13.1/21-27.**

INTRODUCTION

India is a geographically subtropical country with warm and humid climate that provides an appropriate environment for developing and spread of numerous plant pathogens (Amin *et al.*, 2015). *Fusarium solani* is a soil-borne fungus and is worldwide in distribution. *Fusarium solani* produced mycotoxin which is secondary metabolites that creates a serious threat to plants and animals. In case of plant, it causes wilt and rot disease on wide variety of crop at least 111 plants species (Bogale *et al.*, 2008). *Fusarium solani* causes disease in pearl millet and decreases plant yield productivity and consequently economic losses. Pearl millet (*Pennisetum glaucum*) is an economic crop which grown for food and forage in India, Africa and worldwide. It belongs from family Poaceae. India was the first producer and developed hybrids seeds of pearl millet in 2014-15 with the total production (Malik, 2015). Pearl millet contains carbohydrates, proteins, vitamins, fats and high amount in minerals *i.e.* iron, zinc, calcium, magnesium, phosphorus, potassium, sodium, copper, manganese, selenium and dietary fibre content that help human health (Prasad and Dwivedi, 2017).

The chemical affects serious threat to the environment, health hazardous and toxicity of some beneficial microbes present in soil which promote plant growth (Dwivedi and Prasad, 2016). The use of medicinal plant extract is an eco-friendly way to control *Fusarium solani*. The aqueous medicinal plant's extract has effective antagonistic properties against pathogen at

Appendix - II Conferences and Workshops attended

Conferences attended

- Presented Poster entitled **"Nickel tolerant *Trichoderma* sp. isolated from Electroplating wastewater: Removal ability and mechanism"** in **"International Conference on Environmental Sustainability: Innovations, Traslations Dimensions and Way forward"** held on 11th to 12th February, 2020 at Department of Environmental Science, Babasaheb Bhmrao Ambedkar University, Lucknow.

- Presented poster entitled **"Tolerance of a Filamentous fungus against some chemicals Isolated from Rhizospheric soil of Pearl Millet"** in **"Ist North Indian Science Congress"** healed on **January 10th-11th, 2018** at **Babasaheb Bhimrao Ambedkar University, Lucknow, Uttar Pradesh, India.**

Workshops attended

- Attended one day work shop on "**Publication Ethics and Patenting"** organized by Department of Environmental Science, Babasaheb Bhimrao Ambedkar University, Lucknow at **10th of February, 2020**.

- Participated in three days Hands-on-Workshop on "**Molecular Characterization of Microorganism**" organized by **Division of Biotechnology, CytoGene Research and Development, Lucknow** during the period of **9th to 11th November, 2018**.

- Participated in two days Workshop on "**High Performance Liquid Chromatography (HPLC) & Its Application**" organized by **Division of Biotechnology, CytoGene Research and Development, Lucknow** during the period of **21st** to **22nd April, 2018**.

- Participated in the Workshop on "**Socio-environmental Dimensions in the Rejuvenating River Gomati**" on 23rd April, 2018 organized by **Department of Environmental Science, Babasaheb Bhimrao Ambedkar University, Lucknow** in association with **Lokbharti.**

Honor and Award

- **International Distinguished Researcher** in **Environmental Microbiology**, **Research Leadership Awards of the Year 2020** awarded by **RULA Awards** accredited by **World Research Council**, **United Medical Council** and **Internatinal Journal of Research Under Literal Access (IJRULA)**.

- ***Research Excellence Award*** in **Life Science** of the year 2021 by Vice Cahncellor, **Babasaheb Bhimrao Ambekar University, Lucknow, India.**

Document Information

Analyzed document	Thesis(1).docx (D93710626)
Submitted	1/27/2021 8:08:00 AM
Submitted by	O. P. Saini
Submitter email	gbl.bbau@gmail.com
Similarity	3%
Analysis address	gbl.bbau.bbau@analysis.urkund.com

Sources included in the report

W	URL: https://www.nature.com/articles/s41598-017-01885-z Fetched: 1/27/2021 8:10:00 AM	5
W	URL: https://www.nature.com/articles/s41598-020-65534-8 Fetched: 1/27/2021 8:10:00 AM	3
W	URL: https://www.researchgate.net/publication/308661968_Microbes_as_Potential_Tool_for_ ... Fetched: 3/26/2020 9:15:49 AM	4
W	URL: https://www.researchgate.net/publication/26876965_Interference_of_chromium_with_bi ... Fetched: 12/30/2020 7:51:58 AM	6
W	URL: https://www.nature.com/articles/s41598-020-61505-1 Fetched: 1/27/2021 8:10:00 AM	2
W	URL: https://www.researchgate.net/publication/223598037_Biosorption_of_Chromium_From_Aq ... Fetched: 12/29/2020 6:03:25 AM	4
W	URL: https://www.researchgate.net/profile/Kun_Yin3/publication/328681212_Microorganism_ ... Fetched: 11/1/2019 11:02:11 AM	6
W	URL: https://www.researchgate.net/publication/225225135_Metal_Tolerance_and_Biosorption ... Fetched: 12/10/2019 11:37:14 AM	3
W	URL: https://www.researchgate.net/publication/323830155_Biological_approaches_to_tackle ... Fetched: 2/26/2020 8:05:37 PM	8
W	URL: https://www.ncbi.nlm.nih.gov/pmc/articles/PMC6180975/ Fetched: 10/21/2019 5:48:22 AM	6
W	URL: https://www.researchgate.net/publication/244144296_Phytoremediation_of_chrome-VI_o ... Fetched: 3/19/2020 10:41:50 AM	1
W	URL: https://journals.plos.org/plosone/article%253Fid%253D10.1371/journal.pone.0227953 Fetched: 1/27/2021 8:10:00 AM	4
W	URL: https://www.researchgate.net/publication/23493670_CrVI_reduction_from_contaminated	